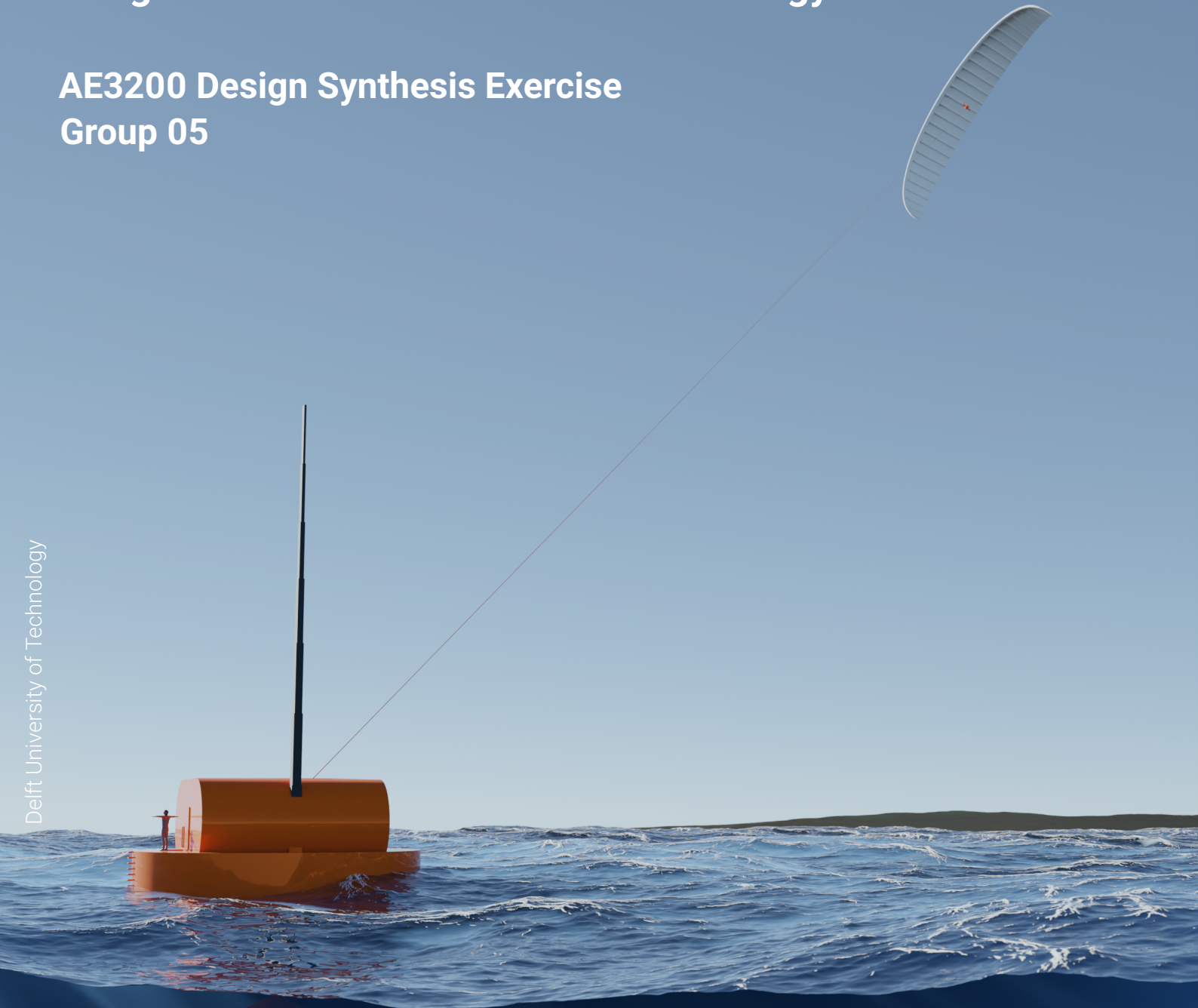


WaveWings

Integrated Airborne Wind and Wave Energy Converter

AE3200 Design Synthesis Exercise
Group 05

Delft University of Technology



This page was intentionally left blank

WaveWings (Group 5) Design Synthesis Exercise AE3200

Final Report

<u>Student Name</u>	<u>Student Number</u>
T.A.M. Clara	5258367
T.Y.A. De Laere	5559855
D.G.A. van Ginkel	5543452
L.D.I. van Vliet	5241952
J.A.A. Bredael	5583810
R. Dux	5477069
R.M. Leal	5084954
J.W.L. Matthé	5539153
G. Fernández-Nespral	5228174
M. Güell Ybarra	5289033

Tutor: Dr.-Ing. Roland Schmehl (Wind Energy, TU Delft)
Coach: Dr. Ir. Furkat Yunus (Control & Operations, TU Delft)
Coach: Oriol Cayón Domingo (Wind Energy, TU Delft)

June 25, 2024
Delft University of Technology
Faculty of Aerospace Engineering, Delft, the Netherlands

Preface

Between April-June 2024, we, Group 05 “WaveWings”, had the opportunity of exploring existing Airborne Wind Energy and Wave Energy Converter technologies with the aim of establishing an integrated solution as part of the Design Synthesis Exercise (AE3200) at Delft University of Technology in the Netherlands.

We hope that this report will serve as a strong building block for integrated wind and wave energy designs and stimulate further research on the WaveWings concept. We hand over this project as a token of gratitude for a newly-discovered AWES and WEC community with the hope of sparking conversation. By focusing on conceptual work, we hope to bring these technologies to public light, identify market opportunities, project economic performance, and to assist in transforming academic knowledge into products.

Evidently, we would like to recognize and thank Dr.-Ing. Roland Schmehl for the wealth of knowledge and experience in AWES, Dr.Ir. Furkat Yunus for knowledge in noise emissions, Ir. Oriol Cayón Domingo for providing aerodynamic models, Dr.Ir. Antonio Jarquin Laguna for the patience required in introducing Maritime WEC systems to Aerospace engineers, and Ir. Rishikesh Joshi for the development of economic models, Kirsten Coutinho for assistance in LCA kite calculations, Ing. Sofia Trombini for discussions on control theory, Felix Bartels from OCEANERGY for his insight on launch and retrieval designs of kites, and to Prof. Dr. Lorenzo Fagiano for establishing the concept.

Thank you to Kitepower for accommodating a visit of the facilities to allow us to grasp the practical implementation of these systems, and to the contributors of the AWEC 2024 in Madrid that opened our eyes to the ongoing developments whilst deepening our understanding.

Group 05, Delft, June 2024

Executive Overview

Mission Need Statement:

WaveWings aims to exploit the synergy between coupled airborne wind energy and wave energy modules in order to construct a 1 GW renewable energy farm in an effort to contribute to the European Union's net-zero 2050 goals.

Project Objective Statement:

To produce a detailed and scalable design of an energy generator consisting of an airborne wind energy system and a wave energy converter with ten students in ten weeks time.

Requirements and Constraints

A foundation block of WaveWings is the stakeholder requirements and constraints. The requirement is to design integrated WaveWings units that extract wind and wave power synergistically, producing 2.5 MW of power of which 2.3 MW is from wind power alone. In total the farm should produce 1 GW of power. Further important requirements and constraints are related to sustainability and finances. Namely, the farm shall provide a 50-80% levelized cost of energy reduction compared to conventional off-shore renewables.

Sustainability Strategy

The Sustainable Development Strategy chapter outlines the WaveWings project's commitment to sustainability through rigorous design and operational guidelines. It details the project's sustainability requirements and the organizational approach to achieving them, which is structured around three pillars: environmental, social, and financial sustainability. The strategy includes specific considerations such as material choices, farm location, resource management, and local resource utilization. Indicators like Global Warming Potential (GWP), Cumulative Energy Demand (CED), and the levelized cost of energy (LCOE) are used to measure the project's sustainability impact. The Sustainability Manager plays a key role in ensuring these aspects are integrated and evaluated throughout the design process.

Concept Configuration

Multiple trade-offs are performed to determine the best solutions for each subsystem in the WaveWings design, by assigning final scores over a scale of 50. Once a kite, launch system, WEC, PTO, and anchoring system are chosen, the way they are integrated is shown and explained.

Three types of kites were considered during the evaluation of kite concepts: Leading-Edge Inflatable (LEI) kites, Ram-Air kites, and Semi-Rigid kites. The LEI kite has inflatable tubes providing stiffness, reducing the need for bridle lines, making it easier to control and launch. It was found that the Ram-Air kite, although lighter and having higher aerodynamic performance compared to the LEI kite, requires extensive bridle lines and is less stable. Finally, the Semi-Rigid kite, offers high aerodynamic performance but is difficult to control and prone to damage. In the end, the trade-off favoured the LEI kite due to its balance of control, ease of launch, crashworthiness, and an overall score of 37.5, compared to 34.5 for the Ram-Air and 25.5 for the Semi-Rigid kite.

The trade-off of the launch system of the kite considered the Upright Launch Tower, the Upside-down Hanging Tower, the Robot-Assisted Water Launch, and the Water Launch. The Upright Launch Tower, utilizing a retractable mast, is a proven technology and offers good control for large kites, scoring 34. The Upside-down Hanging Tower is less stable for large kites, especially since the tower would cause large moments on the buoy platform, scoring 20. The Robot-Assisted Water Launch and Water Launch both scored 32, benefiting from allowing the kite to take-off at low cut-in wind speeds and designed for water landings, but both were deemed too complex due to its increased amount of systems and unproven concepts. Thus the upright launch tower was selected,

Three different wave energy converter (WEC) concepts were traded-off: point absorbers, line attenu-

ators, and raft-type attenuators. Point absorbers, such as CorPower's unit, were shown to be the preferred choice due to their potential synergy with Airborne Wind Energy Systems (AWES) with their main degree of freedom being the vertical heaving motion, high survivability in extreme wave conditions (up to 18 meters wave heights), and efficient hydrodynamic performance (30%). The point absorber scored 47.5, making it choice for the WEC concepts. In comparison, line attenuators and raft-type attenuators, such as those by Pelamis and Mocean Blue X respectively, scored lower due to their lower Technology Readiness Levels (TRL), lesser or non-proven survivability in high wave environments, and higher costs.

The WaveWings must be effectively anchored to the sea floor to avoid drifting and to be stable for power absorption in heave motion. Three mooring systems were compared based on their anchoring efficiency, cost, installation complexity, time, and noise generation during installation and operation. The Gravity Anchor, a straightforward solution involving the deployment of precast concrete anchors, scored 29.5, because of its ease of installation and lower noise emissions. The Driven Pile, with a score of 33.5, offers high anchoring efficiency but is more complex to install and generates significant noise when installed. The Suction Pile was chosen after the trade-off, scoring 39 due to its anchoring efficiency and lower environmental disturbance.

With the trade-offs completed for the kite, launch tower, WEC, WEC PTO, and anchoring systems, the integration of these systems is now considered. In Figure 1 and 2 the preliminary design of a wave wings unit can be seen. In Figure 1 the buoy in closed configuration can be seen. In yellow the WEC floating body can be seen. In blue the maintenance door at a human scale is displayed to show the scale of the system, and in grey, the submerged body, which acts as a ballast can be appreciated. In black, the operation doors are displayed. These can be opened independently depending on the configuration that the system is working on. If the kite is being deployed or retrieved, all doors will be opened as seen in Figure 2. It is important to note that the kite shown in Figure 2 is not set to scale and a accurate 3D model will be done in later stages.

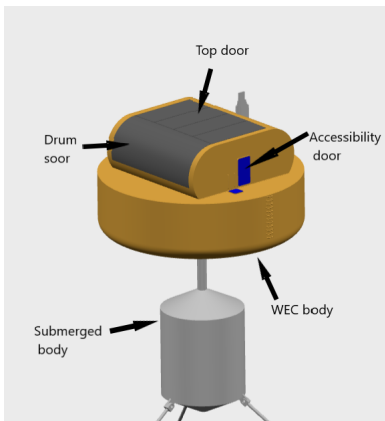


Figure 1: Closed concept layout

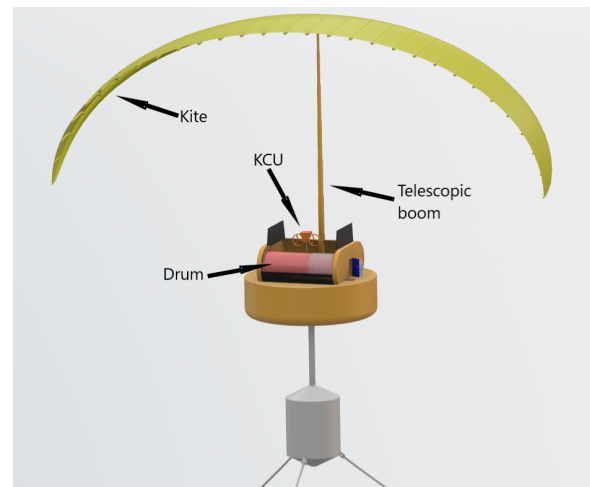


Figure 2: Kite deployment and launch configuration with open doors

Market Analysis

The target market of the WaveWings farm is the Irish offshore wind sector of renewable energy. Bottom-fixed and floating horizontal-axis wind turbine (HAWT) offshore farms are the current competitors in this market.

The most important stakeholders that are identified are the government and customer stakeholders. These have high influence and high interest in the WaveWings farm. The government can implement financial incentives, require permits and regulations to be followed. The customers are interested in price-competitiveness, and are the consumers of the electricity the farm produces. The most important driver for purchase of renewable energy is for customers and governments to meet sustainability

goals and reduce greenhouse gas emissions.

The offshore wind energy capacity in Ireland is growing annually with a rate of 69%, the trends are in the favor of WaveWings for integration into the market. By 2030, Ireland will have an installed offshore wind capacity of 5 GW, resulting in a market share of 20% for WaveWings.

The location selected has an ocean and marine energy testing and validation facility, which will be utilized by the WaveWings farm. This facility allows the initial phases of the project to be more cost effective than in the case no existing facilities were present.

Constructing any facility requires permitting and regulations to be followed. Several documents are needed to obtain the permits, and include documents such as zoological assessments and noise pollution reports. The regulations that has to be followed is the airspace regulation imposed by the Irish government. The Irish government provides no financial incentives as of 2016, so no financial breaks are expected for the WaveWings farm.

The levelised cost of electricity (LCOE) target range is required to be between 32 and 81 EUR/MWh.

The positioning in the offshore wind energy market is initially favorable, WaveWings will have a lower LCOE than both bottom-fixed and floating offshore HAWT, but is expected to be surpassed by bottom-fixed HAWT in 2035 and floating HAWT in 2040. For an expected deployment year of 2030, it will be more profitable than floating offshore HAWT for half of its lifetime.

Airborne System

The airborne system consists of all airborne subsystems of the WaveWings unit. This includes the kite, the bridle system, the kite control unit (KCU) and the tether. All these systems are designed to have a rated power output of 2.3 MW at a rated wind speed of 12.5 m s^{-1} .

The first subsystem which is designed is the kite, for this, the airfoil needs to be chosen. During the trade-off phase of this project, it was decided that the kite would be a leading edge inflatable kite (LEI). This means that a LEI airfoil needs to be analysed. For this, the model of Ir. J. Breukels [1] is used. Different values of leading edge thickness and camber were simulated and evaluated on its C_l^3/C_d^2 performance. This performance indicator was chosen because it is the aerodynamic part of the crosswind power equation by Loyd [2]. From this analysis, it was found that an airfoil with a leading edge thickness of 10% and a camber of 8% is optimal for crosswind power generation.

After the airfoil is designed, the 3D shape of the kite needs to be designed. For this a few assumptions were made. Firstly, the leading edge of the kite is elliptic and the trailing edge is straight. The curvature of the kite is the top half of an ellipse. These assumptions were made by comparing to sporting kites. To simulate different geometries, the Vortex step method (VSM) of Ir. O. Cayon was used. An iteration over aspect ratio and curvature was performed. This iteration took into account the aerodynamic efficiency of generating power, and thus kite size, and the ability of the kite to turn. The final kite design has an aspect ratio of 6.3 and an elliptical curvature ratio of a 1.6 circular arc.

A structural analysis of the kite shows that there is a maximum distance of 2.00 m between the struts. The material which is selected for the kite is ALUULA Vaepor™ due to its higher stiffness and strength when compared to other materials.

The capacity factor was calculated using wind speed data at the location and equals 59%. The kite surface was determined to be 400 m^2 . The average cycle time was determined to be 144 s. At a rated wind speed of 12.5 m s^{-1} the kite is reeling out 70% of the time and producing power, the other 30% it is reeling in and consuming power.

An overview of the most important parameters of the airborne system is given in tables 1 and 2. The kite is visualised in Figure 3.

Table 1: AWES design parameter overview

Parameter	Value
Airfoil Camber	8%
Leading Edge thickness	10%
Aspect ratio	3.5
Span	50.0 m
Planform area	400 m ²
Elliptical curvature ratio	1.6
Kite mass	456.1 kg
KCU mass	110 kg
Strutt spacing	2.00 m
Flat surface area	470 m ²
Flat span	64.6 m
Flat aspect ratio	8.9
Tether material	DYNEEMA® SK78
Tether length	1100 m
Tether diameter	56 mm

Table 2: AWES performance parameter overview

Parameter	Value
Powered angle of attack	13.5°
Lift coefficient	1.423
Kite drag coefficient	0.113
Bridle drag coefficient	0.012
Tether drag coefficient	0.027
Tether operational length	400-1000 m
Elevation angle	30°
Cut-in wind speed	4.4 m s ⁻¹
Rated wind speed	12.5 m s ⁻¹
Power (reel-out)	3.6 MW
Power (reel-in)	-20 kW
Cycle time	144 s
Rated power	2.3 MW
Capacity factor	59%
Yearly flight hours	6758 hours

**Figure 3:** Render of the kite

Floating System

The design of the floating Buoy with PTO unit aboard for power absorption involves the optimization of a Wave Energy Converter (WEC) by implementing frequency domain modelling using linear wave theory to estimate the time-averaged absorbed power of the WEC. The motion of the buoy, assumed to be limited to heaving (vertical) motion, is modelled using Newton's second law. The key forces

considered are the hydrostatic, wave excitation, wave radiation, and PTO forces.

The simulation pipeline begins with the BEMSolver, utilizing the CAPYTAINE Python library to determine the WEC's hydrodynamic coefficients numerically. These coefficients, such as the hydrodynamic damping coefficient, added mass, and wave excitation force, are critical inputs derived using a Boundary Element Method (BEM) solver for a specific WEC geometry. The latter are used as inputs in a custom code that computes the maximum power output of the WEC by tuning the PTO damping and stiffness coefficients.

A sensitivity analysis was performed to explore the impact of key design variables, including the aspect ratio (AR), submergence factor (SubF), and safety factor (SafF), on the absorbed power to narrow down the design space. Varying aspect ratio while maintaining the submergence factor and safety factor constant reveals that higher aspect ratios, although yielding lower average power across broad frequency bands, are optimal within the wave frequency bands of the chosen farm site. Simulations demonstrate that increased submergence generally enhances power absorption at higher frequencies. However, the optimal design balances these factors, choosing $AR = 4.0$, $SubF = 0.66$, and $SafF = 4.6$, optimized for the median wave frequency ($\omega = 0.8331 \text{ rad s}^{-1}$).

Power tuning involves adjusting the PTO damping and stiffness to find a global maximum for power output. The WECSolver software automates this process, ensuring compliance with design constraints, such as buoy stability and non-tipping conditions. The chosen parameters yield an average power of 151.8 kW and a capacity factor of 63.2%.

The submerged buoy (SB) is designed for stability and buoyancy, with dimensions of 5.285 meters in both diameter and length, and a volume of 116 cubic meters. The SB's mass is 58.1 tons, including a ballast of wet sand with a density of $1,682 \text{ kg/m}^3$ to ensure stability. The force applied by the PTO is 527.4 kN, and the shell thickness is 0.2 meters.

The Power Take-Off (PTO) subsystem, essential for converting mechanical energy into electrical energy, operates at a working pressure of 350 bar. The WEC is designed to generate 200 kW at rated conditions. Given an efficiency of 95% for both the pump and the motor, the actual power absorbed by the pumps must be 221.6 kW. The AWES PTO subsystem includes three hydraulic cylinders, a hydraulic motor with a mass of 700 kg, and a generator with a mass of 7,000 kg.

The integrated PTO system has a total mass of approximately 36 tons considering a conservative scaling factor of 1.2 times the mass of the AWES PTO. This integration allows the WEC to provide additional power in case of a failure in the AWES system.

The selected HTC1301-0220 telescopic marine crane from MacGregor can lift up to 2 tons to a height of 20 meters, making it more than capable of handling the 500-kilogram kite system. This crane is typically used aboard vessels therefore it will be suitable for a maritime buoy. Retrofitting it to extend and retract vertically instead of extending both laterally and vertically, will minimize the moment caused by the kite's weight, although allowing the crane to deal with the drag-induced moment during take-off of the kite. The crane operates on electrical power, eliminating the need for combustion sources, allowing it to be powered by the onboard wind and wave power, and thus increasing WaveWings' overall sustainability.

Overall, the design of the floating buoy integrates a Wave Energy Converter (WEC) functioning on hydraulic PTO units, counter-balanced by a submerged buoy, to which the AWES PTO drum will be attached, and the use of a crane to launch and retrieve the kite.

Control System

The control system is crucial in combining the operations of the AWES and the WEC systems. The goal of the control system is to maximize the electricity generation, all while respecting operational constraints, such as structural limitations and stability requirements.

The operations of the WaveWings system consists of multiple different phases, which impose different constraints on the control system. The AWES system operations consist of launch, reel-out and

reel-in as well as retrieval phases. During the launch, reel-in and retrieval phases, precise manoeuvring is required. During reel-out, which constitutes about 70 % of the total operations time, these constraints are relaxed, and optimization can be applied. The WEC system operations consist of the energy harvesting phase as well as a storm-safe mode which is only triggered during extreme weather conditions to avert damage to the buoy.

A control architecture, illustrated in Figure 4, has been developed to serve as the basis of a future, more detailed design. It presents an overview of the different components of the control system and their relative hierarchy. Each layer is connected with its neighbours, thus data and control decisions can flow both ways. The system & environment block represents the physical world, thus encompassing all kinds of environmental effects, like the wind and wave conditions, but also the dynamics of the physical WaveWings system. Important components of the control system are the sensors and actuators, which are responsible for interacting directly with the environment, gathering data and executing control decisions. The joint controller is responsible of providing instructions to ensure an optimal interplay of all the subsystems. The farm is connected to the outside world through the operator. The focus of this project is to explore the possibility of synergy between the AWES and WEC system. Thus, possible strategies implemented by the joint controller are investigated.

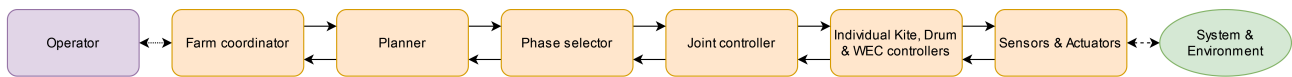


Figure 4: Control Architecture of the WaveWings system.

A baseline strategy consisting of decoupling the dynamics of the AWES and the WEC is developed to be employed for the critical phases of AWES launch, reel-in and retrieval. Using a constant tether force strategy for the drum controller, the tether force is stabilized, thus reducing the impact of the floating and airborne systems on each other to a static force. In order to create synergy between the AWES and WEC, a WEC amplification strategy is explored for the AWES reel-out phase. Implementing a constant velocity drum controller, oscillations in the tether force are produced by the kite flying a figure eight trajectory and by the movement of the floater. By matching the period of the tether force oscillations to an odd multiple of the wave period, the movement of the floater can be amplified, thus promising increased WEC power output. Using this strategy, it might be possible to produce more power by combining the AWES and the WEC than if they are kept separate.

Farm Design

As the WaveWings unit is integrated into a 400-unit farm, it is important to design the farm layout. Characteristics of the layout is mostly governed by the electrical infrastructure. The three main criteria leading the decision-making of the farm layout are reliability, cost, and sustainability. Reliability is assessed by the amount of affected units and lost power of the farm due to subsea cable failure. Cost is closely related to the length of the cable and its specified voltage. Sustainability is affected by the total enclosed area of the farm, as well as cable-laying adjustments made to not disturb seafloor architecture. These criteria are used to assess the main configurations used for offshore renewable energy farms: string layout, star layout, and the string-and-star configuration layout. The combination layout not only is more applicable for a 400-unit farm, but it also combines the advantages of the string and star layouts, and is thus the chosen layout type.

The source type is mainly determined by the distance to shore, which is closely related to the reactive power consumption of the subsea cables. Considering this with the 70 km distance to shore of the WaveWings farm, High Voltage Alternating Current (HVAC) transmission to shore is chosen. To keep consistency in the farm, all subsea cables, including interarray cables within a star and radial feeder cables linking stars, are 3-phase AC made of cross-linked polyethylene (XLPE).

The layout is tested in Python by arranging different number of units to a star, and printing cable lengths, and enclosed area of the farm. It is found that the best string-and-star combination layout is 50 stars each with 8 units, using 22 kV inter-array cables within the star. At the center of each

star is a floating platform that houses a MV to HV transformer. This offshore transformer steps up the voltage from 22 kV to 66 kV. Then, there are 25 radial feeder cables at 66 kV each connecting two star groups. The 25 radial feeders will be split into 5 main radial feeders of 66 kV that join to 5 offshore collection stations of the farm. The farm has a multi-link power transmission to shore using 5 links. There are five onshore stations each with a back to back converter (B2B) step the voltage to the onshore grid-compliant power by being placed in series to each multi-link. Aside from these B2B transformers onshore, each WaveWings unit houses its own transformer. The diagram of the farm layout, offshore substations, and power transmission to shore are depicted in Subsection 10.6.2.

Financial Analysis

The financial analysis provides a comprehensive overview of the project's economic feasibility, utilizing a detailed custom economic model developed for the project. The model divides capital and operational expenditures (CAPEX and OPEX) into three main modules: AWES, WEC and infrastructure. It relies on various sources for analytical and empirical relations, and takes over 50 inputs ranging from general project parameters such as the lifetime to component-specific parameters like kite surface area. The final output includes key performance indicators (KPIs) and cost breakdowns, allowing for a thorough understanding of the project's economic aspects.

The AWES module estimates costs primarily related to the kite, tether, and ground station. Main cost drivers in this module include the tether's CAPEX and OPEX, which are influenced by the specific weight and replacement rate of the tether. The generator and hydraulic components also contribute significantly to the costs due to their high power requirements and frequent replacement needs. However, even taking into account the fact that only 700 m of each tether are replaced at a time, this cost still leads the others from this module.

The WEC module uses a different approach to estimate costs, focusing on the mass and material costs of the hull and mechanical components. As such, it provides a slightly different cost breakdown, which is driven by material usage throughout the WEC.

The infrastructure module adapts a model used for floating offshore wind turbine farm analysis, modified for the chosen farm location off the west coast of Ireland. This module breaks down CAPEX components into development, installation, electrical, mooring, and end-of-life decommissioning costs. Installation, electrical infrastructure, and mooring costs are identified as the most significant contributors.

The results of the economic model show that AWES costs represent the largest portion of total expenses, mainly due to tether maintenance. Infrastructure expenses follow this, with a significant contributions from electrical infrastructure and OPEX costs. The total project cost for the 400-unit farm over 20 years is dominated by these components, with a combined expenditure of approximately €3.1 billion.

In addition to this, key performance indicators (KPIs) including weighted average cost of capital (WACC), annual energy production (AEP), LCOE, levelized revenue of electricity (LROE), net present value (NPV), and internal revenue rate (IRR) are calculated by the economic model. This provides a general view of the project's finances. The most important of these metrics is the LCOE, which is found to be €49.4/MWh. This value fits within the project requirement of a 50-80% reduction in LCOE compared to other renewables. Furthermore, the rest of the KPIs indicate that while the project has large initial costs, its long-term profitability and efficiency rely on reducing operational expenditures and extending component lifetimes as much as possible. An overview of this cost breakdown is shown in Figure 5.

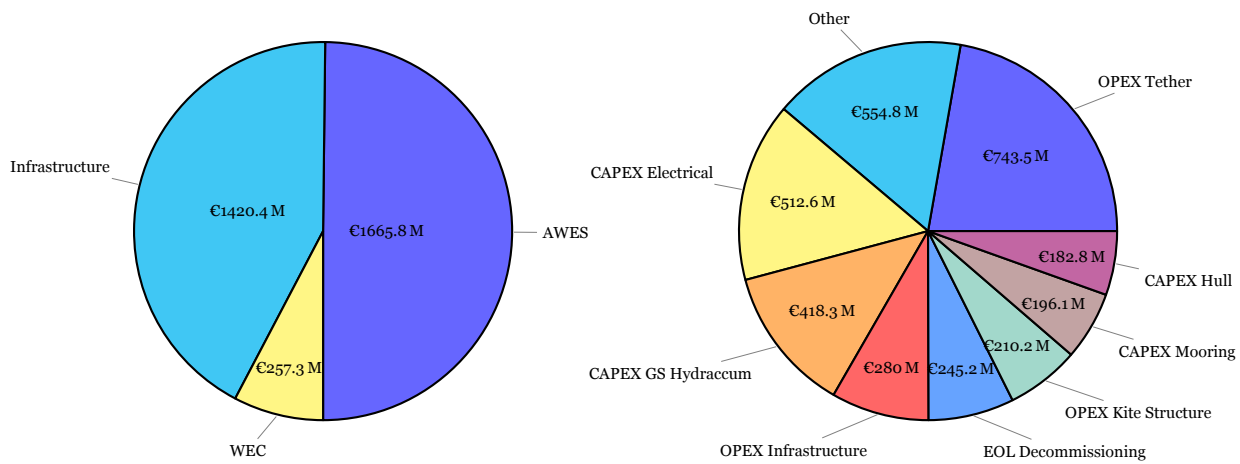


Figure 5: Cost contribution breakdown, along with the cost of each component in millions of euros

A additional part of the financial analysis involved mapping the LCOE in the region around the selected farm location. The LCOE mapping revealed that it is still possible to further reduce the LCOE of the WaveWings farm by either moving closer to the coastline, or to a nearby low-LCOE region.

Risk Analysis

By carrying out a risk analysis, issues that may arise during the operation of the unit can be accounted for, assuring a certain level of expected reliability, functionality, and safety. Research into these risks are drawn from experience in the petroleum industry, offshore platforms, wind turbine technologies, and airborne wind energy systems (AWES). A comprehensive Strength-Weaknesses-Opportunities-Threats (SWOT) analysis guides the enhancement of strengths and mitigation of weaknesses early in development. Key subsystems such as the Kite, Kite Control Unit (KCU), Buoy, Mooring, Communications, and Power are analyzed through Failure Mode and Effects Analysis (FMEA) to identify potential risks, consequences, and mitigation strategies. Subsequently, risk maps can be used to visualize and quickly identify critical risks to address. Due to the placement of the product in deep offshore, mitigation strategies are crucial to ensuring the autonomy of the system whilst considering the effect of a grid layout due to interferences between neighbouring units.

Risks marked as TR-KCU-1, TR-KCU-2, TR-PWR-1, TR-PWR-2, and TR-GRD-1 are associated to high-risk levels; these require appropriate mitigation strategies to avoid catastrophic interruptions to the product's functionality. TR-KCU-1 addresses poor Kite Control Unit (KCU) characteristics and synchronization with launch tower elements, which could result in the AWES landing in water, making autonomous recovery impossible and likely leading to the loss of the kite. The mitigation strategy involves incorporating onboard inflatable elements with CO₂ cartridges for rapid inflation and synchronizing tether reel-in to prevent drifting. TR-KCU-2 pertains to wind turbine failure, causing a complete loss of power to the KCU and subsequent loss of control over the system. The mitigation strategy focuses on implementing a robust testing program to determine the turbine's durability and resilience under various operational conditions. TR-PWR-1 involves wave conditions deviating from nominal design parameters, leading to the over-extension of the Power Take-Off (PTO) system and significant damage to the integrated unit. To address this, a storm-mode design is proposed, allowing the system to submerge during extreme weather conditions or securely shut down the PTO system to constrain moving parts. TR-PWR-2 highlights the risk of hydraulic PTO leakage due to overpressure, which could cause environmental damage and reduced power output. This risk is mitigated by close health monitoring of the system and the use of biodegradable hydraulic fluids to minimize environmental impact. TR-GRD-1 concerns the deep offshore placement of systems, which limits accessibility for maintenance crews and demands sustained reliability and autonomy to minimize downtime and associated costs. Mitigation involves utilizing support vessels to limit displacement times, especially during testing phases, ensuring that maintenance can be conducted efficiently.

Sustainability Evaluation

The sustainability evaluation of the WaveWings project demonstrates significant potential in reducing environmental impact compared to conventional energy sources. The WaveWings system achieves a Global Warming Potential (GWP) of 17.97 kgCO₂/MWh, with a 30-60% reduction compared to the 25.6-45.2 kgCO₂/MWh range for conventional floating offshore wind turbines. WaveWings is projected to have a total CO₂ equivalent saving of 54.69 million tonnes over its 20-year lifetime. It was also found that 35% and 31% of the GWP of the devices comes from the Operations and Maintenance stages and the buoy and components manufacturing. While the other 33% comes from other parts like the power take of systems, electrical systems and mooring, or transport and installation and end-of-life stages. Additionally, each unit uses 84.3% less material than a comparable floating HAWT, fulfilling the requirement to minimize material usage. The Energy Payback Time (EPBT) is calculated at 0.15 years, indicating a swift return on environmental investment. However, the project does not meet the stringent requirement of achieving a 70-95% reduction in GWP. Furthermore, ecological considerations were addressed by situating the farm outside regions of ecological importance to protect marine life and habitats, thus satisfying the requirement to avoid ecologically sensitive areas. Further studies will be performed in future stages of the project in order to further assess the noise impact of the farm and the proper ecological impact on the exact farm location.

Verification & Validation

Verification and Validation procedures seek to acknowledge the suitability, accuracy, and assumptions taken when generating models; these can be pre-existing from literature or can be made in-house by the WaveWings team.

A WEC simulation includes a BEMSolver [3] adopted in-house from “CAPYTAINE” that works hand-in-hand with a WEC-Sim [4] module that extracts hydrodynamic coefficients and a WECSolver [5] made in-house that can compute the power output of the WEC platform. Verification of the software was carried out manually by replicating theoretical equations and cross-checking with the results of the simulations. Validation remains limited due to the necessity for additional numerical and experimental prior to the manufacturing of a full-scale prototype.

In parallel, a floating AWES simulation is used to design the control strategies, as developed by A. Cherubini et al. [6, p.137-163], validated against a software with an identical purpose as developed by S. Trombini et. al [7]. Verification of these softwares are assumed to be sufficient provided that they originate from peer-reviewed and published papers. Similarly, due to the alignment in results, the software was considered to be sufficiently validated.

Last but not least, the economic model used to project a significant range of economic parameters depending on AWES, WEC, and infrastructure sizing was implemented. Although not all modules of the code could be verified due to limited available data, the validity of the infrastructure segment could be validated against a case study specific to the Irish coast [8].

Implementation Plan

The implementation plan aims to present the procedure after the design process is finished. This can be split into a number of phases. These are the small scale testing, the securing of the supply chain, the manufacturing, the electrical grid installation, the mooring installation, the deployment and testing, the operation and maintenance and the deconstruction. Many of the phases before the operation of the wind farm can be parallel, so the time of the installation and testing of the entire farm has been estimated at 8.5 years. Afterwards it should be prepared for 25 years of operation before deconstruction.

Following these phases it is important to investigate in a RAMS analysis. This will delve deeper in the reliability, the availability, the maintainability and the safety of the WaveWings farm. The reliability of the WaveWings project will be preserved by quantifying systems in flight hours or in mean time to failure. These values will be monitored and for most components a Risk Priority Number (RPN) has

been calculated to give priority to the more vulnerable components. For availability it is made sure that the performance of the WEC is closely monitored to make sure the reactive power is constant. Maintainability is important to analyse, because an AWES needs more maintenance than normal wind turbines. It is therefore decided that individual buoys need more than 10 visits a year, after going over an in-depth maintenance plan for every subsystem. Finally is the safety. During operation there are no people on board, which does not lead to a lot of safety issues, however it is necessary to wear protective clothing.

Next is the production plan. The aim is to split the manufacturing of a single WaveWings unit into different steps. This is presented in the flow chart in Figure 6.

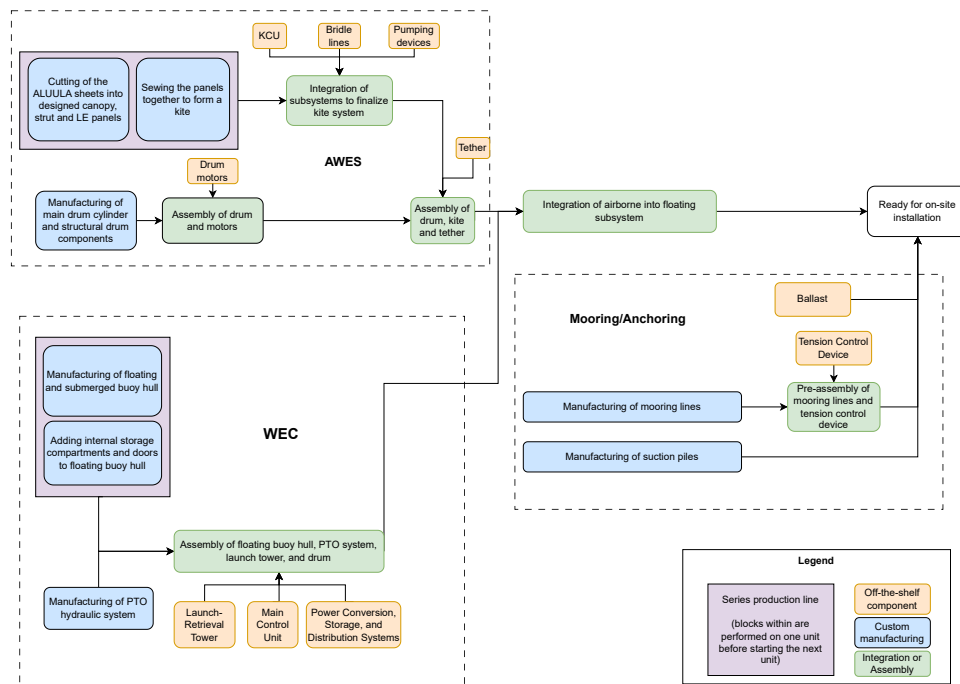


Figure 6: Production plan flow chart. The last unit is produced 4 years after the first unit.

This gives an insight in how the different materials and off-the-shelf components form the final WaveWings buoy and what the steps are within the manufacturing process.

Afterwards is the logistics description. This shows all possible companies that could be consulted in the logistic operation of the project. For these companies the main criteria is their expertise and also their location. Most companies are either based in the Netherlands or in Ireland close to the farm site. Most of the off-the-shelf components have been coupled to a company. The main consulting company for the WaveWings project is SmartBay, which has testing facilities close to the farmsite.

Finally is the future developments. This delves deeper into the steps taken after the operation of the WaveWings project. If the project is a success, there should be looked at expansion and scaling of the manufacturing capacity. It is also necessary to keep up to date with the technological advancements. The control system for example can still be optimized over time. Next to that it is also important to reevaluate environmental impact by examining for example material advancements. Finally the market and policy development have to be investigated. The need of energy and therefore the utility of the farm changes over time. This means that the market analysis needs to be reevaluated over time.

Contents

Executive Overview	ii		
Nomenclature	xv		
1 Introduction	1		
2 Requirements	2		
3 Sustainable Development Strategy	4		
3.1 Requirements	4		
3.2 Pillars and Indicators to Sustainable Development	4		
3.2.1 Monitoring of Sustainability Indicators	5		
4 Concept Configuration	6		
4.1 Concept Description	6		
4.1.1 Kite Concept Description	6		
4.1.2 Launch Concept Description	6		
4.1.3 WEC Concepts	7		
4.1.4 Anchoring Concepts	8		
4.1.5 AWES Power Take-Off	9		
4.1.6 WEC Power Take-Off	9		
4.2 Trade-Off Summary	9		
4.3 Configuration Layout	12		
4.4 Systems Tree and Description	15		
4.5 Functional Analysis	15		
4.6 Hardware and Software Diagram	19		
5 Farm Location	20		
5.1 Requirements	20		
5.2 Farm Location Selection	20		
5.3 Operating Conditions	23		
5.3.1 Nominal and Extreme Wave Conditions	23		
5.3.2 Nominal and Extreme Wind Conditions	23		
6 Market Analysis	25		
6.1 Market Identification	25		
6.1.1 Stakeholder Analysis	26		
6.1.2 Market Trends	27		
6.1.3 Utilities	28		
6.2 Permits, Regulations, and Incentives	28		
6.2.1 Permits	28		
6.2.2 Regulations	28		
6.2.3 Incentives	29		
6.3 LCOE Target	29		
6.4 Market Positioning	30		
6.5 SWOT Analysis	31		
7 Airborne System	32		
7.1 Requirements	32		
7.2 Airfoil Design	32		
7.2.1 Airfoil Camber	32		
7.2.2 Leading-Edge Thickness	33		
7.3 Kite Design	34		
7.3.1 Aspect Ratio	34		
7.3.2 Curvature	35		
7.3.3 Strut Design	36		
7.3.4 Material Selection	37		
7.3.5 Kite aerodynamic overview	37		
7.4 Bridle System	38		
7.5 Performance Evaluation	39		
7.5.1 Theory	39		
7.5.2 Operations	40		
7.5.3 Cut-in wind speed	42		
7.5.4 Capacity Factor, Average Power, and Yearly Flight Hours	42		
7.5.5 Kite Projected Surface Area	43		
7.5.6 Kite Mass	43		
7.5.7 Sensitivity Analysis for Power Curve	43		
7.6 Tether	44		
7.6.1 Length, Diameter, Material, and Mass	44		
7.6.2 Lifetime due to Dynamic Bending	44		
7.6.3 Lifetime due to Creep	44		
7.7 Kite Control Unit	45		
7.8 Airborne System Overview	45		
8 Floating System	47		
8.1 Requirements	47		
8.2 Floating Buoy with PTO Unit	48		
8.2.1 Frequency Domain Modelling	48		
8.2.2 Simulation Pipeline	49		
8.2.3 Sensitivity Analysis	51		
8.2.4 Tuning for Maximum Power	53		
8.2.5 Results and Recommendations	54		
8.2.6 Stability of a Floating Body	56		
8.3 Submerged Buoy (SB)	56		
8.4 Mooring Subsystem	57		
8.5 Anchoring Subsystem	57		
8.6 Main Control Subsystem	58		
8.7 Drum Subsystem	58		
8.8 Launch-Retrieval Tower	59		
8.9 Power Subsystem Characteristics	60		
8.9.1 Electrical Block Diagram	60		
8.9.2 Power Take-Off Subsystem	61		
8.10 Material Selection	65		
8.11 Communications and Data-Handling	66		
8.11.1 On the Subsystem-Level	66		
8.11.2 On the Farm-Level	66		
9 Control System	69		
9.1 Control System Requirements	69		

9.2 Operations Overview	69	11.4 Sensitivity Analysis and LCOE Mapping	88
9.2.1 AWES Launch	69	12 Risk Analysis	91
9.2.2 AWES Reel-Out	70	12.1 Requirements	91
9.2.3 AWES Reel-In	70	12.2 SWOT Analysis	92
9.2.4 AWES Retrieval	70	12.3 Technical Risk Assessment	92
9.2.5 WEC Energy Harvesting	70	12.4 Risk Maps	95
9.2.6 WEC Storm-Safe Mode	70	13 Sustainability Evaluation	97
9.3 Control Architecture	70	13.1 Requirements	97
9.4 Subsystem Control	71	13.2 Life Cycle Assessment	97
9.4.1 Kite	71	13.2.1 Goal and Scope Definition	98
9.4.2 Drum	71	13.2.2 Inventory Analysis	99
9.4.3 WEC	72	13.2.3 Impact Assessment	101
9.5 Control Strategy	72	13.2.4 Comparison to Floating HAWT	102
9.5.1 Simulation Approach	72	13.3 Additional Evaluation Criteria	102
9.5.2 Baseline Strategy	72	14 Verification & Validation	104
9.5.3 WEC Amplification Strategy	73	14.1 Compliance Matrix	104
9.5.4 Further Considerations	75	14.2 Model Validation & Code Verification	109
10 Farm Design	76	14.2.1 WEC Simulation	109
10.1 Requirements	76	14.2.2 Floating AWES Simulation	109
10.2 Strategy	76	14.2.3 Economic Model	109
10.3 Types of Configurations	77	15 Implementation Plan	110
10.3.1 String Layout	77	15.1 Implementation Summary	110
10.3.2 Star Layout	77	15.2 Reliability, Availability, Maintainability, and Safety (RAMS)	114
10.3.3 String-and-Star Combination	77	15.2.1 Reliability	114
10.4 Source Type and Transmission to Shore	78	15.2.2 Availability	114
10.5 Power Electronics	78	15.2.3 Maintainability	115
10.6 Layout Determination	78	15.2.4 Safety	116
10.6.1 Testing of Configurations	79	15.3 Production Plan	116
10.6.2 Final Layout	79	15.4 Logistics Description	117
11 Financial Analysis	81	15.5 Future Development	118
11.1 Requirements	81	16 Budgets	119
11.2 Economic Model Description	81	16.1 Power Budget	119
11.2.1 AWES Module	82	16.2 Mass Budget	120
11.2.2 WEC Module	83	17 Conclusion	121
11.2.3 Infrastructure Module	84		
11.2.4 Key Performance Indicators	85		
11.3 Economic Model Results	87		

Nomenclature

Abbreviations

AEP Annual Energy Production
 AWES Airborne Wind Energy System
 BEM Boundary Element Method
 BEMIO Boundary Element Method Input/Output Tool
 BEMSolver Boundary Element Method Solver
 CAD Computer-Aided Design
 CAGR Cumulative Annual Growth Rate
 CAPEX Capital Expenditure
 CAPYTAINE CAPYTAINE Software
 CDH Communications and Data-Handling
 CED Cumulative Energy Demand
 CFRP Carbon Fibre Reinforced Polymer
 CON Constraint
 CTF Cycles To Failure
 CUS Customer
 DEV Developers
 DTO Design Option Tree
 EMFs Electro-Magnetic Fields
 ENV Environment
 EPBT Energy Payback Time
 EU European Union
 FBD Free Body Diagram
 FH Flight Hours
 FIT Feed-In Tariffs
 FMEA Failure Mode and Effects Analysis
 FTA Failure Tree Analysis
 GOV Government
 GWP Global Warming Potential
 HAWT Horizontal Axis Wind Turbine
 HVAC High Voltage Alternating Current
 HVDC High Voltage Direct Current
 IMU Inertial Measurement Unit
 IQR Interquartile Range
 IRR Internal Rate of Return
 KCU Kite Control Unit
 KPIs Key Performance Indicators
 LCA Life Cycle Analysis
 LCOE Levelised Cost of Electricity
 LEI Leading-Edge Inflatable
 LROE Levelised Revenue of Electricity
 LRT Launch Retrieval Tower
 MCU Main Control Unit
 MG Metacentric Height
 MTTF Mean Time To Failure
 MV Medium Voltage
 NEMOH NEMOH Software
 NPV Net Present Value
 O&M Operations and Maintenance

OPEX Operational and Maintenance Expenditure
 ORE Offshore Renewable Energy
 OWC Oscillating Water Column
 PDO Power Density Output
 PGO Power Grid Operator
 PTO Power Take-Off
 RAMS Reliability, Availability, Maintainability, and Safety
 REFIT Renewable Energy FIT Tool
 REQ Requirement
 ROV Remotely Operated Vehicle
 rpm Rotations Per Minute
 RPN Risk Priority Number
 SB Submerged Buoy
 SWOT Strength-Weaknesses-Opportunities-Threats
 T&I Transport and Installation
 TFO Tether Force Oscillation
 TRL Technological Readiness Level
 UN United Nations
 USR User
 V & V Verification and Validation
 VHF Very High Frequency
 VSM Vortex Step Method
 WACC Weighted Average Cost of Capital
 WBS Work Breakdown Structure
 WEC Wave Energy Converter
 WEC-Sim Wave Energy Converter Simulation Software
 WECSolver Wave Energy Converter Solver
 WFD Work Flow Diagram
 XLPE Cross-Linked Polyethylene

Symbols

β Elevation Angle $^\circ$
 λ Wavelength m
 ω Wave frequency rad
 ω Wave frequency rad s^{-1}
 ρ Density k/m^3
 σ Stress Pa

Miscellaneous

\bar{P}_a Time averaged absorbed power W
 η Efficiency –
 \hat{F}_e Complex amplitude of wave excitation force N
 \hat{u} Complex amplitude of vertical velocity –
 A Area m^2
 a Buoy acceleration m s^{-2}
 A_{body} Amplitude of body motion m
 A_{wave} Wave amplitude m
 AR Aspect Ratio, Diameter over Height –
 b Kite span m
 C Cost €

c	Damping Coefficient	–	L_{in}	Cable Length	m
C_f	Capacity Factor	-	M	Inertial matrix	kg
C_D	Drag Coefficient	–	m	Mass	kg
C_L	Lift Coefficient	–	M_r	Added mass	kg
D	Drag	N	n	Number of	–
d	Diameter	m	P	Power	W
d_t	Tether Diameter	m	p	Pressure	Pa
E	Young's Modulus	Pa	P_d	Mean absorbed wave power	W
F	Force	N	P_w	Wave power flux per unit	kW m^{-1}
F_e	Wave excitation force	N	Q	Nominal Tension	N
F_{hs}	Hydrostatic force	N	R	Damping Coefficient	kg s^{-1}
f_{out}	Reel-out factor	-	r	Turning Radius	m
F_{PTO}	PTO Force	N	S	Projected Area	m^2
F_r	Wave Radiation Force	N	$SafF$	Safety Factor	-
g	Gravitational acceleration	m s^{-2}	$SubF$	Submergence Factor	-
h	Altitude	m	T	Tension	N
H_s	Wave Height	m	T_e	Wave Period	s
h_{buoy}	Buoy height	m	t_{inst}	Installation time	day
h_{water}	Water depth	m	V	Volume	m^3
K	Stiffness Coefficient	N m^{-1}	v	Speed	m s^{-1}
K_{hs}	Hydrostatic coefficients	-	X	Reactance	N s m^{-1}
L	Lift	N	Z	Impedance	N s m^{-1}
l	Length	m	z_0	Aerodynamic roughness length	m

1 | Introduction

By exploring Airborne Wind Energy and Wave Energy Converter solutions, the WaveWings project was founded with the aim of harnessing the benefits of an integrated energy generation platform whilst upscaling to a 1 GW renewable energy grid that would contribute to the European Union's net-zero 2050 goals. Critical thinking throughout the report led to the establishment of a cost-effective solution to increase renewable energy production whilst focusing on sustainability, market viability, and technological feasibility.

Mission Need Statement:

WaveWings aims to exploit the synergy between a coupled airborne wind energy and wave energy module in order to construct a 1 GW renewable energy grid in an effort to contribute to the European Union's net-zero 2050 goals.

Project Objective Statement:

To produce a detailed and scalable design of an energy generator consisting of an airborne wind energy system and a wave energy converter with ten students in ten weeks time.

In Chapter 2, stakeholder requirements are established to guide the development of the product. In Chapter 3, a sustainability strategy is elaborated upon to showcase procedural decisions made throughout to ensure the product would meet our requirements whilst accounting for hurdles from a project management perspective. In Chapter 4, all concepts originally introduced as a trade-off are summarized for consideration in the final design. In Chapter 6, a market analysis establishes and identifies market opportunities, considers required permits, regulations, and incentives, and presents performance indicators to measure the product's commercial feasibility. In Chapter 7, the Airborne Wind Energy System (AWES) concept is established by decomposing the study into airfoil, kite, and bridle line design. Subsequently, a performance evaluation is carried out through the use of a model to confidently support the chosen design. Afterwards, the tether and Kite Control Unit (KCU) characteristics are defined. In Chapter 8, the floating buoy with the hydraulic Power Take-Off (PTO) unit is sized using literature and a variety of models, the submerged buoy used as a counter-weight to the floating buoy for assured functionality of the PTO is sized, and a thorough consideration of power subsystems on both AWES and WEC are presented. Additionally, material selection and communication and data handling considerations are added to address aspects related to system integration. In Chapter 9, all operational modes of the system are defined before diving into the control architecture, the subsystems requiring control protocols, and control strategies for all the stated subsystems accompanied by results from simulations. In Chapter 10, the sizing strategy for the various farm configurations is established before proceeding to a description of the required electrical infrastructure. In Chapter 11, a financial analysis seeks to establish a robust economic model accompanied by key performance indicators to motivate the feasibility of the product based on the original requirements. Furthermore, contour maps for the Levelised Cost of Electricity (LCOE) for the chosen farm location on the west coast of Ireland are used to confirm the incentive behind the chosen site. In Chapter 12, a technical risk assessment is carried out by using a Strength-Weaknesses-Opportunities-Threats (SWOT) analysis, a Failure Mode and Effects Analysis (FMEA), and visualizations through the use of risk maps. In Chapter 13, a sustainability evaluation is carried out based on the points presented in Chapter 3. In Chapter 14, a compliance matrix highlights the ability or shortcomings in meeting requirements followed by verification and validation procedures for all the models/software used throughout the sizing methods. In Chapter 15, an implementation plan outlines future phases of the product's deployment from a manufacturing, operations, maintenance, and decommissioning perspective. Additionally, a Reliability, Availability, Maintainability, and Safety (RAMS) analysis is provided before proceeding to a production plan, logistics description, and room for future developments. Last but not least, in Chapter 17, conclusions are drawn from the study along with recommendations for next steps that would advance or refine the study.

2 | Requirements

When designing the WaveWings system, requirements are used as guidelines that outline the necessary functionalities, capabilities and characteristics of the final design. A list of stakeholder requirements is presented in Table 2.1. These requirements are the most important and high-level requirements. A full list of the requirements and their compliance can be found in Section 14.1.

Table 2.1: List of Stakeholder Requirements

Identifier	Requirement
USR-REQ-1	The farm shall produce 1 GW of rated electrical power.
USR-REQ-1-1	One unit shall produce 2.5 MW of rated electrical power.
USR-REQ-1-1-AWE	The AWES part of one unit shall produce 2.3 MW of rated electrical power.
USR-REQ-1-1-AWE-8	The AWES part shall produce maximum power at 12.5 m/s rated wind speed.
USR-REQ-1-1-WEC	The WEC part of one unit shall produce 0.2 MW of rated electrical power.
USR-REQ-1-1-1	The AWES and WEC shall perform better than the two systems individually.
USR-REQ-1-2	The farm shall consist of 400 units.
USR-REQ-2	The farm shall have a capacity factor between 50% and 60%.
USR-REQ-3	The farm shall be connected to an onshore electrical grid.
USR-CON-1	The farm shall provide a 50-80% LCOE reduction compared to other off-shore renewables.
USR-CON-1-1	The farm shall provide total cost savings of 40% compared to individual deployment of airborne wind and wave energy systems.
USR-CON-1-2	Each unit shall provide a 25-30% manufacturing cost reduction compared to separate corresponding units of airborne wind energy and wave energy generation.
USR-CON-2	The farm shall provide a 70-95% reduction in GWP compared to the current average electricity generation.
USR-CON-2-1	The farm shall save 1.34 million tons of CO ₂ per year compared to average emissions for electricity generation in 2023.
USR-CON-2-2	Each unit shall use 90% less material than a comparable floating HAWT.
USR-CON-3	The design shall include a high-level FMEA and FTA.
USR-CON-7	The AWES subsystem shall use the soft kite pumping concept.
USR-CON-8	The farm shall be placed in the EU.
USR-CON-9	The farm shall be placed where the sea is deeper than 60 meters.

Some requirements that were stated in the beginning of the design phase were later deleted due to several reasons. Table 2.2 shows these deleted requirements and the reason for deleting them.

Table 2.2: List of deleted requirements

Identifier	Requirement	Rationale
USR-REQ-1-1-AWE-5-1	The AWES shall have a minimum apparent wind speed that relates to CL/CD.	Minimum apparent was not used in the design.
USR-REQ-1-1-AWE-5-4-1	The AWES shall maximise the glideslope to minimize the reel in power.	This could not be done as limited research was available.
USR-REQ-1-1-AWE-6-2	The AWES shall have a launch velocity of at most TBD m/s.	A requirement for maximum cut-in speed was deemed irrelevant.
USR-REQ-1-1-AWE-7-2	The kite shall be retrievable from the water.	The chosen design does not use a water landing method for retrieval.
USR-CON-1-4	Developers shall be aware of the financial constraints imposed by large-scale assembly of units into a farm.	This was determined not relevant for the current stage.
USR-CON-2-2-AWE-1	The AWES shall have a maximum mass of TBD kg.	There was no maximum mass determined upfront for the AWES.
USR-CON-2-2-WEC-1	The WEC shall have a maximum mass of TBD kg.	There was no maximum mass determined upfront for the WEC.
USR-CON-4-1	The noise level during operation shall not exceed 90 dB [9].	This could not be done as limited research was available.
USR-CON-4-2	The noise level during installation shall not exceed TBD 100 db[9].	This could not be done as limited research was available.

Other requirements were changed, thus the original one was deleted and a new one was created with a new identifier. These are shown in Table 2.3.

Table 2.3: List of changed requirements

Identifier	Requirement
USR-REQ-1-1-AWE-4-6	The tether shall resist the tension force of TBD kN.
USR-REQ-1-1-AWE-4-12	The tether shall resist the tension force of the nominal tether force times the tether safety factor.
USR-REQ-1-1-AWE-5-4-2	The generator shall be capable of generating 3.6 MW of power.
USR-REQ-1-1-AWE-5-4-3	The AWES PTO shall be capable of handling 3.6 MW of power.

3 | Sustainable Development Strategy

Sustainable development is an important aspect of the WaveWings project and is considered throughout the design of the product. Firstly, the sustainability requirements are listed in Section 3.1. To achieve those requirements, an organizational approach to sustainability is defined in Section 3.2 by a choice of pillars to sustainable development and indicators which can quantify if the requirements are met. The implemented organizational strategies guide the design process at every stage. Throughout the design, the Sustainability Manager actively ensures that the sustainable development strategy is considered. Once the design is finalized, the Sustainability Manager evaluates if the chosen indicators meet the requirements in Chapter 13.

3.1 | Requirements

Table 3.1: Requirements for sustainability of the farm and individual units

Identifier	Requirement
USR-CON-2	The farm shall provide a 70-95% reduction GWP compared to the current average electricity generation.
USR-CON-2-1	The farm shall save 1.34 million tons of CO ₂ per year compared to average emissions for electricity generation in 2023.
USR-CON-2-2	Each unit shall use 90% less material than a comparable floating HAWT.
USR-CON-4	The farm shall adhere to Irish environmental laws.
USR-CON-4-6	The system shall use non-toxic materials.

3.2 | Pillars and Indicators to Sustainable Development

The first step in achieving the sustainability requirements listed in Section 3.1 is to establish organizational strategies that will ensure design choices are regularly made with sustainability in mind. Three pillars to sustainability are used as the foundation for the WaveWings project: financial, social, and environmental sustainability. For each of the pillars, potential design considerations are listed below along with indicators that can be used to quantify sustainability. The Sustainability Manager is responsible for enforcing the consideration of these points throughout the design as outlined in Subsection 3.2.1

Environmental sustainability can be achieved in the design areas listed below and can be quantified by parameters such as the *Global Warming Potential (GWP)* and the *Cumulative Energy Demand (CED)* which are used in the life cycle analysis (LCA) in Section 13.2. Other indicators are *tons of CO₂* emitted and the levelized cost of energy *LCOE*.

1. Choice of materials explained in Chapter 13.
2. Choice of farm location that minimizes environmental harm. This is done in Chapter 6.
3. Management of resources used during the design phase (i.e. printing of documents vs. using digital copies, facilities used for simulation and validation).
4. Selection of manufacturers that are as close to the deployment site as possible. This is detailed in Chapter 6 and Chapter 11

Social sustainability can be achieved by considering the design areas below and can be quantified by the cost of energy for consumers:

1. Providing a reliable and low-cost source of energy to consumers.
2. Utilizing local resources to benefit the social (and economical) development of local businesses. Detailed in Chapter 11.

Financial sustainability can lead to the lowering of the cost of energy and thus a higher return on investment. This can be achieved by:

1. Optimizing the synergy between the AWES and WEC components to reduce material costs and increase power output per unit Chapter 9
2. Choice of farm location: a market analysis must be performed to determine a site where incentives lead to the highest possible return on investment in Chapter 6.
3. Criteria used during design trade-offs must encourage lower-cost designs, aligning with the UN's goal for affordable clean energy. This is shown in Chapter 4.

3.2.1 Monitoring of Sustainability Indicators

The aforementioned environmental, social, and financial indicators of sustainability are evaluated in the midterm and final reviews of the WaveWings design. A detailed reporting of the LCA and how indicators such as GWP, CED, and LCOE are calculated is done in Chapter 13. Finally, an evaluation of compliance to the requirements listed in Table 3.1 is performed in Chapter 14.

4 | Concept Configuration

In this chapter, the concept configuration will be discussed. First, several concepts are explained in Section 4.1. These concepts will then go through a trade-off in Section 4.2 to determine the final concept that will be designed. The layout of the design will then be explained in Section 4.3. A systems tree where all the subsystems in the design are discussed is shown in Section 4.4. The functional flow and functional block diagrams showing how the system works are then presented in Section 4.5. Afterwards, the hardware diagram is explained and presented in Section 4.6.

4.1 | Concept Description

Several concepts were considered for the final design. The concepts discussed in this section were traded off to each other in Section 4.2.

4.1.1 Kite Concept Description

In this section, the three kite concepts selected in the midterm report are further explained. The structural and aerodynamic characteristics of the three kite concepts will be discussed.

Leading-Edge Inflatable kite

A leading-edge inflatable (LEI) kite is a kite which has inflatable tubes running along the leading edge and a few inflatable struts in the chordwise direction. The purpose of these inflatable tubes is to add some stiffness to the kite so that it can better maintain its aerodynamic shape when the kite is loaded. Secondly, the inflatable tubes form a stiff structural frame through which the aerodynamic forces can be transmitted to the bridle line system. This decreases the number of bridle lines needed when compared to similar ram-air kites.



Figure 4.1: TU Delft V3 LEI Kite [10]

Ram-Air Kite

Ram-air kites, sometimes called foil kites, consist of a double canopy without any stiff structural elements. They can be a bit lighter due to this, but they need an extensive system of bridle lines to keep their shape during operations. Because of their double skin design, the airfoil is better defined than the LEI airfoil. So the airfoil is capable of better aerodynamic performance than the LEI airfoil. To maintain the airfoil shape, openings at the leading edge of the kite need to be made. These openings allow the kite to inflate by using the air pressure at the stagnation point.

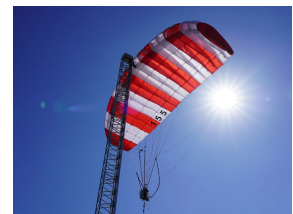


Figure 4.2: SkySails Ram-Air kite [11]

Semi-Rigid Kite

The semi-rigid kite concept which will be considered is based on the Kitegen semi-rigid wing. The kite consists out of several rigid wings which determine the aerodynamic shape of the kite and a double skin. The main benefit of having rigid ribs is that they improve the aerodynamic efficiency of the kite towards a lift-over-drag ratio of 28 while having a lift coefficient of 1.0. Doing the reverse math, it is found that the drag coefficient Kitegen claims to have is 0.036. We determined that these numbers are very optimistic as they are way higher than the aerodynamics for the other concepts.



Figure 4.3: Kitegen semi-rigid kite [11]

4.1.2 Launch Concept Description

Choosing a launch concept is an important part of the design. After some research and a brainstorming session with the team, 4 concepts were chosen for the trade-off. These concepts are explained below.

Launch Tower (Upright)

This concept uses a retractable launch mast placed on the buoy that launches and retrieves the kite. To launch the kite, a telescopic mast lifts the folded kite out of the storage compartment located at the bottom of the mast. When the wind is sufficient, the kite is released and starts to gain altitude. A thin tether is used to connect the top of the mast to the leading edge of the kite at all times. To retrieve the kite, it gets winched back and the mast is extended again. When the kite gets close to the mast a secondary winch pulls the tether connected to the leading edge. The kite and its control unit are stored in the storage compartment. The SkySails Power PN-14 system uses this concept as well and has proven that it works [12].

Launch Tower (Upside-down Hanging)

This tower concept relies on the kite performing a cross-wind manoeuvre to take off. It consists of a tower with multiple support arms connected to the top of the floating platform. The support arms can be folded after the kite is rolled by the lower horizontal arm and its pinching mechanism. After being folded, the structure can be stored within the floating platform. The tower allows the kite to be retrieved without first touching the water. This way of launching has been demonstrated by a TU Delft concept [13].

Robot-Assisted Water Launch

The robot-assisted launch concept relies on inducing wind speed to the kite to allow take-off during conditions of wind speed that are lower than the cut-in wind speed of the kite. The kite must be secured at a distance away from the winch system and then as the tether is reeled in, the kite is unsecured and the kite begins its ascent. The robot is unattached to the buoys and has its own charging station, allowing it to be shared across different units.

Water Launch

This concept is the same as the Marine Robot-Assisted Launch minus the marine robot. That is, the kite is positioned to its launch position by the wind and/or waves themselves without the help of a robot. The system relies on the kite control unit decreasing the angle of attack of the kite during positioning pre-launch such that the kite does not lift-off from the water pre-maturely.

4.1.3 WEC Concepts

From the design option tree in the midterm report, it can be determined that point absorbers, line attenuators and raft-type attenuators are the surviving concepts that will be considered in the trade-off process performed in Section 4.2. Following is a description of the design options.

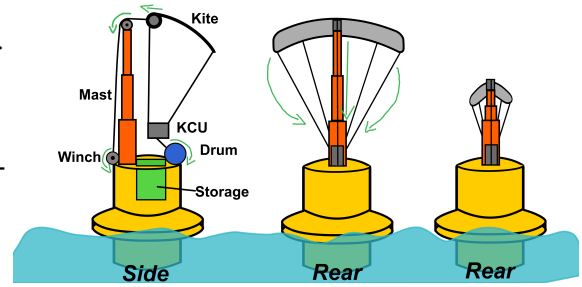


Figure 4.4: Sketch of a launch tower concept with a kite in upright position attached to the top of the mast

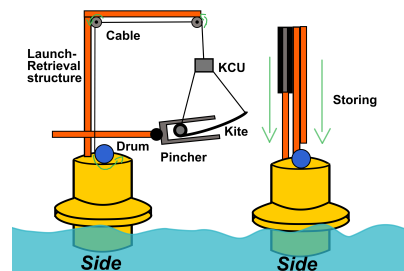


Figure 4.5: Launch tower with the kite hanging upside-down from the mast

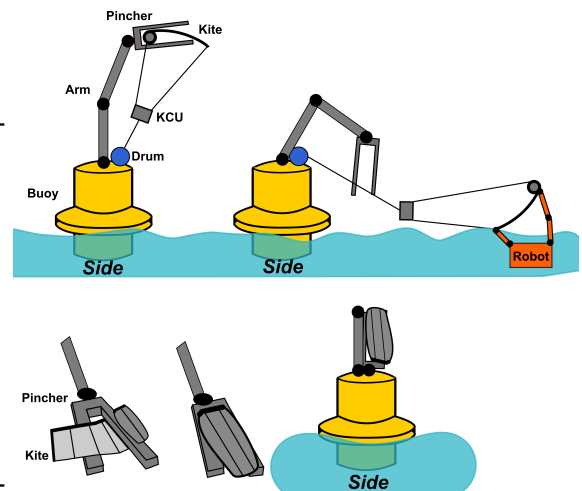


Figure 4.6: Marine Robot-Assisted Launch concept sketch

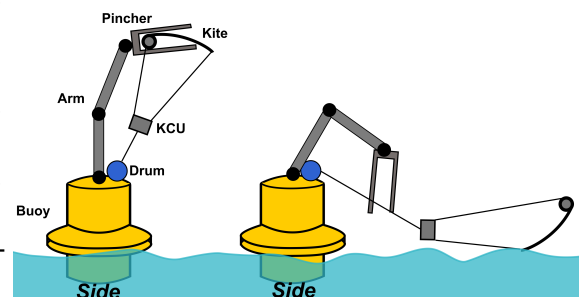


Figure 4.7: Water launch system sketch

Point Absorber

Point absorbers are a type of WEC that creates energy due to the relative motion between a heaving buoy and a fixed point at the bottom of the sea. The buoy moves up and down with the waves, while the fixed point, often an anchor or a submerged structure, remains stationary. This relative motion is used to drive a mechanical system that converts kinetic energy into electrical energy. It has one degree of freedom: the vertical heave of the buoy. The CorPower point absorber is the prototype used for reference as seen in Figure 4.8.



Figure 4.8: CorPower point absorber [15]

Line Attenuator

Line attenuators are elongated WECs, snake-like in nature. Due to the design, the device maximizes power absorption when aligned perpendicular to the wavefront. Line attenuators consist of multiple segments, which are connected by flexible joints. The movement between the different segments leads to power generation. It has multiple degrees of freedom, constituting from the multiple flexible joints. The Pelamis is the prototype used for reference as seen in Figure 4.9.



Figure 4.9: Pelamis line attenuator [16]

Raft Attenuator

Raft-type attenuators are similar to line attenuators. They also maximize power absorption when aligned perpendicular to the wavefront. However, this attenuator consists of two rafts connected by a hinge. It thus has one degree of freedom, which is the rotation of the hinge. The Mocean Blue X is the prototype used for reference as seen in Figure 4.10.



Figure 4.10: Mocean Blue X [17]

4.1.4 Anchoring Concepts

In order to maintain the system within a certain area a mooring system needs to be attached to the floor. In the following section, 3 mooring systems will be considered and later traded off in Section 4.2. Keep in mind that even though there are more mooring systems, only the three discussed below are of importance due to the sea floor or sustainability constraints.

Gravity Anchor

The principle of this type is simply dropping the anchor to the seafloor. It is typically made of precast concrete, as this is viable to home new biodiversity. The main contributor to holding capacity is the weight of the anchor itself. It can be placed in mud, sand, and rocky seafloor. The concept is shown in Figure 4.11.

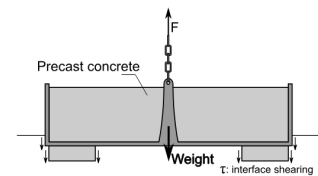


Figure 4.11: Gravity anchor [18]

Driven Pile

The pile is lowered to the seafloor. Then, driving equipment is properly aligned to the pile before driving it through the seabed. This is typically done offshore using large steam, hydraulic, or vibrational hammers. As the site location has a seafloor composed of clay, a vibrational hammer is the best option. Embedding greatly increases holding capacity. This type is restricted to clay and sand, as rocky terrain is impossible to drive into. The concept is shown in Figure 4.12.

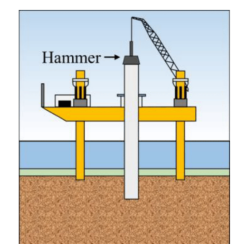


Figure 4.12: Driven pile [19]

Suction Pile

A steel cylindrical shell is lowered to the seafloor. Then, water is allowed to pump in and out of the shell, and an open bottom allows soil to enter the internal volume of the caisson, embedding the pile and increasing holding capacity [14]. This pile type is restricted to clay and sand but performs much better in clay. The concept is shown in Figure 4.13.

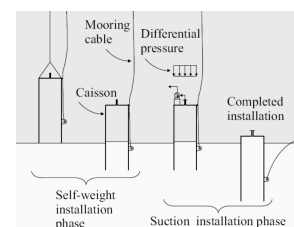


Figure 4.13: Suction pile [20]

4.1.5 AWES Power Take-Off

To convert the force in the tether of the kite to electrical energy a power take-off system is needed. This will be done by a generator and hydraulic pumps which are driven by the rotations of the drum. This system also needs to be able to reel in the kite, to do this the hydraulic pumps are used to rotate the drum.

4.1.6 WEC Power Take-Off

The power take-off subsystem of the wave energy converter is the subsystem that allows the WEC to convert wave energy into electricity. Three concepts will be described in this subsection, which is traded off in Section 4.2.

Hydraulic

The working principles of a hydraulic power take-off system PTO subsystem are described by J.F. Gaspar et al. (2016) [21]. To summarise, a basic hydraulic PTO subsystem has a single-acting actuator with either one or two rectification non-return valves and one generation station. Hydraulic accumulators stabilize the hydraulic power that reaches the generator. The accumulator that is located at the high-pressure side is used to store energy while the one at the low-pressure side to avoid the emergence of pump cavitation. A schematic of this principle is provided in Figure 4.14.

Mechanical Drive/Gearbox

Mechanical drive or gearbox PTO subsystems use an electric generator to directly convert energy captured by the WEC into electricity; a gearbox is used to drive the electric generator [22]. A schematic of a mechanical drive PTO subsystem is provided in Figure 4.15.

Direct Drive

Direct drive PTO subsystems have a greatly reduced mechanical complexity due to the lower amount of moving parts. This subsystem requires a translator and a stator, which when undergoing relative motion to each other are able to produce electricity. The translator consists of permanent magnets, and the stator is constructed using coil windings [22]. A schematic representation of a direct drive PTO subsystem is given in Figure 4.16.

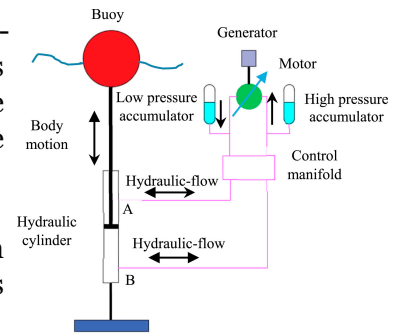


Figure 4.14: Schematic of the hydraulic PTO subsystem [22]

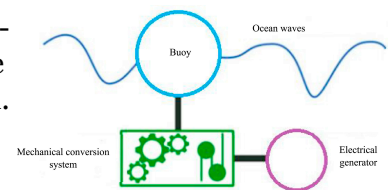


Figure 4.15: Schematic of the mechanical drive PTO subsystem [22]

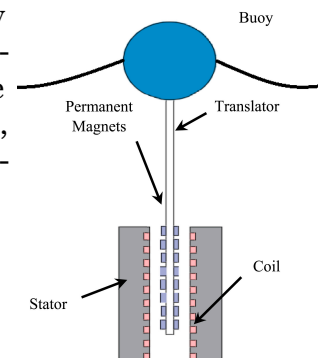


Figure 4.16: Schematic of the direct drive PTO subsystem [22]

4.2 | Trade-Off Summary

In order to select a final design, a trade-off is done for all five groups of concepts above. Each trade-off has its trade-off criteria with corresponding weights. All the weights add up to 10. Each design receives a score for each criterion. The total score is calculated by multiplying the score of each design with the weight of the corresponding criterion. The design with the highest score then wins the trade-off and will be used in the design. The only exception to this is the WEC PTO trade-off. Here the winner was the direct drive system but since it was decided to combine the AWES and WEC PTO systems the final WEC PTO design was a hydraulic PTO. This is further explained in Subsection 8.9.2.

Table 4.1: Trade-off table for kite

Criterion \ Design	Aerodynamic performance, weight = 2.5	Specific Mass [kg m ⁻²], weight = 2.5	Control, weight = 1.5	Launch, weight = 1.5	Crashworthiness, weight = 1	Storage, weight = 1	Total score
Leading Edge Inflatable Kite	646 [score = 3]	0.44 [score = 4]	Easier to control due to the stiff tubes [score = 4]	Easy take-off and landing due to stiff structure [score = 4]	Floats, Rigidity unlikely that lines tangle [score = 4]	Needs deflation [score = 4]	37.5
Ram-air Kite	609 [score = 3]	0.25 [score = 5]	Unstable due to lack of stiff elements [score = 2]	No stiff structure thus more difficult [score = 3]	Can sink, lines can get tangled [score = 4]	Can be easily folded [score = 5]	34.5
Semi-rigid Kite	784 [score = 5]	1.5 [score = 1]	Due to lack of span-wise stiff elements, hard to control [score = 2]	No stiff structure thus more difficult [score = 3]	Rigid elements can break and tear fabric, can sink [score = 1]	Size reduction in spanwise direction [score = 2]	25.5



Table 4.2: Trade-off table for launch options

Criterion \ Design	TRL, weight = 2	Retrieval, weight = 2	Mass, weight = 2	Storage, weight = 2	Cut-in windspeed, weight = 2	Total Score
Launch Tower (Up-right)	8 [score = 4]	Good control, can handle large kites - cannot be retrieved from water [score = 3]	Mast structure only used to position and retrieve kite [score = 3]	Proven design [score = 5]	Static launch increases cut-in windspeed [score = 2]	34
Launch Tower (Hanging Upside-down)	6 [score = 3]	Difficult to handle large kites - cannot be retrieved from water [score = 2]	Large moments mean large heavy structure needed [score = 1]	Quite complex [score = 2]	Static launch with swinging motion [score = 3]	20
Robot-Assisted Water Launch	2 [score = 1]	Designed for water landing - high chance of retrieval due to help from robot [score = 5]	Only retrieval mechanism needed, no mast. Added mass of robot [score = 4]	Quite complex [score = 2]	Lower cut-in windspeed [score = 4]	32
Water Launch	2 [score = 1]	Designed for water landing - high chance of retrieval [score = 4]	Only retrieval mechanism needed /no mast [score = 5]	Quite complex [score = 2]	Lower cut-in windspeed [score = 4]	32



Table 4.3: Trade-off table for WEC

Criterion						
Design	Synergy Adaptation with AWES, weight = 3.5	TRL, weight = 1.5	Survivability, weight = 1	Cost [€/MWh], weight = 1.5	Hydrodynamic Efficiency, weight = 2.5	Total score
Point absorber	Synergy possible, heaving can be amplified [score = 5]	7-8 [15] [score = 4]	With- stands 18 m waves [23] [score = 4]	≈100 [24] [score = 5]	30% [score = 5]	47.5
Line attenuator	Synergy possible, tuning possible, though multiple hinges gives multiple DoF [score = 3]	4 [score = 2]	Tested in 8 m waves [25] [score = 3]	735.94[26] [score = 1]	15% [score = 3]	25.5
Raft type attenuator	Synergy possible, tuning possible, one hinge [score = 4]	6-7 [score = 3][27]	Max to 2.3 m waves [28] [score = 3]	≈165 [29] [score = 4]	15% [score = 3]	35



Table 4.4: Trade-off table for WEC PTO

Criterion					
Design	Maintenance, weight = 3	Cost, weight = 1	Efficiency, weight = 4	Sustainability, weight= 2	Total score
Hydraulic	High, wear in piston seals and extreme events can damage whole system [score = 2]	Well developed [score = 5]	Converts in many steps but can use both translation and rotational motion, 69% to 80% [22] [score = 3]	Made out of steel and transformer oil, oil leaks are possible [score = 3]	29
Mechanical drive / Gear-box	High, many moving parts [score = 1]	Depen- dent on size [score = 3]	Max of 3 conversions, 97% [22] [score = 4]	Made out of steel [score = 5]	32
Direct drive	Low, few moving parts and no mechanical interface required [score = 5]	Uses Rare Earth Metals [score = 2]	Converts into electricity in one step, relatively high [score = 4]	Rare Earth Metal mining is not sustainable [score = 1]	35

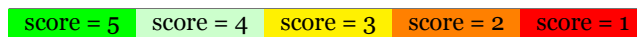
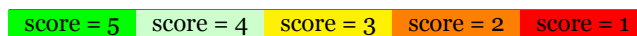


Table 4.5: Trade-off table for Anchoring

Criterion						
Design	Anchor efficiency, weight = 4.5	Cost, weight = 1.5	Installation complexity, weight = 2	Installation time, weight = 1	Install- ation noise, weight = 1	Total score
Gravity	0.3-0.6 [score = 1]	medium [score = 4]	low; simply dropped [score = 5]	low [score = 5]	Silent [score = 4]	29.5
Driven pile	12-100 [score = 4]	high [score = 3]	high; pile is lowered then align driving equipment [score = 3]	high [score = 3]	high [score = 2]	33.5
Suction pile	9-240 [score = 5]	high [score = 3]	high; pile is lowered, hammered, and then begin pumping control [score = 2]	medium [score = 4]	Silent [score = 4]	39



4.3 | Configuration Layout

Now that the design concept has been performed and understood, the concept layout can be seen. In the following section, the model made and its functionality will be shown and explained.

As explained in the previous section, the design chosen is a single-body system point absorber for the WEC system and a leading-edge inflatable kite for the AWES system. Apart the launch tower will be a telescopic beam, and the system use hydraulic PTOs.

In Figure 4.17 a figure showing the closed concept can be seen. In yellow, one can see the WEC floating buoy, in black the doors required for the AWES are seen, in blue the accessibility door can be seen, and in grey, the submerged body, which contains the ballast, and the telescopic boom can be seen. Such a configuration would be used in stormy conditions when the AWES system is not in operation. In Figure 4.18 the configuration for deployment can be seen. It can be seen how the doors in front of the drum and in top of the buoy have been opened in order to deploy the kite. The drum door is rolled inside the buoy, and the top doors are opened vertically as shown in the image. Also, the telescopic boom is deployed in order for the kite to have some initial height during launch. Apart, the kite during launch can be seen. It is important to note that the kite shown in this image is not in an accurate scale, since the model of the kite was not made due to time constraints.

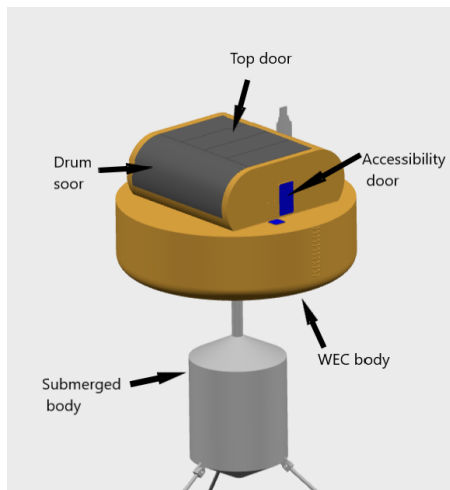


Figure 4.17: Closed concept layout

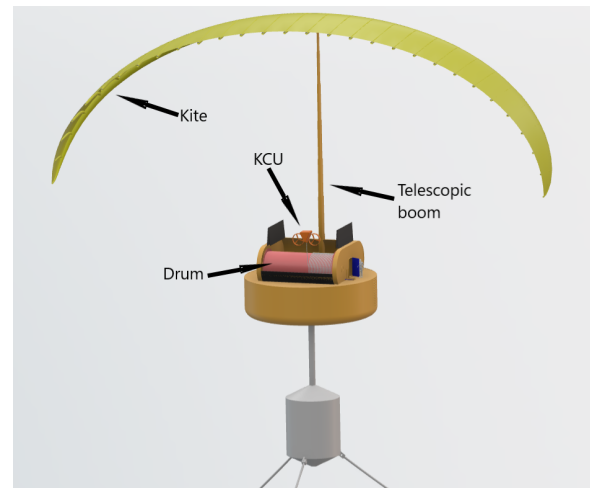


Figure 4.18: Launch and retrieval mode with open doors

In Figure 4.19 the flying configuration of the kite can be seen. As a preventive measure, the telescopic boom is kept deployed and the top doors closed. The further stage of the project the drum door will be updated in order for the drum door to stay closed while operations. This will be done in order to increase the survivability of the systems by reducing the exposure to the environments. In Figure 4.20 the inside layout of the system can be seen. A human model is placed next to the accessibility door (blue door) in order to show the scale of the buoy. While maintainability the top doors are kept closed for the comfort of the workers. In the image, the accessibility stairs outside of the buoy can be seen as well as inside stairs in order for workers to be able to access different sections of the buoy. One of the accumulators is also placed on the top floor of the system for scale references. It is important to note that in further stages, the placement of more specific parts like piping, cables generators and more will be done.

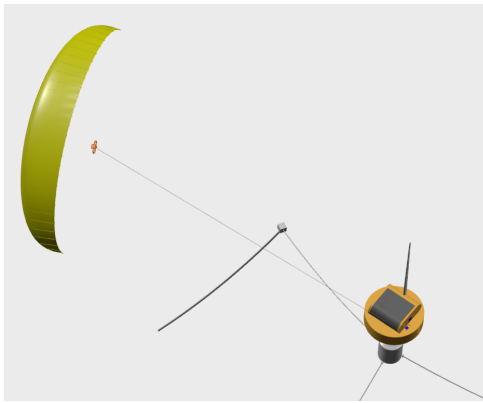


Figure 4.19: Flying configuration

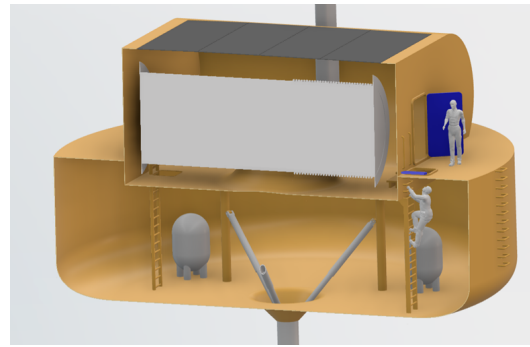


Figure 4.20: Accessibility of the buoy

In Figure 4.22 and Figure 4.23 the WEC PTO pistons can be seen in both the highest and lowest configuration when the highest operational wave height of 5 m is experienced. It is clear that enough room is left on the buoy in order to leave the pistons move. Such movement is needed due to the relative movement between the body and the submerged body in order to generate power. Finally, in Figure 4.21 the expected mooring can be seen. It can be seen in the image that the mooring system used is a semi-taut system. Such a system is used in order to provide stability for first-order frequency waves while still providing freedom of movement for second-order waves such as tides. This system is composed of two mooring lines, one attached to the sea floor via a suction pile and the other attached to the submerged body. The attachment in between both lines consists of a submerged buoy that keeps the lines in tension.

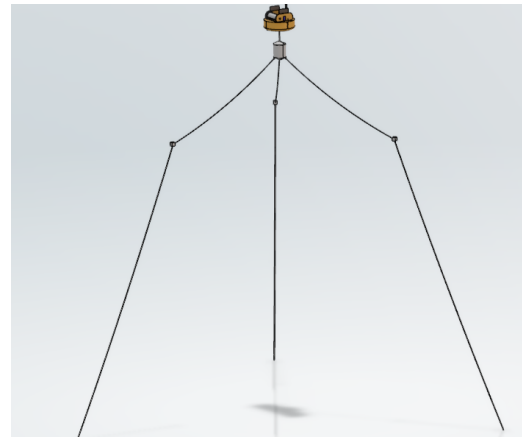


Figure 4.21: Mooring configuration

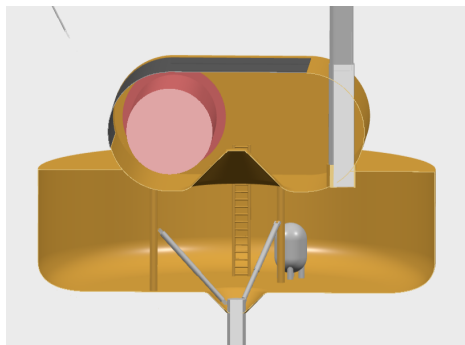


Figure 4.22: High wave configuration

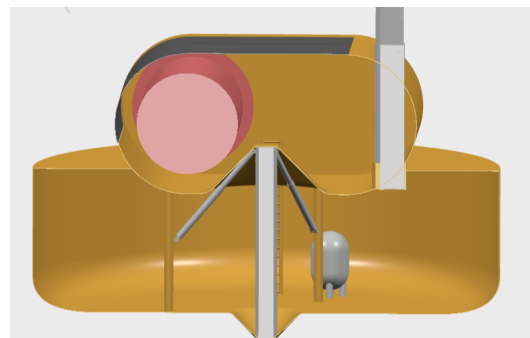
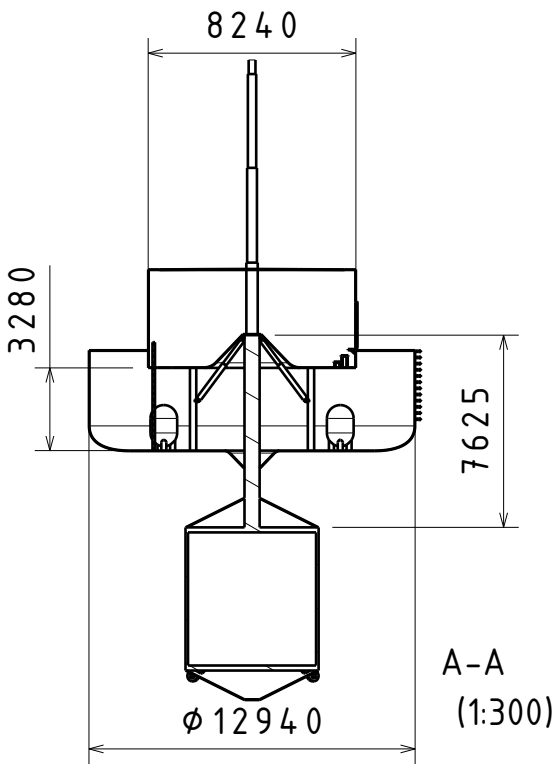
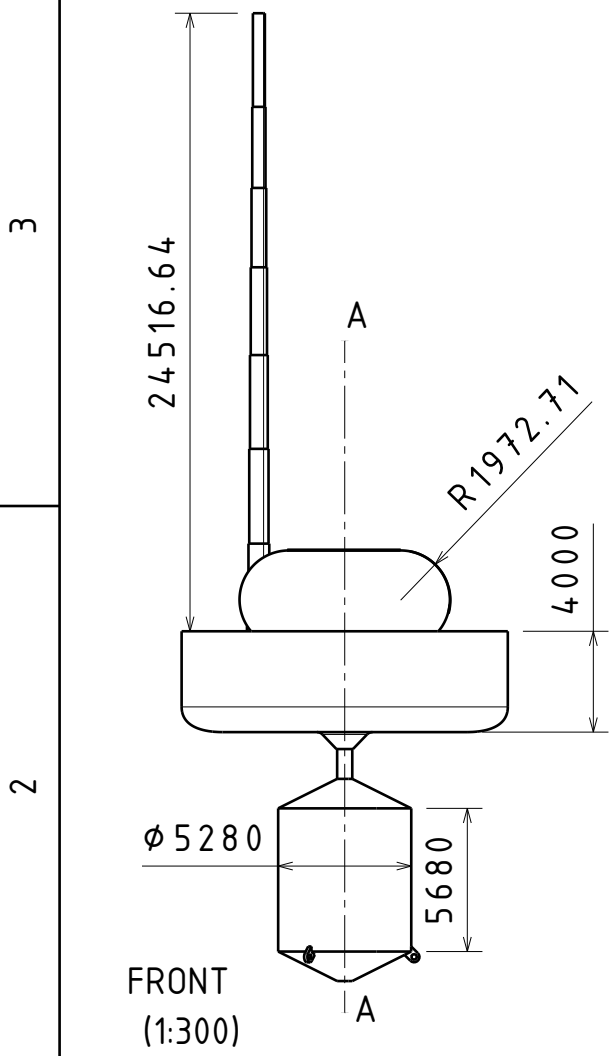
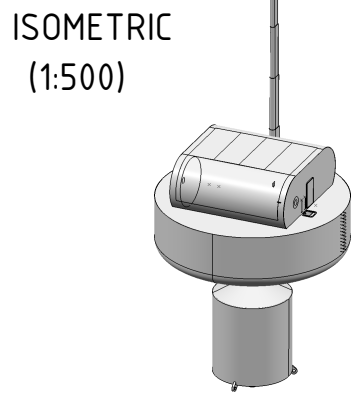
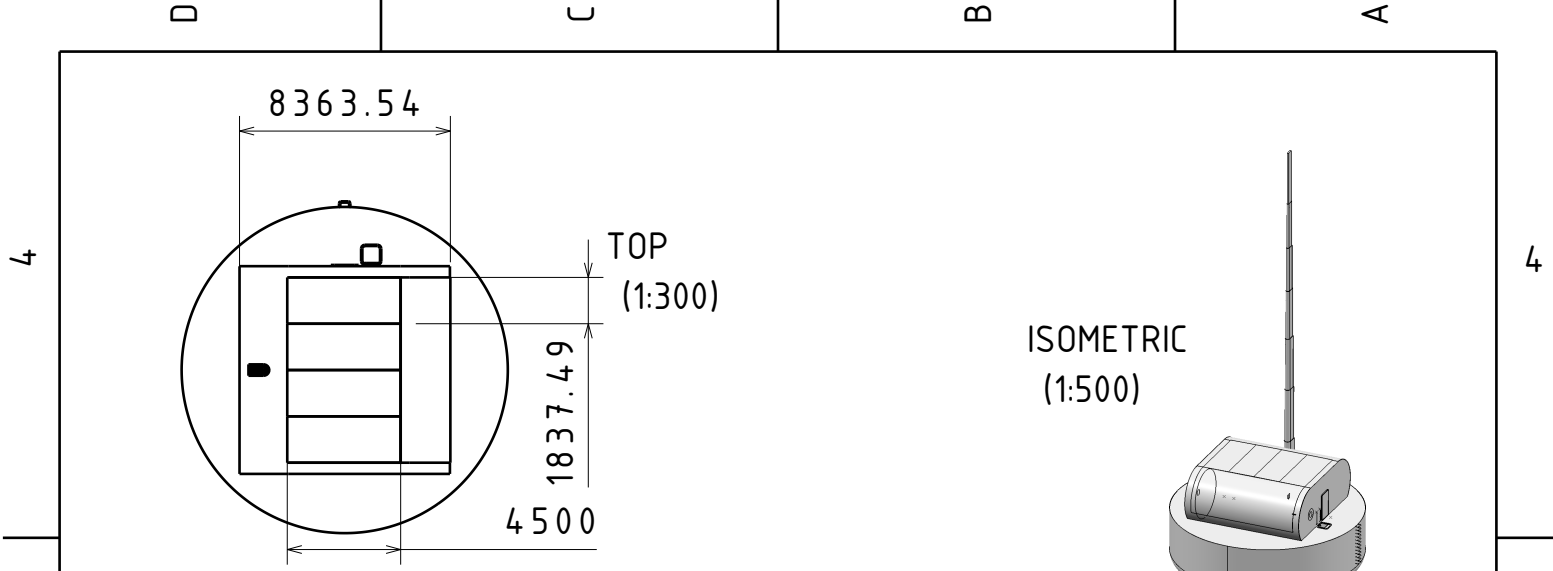


Figure 4.23: Low wave configuration

The following page shows a technical drawing of the model in the closed configuration of the WaveWings device. The dimensions shown are set in order to show have a better view of the size of the device. Measurements like the height and diameter of the buoy and submerged body are calculated in Section 8.2 and 8.3 respectively. Other dimensions like the length of the rod attached to the submerged body are based on the clearance constraints for the highest operational wave height of 5 m. The radius and lengths of the top floor area of the device are made large enough in order to host the drum and folded kite inside, which are sized in Section 8.7 and 7.3, and as such it has a width of 8.24 m and a height of 3.944 m. Finally, other sizes like the telescopic boom size and the door sizes are shown in order to understand the size of the components. Other sizes should be specified in further stages of the project.



This drawing is our property. It can't be reproduced or communicated without our written agreement.		Tu Delft University			
		DRAWING TITLE			
DRAWN BY DSE Group 5		DATE 19/06/2024		G5 final assembly drawing	
CHECKED BY DSE Group 5		DATE 19/06/2024		SIZE A4	DRAWING NUMBER 1
DESIGNED BY DSE Group 5		DATE -/06/2024		SCALE 1:250	WEIGHT(kg) NA
				SHEET 1/1	

4.4 | Systems Tree and Description

In order to clearly represent an exhaustive list of systems used in the WaveWings product, a system tree is shown in Figure 4.24. Nodes are sorted by specificity where the product trickles down into segments, systems, subsystems, and components, in that specified order. As an overview, airborne and floating systems are associated to the device segment whilst the farm segment addresses the broader implications of up-scaling the project to 400 units where electrical infrastructure considerations are essential. Due to the integrated nature of the unit, it should be noted that the power-generating “ground” segment of the AWES is now placed unto the floating body supported by the buoy. Hence, the floating body holds the majority of the subsystems including the Power Subsystem, Main Control Unit (MCU), Buoy and Mooring Subsystems, Communications Subsystem, and the Launch and Retrieval Subsystem.

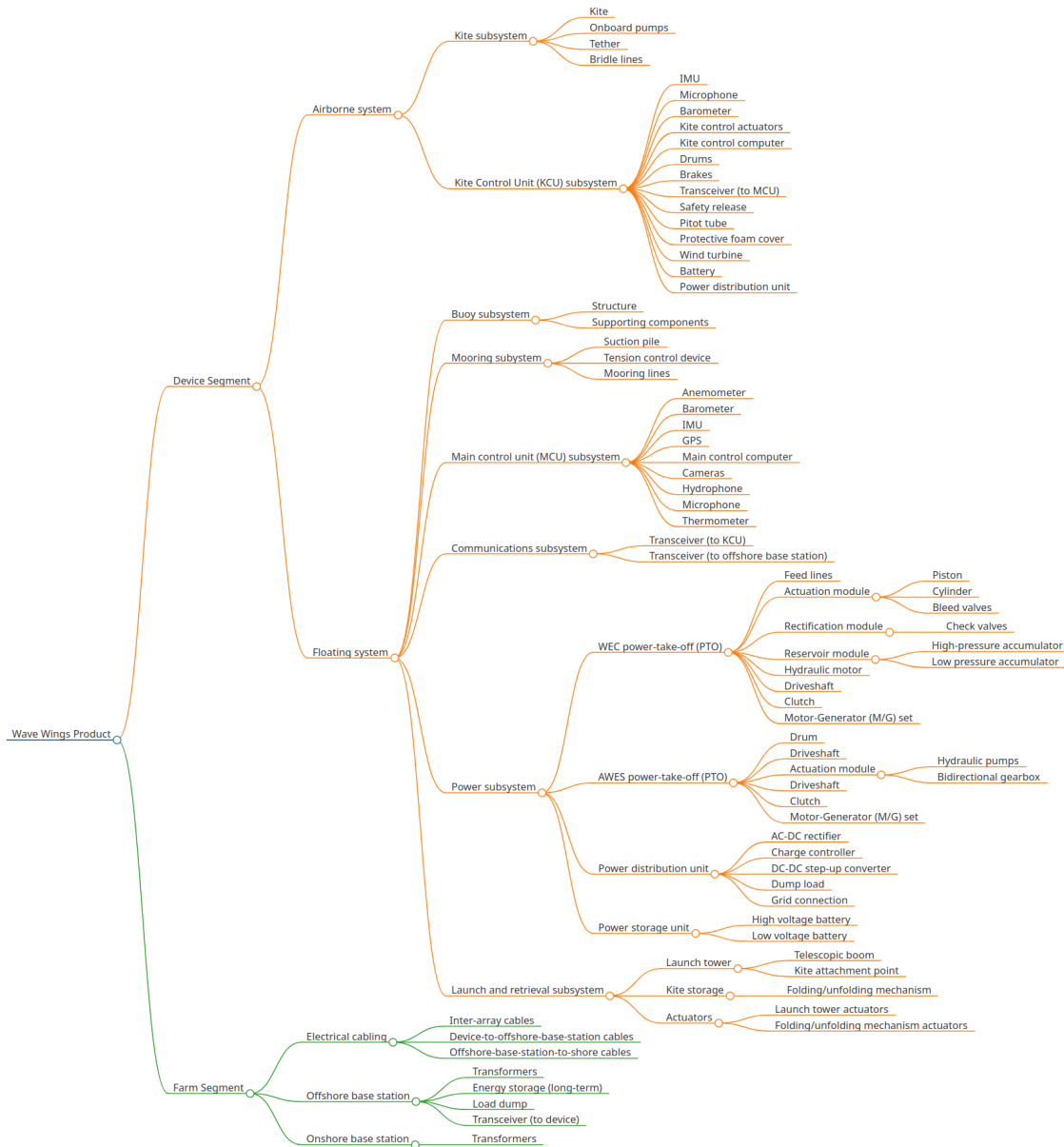
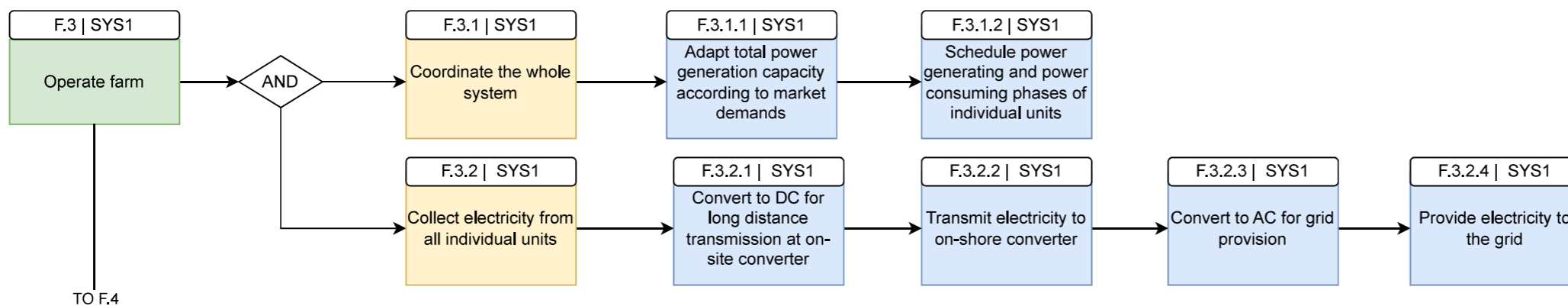
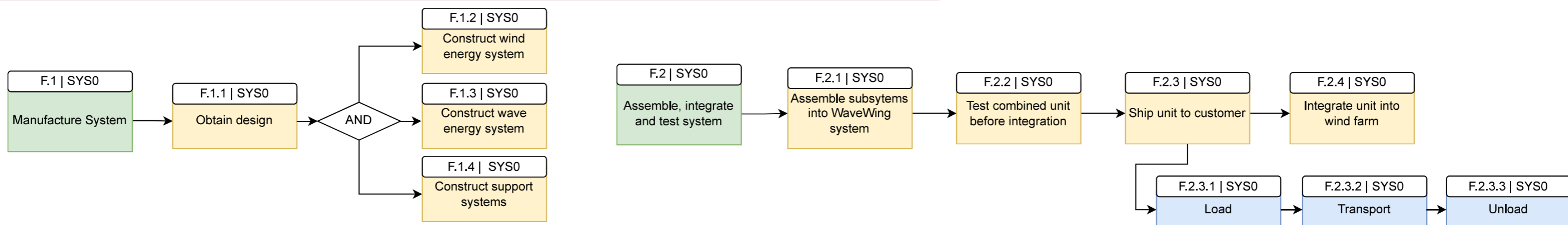
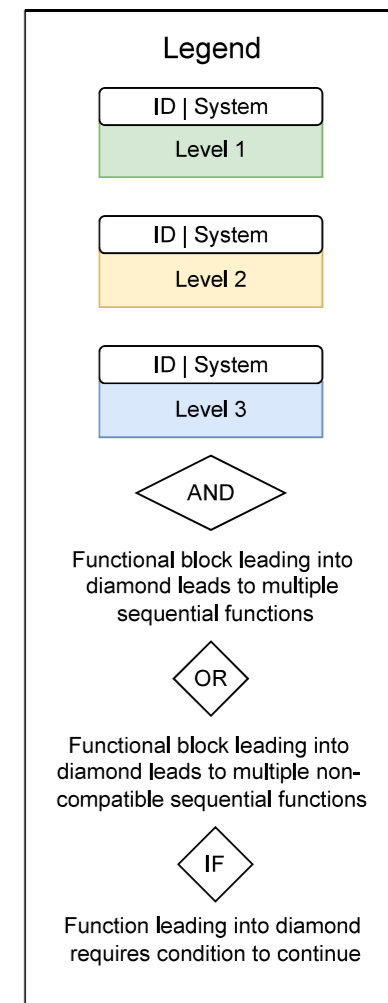
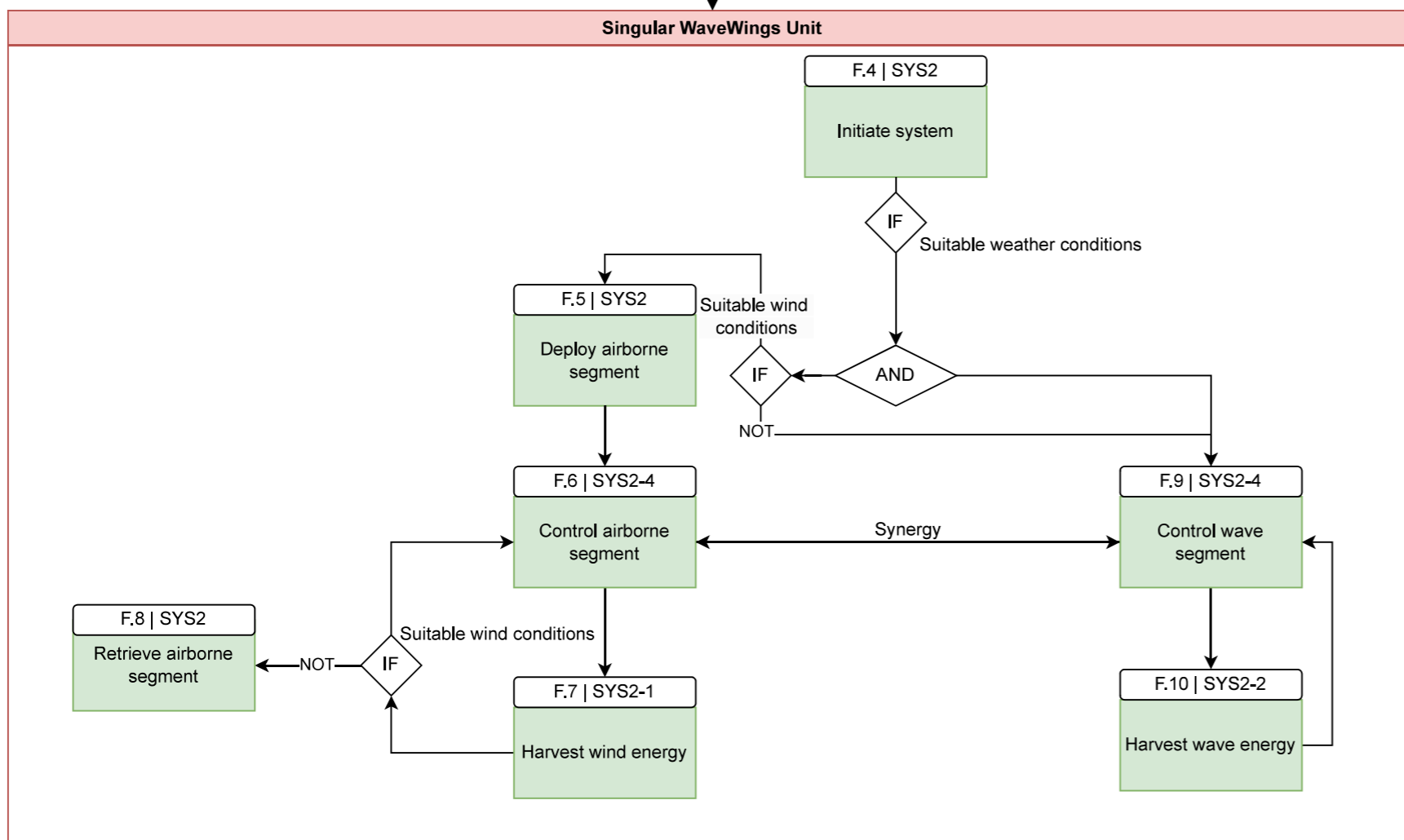
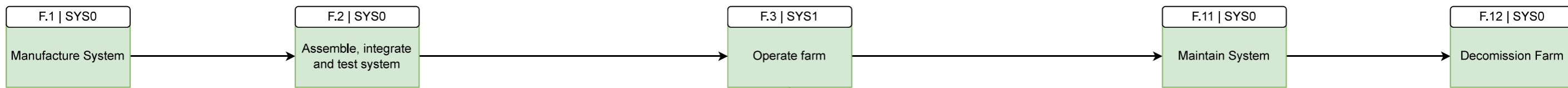
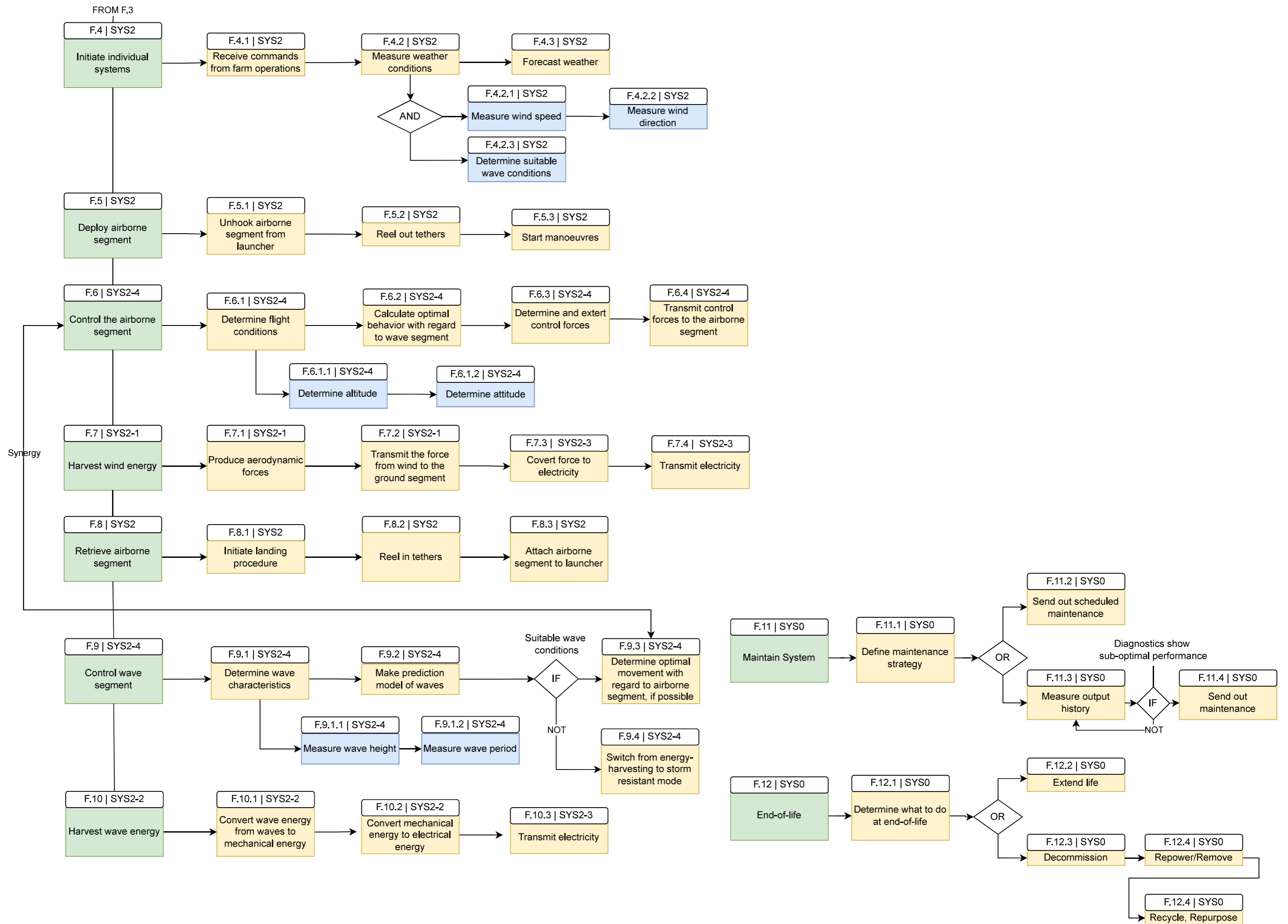


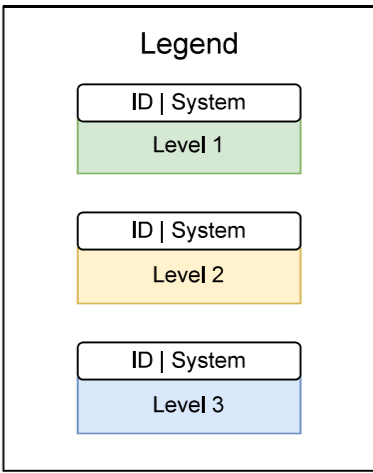
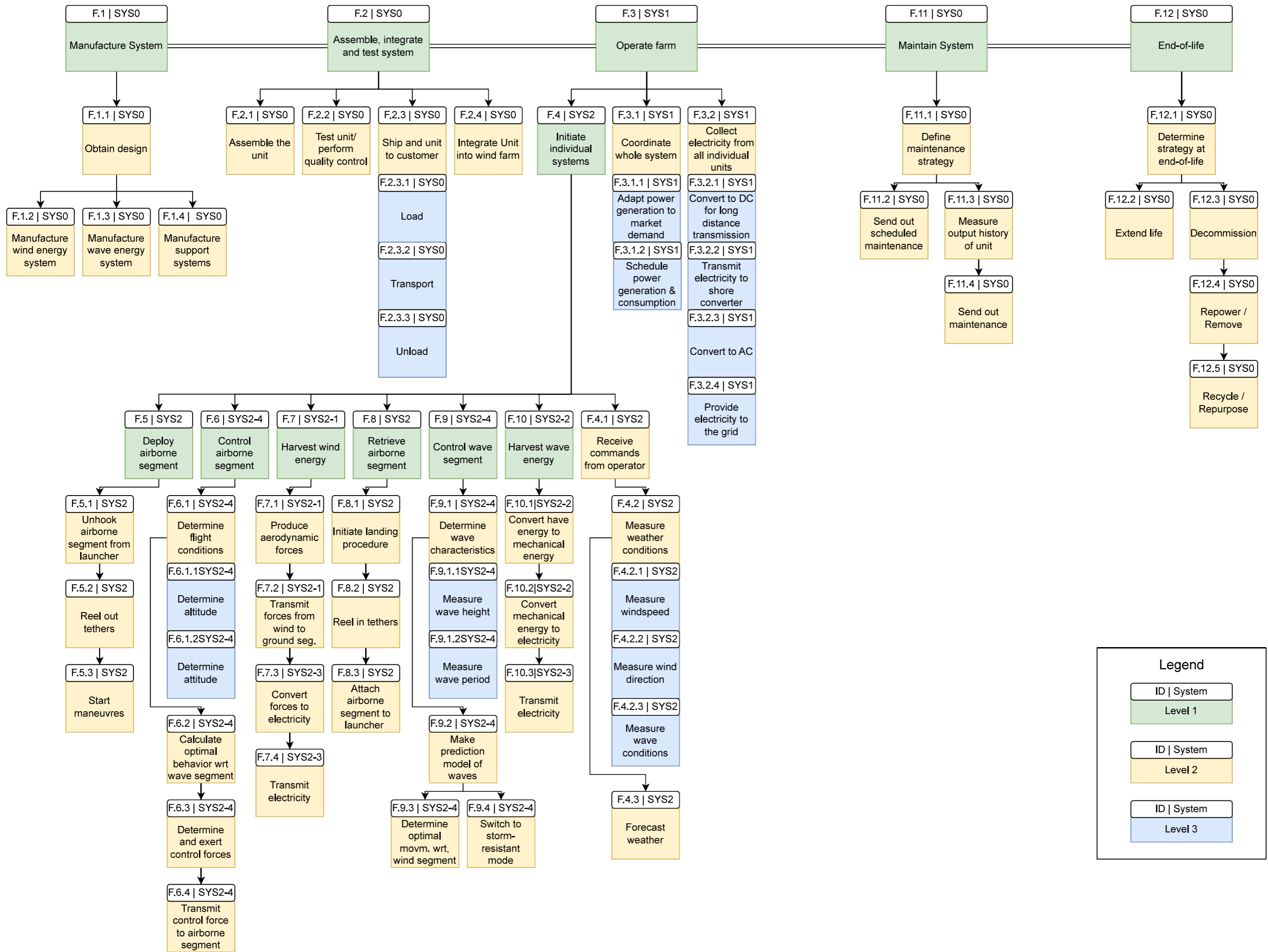
Figure 4.24: Systems Tree

4.5 | Functional Analysis

The functional analysis of the WaveWings units is displayed by functional flow diagrams, which highlight the interrelations and dependencies of the functions performed by the unit. Each phase of the WaveWing units also has its functions defined in the functional breakdown structure.







4.6 | Hardware and Software Diagram

The hardware and software of the airborne and floating systems are presented in Figure 4.25. The legend specifies the subsystem in different colors. The relationships from power, physical connections, and data-transfer is also depicted in varying arrow heads. Some boxes indicate whether it was designed by the team or an off-the-shelf component was selected. For other boxes, it is stated that it is a future design. In the diagram, it can be seen that the airborne and floating systems are linked through the main tether and support tether. Also, the most critical components, which handle the most flow, are the main control computer, the kite control computer, and the power distribution unit. These components, shall they fail, cause system failure. Thus, this diagram suggests to increase the reliability and conduct a proper risk analysis for those components.

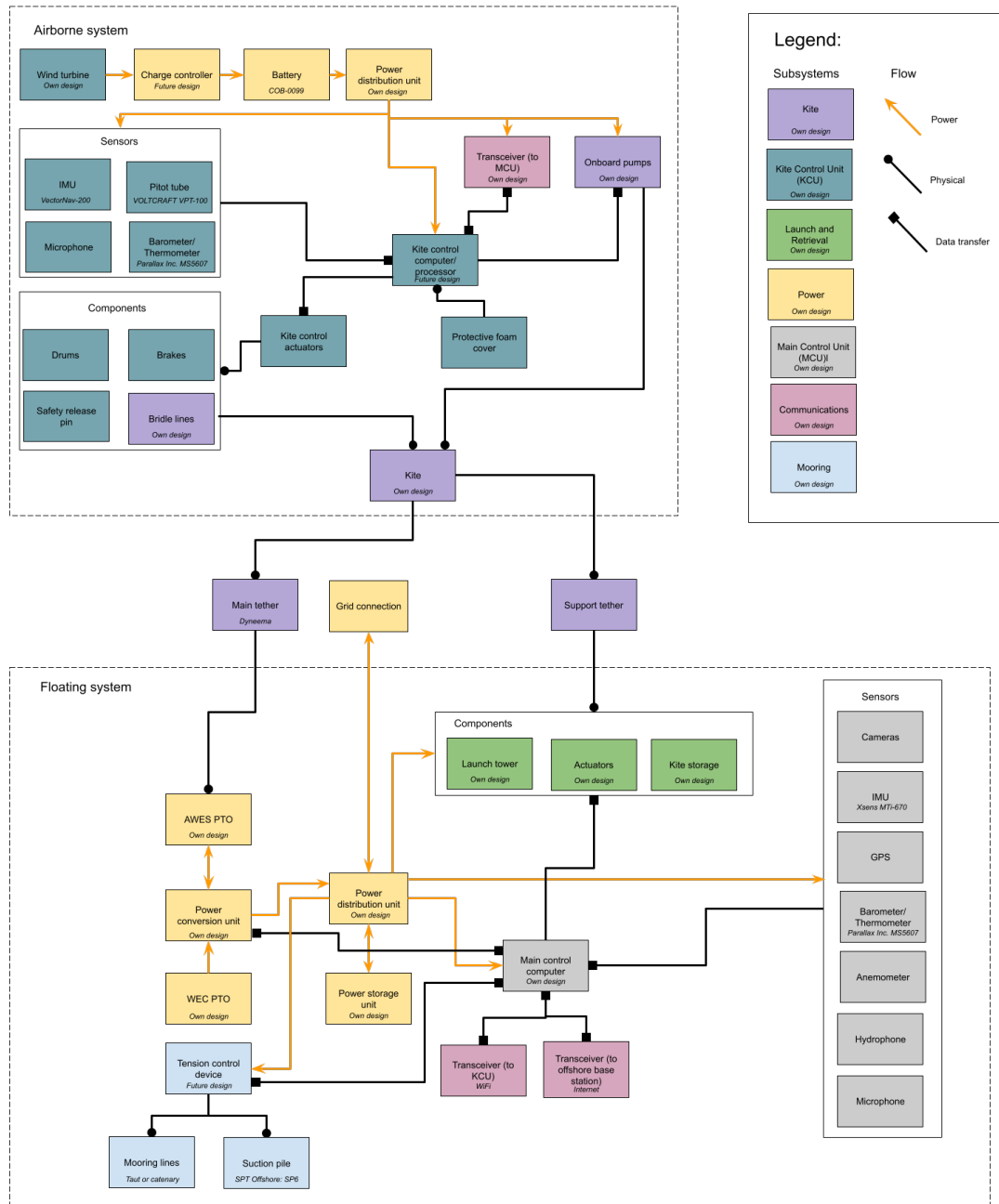


Figure 4.25: Hardware and Software diagram

5 | Farm Location

This section describes the procedure for narrowing down the site location for the WaveWings farm. First, the site-location-dependent requirements are stated in Section 5.1. After this, the farm location selection method and results are discussed in Section 5.2. Following this, the operating conditions for the selected location are described in Section 5.3, as this provides the basis for some site-specific requirements.

Note that certain economic aspects are considered for this site selection, but are only discussed in Chapter 6. As a result, the interconnection of these two chapters is as follows: this chapter selects a site and justifies the selection with a select number of criteria. The market analysis then further justifies it by looking into economic and logistic aspects.

5.1 | Requirements

Table 5.1 mentions all the requirements related to the market and economic performance of the project, in addition to some constraints on the farm location.

Table 5.1: Requirements for the farm location

Identifier	Requirement
USR-CON-1	The farm shall provide a 50-80% LCOE reduction compared to other off-shore renewables.
USR-CON-1-1	The farm shall provide total cost savings of 40% compared to individual deployment of airborne wind and wave energy systems.
USR-CON-1-2	Each unit shall provide a 25-30% manufacturing cost reduction compared to separate corresponding units of airborne wind energy and wave energy generation.
USR-CON-1-3	Detailed cost estimations shall be carried out for all components of the system, both for a single unit and for a 1 GW farm.
USR-CON-1-5	The system shall have a mission lifetime of 20 years.
ENV-CON-4-3	The farm shall not be placed in a marine protected area.
ENV-CON-4-4	The farm shall not be placed in a sea-life migrating route.
ENV-CON-4-5	The farm shall consider migratory routes of birds.
GOV-CON-6	The farm shall be positioned 25 km or more from shore.
GOV-CON-8	The farm shall be placed in the EU.
USR-CON-9	The farm shall be placed where the sea is deeper than 60 meters.
USR-REQ-1-1-AWE-1	The unit shall operate at a location with a median surface wind speed of 11 m/s.
USR-REQ-1-1-WEC-1	The unit shall operate at a location with 70 kW/m.

5.2 | Farm Location Selection

In order to align itself with the UN sustainable development goals and EU the 2030 agenda, the European Union energy market needs to incorporate more renewable energy resources. As such the focus of this study is on the European market and environmental conditions.

The first restriction for the site of the farm is the depth. Since offshore bottom fixed wind turbines are already a well-established market with high economical performance and relatively low environmental impact. As such for the Wave Wings project to find a non-established mar-



Figure 5.1: General Bathymetric Chart of the Oceans (GEBCO) 2022 Bathymetry contours [30].

ket, the depth region should not directly compete with bottom fixed offshore wind turbines [31]. Bottom-fixed offshore wind turbines become non-economically feasible at greater depth than 60 m, at which point floating wind becomes more feasible. In [32] it is recommended that the greatest depth for installation of WEC devices is 250 m depth. As such the market segment for the Wave Wings devices will be for greater than 60 m depth. In Figure 5.1 the bathymetry data from Europe's seas and oceans can be seen. In dark blue the regions with water depth shallower than 60 m can be seen, and in light blue the regions in between 60 and 250 m can be seen. As such, the farm will be restricted to such areas.

The next step after deciding on the first constraint is to look at suitable locations considering wind and wave power. In Figure 5.2a and 5.2b, the regions of interest in terms of wind capacity factor and wave mean power can be seen respectively market by white ovals. The zones of biggest interest regarding wind, are those with capacity factors of 50% or higher, and the main regions regarding wave energy are those with a mean wave power greater than 20 kW m^{-1} [32]. By comparing both maps it is clear that the regions of interest for both requirements are the Western coast of Ireland and the Northern-West region of the Iberian peninsula. Due to the high wave power, it is decided the region of interest will be the Western coast of Ireland.

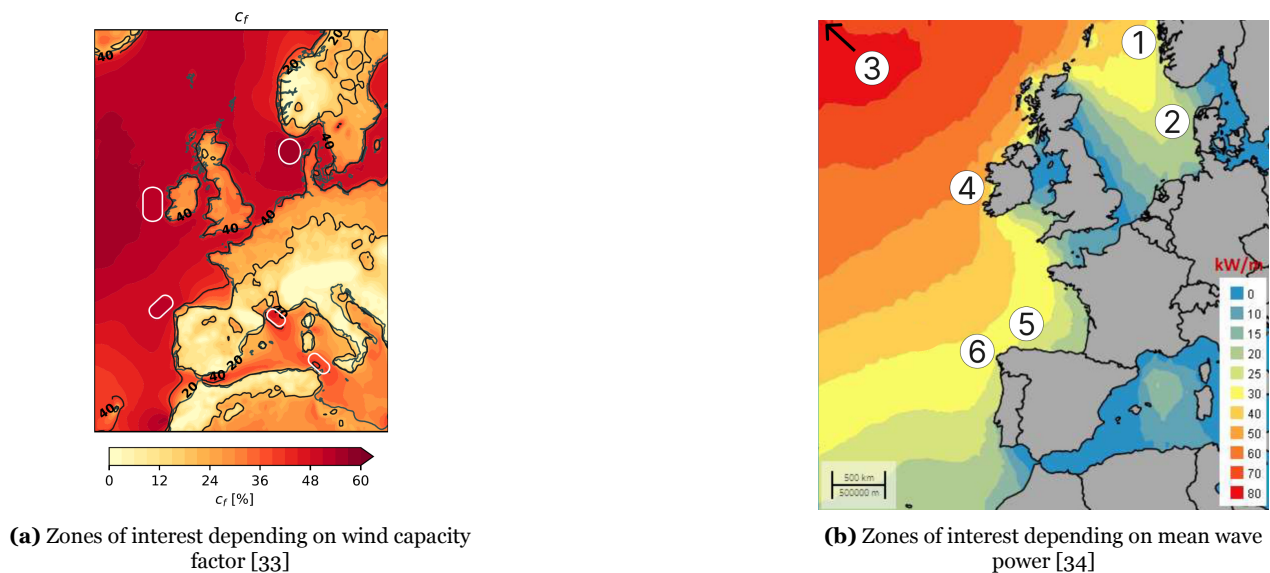


Figure 5.2: Zones of interest in the European Regions

In order to ensure alignment with the 14th sustainable goal, a final check needs to be performed before continuing in the more detailed farm location survey. This check consists on verifying that no regions of ecological importance are placed near the region of interest. In Figure 5.3 the regions of marine ecological importance can be seen. It is clear from the map that the West coast of Ireland has no main region of ecological importance. It is important to note that further studies will be performed in this aspect in further sections of this study in order to ensure the sustainable development of the farm.

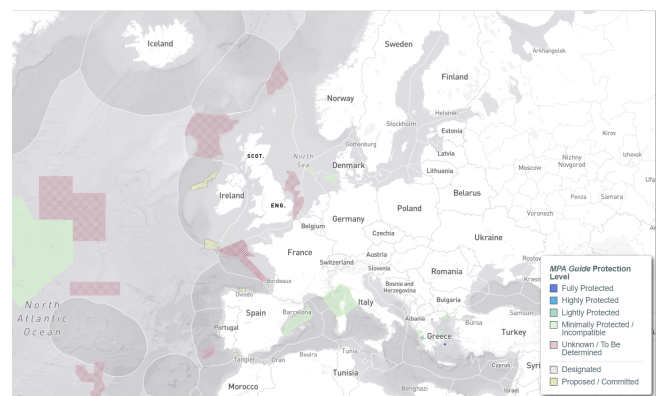


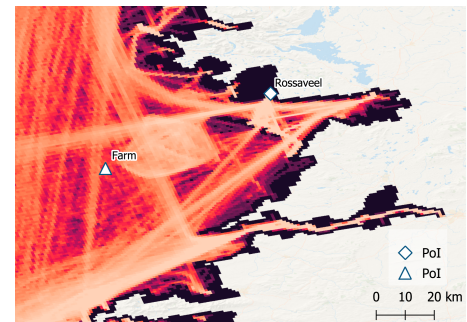
Figure 5.3: Marine protected regions in the European Union [35]

To increase the accuracy of the LCOE estimate, a more specific location is proposed. As a detailed optimization procedure for the selection of the farm location is out of the scope of this phase of the project, a suitable location is selected through an assessment of the resources available and several

constraining parameters. For this, the chosen parameters are those recommended by A. Martinez and G. Iglesias (2021) [36], but extended to include the distance to nearby ports, location of nearby wind farms, the distance to the closest shore, route density, bathymetry data, and operating conditions (described in Section 5.3).



(a) Map indicating points of interest (PoI), nearby farms [37] and key distances



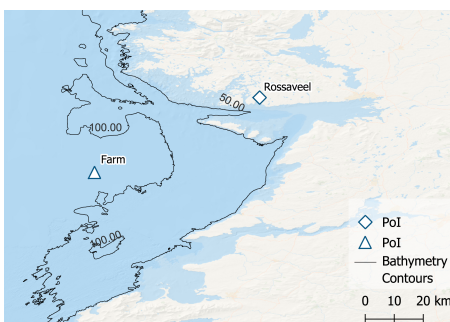
(b) EMODnet route density average from 2019 to 2023 [37]

Figure 5.4: Maps showing points of interest and trade routes near the proposed farm location

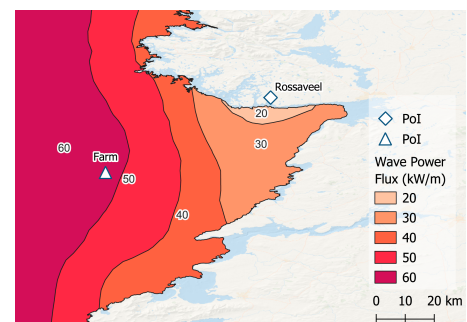
Figure 5.4a shows a cropped map of the western coast of Ireland, with the proposed location of the offshore wind farm (coordinates $52^{\circ}52.9771^{\circ}\text{N}$, $10^{\circ}23.4687^{\circ}\text{W}$). As can be seen, the port of Rossaveel has been chosen, and is calculated to be around 70 km away from the farm. To justify this farm location decision, it can be seen that there are a number of existing offshore wind farm proposals in the area, as well as a wind farm testing location called SmartBay¹, 1.5 km from the port. This test site includes facilities such as data buoys, a subsea observatory and other pieces of critical infrastructure and support (e.g. vessels and installation machinery) which could be used for both the development and installation of the WaveWings devices.

An additional consideration to make when selecting suitable farm locations is that its construction should not greatly affect existing shipping routes or fishing areas. Figure 5.4b Shows the mean route density in the area of the proposed location over 4 years. As can be seen, a popular fishing area exists just east of the location, and shipping routes pass by just west and north of the location. However, the proposed location does not stand in the way of any of these.

Following this, Figure 5.5a shows the bathymetry contours in the region where the farm location is proposed. As can be seen, the sea floor depth in the region is in between 100 m and 200 m. This aligns with the observations made in the Baseline Report [38]. For simplicity, this value is assumed to be 150 m for future calculations. Figure 5.5b shows the mean wave power flux in the region around the farm. Once again, to confirm with the location requirements defined in the Baseline Report [38], it can be seen that the power flux in the proposed location is approximately 60 kW m^{-1} . This is sufficient to allow WaveWings to generate the desired power.



(a) GEBCO 2021 Bathymetry contours [30]



(b) Mean annual wave power flux [39]

Figure 5.5: Maps showing bathymetry and mean power flux data for the proposed farm location

¹<https://www.smartbay.ie/>

as shown by Equation 5.1 and Equation 5.2 below.

$$v_{\log} = v_{\text{ref}} \frac{\log\left(\frac{h}{z_0}\right)}{\log\left(\frac{h_{\text{ref}}}{z_0}\right)} \quad (5.1)$$

$$v_{\text{pow}} = v_{\text{blend}} \left(\frac{h}{h_{\text{blend}}}\right)^{\alpha} \quad (5.2)$$

Here, the aerodynamic roughness length $z_0 = 0.0002$, the blending height $h_{\text{blend}} = 60$ m and $\alpha = 0.11$, as is recommended for offshore areas. The values h_{ref} and V_{ref} correspond to a reference altitude and velocity (data point) on which the profile is based on. This data point is extracted from a time series dataset provided by the Sustainable Energy Authority of Ireland (2024) [45] containing wind speeds at 20 m altitude at the selected farm location for 2013. This velocity altitude profile is then used in conjunction with the data from sea [45] to construct Figure 5.8, which shows the probability distribution of various wind speeds for the farm location, at both 20 m and 350 m altitude.

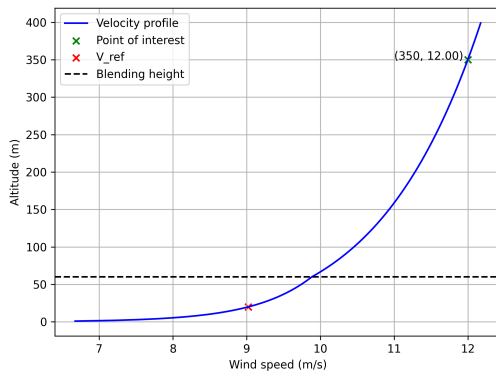


Figure 5.7: Wind velocity profile plotted with altitude, at the proposed location

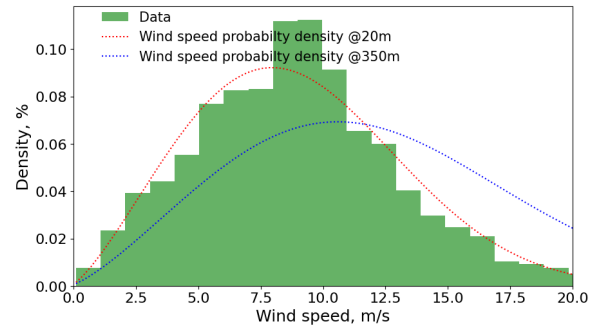


Figure 5.8: Wind velocity probability density distribution at the proposed location

Following from this analysis, it can be seen that the farm location experiences wind speeds of approximately 12 m s^{-1} at a height of 350 m (Figure 5.7). This is in line with “*USR-REQ-1-1-AWE-8*: The AWES part shall produce maximum power at 12.5 m/s rated wind speed.” *USR-REQ-1-1-AWE-1* is not satisfied as the median surface wind speed is equal to 9 m s^{-1} . This is probably due to that the requirement was not formulated properly and the median required wind speed was overestimated.

During storms, sustained winds and gust of up to 32 m s^{-1} and 44 m s^{-1} respectively should be expected [43]. By the definition of the Irish Meteorological Service, a sustained wind is the average wind speed over 10 min while a gust is the average wind speed over 3 s.

6 | Market Analysis

A market analysis is performed to determine the financial feasibility of the integrated wave-wind design in terms of demand and potential supply based on the integrated technology. It should be noted that no competitors exist in the realm of offshore platforms with equipped wave energy converters coupled to airborne wind energy systems. Although there are leaders in the constituents of the product this project is developing, market implementation at scale remains limited with varying technology readiness levels. Generally speaking, it is true that research and development is active with extensive testing programs and a community that is ready to share knowledge on the approaches to developing these technologies. For example, it is only as of March 2024 that SkySails, working in the development of AWES, validated their power curves [11]. The limited maturity of the technology proves that research is at the center of the industry and that competition on a commercial level is not prominent.

Research has determined that there are no widely known commercial AWES projects. However, Makani, a project developed by Google, created a 600kW rigid kite that was connected to a floating structure¹. The project was discontinued not due to engineering challenges but due to the withdrawal of investment in the company’s solution. Makani’s estimated LCOE is half of conventional HAWT of similar power output. The current leader in point absorber WECs is CorPower with a unit capable of generating 300kW. CorPower’s LCOE is estimated to be 70 €/GWh².

In this chapter, the specific markets which the WaveWings units target are first discussed. This is done through a market identification in Section 6.1, which includes an overview of relevant stakeholders, market trends and utilities. Note that this makes use of the outcomes of Chapter 5. To add detail to the analysis, permits, regulations and incentives present in the proposed farm location are also discussed, in Section 6.2.

Following this, and taking into account USR-CON-1 requirement, “The farm shall provide a 50-80% LCOE reduction compared to other off-shore renewables.” the LCOE of current off-shore renewables is found, in Section 6.3. This value is then scaled to the power output of the WaveWings farm in order to find a specific LCOE reduction target. The feasibility of this target is also discussed in the same section.

Finally, a market positioning analysis is carried out in Section 6.4, in which the WaveWings product’s performance is evaluated and compared to competitors. Additionally, a measure of the estimated market share and financing strategy is also provided.

6.1 | Market Identification

To perform a thorough market analysis of the WaveWings project it is first necessary to determine which markets are targeted. A market consists out of stakeholders, their needs, and their requirements. Furthermore, a market has current trends that need analysing, existing utilities that can be utilized, and competitors that need to be out-performed.

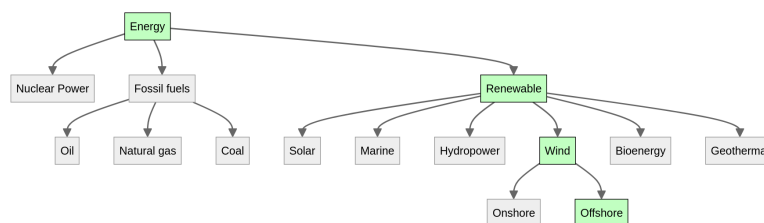


Figure 6.1: Market breakdown

¹<https://x.company/projects/makani/>

²<https://euscores.eu/co-location-of-offshore-wind-wave-and-offshore-solar-energy-could-lead-to-unprecedented-lcoe-reduction/>

As shown in Figure 6.1, the selected target market in this case is the offshore wind energy market. This is a subset of the wind energy market, which in turn is a subset of the renewable electricity market. Other forms of energy production that are non-renewable (i.e. nuclear and fossil fuels) are not considered in this analysis. This specific market is selected due to the lack of an established wave energy market, and also taking into account the fact that, according to the requirements, the wind energy production for WaveWings is far greater than that of wave energy.

Following from the conclusions of the farm location study Chapter 5, the geographic market is narrowed down to the Irish offshore energy production industry. As a result, details can be discussed that relate to this specific geographic region. Figure 6.2 visualizes all the operational and planned offshore wind and ocean energy farms, and also the WaveWings farm location. Test sites are also represented in the figure. Each red square and blue triangle indicates where the competitors that the WaveWings farm have are situated. The information of these sites is available on [37]. The green circle is where the WaveWings farm is planned to be located. Surrounding the WaveWings are multiple wind farms, allowing the use of similar services and infrastructure.

6.1.1 Stakeholder Analysis

It is important to identify the major stakeholders of offshore wind energy production, as this allows for a more relevant requirement discovery process and for the target markets to be identified. The stakeholders that have been identified are: operators that will serve as the operators of the product, governments that will regulate the market of these new technologies and set up incentives, environmental groups that want to insure the respectful installation of these units in a marine ecosystem, developers that are at the heart of the design, research, and installation of the product, customers that buy electricity from the farm and provide it to the end-users, and competitors that will be competing for the same market as the offshore energy plant. The identifiers for these stakeholders are defined in the following list.

- 1. OPR Operators
- 2. GOV Government
- 3. ENV Environmental groups
- 4. DEV Developers
- 5. CUS Customers
- 6. COM Competitor

The interest and influence of these stakeholders on the project are depicted in Table 6.1, with high interest and high influence stakeholders needing to be informed and satisfied the most. As can be seen, the most important stakeholders are GOV (Government) and CUS (Customer), as this stakeholder is characterized by high interest and high influence.

Table 6.1: Interest-Influence-Stakeholder Chart. One must keep high-interest stakeholders informed and satisfied.

High Interest	COM	ENV	GOV, CUS
Medium Interest			DEV
Low Interest		OPR	
	Low Influence	Medium Influence	High Influence

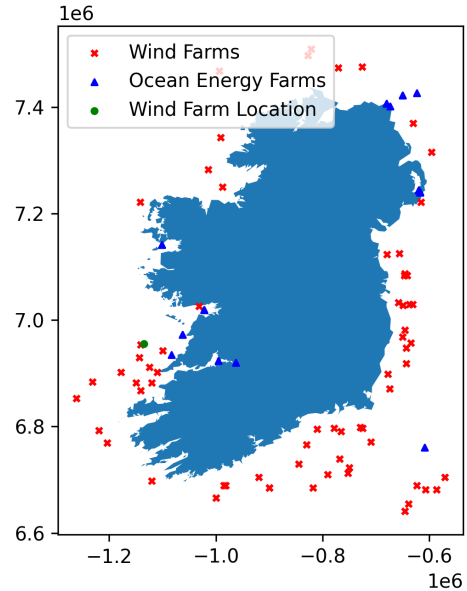


Figure 6.2: Irish shoreline with nearby existing, planned and test sites for wind and ocean energy [37]

The main drivers and requirements of the customer stakeholder are mentioned in Figure 6.3, obtained from a survey of renewable energy projects. These are the main points of interest for the customer

stakeholder, the needs of the customers.

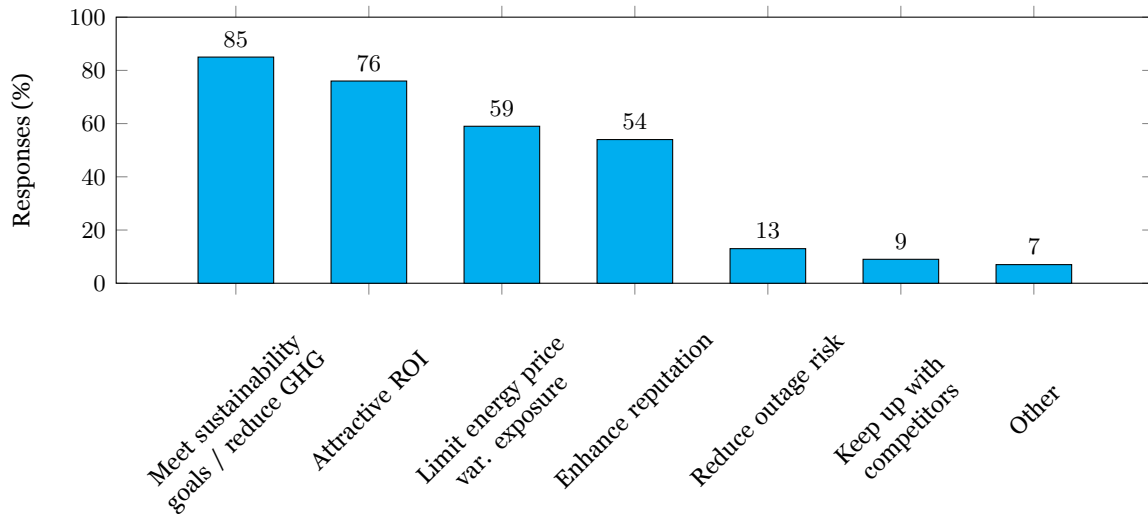


Figure 6.3: Drivers of intent to purchase [46]

Inspecting Figure 6.3 indicates that customers are mostly interested in meeting sustainability goals and reduce greenhouse gas emissions. The second most attractive characteristic for customers is the return on investment, it is financially attractive to invest in offshore wind energy. A more in depth analysis of other key performance indicators are mentioned in Section 6.4. The third most important factor is that customers desire a less volatility in energy price variation. Oil and gas prices can be volatile, while renewable resources are without costs.

6.1.2 Market Trends

To successfully enter a market, current and future developments must be considered. For this, market trends and dynamics are analyzed. A common metric for measuring market growth is cumulative annual growth rate (CAGR). In this case, this indicates how much every energy source has grown per year. The CAGR of the Irish renewable power market installed capacity is visualized in Figure 6.4.

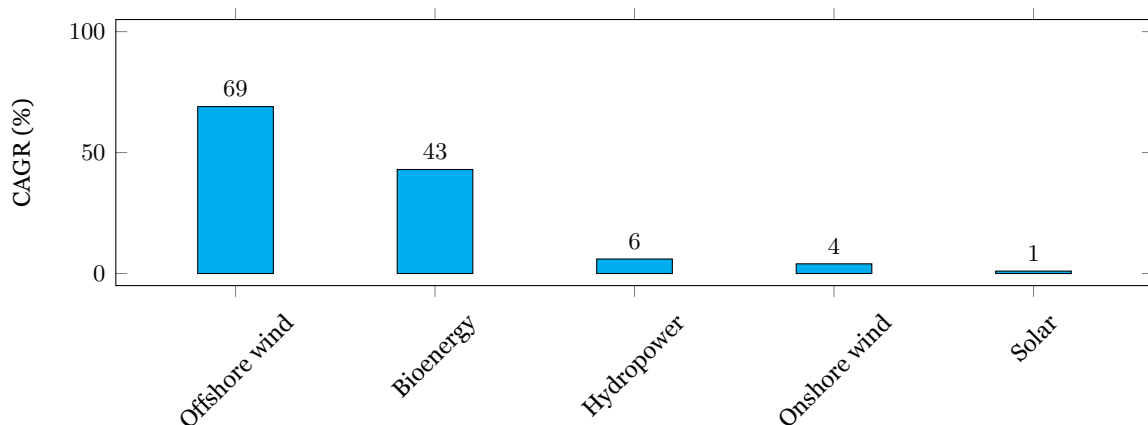


Figure 6.4: CAGR of energy sources in Ireland [47]

By considering Figure 6.4, it is determined that offshore wind is the fastest growing energy source in Ireland, with a CAGR of nearly 70%. This is followed by bioenergy, hydropower and offshore wind. From this, it is clear that offshore wind is a key player in the Irish energy production market. This means that the WaveWings project has the potential to become a key player in the Irish energy industry, given that it performs in the offshore wind market. Furthermore, taking into account the fact that the current target for installed offshore wind capacity is 5 GW in 2030 [48], the WaveWings farm

could secure a market share of 20% of all installed offshore wind capacity. All of this, in a rapidly growing market.

6.1.3 Utilities

Existing utilities present opportunities for the WaveWings farm to exploit. Available utilities at Rossaveel, Ireland include SmartBay, Ireland's national observation and validation facility for the marine and ocean energy sector [49]. SmartBay has a useful asset, the testing facility. This asset can be used for developers wishing to undertake low-cost sea trials and validation of devices and components at various technology readiness levels. During the development phase of the WaveWings project, SmartBay will be used to validate and test the product. Also available at SmartBay are data buoys, which allow for the validation of sensors on the WaveWing units. Furthermore, SmartBay has a subsea observatory. This observatory has a hydrophone, which can measure noise levels of ocean devices, so the WaveWings device can be validated regarding noise pollution regulations, mentioned in Section 6.2, and as specified by *USR-CON-4-1*.

6.2 | Permits, Regulations, and Incentives

The government is the main stakeholder that has a high influence on the project. They can require certain permits to be received, imply regulations on the project, and can provide incentives for green energy.

6.2.1 Permits

The permitting process required for the farm is lengthy, as the WaveWings farm requires a large amount of documentation. The documentation include the following items [50]:

- Design stage report
- Discharge documentation
- Environment section
- Fisheries Ireland report
- Noise impact assessment
- Site layout, access plan
- Noise monitoring location map
- Planning and environmental report
- Reinstatement program
- Ornithology assessment
- Marine biology assessment
- Other zoological assessments

The formulating of the documents should happen as soon as possible, as the application procedure can be lengthy and time-consuming.

6.2.2 Regulations

A set of regulations that have to be followed to obtain a permit to fly when constructing the farm in Ireland is the airspace regulations. The steps to obtain the permit are listed below [50].

- Registration of AWES kite
- Request restricted airspace
- SORA assessment, determine SAIL category
- If SAIL III, Design Verification approval (e.g. via EASA)
- Operational documents approval via DUTO (declared UAS training organization) ³

The steps to obtain the permit to fly should be started as soon as possible, as the application procedure can be lengthy and time-consuming. Input has been provided to the policy framework by AWEurope to change the consideration of AWE as a special type of unmanned aircraft system.

³<https://www.iaa.ie/general-aviation/drones/rpas-training-facilities>

6.2.3 Incentives

Governments can implement financial incentives for energy companies to more profitably provide green energy. Feed-In Tariffs (FIT) are a possible incentive, a policy designed to support the development of renewable energy sources by providing a guaranteed, above-market price for producers. These usually involve long-term contracts. The Renewable Energy FIT (REFIT) mechanism was introduced for wind and hydropower in 2006 to assist Ireland to meet its obligation to increase the consumption of renewable electricity to over 13% of the total electricity consumption by 2010 (as per EU Directive 2001/77/EC). However, all REFIT programs were closed by 2016 for new projects. During the 2006-2016 period REFIT was instrumental in the rapid growth of the renewable power market in the country. To further encourage the growth of renewables, the Irish government started to draft a framework to introduce an auction system to support renewables.

In short, Ireland does not provide any support schemes for renewable systems, and thus no financial breaks are expected over the lifetime of the farm.

6.3 | LCOE Target

According to the conclusions made in Subsection 6.1.2, the performance of the WaveWings product is imperative for success in the identified industry. As such, a specific LCOE target is calculated. For this, relevant offshore technologies are considered, including solar energy, wave energy, floating wind and fixed wind. Their average LCOE and global installed capacity as of 2021 are shown in Figure 6.5. It is observed that the LCOE decreases logarithmically with capacity. Thus, a logarithmic trendline of the averages is plotted in Figure 6.5. From the trendline, it is interpolated that the LCOE of an arbitrary 1GW off-shore renewable farm is 161 €/MWh. For a 50-80% reduction in LCOE, this means a target LCOE range between 32 and 81€/MWh is desired.

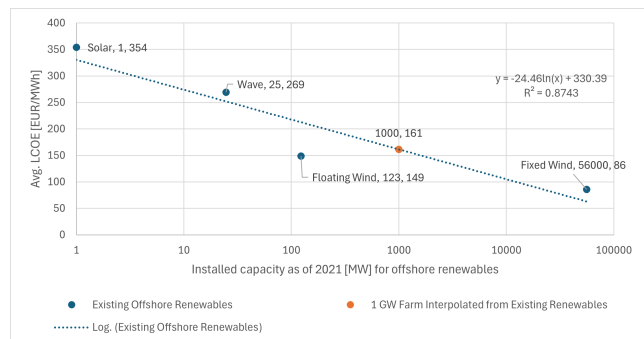


Figure 6.5: Average LCOE plotted against installed capacity as of 2021 for off-shore Renewables

The feasibility of this target is evaluated by comparing it to current statistics from existing projects. For instance, September 2017 estimates made by EnerKite and Kitepower yield an LCOE range of 46 to 150 €/MWh for onshore kite farms [51]. Research provided by Lorenzo Fagiano on High Altitude Wind Energy estimates an LCOE range of 30-35 \$/MWh for onshore kite farms [52]. Note that onshore energy production potential is significantly less than off-shore, thus lower LCOE values can be expected for off-shore AWES farms. All in all, the latter upper and lower estimates on the LCOE ranges of onshore AWES wind farms suggest that off-shore AWES wind farms could feasibly attain the desired LCOE range of this project.

Current WEC technologies have a much higher LCOE compared to AWES. The most market-ready company, CorPower, estimates an LCOE of 70€/MWh for 600MW of installed capacity. This capacity is 60% of the target capacity of the project's wind farm so the LCOE value is comparable in scale. Since the CorPower-estimated LCOE value for WECs falls within the 1GW farm target LCOE range, it is expected that the LCOE of an integrated wind-wave system can meet the desired LCOE range of 32 and 81€/MWh.

The worldwide market is targeted to produce 47,700 TWh/year of electricity by 2050; Europe will aim for 4,800 TWh/year. A 1GW farm operating at a capacity factor in the range of 50-60 % yields a response in demand of 0.09125-0.1095% of the European market. Note that the mobility of the platform will target the 2400 European islands that do not have access to large-scale mainland energy systems with a demand of 60 TWh/year as of 2016, which would respond to 7.30-8.76% of the demand with the envisioned 1 GW farm.

6.4 | Market Positioning

To carry out a proper evaluation of the market positioning of the WaveWings project, a set of key performance indicators (KPIs) are evaluated. These cover financial performance aspects of the WaveWings devices. Due to a general lack of data availability for some offshore wind turbine projects, not all the KPIs calculated by the economic model in Chapter 11 are considered here. As a result, only the LCOE is considered in this section, with further conclusions regarding some KPIs being mentioned in Chapter 11.

Following from the results of the economic model, the LCOE for the WaveWings farm is estimated to be €49.4/MWh. According to the LCOE target established in Section 6.3, it is confirmed that this value meets the requirements of the project. Additionally, Figure 6.6 shows this value along with LCOE forecasts up until the final year of operations for the WaveWings farm, for offshore floating and bottom-fixed wind turbines.

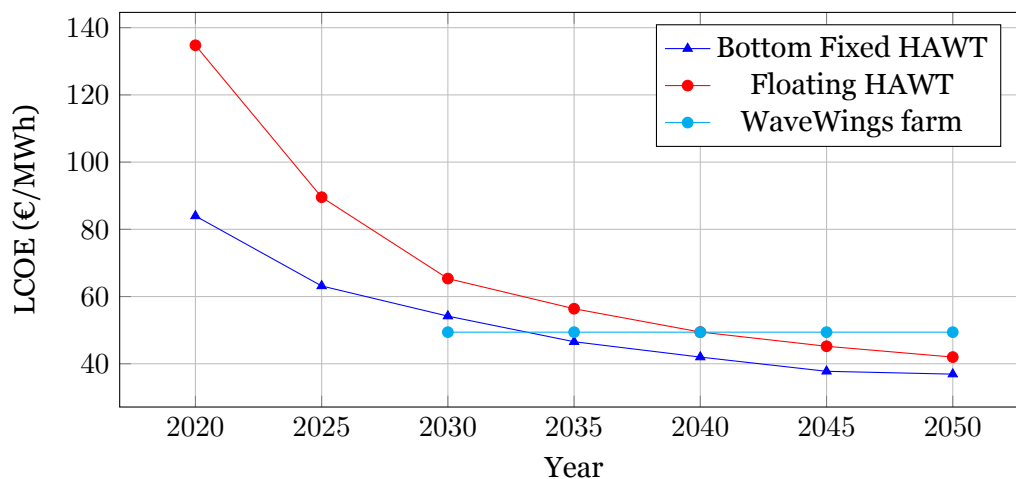


Figure 6.6: Predicted LCOE for offshore HAWT in Ireland [53], compared to the WaveWings estimated LCOE

As can be seen, the predicted LCOE values highlight several key points. First of all, bottom fixed HAWT, despite starting with a relatively high LCOE in 2020, sees a significant cost reduction to approximately €37/MWh by 2050. According to Wind Energy Ireland [53], this is driven by technological advancements, economies of scale and an improved supply chain efficiency. On the other hand, floating HAWT is initially more expensive than bottom-fixed HAWT. It also experiences a significant LCOE reduction, reaching around €42/MWh by 2050. Nevertheless, at the time of the WaveWing farm commissioning in 2030, the LCOE is still 10 years ahead of Floating HAWT. Despite the higher costs compared to bottom-fixed HAWTs, floating turbines are gaining popularity due to their suitability for deeper waters where fixed structures are not feasible.

The LCOE for the WaveWings farm is assumed to remain constant throughout the deployment period, with a value of €49.4/MWh. This suggests that the WaveWings project will maintain price competitiveness with floating HAWT until the year 2040. Beyond this timeframe, however, the predicted LCOE for new offshore wind projects is expected to decrease below the estimated WaveWings LCOE. This indicates that while WaveWings will remain competitive in the near term, there may be increasing pressure to reduce costs further or innovate to sustain its competitive edge beyond 2040.

In addition to this, the WaveWings project is projected to capture a significant market share in the Irish offshore wind sector. As touched upon in Subsection 6.1.2, the expected target of 5 GW installed offshore capacity in Ireland will be partially filled by the 1 GW WaveWings farm. As a result, the expected market share of offshore wind by the WaveWings farm is 20% by 2030. Continued market analysis and strategic partnerships will be essential in achieving these growth targets and maintaining a secure position within this rapidly evolving industry.

6.5 | SWOT Analysis

A SWOT analysis is needed to complete the market analysis. A SWOT diagram indicates the strengths (helpful internal aspects), weaknesses (harmful internal aspects), opportunities (helpful external aspects), and threats (harmful external aspects). The SWOT analysis is presented in Table 6.2. Strengths and opportunities are found in the synergy of wave and wind power in an integrated design while weaknesses and threats are identified for the novelty of the technology. Some points in the SWOT diagram also lead to new requirements or linked to existing requirements to show that proper measures are taken to reduce weakness and threats and enhance strengths and opportunities.

Table 6.2: SWOT Diagram

	Helpful	Harmful
Internal	<p>Strengths</p> <ul style="list-style-type: none"> Combining AWES and WEC technologies can lead to a lower LCOE than conventional wind turbines since they share the same infrastructure and the power production is increased compared to individual systems. The associated requirements are USR-CON-1 and USR-CON-1-1. AWES can extract energy from more reliable and powerful winds at high altitudes. The associated requirements are USR-REQ-1 and USR-REQ-1-1. Combining AWES and WEC leads to a design that uses less material than an individual WEC or AWES and less material than a conventional wind turbine. The associated requirement is USR-CON-1-2. 	<p>Weaknesses</p> <ul style="list-style-type: none"> AWES is a relatively new technology and WEC is not widely commercialised yet. Combining both technologies into a single platform has never been done before. This ambition is translated to requirements DEV-CON-7 and USR-CON-1-1-CTR-1. Control strategies are more complicated than with conventional wind turbines, which requires both robust and reliable software as well as suitable risk management. This is reflected in requirements USR-REQ-2-3-AWE-1 and USR-REQ-2-3-AWE-2.
External	<p>Opportunities</p> <ul style="list-style-type: none"> As shown by the surge in fossil fuel prices due to the Russian-Ukrainian war, Europe needs to build energy self-sufficiency. The EU is investing more than €210 billion forenergy efficiency and renewable energy by 2027 for this purpose [54]. The 2012 global primary power demand is 18TW. High altitude off-shore wind resources worldwide have an 1800 TW power production potential whereas lower altitude winds that wind turbines extract energy from only have 400TW of power production potential; wind energy extraction is not limited by geophysical limits [55]. 	<p>Threats</p> <ul style="list-style-type: none"> Shipping routes, fishing industry, oil and gas exploration, and military use of off-shore areas can hinder the approval of an off-shore wind-wave farm [56]. Natural areas would prohibit the installation of a farm. Requirements ENV-CON-4 and ENV-CON-5 stem from this.

7 | Airborne System

To describe the subsystems in detail, the WaveWings unit is sub-divided into an airborne system and a floating system. The airborne system, described in this section, consists out of the kite, the KCU, and tether. The floating system, described in Chapter 8, consists out of the buoy, the PTO, the submerged body, the mooring, the ballast, the anchor, the main control system, the drum subsystem, and the launch-retrieval tower. The airborne system is the main component of the integrated WaveWings design. It should provide more than 90% of the energy of the WaveWings unit. Firstly the requirements will be presented. Following is the kite design and the bridle system. Afterwards, the performance will be evaluated. Finally, the tether and KCU will be discussed.

7.1 | Requirements

Table 7.1 shows a list of requirements that the airborne system should comply with. In Section 14.1 an overview is presented where all the requirements and their compliance are shown.

Table 7.1: Requirements for airborne system

Identifier	Requirement
USR-CON-7	The AWES subsystem shall use the soft kite pumping concept.
USR-REQ-1-1-AWE	The AWES part of one unit shall produce 2.3 MW of rated electrical power.
USR-REQ-1-1-AWE-2	The AWES shall produce a maximum of 3.6 MW of power during reel-out.
USR-REQ-1-1-AWE-2-1	The AWES shall maximise CL^3/CD^2 for peak power generation.
USR-REQ-1-1-AWE-6-1	The AWES shall have a launch velocity of 5.0 m s^{-1} or lower.
USR-REQ-1-1-AWE-4	The AWES shall survive operational environmental conditions.
USR-REQ-1-1-AWE-4-1	The kite shall have a system to absorb lightning strikes.
USR-REQ-1-1-AWE-4-2	The AWES shall resist hail of size 3 centimetres.
USR-REQ-1-1-AWE-4-3	The AWES shall endure 32000 hours of UV radiation.
USR-REQ-1-1-AWE-4-4	The kite shall survive a soft landing in the water.
USR-REQ-1-1-AWE-4-5	The AWES shall operate between -15°C to 35°C .
USR-REQ-1-1-AWE-4-9	The AWES shall be modelled with control simulation software for tether fatigue.
USR-REQ-1-1-AWE-4-10	The kite shall withstand aerodynamic forces at maximum velocity.
USR-REQ-1-1-AWE-4-11	A fatigue analysis shall be carried out on the AWES structures under cyclic loading.
USR-REQ-1-1-AWE-4-12	The tether shall resist the tension force of the nominal tether force times the tether safety factor.
USR-REQ-1-1-AWE-8	The AWES part shall produce maximum power at 12.5 m/s rated wind speed.
USR-REQ-1-1-AWE-9	The kite shall be able to turn with a maximum turning radius of 100 m during operations.
USR-REQ-1-2-1-3	The AWES shall be equipped with warning lights.
USR-REQ-2	The farm shall have a capacity factor between 50% and 60%.

7.2 | Airfoil Design

7.2.1 Airfoil Camber

The first airfoil parameter which will be determined is the camber of the airfoil. This is a measure of the curvature of the airfoil. It represents the maximum distance between the the canopy and the straight line from the leading edge to the trailing edge of the airfoil. as can be seen in Figure 7.1a, an increase in camber causes an increase in maximum lift coefficient which improves the performance, but is also

causes the drag coefficient to increase. To find the optimal value for the camber, multiple airfoils are simulated using Breukels his method [1]. For each airfoil, the performance indicator C_l^3/C_d^2 , which is the aerodynamic part of Loyd [2] his crosswind power equation, is calculated and the camber with the highest C_l^3/C_d^2 is selected. This result is shown in Figure 7.1b.

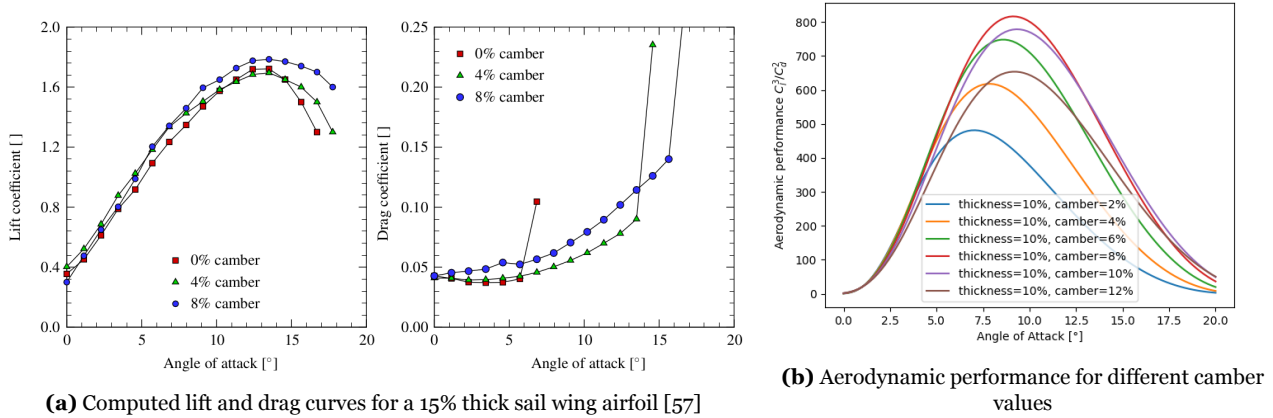


Figure 7.1: Aerodynamics for different camber values

As can be seen in Figure 7.1b, the optimum value for camber is 8%. It is important to remember that a soft kite is being designed, so the geometry of the wing will change during flight. This means that the kite will not always have this optimum camber value, to account for this, a sensitivity analysis is performed where the kite will be simulated with a camber of 6% and a camber of 10%. This would change the overall size of the kite to 416 m² and 404 m² respectively.

7.2.2 Leading-Edge Thickness

The second parameter which will be decided upon is the leading edge thickness. Increasing the leading edge thickness increases the slope of the lift curve slightly, hereby increasing the lift coefficient for lower angles of attack. But increasing the leading edge thickness also decreases the maximum lift coefficient and increases the drag. Similar to the camber determination, different leading edge thicknesses are simulated using Breukels his method [1]. The different airfoils are then compared on their maximum C_l^3/C_d^2 value.

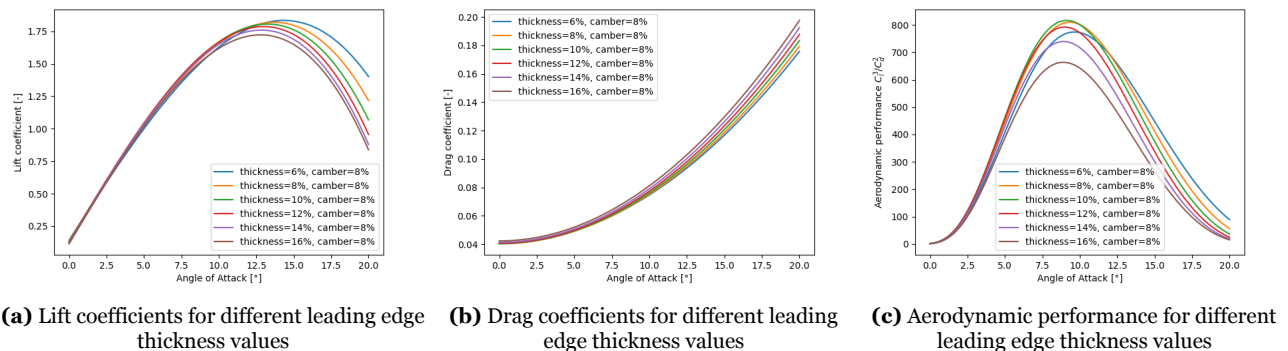


Figure 7.2: Aerodynamics for different leading edge thickness values

As can be seen in Figure 7.2c, the airfoil with a 10% leading edge thickness has the highest C_l^3/C_d^2 value. This is why this leading edge thickness is chosen. It is important to note that the leading edge thickness is also influenced by the structural design of the kite, but at this stage of the design that is not yet taken into account. As a sensitivity analysis, the thicknesses of 8% and 12% will also be simulated. They would change the projected area to 409 m² and 402 m² respectively.

7.3 | Kite Design

Now that the airfoil of the kite has been determined, the 3D shape of the kite can be decided upon. There are three main geometric parameters which are designed. Firstly, the aspect ratio of the kite is decided. After this the curvature of the kite will be determined. Lastly, the positioning of the struts will be discussed.

During the design phase, an iteration was present between the curvature and aspect ratio as they influence each other. In the report, only the plots of the final iteration are presented.

7.3.1 Aspect Ratio

The aspect ratio of the wing is one of the most important design parameters because it is influenced by a lot of factors. Firstly, the aspect ratio has influence on the aerodynamic performance. A higher aspect ratio will reduce the induced drag, making the kite more efficient. However there are also downsides on having a high aspect ratio. Most of these stem from the fact that a high aspect ratio means that the span will be high. This has an influence on the structural integrity of the kite as it will require a more extensive bridle system to support the shape. This higher span also influences the turning performance as the apparent wind speed at the outside of the turn will be higher than the apparent wind speed at the inside of the turn (Figure 7.3). Because of this, the drag at the outside of the turn will be higher than the drag at the inside of the turn, inducing a moment which counteracts the turning motion.

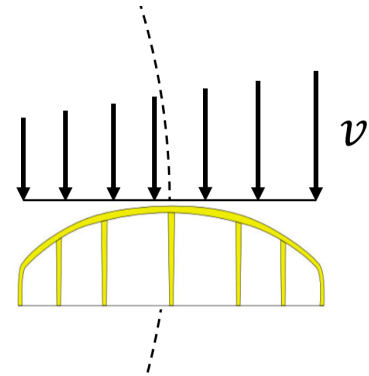


Figure 7.3: Apparent wind speed during turns

Before the aspect ratio can be decided, the overall concept of the kite needs to be decided upon. It is decided that the leading edge of the kite is a semi-ellipse. The trailing edge of the kite is a straight line. The choice for an elliptical leading edge is based on the elliptical lift distribution this induced, which is the most efficient lift distribution. The trailing edge is decided to be straight, this decision was made by comparison with LEI sporting kites which have a straight trailing edge and it is also a simplification to save time and resources.

To determine the aspect ratio of different kites, the projected span and projected surface area are used. Equation (7.1) gives how the aspect ratio is calculated.

$$AR = b_{proj}^2 / S_{proj} \quad (7.1)$$

A range of different aspect ratios are simulated using the vortex step method (VSM). The kites which are simulated all have the curvature of a 120° circular arc. The results of the simulation can be seen in figures 7.4, 7.5 and 7.6. Figure 7.7 gives the aerodynamic performance, but with added bridle and tether drag evaluated at $S=390 \text{ m}^2$.

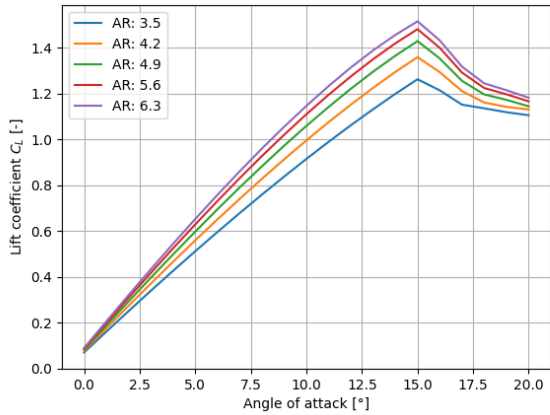


Figure 7.4: Kite lift curves for different aspect ratios

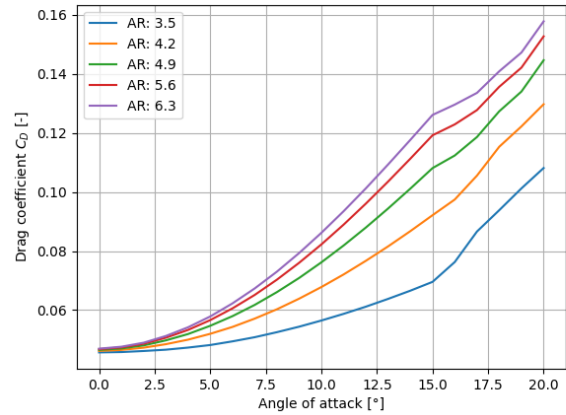


Figure 7.5: Kite drag curves for different aspect ratios

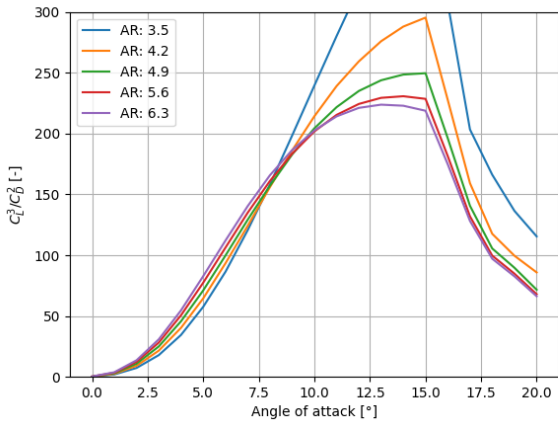


Figure 7.6: Kite aerodynamic performance curves for different aspect ratios

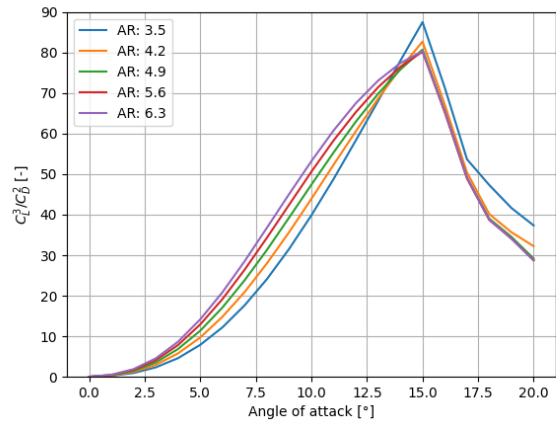


Figure 7.7: Kite aerodynamic performance curves including bridle and tether drag for different aspect ratios

The most important of the plots presented above is Figure 7.7, it shows the power coefficient with the most realistic drag component. On this graph it can be seen that a higher aspect ratio means that the power coefficient is higher for most of the AOA range. Only for the peak lift coefficient this changes. But as the kite won't be flying at peak lift coefficient to prevent instabilities, we conclude that the aspect ratio should be as high as possible. As very high aspect ratios would make the kite hard to handle during operations, the span should be limited. After discussing with the launch and control group, a maximum span of 50 m was decided upon. This means that the half-span is 25% of the turning radius. With this span set, the aspect ratio was maximized while by iterating it with the kite planform area. From this, a aspect ratio of 6.3 was found.

7.3.2 Curvature

The curvature of the kite is an important metric as this makes sure that the kite has a sufficient sideways force for turning the kite. To design the curvature, we assume that the curvature follows the top half of an ellipse. The choice for an ellipse was made to have the most amount of surface area facing up and generating lift in the vertical direction, the choice for an ellipse also means that the side of the kite is vertical and thus has maximal efficiency for steering the kite. The designing parameter is for the curvature is thus the ellipse ratio, which is the halve span divided by the kite height. As per requirement *USR-REQ-1-1-AWE-9*, the kite needs to be able to have a turning radius of 100 m. This means that the kite needs to be able to produce a sideways force which can induce an acceleration as

described in equation (7.2).

$$F = m \cdot \frac{v_{kite}^2}{r} \quad (7.2)$$

Where m is the combined mass of the kite, bridle system and KCU. v_{kite} is the speed of the kite, which can be calculated using equation (7.3) [58] and r is the turning radius which is set at 100 m.

$$v_{kite} = \sqrt{1 + \frac{L^2}{D} (\cos \beta - f)} v_{wind} \quad (7.3)$$

In this equation, the lift-over-drag ratio is 9.36 as will be calculated in Subsection 7.3.5, the elevation angle (β) is 30° (Subsection 7.5.2), the reel-out factor (f) is 0.48 (Subsection 7.5.2) and the wind speed is 12.5 m s^{-1} . Inserting these numbers, it can be found that the kite speed (v_{kite}) is 45.4 m s^{-1} .

The third unknown parameter in equation (7.2) is the mass of the kite. It is assumed that this mass consists of the kite, the KCU and the bridle system. As calculated in Subsection 7.5.6, the kite mass is 470 kg. The KCU mass is 110 kg. The bridle system is not designed, but its mass is estimated at 100 kg. This gives a total mass of 680 kg. Using these numbers, it is found that the kite needs to generate at least 14.0 kN. A safety factor of 3 will be applied to this force because the mass of the tether which is also turning is not taken into account. Secondly, the impact of the apparent wind difference at the wingtips (Figure 7.3) is also not quantified. The design value for sideways force will thus be 42 kN. This force is translated to a force coefficient by dividing by the dynamic pressure (at sea level conditions, and kite speed of 45.4 m s^{-1}) and the projected (downwards) surface area of 400 m^2 . This gives a side force coefficient of 0.084.

As calculating the aerodynamic coefficients of the steering goes out of the scope of this design synthesis exercise, a different method is needed to calculate this side force coefficient. To estimate the side force coefficient, we simulate the sideways force of half the kite using the VSM. After consulting with an expert in the field¹, it is found that we could estimate this steering force with the sideways force of half a kite. Because this is not an exact representation, a safety factor of two was applied. This means that the sideways force component of half a kite (normalised with the downwards projected surface area of the entire kite), needs to be at least 0.168.

The curvature of the kite is minimised to limit the mass of the kite as a higher curvature means that the ratio of flat area to planform area will be higher. Also a lower curvature means that the sideways area gets limited which reduces the overall drag of the kite. The lowest curvature while still having a side force coefficient of 0.168 is a curvature with an elliptical ratio of 1.6, its side force coefficient curve is given in Figure 7.10.

7.3.3 Strut Design

Struts are an essential part of the design of a kite. Not only do they provide stability, but they also keep the structure of the kite intact. Due to the high loads inside of the wing, it is important that the loads are well spread over the struts and that the canopy does not flutter. Following are therefore the specifications for the strut design.

First is the design of a singular strut. The strut will have a cylinder structure because that is a shape with not much drag [59]. For the Kitepower LEI kites the diameter of the struts is around 70 percent of the leading edge tube. For this kite, this percentage is decided to be quite a lot smaller, because of the leading edge is already very big, and the size of the strut does not have a major influence in the distance between the individual struts. Therefore there has been chosen for design of a lot of smaller struts, with a diameter of 40 percent of the leading edge. Struts are required to handle less load than the leading edge and smaller struts lead to a better aerodynamic performance of the kite, while the wind energy can still be transferred into the entire kite.

Following is the spacing of the struts. To define this, some sort of trade-off is required. This is because more struts decrease the chance of fluttering, but they also increase the drag and therefore decrease

¹Ir. O. Cayon, 17/06/2024

the aerodynamic performance. With less struts there is less drag, but fluttering could occur and the kite has less structural integrity. Therefore to make a choice there have been looked at similar kites. There are no LEI kites of the size for the WaveWings. Therefore the other smaller Kitepower kites have been inspected. Due to the slightly bigger struts, the maximum distance between the struts is estimated at a maximum of 2 meters, to keep structural integrity and decrease the chance of fluttering.

7.3.4 Material Selection

Afterwards, it is also essential to dive into the material selection. The main used material currently for kites is Dacron. There is however a new material on the market with promising attributes called ALUULA Vaepor™. Following will be the advantages and disadvantages for both materials and a final choice will be made.

The difference in the design choice is performance. This is dependent on the strength, stiffness and also the weight required to provide a proper kite. Firstly for the weight, ALUULA mostly weighs around 80 grams per square meter, while Dacron weighs around 160 grams per square meter. For these densities, ALUULA still has a slight strength and stiffness advantage. [60] In total that means that performance-wise ALUULA is the better option.

Looking at the costs there is also quite a difference between the two materials. Kites made from ALUULA are estimated to be 30 percent more expensive than Dacron kites, due to the more complex composite structures [61]. Although this seems like a lot, a bit of the cost can be refuted, by the durability of the kite. The ALUULA material probably does not have to be changed as frequently, due to the stiffness and therefore less damage. This decreases the total cost of keeping the kite operable.

After careful consideration, the kite material has been chosen to be ALUULA Vaepor™. Although the material is very new, Ocean Rodeo [60] claims that the positive results are from more than 2000 hours of testing. Although the cost of the ALUULA Vaepor™ is a bit higher than the Dacron, it does not weigh up to the performance of the ALUULA. That is why it is chosen.

7.3.5 Kite aerodynamic overview

To determine the final lift and drag coefficients of the kite, the VSM simulation was run for a kite with a projected surface area of 390 m², a projected aspect ratio of 3.5 and a curvature of 120°. Figures 7.8 and 7.9 give the lift and drag curve of the kite.

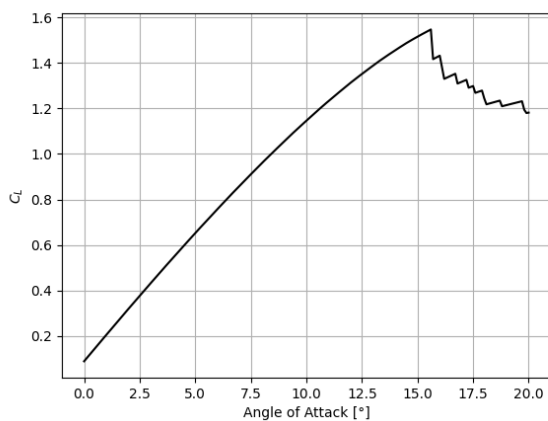


Figure 7.8: Kite lift curve

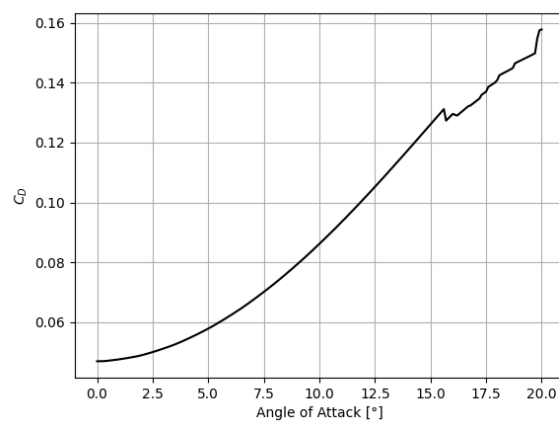


Figure 7.9: Kite drag curve

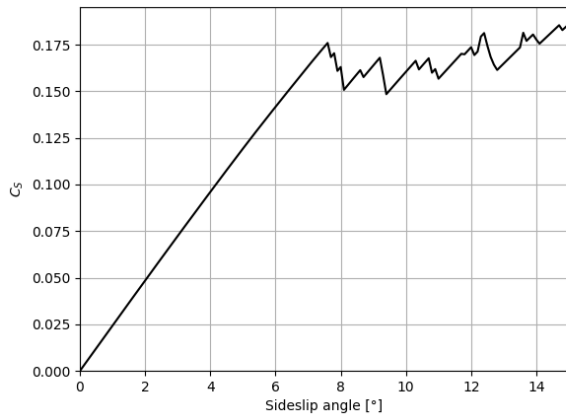


Figure 7.10: Kite side force coefficient curve

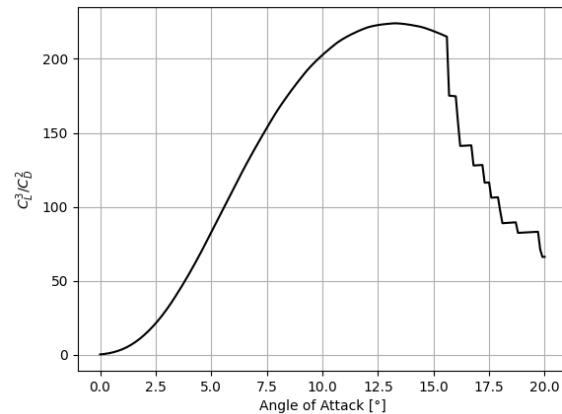


Figure 7.11: Kite power coefficient curve

To avoid stalling, it is decided that the kite will fly at an angle of attack of 2° lower than the stall angle of attack. This means that the kite will have a lift coefficient of 1.423 and a drag coefficient of 0.113. This drag coefficient is increased by 0.012 to take into account the bridle system and by 0.027 for the tether drag. Which makes the total drag coefficient 0.152. This means that the airborne system has a lift-over-drag ratio of 9.36.

7.4 | Bridle System

Here the bridle system will be discussed. Due to the limited time and resources available during this design synthesis exercise, a full design of the bridle system will not be performed. However, it is important to quantify some characteristics of the bridle system. The characteristic which will be looked at in this report is the drag coefficient of the bridle system ($C_{d_{bridle}}$). This is an important parameter as it can make up a significant portion of the total drag of the airborne system, thus a significant impact on the sizing of the kite.

To estimate the bridle system drag coefficient, the drag coefficient of the bridle system of a smaller kite (TU Delft LEI V3A kite [62]) will be calculated. It will then be assumed that the bridle system drag coefficient is equal for the larger kite being designed in this report.

To calculate the value of the bridle drag, a few assumptions are made.

- The entire bridle system moves at the same windspeed as the kite. In reality, the distance of the bridle system to the groundstation is lower than the distance between the groundstation and the kite. This means that the bridle system experiences a lower airspeed than what is assumed, hereby slightly overestimating the drag coefficient. Which makes this assumption conservative.
- The drag coefficient of the tether (normalised to the tether area) is assumed to be 1.1. We assume that the drag coefficient of the bridle system is equal to the drag coefficient of the tether which is assumed to be 1.1 [57]. Depending of the type of bridle line chosen, this value might change.
- It is assumed that all the bridle lines have a diameter of 2 mm. In [62] it is mentioned that the bridle system consists of 200 kgf sleeved line but that the TU Delft team will replace part of the system with 600 kgf sleeveless Dyneema[®] line. The 200 kgf line is assumed to be sleeved Dyneema[®] SK75 line with a diameter of 2 mm, the 600 kgf line is assumed to be 2.5 mm Dyneema[®] sleeveless line². This line is not significantly thicker than the 200 kgf line as it does not include a sleeve. As it is not known how much of the bridle system the Delft team replaced, it is assumed that the entire system has a diameter of 2 mm. The impact of this assumption will be discussed in a sensitivity analysis.

²https://services.crm.service.eu/raiminisite/Image/Download?docid=35383&dl=MIJNRAI_TOP_LIBRARY<tc=M IJNRAI_LOGIN_PRIVATEFILE

As discussed in [62], the total bridle line length is 108.441 m and it is assumed that the bridle line has a diameter of 2 mm. The drag coefficient of the bridle line is 1.1 when normalised to the bridle line area and the projected area of the TU Delft LEI V3A kite is 19.753 m² [62]. To calculate the drag coefficient of the bridle system, equation (7.4) is used.

$$C_{D_{bridle}} = C_{D_{line}} \frac{l_{bridle} \cdot d_{bridle}}{S} \quad (7.4)$$

Filling in all values, this gives a bridle system drag coefficient $C_{D_{bridle}} = 0.012$.

As discussed in the assumptions, the bridle lines were partially replaced by 2.5 mm sleeveless Dyneema[®] line. As a sensitivity analysis for the bridle system, the impact of changing the entire bridle system with 2.5 mm line will be discussed. Using equation (7.4), a bridle system drag coefficient of $C_{D_{bridle}} = 0.015$ is found. This would increase the projected kite area to 416 m².

7.5 | Performance Evaluation

In this section, the performance of the AWES part will be evaluated. This is done using the power curve to determine the capacity factor, kite projected surface area, reeling speeds, drum RPM and cycle times. The power curve is generated by code provided by Roland Schmehl [63] and modified and expanded for use in this project.

7.5.1 Theory

The theory that is used in this code is from [64] which is a further development of Lusincher [57, p. 47-64] who originally developed the operational strategy with 3 wind speed regimes. Figure 7.12 shows the forces and wind speeds at reel-out and reel-in. The maximal cycle power at each wind speed is determined by finding the optimal reel-out and reel-in speed. The optimal reel speeds are found by optimising the reel-out and reel-in factors for maximal cycle power at each wind speed. The reel-out/reel-in factor is defined as $v_{out/in} = f_{out/in} v_w$. To maximise the cycle power the kite is reeled in fast with high power which minimises the time it is not generating power and reels out slowly.

There are three wind speed regimes. In the first wind speed regime, $0 \leq v_w \leq v_{n,T}$, there are no limits on tether force or generator power and the reel-out and reel-in factors stay constant. Equation 7.5 is used for the first regime. In the second wind speed regime, $v_{n,T} \leq v_w \leq v_{n,P}$, the tether force is limited thus the reel-out factor is increasing as can be seen in Figure 7.14a so the system can produce more power. Equation 7.6 is used for the second regime. In the third wind speed regime, $v_{n,P} \leq v_w$, the PTO power limit and tether force limit are reached. The reel-out factor is decreasing with higher wind speeds. Equation 7.7 is used for the third regime.

This code does not include the kite mass during its computations. The power curve is generated using a two-state system where the kite goes from reel-out to reel-in instantaneously. Thus the reel-in phase is not computed for the curved reel-in trajectory as seen in Figure 7.14d but for the ideal reel-in trajectory.

$$p_{c,opt} = \max_{f_o, f_i} \left\{ \left[(\cos\beta_o - f_o)^2 - \frac{\gamma_i}{\gamma_o} \frac{(\sqrt{1 + E_i^2(1 - f_i^2)} - f_i)^2}{1 + E_i^2} \right] \frac{f_i f_o}{f_i - f_o} \right\} \quad (7.5)$$

$$p_{c,opt} = \max_{f_i} \left\{ \left[\frac{1}{\mu_F^2} (\cos\beta_o - f_{n,F})^2 - \frac{\gamma_i}{\gamma_o} \frac{(\sqrt{1 + E_i^2(1 - f_i^2)} - f_i)^2}{1 + E_i^2} \right] \frac{f_i [(\mu_F - 1)\cos\beta_o + f_{n,F}]}{\mu_F f_i - [(\mu_F - 1)\cos\beta_o + f_{n,F}]} \right\} \quad (7.6)$$

$$p_{c,opt} = \max_{f_i} \left\{ \left[\left(\cos \beta_o - \frac{f_{n,P}}{\mu P} \right)^2 - \frac{\gamma_i \left(\sqrt{1 + E_i^2 (1 - f_i^2)} - f_i \right)}{\gamma_o (1 + E_i^2)} \right] \frac{f_i f_{n,P}}{\mu P f_i - f_{n,p}} \right\} \quad (7.7)$$

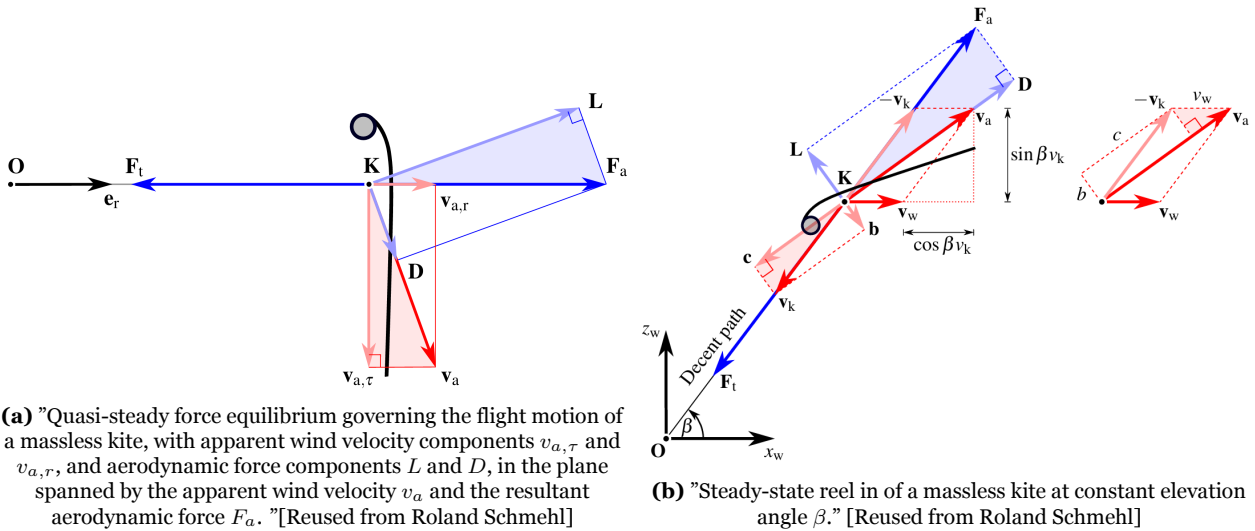


Figure 7.12: (a) quasi-steady force equilibrium and (b) reel-in velocities.

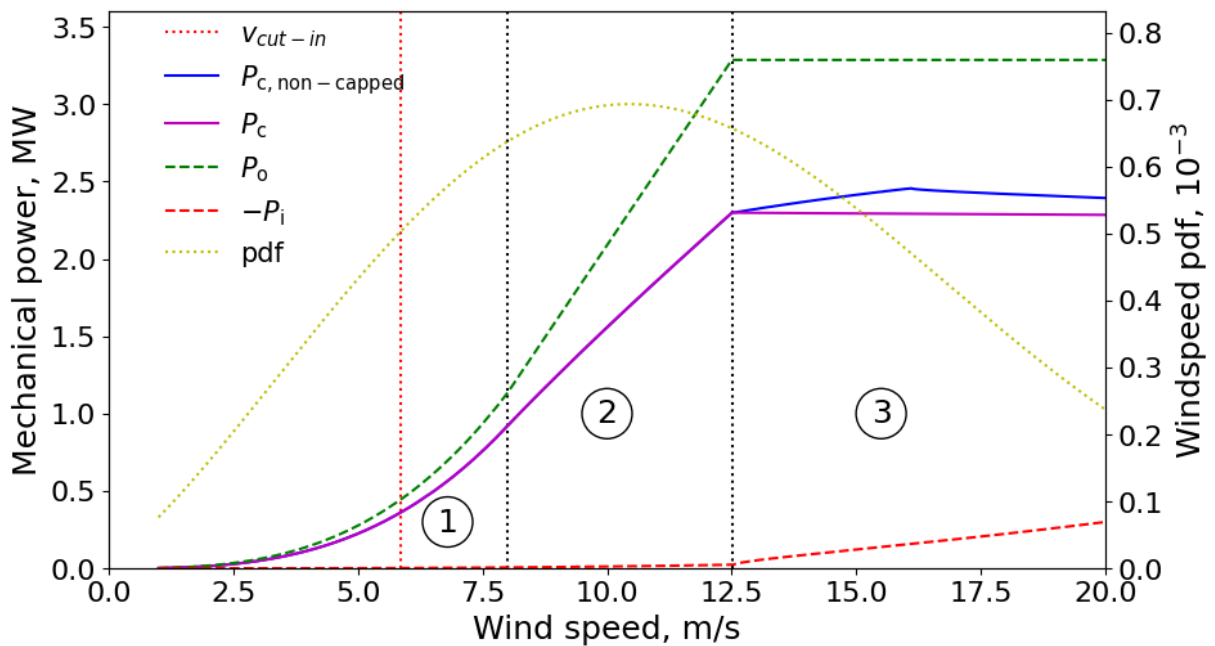


Figure 7.13: Power curve showing the three different wind speed regimes, the cut-in wind speed (v_{cut-in}), cycle power (P_c), reel-out power (P_o), reel-in power (P_i) and the wind speed probability density function (pdf)

7.5.2 Operations

Operational Height

The kite operates from a tether length of 400 m and starts reeling back in from a tether length of 1000 m. This corresponds to an operational length of 600 m. The operational range was determined while sizing the tether and is explained in Section 7.6. The elevation angle during reel out is 30° together with an average tether length during operation of 700 m the average operational height equals 350 m.

The elevation angle was chosen at 30° as this is a good compromise related to altitude, tether drag and tether length [57, p.61]. The power curve computations are done for the average operational height.

Cycle Times

The cycle times are decreasing with higher wind speeds as seen in Figure 7.14c because the reel-out and reel-in speeds are increasing. In wind speed regime 3 the cycle times are starting to become more constant. The percentage of time the kite is reeling out at the rated wind speed is 70%, this is the lowest percentage of all the wind speeds. The highest reel-out percentage is in wind speed regime 1 and equals 81%.

Reeling Speeds

A graph showing the reeling speeds and the drum RPM can be found in Figure 7.14b. The reel-out speed reaches a maximum at the end of wind speed regime 3 of 6 m s^{-1} with an RPM of 41. The reel-in speed reaches its maximum at 20 m s^{-1} with a value of 15.3 m s^{-1} since it is capped at this reel-in speed. The corresponding maximum reel-in RPM is 104. The maximum reel-in speed was calculated and is equal to 18 m s^{-1} as from literature 15 m s^{-1} is realistic [65] and the WaveWings unit will be more advanced than other earlier designs.

Cycle Power

The cycle power is capped since the system produces more power than the rated power limit of 2.3 MW. This is necessary since the power transmission infrastructure is designed for a power output of 2.3 MW per unit. The cycle power is capped by calculating the reel-in factor so that the cycle power does not exceed 2.3 MW. The result of limiting the cycle power can be seen in Figure 7.13 and Figure 7.14 as the magenta line.

Reel-Out Angle

In wind speed regime 3, the generator power limit limits the reel-out power. To ensure the kite does not produce more power than this limit, the tether force is limited by flying the kite at a higher elevation angle. The increase in reel-out angle can be seen in Figure 7.14a. The maximum reel-out angle is 57° .

Reel-In Angle

The reel-in angle, seen in Figure 7.14a, is the optimal angle to reel the kite in. However, in practice the kite almost never reaches this angle. When the kite reaches the end of the reel-out phase it starts reeling in immediately and moves to the optimal reel-in angle. But most times the kite has already been reeled in enough before it reaches the optimal reel-in angle or it reaches it when it has only a few meters still to go. Such a trajectory is visualised in Figure 7.14d, in this figure the trajectory was plotted for reel-out and reel-in at 12.5 m s^{-1} . Note that the power curve and its respective characteristics are calculated assuming the ideal reel-in angle and not by the reel-in trajectory shown in Figure 7.14d.

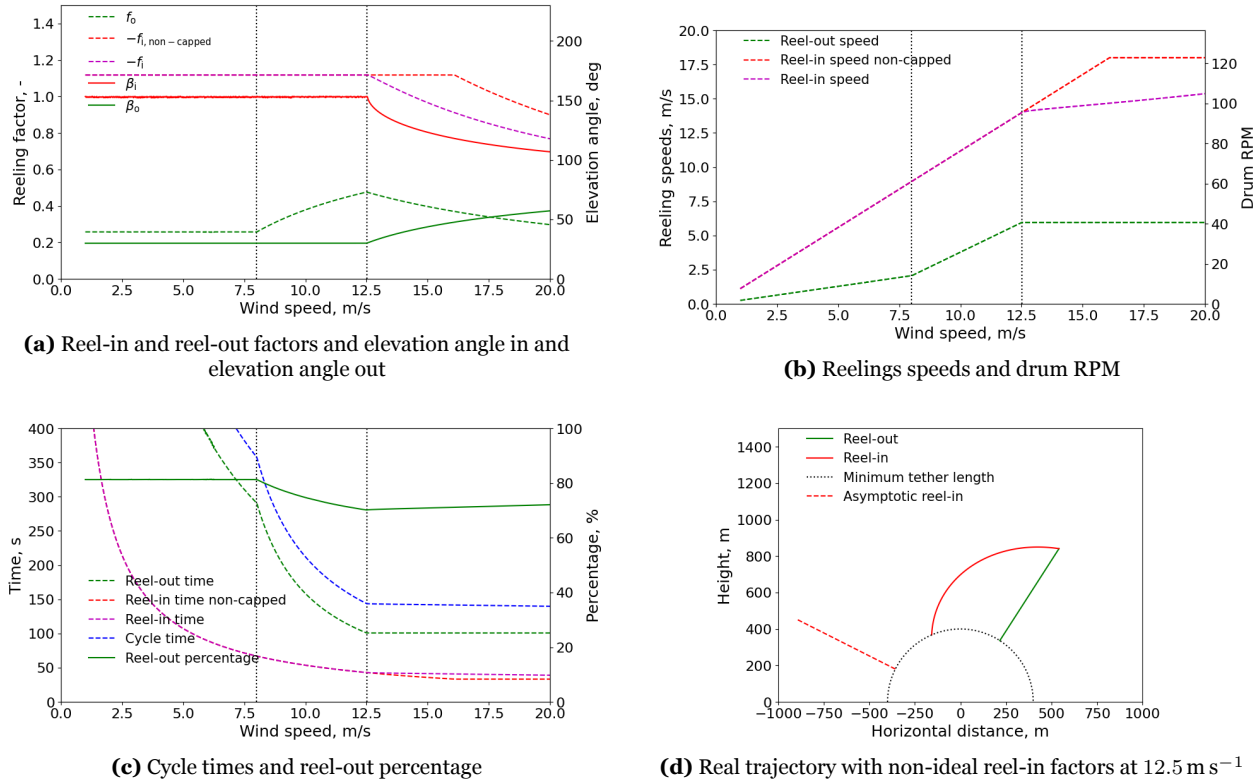


Figure 7.14: Overall Caption for all figures

7.5.3 Cut-in wind speed

Another important performance metric of the kite is the cut-in wind speed. This is the minimum wind speed at which the kite can be launched, so having a lower cut-in wind speed means that the range of wind speeds in which the system can be operated gets larger. This has an influence on the capacity factor of the system. As the launching mechanism is a static launch the calculation for the cut in wind speed is straight forward, the lift force is set equal to 1.2 times the weight of the kite, bridle system and KCU. This safety factor of 20% is included because part of the tether is also lifted, there might be friction in the drum, etc. Equation (7.8) gives the formula for the cut-in wind speed.

$$v_{w_{cut-in}} = \sqrt{\frac{1.2(m_{kite} + m_{bridle} + m_{KCU})g}{\frac{1}{2}\rho S C_L}} \quad (7.8)$$

Where m_{kite} is 456.1 kg, m_{bridle} is estimated to be 100 kg and m_{KCU} is 112 kg. The density is assumed to be the sea level value of 1.225 kg m⁻³, the projected surface area is 400 m² and the lift coefficient is 1.423. Filling in all these values, the cut-in wind speed is calculated to be 4.4 m s⁻¹. This satisfies *USR-REQ-1-1-AWE-6-1*

7.5.4 Capacity Factor, Average Power, and Yearly Flight Hours

The capacity factor is an important metric for wind energy farms. It is defined by the average power divided by the rated power of the system.

The cut-in wind speed of the system defines the wind speed required for flight. This is taken into account when calculating the average power. The cut-in wind speed at the operational height is derived from the cut-in wind speed at 20 m height by the velocity profile which has a value of 5.9 m s⁻¹ and can be seen in Figure 7.13 as the vertical red dotted line.

To calculate the average power the wind speed probability density function from Chapter 5 is multiplied by the capped cycle power for each wind speed and then summed together. This results in an average power of 1.36 MW, which when divided by the rated power of 2.3 MW results in a capacity factor of 59% which satisfies *USR-REQ-2*.

The yearly flight hours can be derived from the wind speed probability density function by taking the sum of it between the cut-in wind speed and the maximum wind speed and then multiplying it by the number of hours in a year. This results in a value of 6758 hours.

7.5.5 Kite Projected Surface Area

The kite projected surface area is determined by taking the lift and drag coefficient from Section 7.3 and varying the nominal tether force and nominal generator power until the capacity factor and rated power satisfy the *USR-REQ-1-1-AWE*. A lot of iterations took place to find the final values for the nominal tether force, nominal generator power and kite surface area. The nominal tether force was also an important factor when sizing the tether thus this had influence on it. In the end, this resulted in a projected surface area of 400 m², which corresponds to a flat area of 470 m². A kite with this projected surface area is able to produce 3.6 MW of power which satisfies *USR-REQ-1-1-AWE-2*.

7.5.6 Kite Mass

The mass of the kite also needs to be known for several reasons. The kite mass is estimated by calculating the specific mass of the TU Delft LEI V3 kite [62]. This kite has a mass of 10.4 kg (not including the mass of the air in the tubes) and a flat area of 25 m². After discussing this with experts from the field³, it was decided that a scaling factor of 1.25 is required to scale the mass of the kite. Equation (7.9) is used to determine the mass of the kite.

$$m = m_{V3} * \left(\frac{S_{flat}}{S_{V3,flat}} \right)^{1.25} + V_{tubes} \cdot \rho_{tubes} \quad (7.9)$$

As the mass of the TU Delft LEI V3 kite does not include air, this is included separately. After reviewing sporting kite literature, it is found that kites are usually pumped up to an over-pressure of 8 psi (=552 hPa). This means that the total pressure is 154% of the sea level pressure. Using the ideal gas law and assuming the pressure and volume doesn't change, it is found that the air density in the tubes is 154% of the sea level density or 1.887kg/m³. The tube volume is determined by integrating the leading edge volume which is 25.9 m³ and adding 10 m³ to take into account the struts. Inputting the density, a flat surface area of 470 m² and a tube volume of 35.9 m³, a kite mass of 456.1 kg is found.

7.5.7 Sensitivity Analysis for Power Curve

A sensitivity analysis is performed to study the effect of varying the cut-in wind speed and kite area. Each variable is varied by ±20% and the effect on the rated power and the capacity factor is noted down in Table 7.2.

Table 7.2: Result of sensitivity analysis power curve

Cut-in wind speed	-20%	Reference	+20%
Capacity factor %	59.76	59.11	57.78
Kite projected surface area	-20%	Reference	+20%
Rated power MW	2.07	2.30	2.30
Capacity factor %	54.63	59.11	62.01

As expected the capacity decreased with an increase in cut-in wind speed and vice versa. Decreasing the kite projected surface decreased the rated power and capacity factor. When increasing the projected surface area the rated power does not increase since it is capped by the nominal generator power.

³Dr.-Ing. R. Schmehl and Ir. O. Cayon, 19/06/2024

7.6 | Tether

The tether is a vital part of the airborne system as it connects the kite to the ground station and delivers the force generated by the kite to the drum, which powers the PTO. In this section, the tether will be sized and the lifetime will be determined. The results from the tether sizing can be seen in Table 7.3.

7.6.1 Length, Diameter, Material, and Mass

First, the length is determined. The operational range is 600 m. The operational range is the length of the kite's tether to reel in and reel out during operation. Extra tether is added to this operational range to ensure safe operation. The amount of extra tether is calculated by multiplying the maximum reel-out speed, 6 m s^{-1} , with 15 sec.

These 15 seconds are the time the system has to go from reel-out to reel-in without using all of the rope. Thus the total tether length is 1100 m rounded off. The operational range was determined with respect to the bending lifetime since a longer tether increased the cycle time which decreased the amount of cycles per year.

Next is the tether diameter, the diameter was chosen by multiplying the tether safety factor of 4 with the nominal tether force to determine the needed break load and then an appropriate diameter was chosen. From Section 7.5 the nominal tether force was chosen to be 613 kW thus the diameter is 56 mm.

The chosen material for the tether is Dyneema® SK78 as it is extremely strong and very light and the polyurethane coating resists UV radiation. The UV resistance means it satisfies *USR-REQ-1-1-AWE-4-3*. The specific density of the tether with a diameter of 56 mm is 172 kg m^{-1} ⁴. This results in a tether mass of 1874 kg.

7.6.2 Lifetime due to Dynamic Bending

The tether is bent constantly under high loads during reeling in and out. This damages the tether and it will need to be replaced. Thus the bending lifetime of the tether needs to be estimated.

This is done by dividing the cycles to failure (CTF) by the amount of single bends under high load per year. The cycles to failure of this rope is determined to be 500000 from figure 33.17 in [57, p. 563-587] with nominal stress in the tether of 249 MPa and a $\frac{D_{drum}}{d_{tether}}$ ratio of 50.

The amount of single bends per year is determined by having 6758 kite fly-hours per year, which was a result in Subsection 7.5.4, with an average cycle time of 166 s and 2 bends under high load per cycle. Two bends per cycle are due to one bend on the drum and one bend on the guide wheel that makes sure the tether is placed correctly on the drum. This is then all combined in Equation 7.10 with an added safety factor of 1.25.

$$Bending\ lifetime = \frac{CTF}{1.25 \cdot 2 \cdot \frac{flight\ hours \cdot 3600}{t_{avg-cycle}}} \quad (7.10)$$

The result is that the tether has a bending lifetime of 1.36 years.

7.6.3 Lifetime due to Creep

The tether will retain a permanent elongation over time when loaded [57, p. 563-587]. This will result in a thinner tether and thus increase the stress in the tether will increase. Eventually, the tether will rupture. The creep rupture lifetime can be taken from figure 33.16 in [57, p. 563-587]. With a nominal tether stress of 249 MPa it has a safe working life of 20 years. There are factors that increase this safe working like day/night temperature factor, season temperature factor and loading factor [57, p. 563-587]. However since the creep lifetime is already satisfactory, these factors will not be needed.

⁴<https://www.vanbeelengroup.nl/en/products/categorie/rope/d12-sk78.html>, accessed on June 24, 2024

Table 7.3: Tether characteristics

Parameter	Values	Unit
Length	110	m
Diameter	56	mm
Mass	1874	kg
Lifetime	1.35	years

7.7 | Kite Control Unit

The kite control unit (KCU) is positioned between the tether and the bridle system. It controls the movement of the kite during reel-out, reel-in, launch and retrieval. To estimate the mass of the KCU a reference system with a kite of 25 m² and a KCU mass of 7 kg is used to upscale the KCU [57, p. 410]. This resulted in a KCU mass of 112 kg. The KCU needs power to steer the kite. Using information received by Kitepower, the KCU power can be estimated by upscaling a smaller system to the WaveWing system. Kitepower's KCU needed 200 W for a 20 kW system, upscaling this to 2.3 MW system results in a KCU power of 23 kW.

The KCU will include actuators, drums and brakes to steer the kite. For communication and data gathering it will include a computer, an transceiver, a microphone, a barometer, pitot tube and an IMU. It also includes a protective foam cover to protect the KCU during launch and retrieval if it bumps against something on the buoy. To power the KCU it will contain a wind turbine, a battery and a power distribution unit. Lastly, it includes a safety release pin to directly depower the kite when it is uncontrollable and could damage the drum and other subsystems located on the buoy. The KCU will be equipped with a warning light to satisfy **USR-REQ-1-2-1-3**.

7.8 | Airborne System Overview

In this section, a overview of all the design and performance parameters of the airborne system are provided in tables 7.4 and 7.5. The kite shape is visualised with the means of a technical drawing.

Table 7.4: AWES design parameter overview

Parameter	Value
Airfoil Camber	8%
Leading Edge thickness	10%
Aspect ratio	3.5
Span	50.0 m
Planform area	400 m ²
Elliptical curvature ratio	1.6
Kite mass	456.1 kg
KCU mass	110 kg
Strutt spacing	2.00 m
Flat surface area	470 m ²
Flat span	64.6 m
Flat aspect ratio	8.9
Tether material	DYNEEMA® SK78
Tether length	1100 m
Tether diameter	56 mm

Table 7.5: AWES performance parameter overview

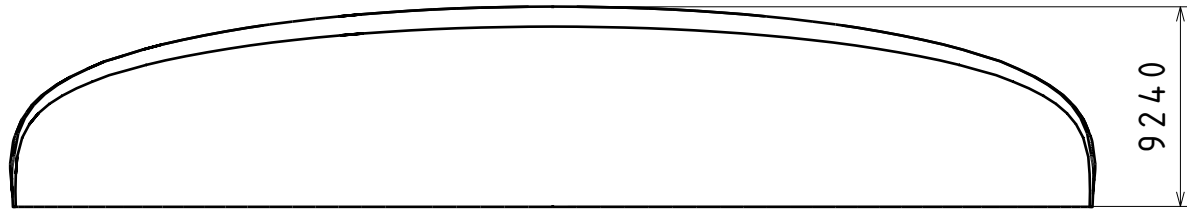
Parameter	Value
Powered angle of attack	13.5°
Lift coefficient	1.423
Kite drag coefficient	0.113
Bridle drag coefficient	0.012
Tether drag coefficient	0.027
Tether operational length	400-1000 m
Elevation angle	30°
Cut-in wind speed	4.4 m s ⁻¹
Rated wind speed	12.5 m s ⁻¹
Power (reel-out, rated)	3.6 MW
Power (reel-in, rated)	-20 kW
Cycle time	144 s
Rated power	2.3 MW
Capacity factor	59%
Yearly flight hours	6758 hours

D

C

B

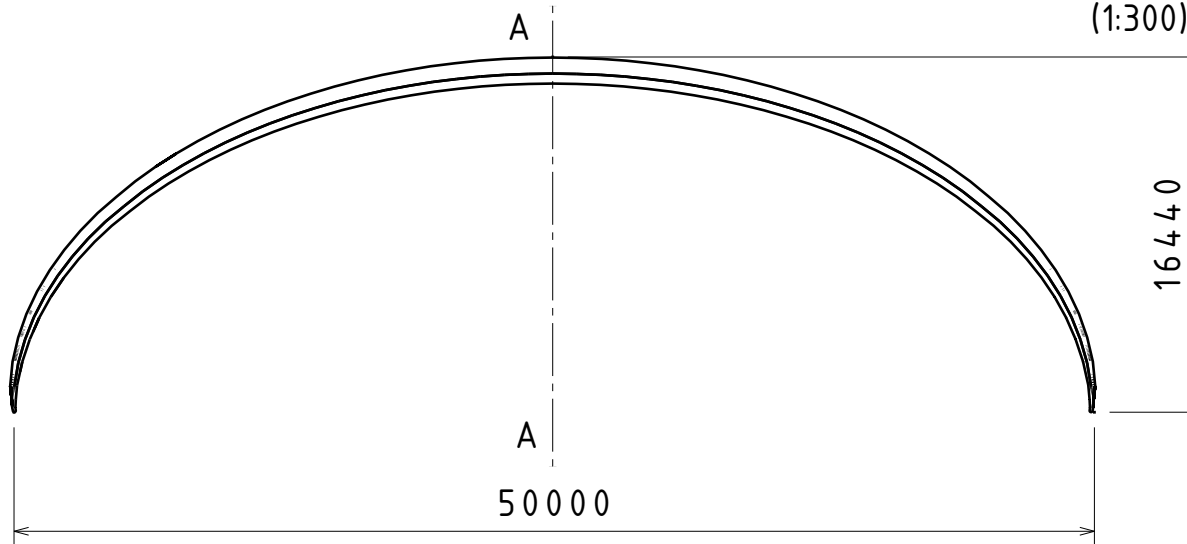
A



9240



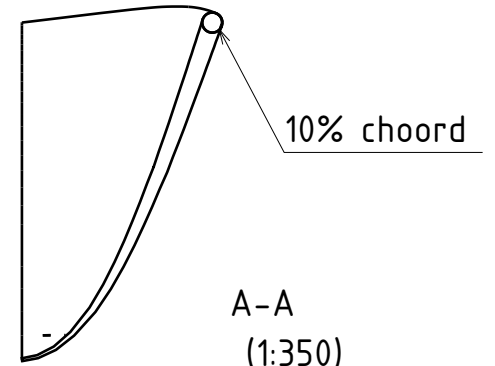
TOP
(1:300)



16440

50000

FRONT
(1:300)



10% choord

A-A
(1:350)

This drawing is our property.
It can't be reproduced
or communicated without
our written agreement.

TU Delft University

DRAWING TITLE

Kite Drawing

DRAWN BY
DSE Group 5

DATE
25/06/2024

CHECKED BY
DSE Group 5

DATE
25/06/2024

SIZE
A4

DRAWING NUMBER

2

REV
X

DESIGNED BY
DSE Group 5

DATE
-/06/2024

SCALE

1:300

WEIGHT(kg)

457.1

SHEET

1/1

D

A

8 | Floating System

As mentioned in Chapter 7, this chapter discusses the floating system. The following section will describe all of the systems involved in the floating system. First, the requirements involved will be shown in a requirement table. Afterwards, the floating buoy for the WEC system together with the PTO system will be explained and sized. Afterwards, the submerged body which contains the ballast, the Mooring subsystem and the anchor will be assessed. Then, the main control system, the drum subsystem, and the launch-retrieval tower will be assessed. Finally, the Power Subsystem characteristics, the material selection, and the communication and data-handling will be discussed

8.1 | Requirements

As shown in Table 8.1, these requirements are related to the power, loading, sizing, and environmental characteristics that ensure the robustness of the design, acting as guidelines for the upcoming subsections.

Table 8.1: Requirements for Floating Subsystem (part 1)

Identifier	Requirement
USR-REQ-1-1-AWE-3	The AWES shall convert harvested energy to electrical energy.
USR-REQ-1-1-AWE-4-7	The AWES connection between the tether and the buoy shall withstand a maximum force of 613 kN.
USR-REQ-1-1-AWE-4-8	The AWES structures shall not resonate with waves.
USR-REQ-1-1-AWE-5-4-2	The generator shall be capable of generating 3.6 MW power.
USR-REQ-1-1-AWE-6	The AWES shall launch the system.
USR-REQ-1-1-AWE-6-3	The AWES shall launch the kite in 5 minutes.
USR-REQ-1-1-AWE-7	The AWES shall retrieve the system.
USR-REQ-1-1-AWE-7-1	The AWES shall retrieve the kite in 5 minutes.
USR-REQ-1-1-AWE-7-3	The tether shall be retractable around a drum.
USR-REQ-1-1-WEC	The WEC part of one unit shall produce 0.2 MW of rated electrical power.
USR-REQ-1-1-WEC-2	The WEC shall survive operational environment conditions.
USR-REQ-1-1-WEC-2-1	The WEC shall withstand a salinity of 35 grams per litre.
USR-REQ-1-1-WEC-2-2	The WEC shall operate between 9.5°C to 34.5°C.
USR-REQ-1-1-WEC-2-3	A fatigue analysis shall be carried out on the oscillator of the WEC system.
USR-REQ-1-1-WEC-2-4	Buoy shall not sink; a minimum volume shall be calculated to ensure that at least neutral buoyancy is achieved.
USR-REQ-1-1-WEC-2-6	The WEC shall be waterproof.
USR-REQ-1-1-WEC-2-7	The WEC shall be fully submersible.
USR-REQ-1-1-WEC-3	A unit shall be transportable back to shore.
USR-REQ-1-1-WEC-4	The system shall be anchored to the seafloor.
USR-REQ-1-2-1-2	The WEC shall be equipped with warning lights
USR-REQ-2	The farm shall have a capacity factor between 50% and 60%.
USR-CON-1-5-1	After 20 years the farm shall have a power output of 70% of its initial.

Table 8.2: Requirements for Floating Subsystem (part 2)

Identifier	Requirement
USR-REQ-1-1-WEC-5	Buoy weight shall be at least the induced peak tether load.
USR-REQ-1-1-WEC-6	The SB shall have a maximum acceleration of $0.06m/s^2$
USR-REQ-1-1-WEC-7	The SB shall be stable
USR-REQ-1-1-WEC-8	The SB shall provide more buoyancy than its weight plus the PTO force combined.
PGO-REQ-3-1	The offshore substation and onshore substation must be compatible.
USR-REQ-4	The system shall be able to communicate between the different systems and subsystems.
USR-REQ-4-1	The communications subsystem of the airborne system and the floating system must be compatible.
USR-REQ-4-2	The communications subsystem of the floating system must have a rating of IP65 or higher.
USR-REQ-4-3	The communications subsystem of the airborne system must have a rating of IP65 or higher.
USR-REQ-4-4	The communications subsystem must be redundant in case internet fails.
USR-REQ-4-5	The communications subsystem and the offshore substation must be compatible.

8.2 | Floating Buoy with PTO Unit

This section describes the sizing process of the WEC system, starting with a theoretical background in Subsection 8.2.1, the simulation pipeline in Subsection 8.2.2, a sensitivity analysis to understand the effect of design parameters on the absorbed power in Subsection 8.2.3, followed by a discussion of the WEC sizing results and recommendations and limitations of the process in Subsection 8.2.5.

8.2.1 Frequency Domain Modelling

Numerical and analytical methods exist for estimating the absorbed power of WECs. For this stage in WaveWings project, analytical methods are chosen over numerical simulations due to the increased complexity and computation time of the latter. The time-averaged absorbed power of a WEC is estimated using linear wave theory frequency domain modelling. J. Tan [66] outlined a method that is reproduced here. Firstly, consider that the motion of a rigid floating body subjected to ocean waves and limited to heaving motion only can be described using Newton's second law, as shown in Equation 8.1.

$$Ma(t) = F_{hs}(t) + F_e(t) + F_{pto}(t) + F_r(t) \quad (8.1)$$

Where M represents the inertial matrix of the oscillating buoy, a is the buoy's acceleration, F_{hs} is the hydrostatic force, F_e is the wave excitation force, F_r is the wave radiation force, F_{pto} is the PTO force. According to J. Falnes [67], the EOM can be re-written in the form of complex amplitudes assuming harmonic motion (regular wave conditions) and a linear PTO model, as shown:

$$\hat{F}_e(\omega) = [R_r(\omega) + R_{pto}] \hat{u} + i\omega \hat{u} [M + M_r(\omega)] + i\hat{u} \left[-\frac{K_{pto}}{\omega} - \frac{K_{hs}}{\omega} \right] \quad (8.2)$$

Where $R_r(\omega)$ is the hydrodynamic damping coefficient, R_{pto} is the PTO damping coefficient, ω is the wave frequency, $M_r(\omega)$ is the added mass of the WEC, \hat{u} is complex amplitude of the vertical velocity, K_{pto} is the PTO stiffness coefficient, and K_{hs} is the hydrostatic stiffness. The intrinsic impedance of the heaving buoy $Z_m(\omega)$, where $X_m(\omega)$ is the intrinsic reactance, is introduced as shown:

$$Z_m(\omega) = R_r(\omega) + iX_m(\omega) \quad (8.3)$$

$$X_m(\omega) = \omega[M + M_r(\omega)] - \frac{K_{hs}}{\omega} \quad (8.4)$$

Similarly, the PTO impedance $Z_{pto}(\omega)$ can be written in terms of the PTO reactance $X_{pto}(\omega)$ as shown.:

$$Z_{pto}(\omega) = R_{pto}(\omega) + iX_{pto}(\omega) \quad (8.5)$$

$$X_{pto}(\omega) = -\frac{K_{pto}}{\omega} \quad (8.6)$$

The introduction of these impedance variables allows \hat{u} to be re-written as shown:

$$\hat{u}(\omega) = \frac{\hat{F}_e(\omega)}{Z_m(\omega) + Z_{pto}(\omega)} \quad (8.7)$$

Then, the time averaged absorbed power \bar{P}_a of the WEC can be obtained, for regular wave conditions, using:

$$\bar{P}_a = \frac{1}{2} R_{pto} |\hat{u}|^2 \quad (8.8)$$

In order to use Equation 8.8, the hydrodynamic coefficients $R_r(\omega)$, $M_r(\omega)$, and F_e are determined using a Boundary Element Method (BEM) solver for a given WEC geometry and mass [4, 5]. R_{pto} and K_{pto} are tuned to maximize the power output. ω is the range of wave frequencies expected on-site. Hydrostatic coefficients, K_{hs} , for vertical cylinders undergoing heaving motion are given by Equation 8.9 from R. Riyanto and S. Rahmawati [68].

$$K_{hs} = \rho_w g \pi R^2 \quad (8.9)$$

Where ρ_w is the density of sea water and R is the radius of the WEC. Evaluating \bar{P}_a results in different powers for different wave frequencies.

8.2.2 Simulation Pipeline

In order to strategically size the integrated buoy-WEC system, a simulation pipeline is established. “BEMSolver” shall refer to the use of the “CAPYTAINE” [3] Python library developed by Matthieu Ancellin as a fork to “NEMOH” originally developed at École Centrale de Nantes [69] but adapted to carry out the study parametrically on large sets of design conditions, “BEMIO” shall refer to the use of a “WEC-Sim” [4] tool that can extract hydrodynamic coefficients from the data provided by “BEMSolver”, and “WEC Solver” shall refer to the use of a software developed in-house by the WaveWings 2024 DSE team to perform parametric studies of the design space through correlation with the power output that can be tuned at will [5]. Macroscopically-speaking, the pipeline abides to Figure 8.1. However, for insight into the behaviour of each block, the detailed cascade is shown in Figure 8.2.

In order to use the above-mentioned softwares appropriately, a set of assumptions must be strictly respected to ensure the validity of the results whilst allowing for an evaluation of the limitations of the approach.

BEMSolver Assumptions:

- The fluid is inviscid.

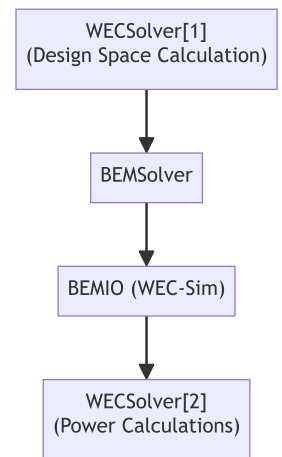


Figure 8.1: Overview WEC Sizing Pipeline

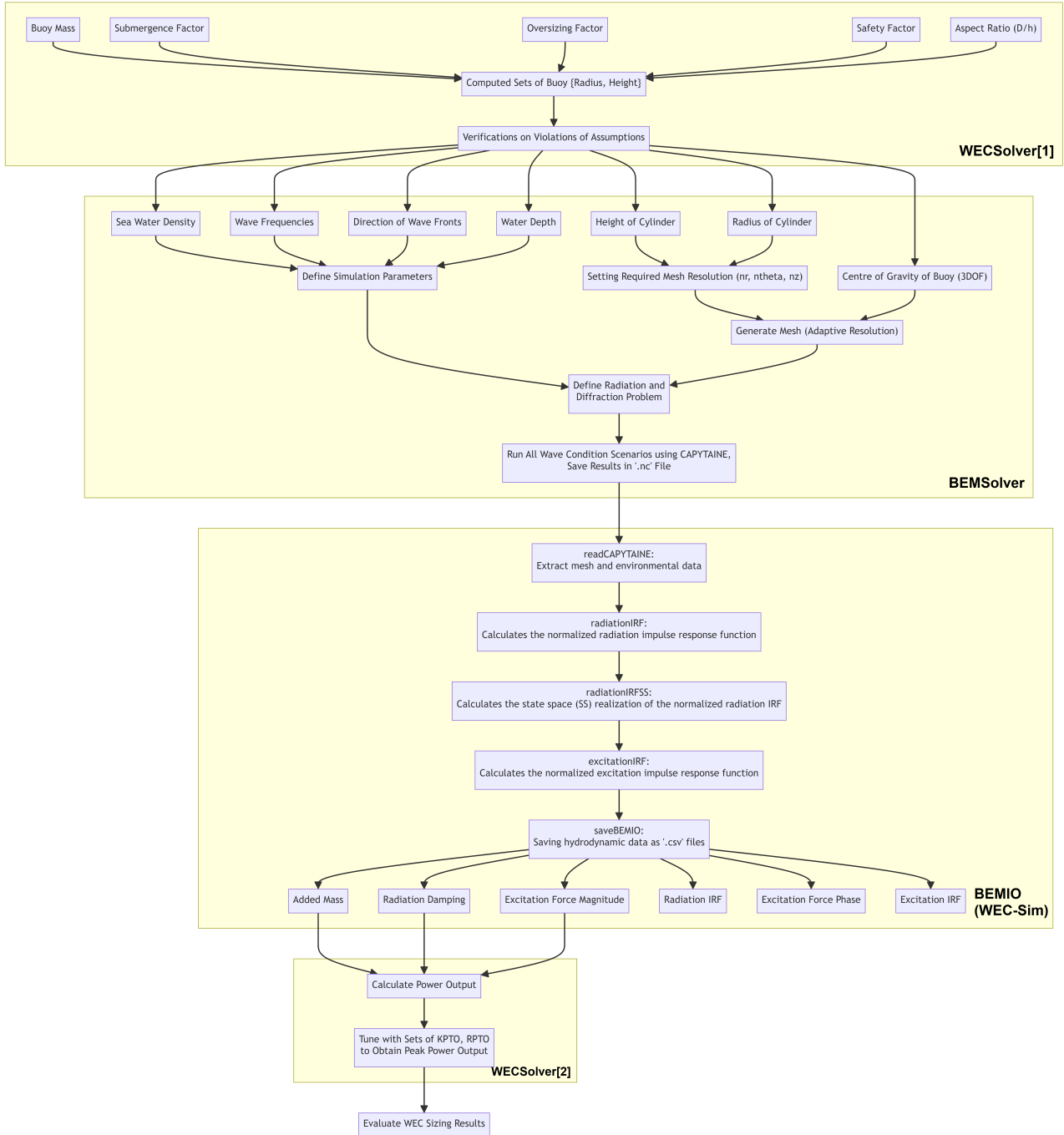


Figure 8.2: Detailed WEC Sizing Pipeline

- The fluid is incompressible, that is $\nabla \cdot \vec{u} = 0$ for flow velocity vector \vec{u} .
- The flow is irrotational, that is $\nabla \times \vec{u} = 0$ for flow velocity vector \vec{u} .
- The wave amplitude is small with respect to the wavelength, that is $A_{wave} \ll \lambda$ where $\lambda = gT^2/2\pi$.
- The amplitude of the body motion is small with respect to its dimension, that is $A_{body} \ll h_{buoy}$.
- The breadth of the buoy is small with respect to the wavelength, that is $2r < 0.10 \cdot \lambda$.
- The sea bottom is flat, and the water depth is denoted as h_{water} ; the medium can be considered of infinite depth if $h_{buoy} > \lambda$ where the sea floor does not impact surface-level dynamics and PTO behaviour.
- The largest panel of the object's surface mesh shall respect $r < \lambda/8$. Adaptive meshing tools are used to generate lowest resolution meshes whilst respecting this limit in order to accelerate the solver.

WEC Solver Constraints:

- Buoy shall not tip-over during rolling and pitching motion before threshold $\theta_{stability}$. This was determined using the stability check defined in Subsection 8.2.6.
- Buoy shall be constrained to heaving motion only along the Z-axis (1 degree of freedom) and shall be the primary source of generated power.
- Regular waves at a defined amplitude and period shall be used as an environment.
- The buoy dimensions are computed such that the buoy has static buoyancy.

8.2.3 Sensitivity Analysis

Sizing a WEC system requires multidimensional thinking; an initial exploration of the influence of design variables on the power output is carried out before tackling the fine-tuning of these parameters in Subsection 8.2.4. For the scope of this project, due to simulation constraints, the shape of the WEC is constrained to a vertical circular cylinder, leaving the parameters listed below as a design space. Since, crucially, the sizing of a WEC system is highly dependent on the frequency ranges induced by the wave environment, power outputs are plotted against relevant parameters in a frequency band ranging from 0.01 rad s^{-1} to 2.01 rad s^{-1} in steps of 0.01 rad s^{-1} . However, this wider frequency interval shall solely be utilized to understand global trends in the optimization process, acting as a sensitivity analysis protocol. Therefore, to refine the search, zoomed-in plots are provided in the range of $0.7241 \text{ rad s}^{-1} < \omega_{env} < 0.9807 \text{ rad s}^{-1}$ since the location survey presented in Chapter 5 establishes an interquartile range of wave frequencies where $\omega_{0.25} = 0.7241 \text{ rad s}^{-1}$, $\omega_{0.50} = 0.8331 \text{ rad s}^{-1}$, $\omega_{0.75} = 0.9807 \text{ rad s}^{-1}$, as shown in Figure 8.8. Notably, however, the design is sized and tuned according to $\omega_{0.50} = 0.8331 \text{ rad s}^{-1}$ as the median condition represents the most encountered wave condition. In order to condense the performance of the sizing to two metrics, the average power output and capacity factor are computed. The average power output is obtained by multiplying a probability density function with the tuned power curve, sized relative to the median condition, over all relevant frequencies. The capacity factor is given by the average power divided by the maximum power of the WEC.

1. AR : Aspect Ratio, Diameter over Height
2. $SubF$: Submergence Factor
3. $SafF$: Safety Factor
4. K_{pto} : Stiffness Coefficient of Power Take-Off Unit
5. R_{pto} : Damping Coefficient of Power Take-Off Unit

Firstly, the aspect ratio (slenderness) AR is varied while keeping $SubF = 0.5$ and $SafF = 1.0$ constant to understand its effect on absorbed power. Since the simulation time is significant, appropriate step sizes and reasonable AR values are used to cover the whole range of feasible dimensions.

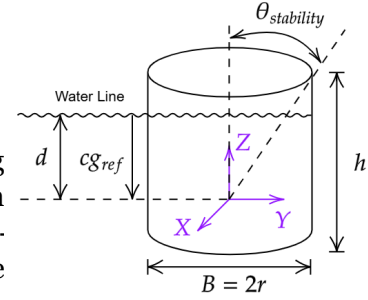
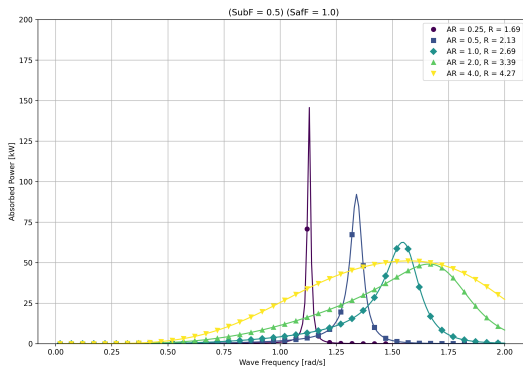
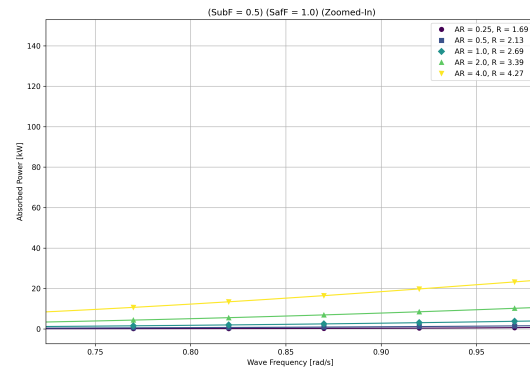


Figure 8.3: Vertical Cylinder Parameters



(a) Wide Frequency Band



(b) Target Frequency Band

Figure 8.4: Sensitivity Analysis for Aspect Ratio

Figure 8.4a demonstrates that higher AR s are correlated with lower average absorbed power but across larger frequency bands whilst lower aspect ratios lead to higher power returns but across narrow frequency bands, centered about lower (leftward shifting) frequencies. When considering the target frequency band in Figure 8.4b, bodies with high AR s are correlated to higher power. Hence, $AR = 4.0$ was chosen to proceed to the next step. Provided that $SubF = 0.5$ for $AR = 4.0$ leads to $R = 4.27\text{m}$, it was discussed with system integration engineers that the packing of all components in the floating buoy would require $R \geq 5.24\text{m}$. Therefore, as a next step, various $SubF$ are tested against $SafF = 1.0$ in an attempt to extract maximum power with the radius requirement in mind. The $SubF$ values used in the simulation are chosen to cover a wide range of feasible values while minimizing simulation time.

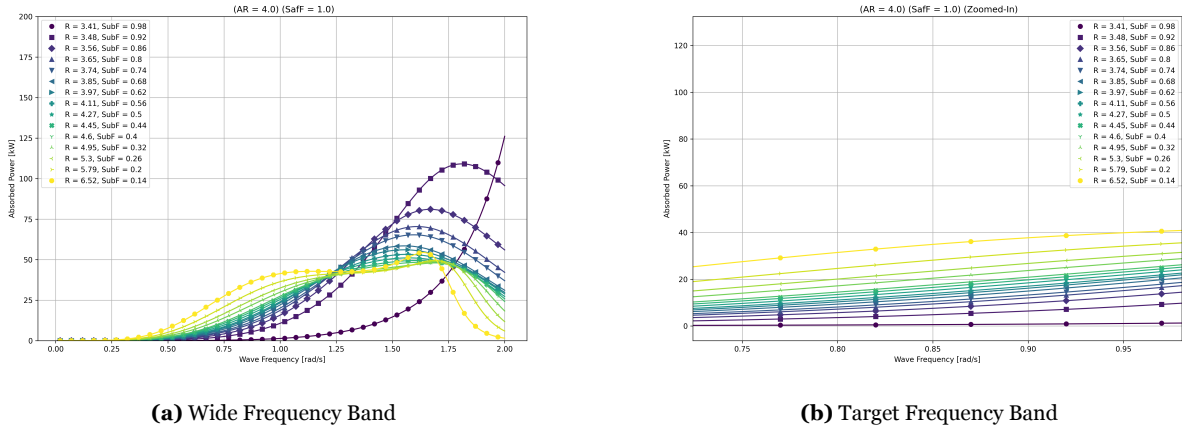


Figure 8.5: Sensitivity Analysis for Submergence Factor

Figure 8.5a demonstrates the unpredictability of optimal designs suited to a target submergence factor due to transient behaviours, highlighting the necessity for sizing the buoy with respect to a target frequency band. However, generally-speaking, higher absorbed power can be found at higher frequencies for increasing submergence factors. Contrarily, for the target frequency band, Figure 8.5b demonstrates that decreasing submergence leads to a quasi-monotonic increase in absorbed power in the target frequency band. Choosing the dimensions that lead to the highest absorbed power in the target frequency band gives: $AR = 4.0, R = 6.52, SubF = 0.14, SafF = 1.0$. However, since the safety factor had not yet been iterated, it shall be increased as a function of optimal $SubF$ until violations are met at $SubF = 0.94, SafF = 6.5$. The range of $SafF$ used in the simulation is chosen to cover a wide range of feasible values while minimizing simulation time.

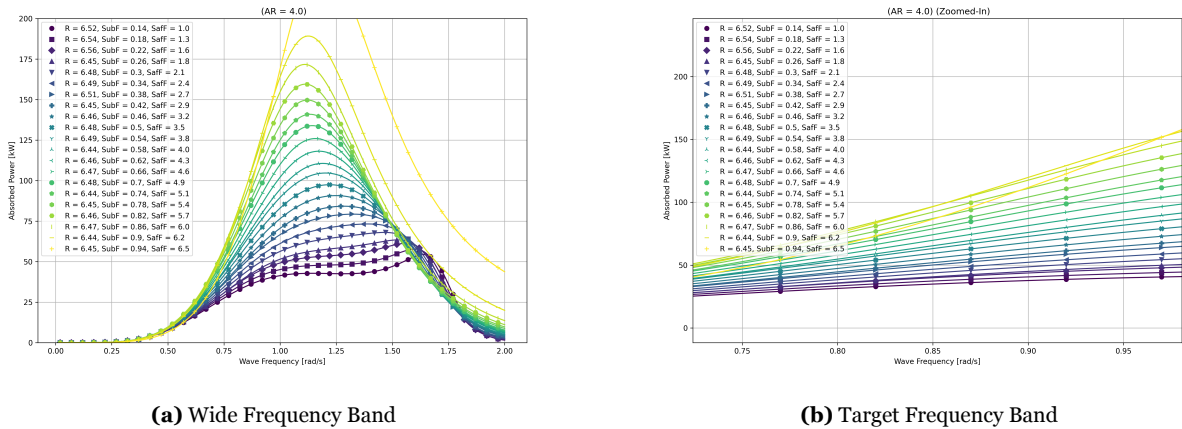


Figure 8.6: Sensitivity Analysis for Safety Factor

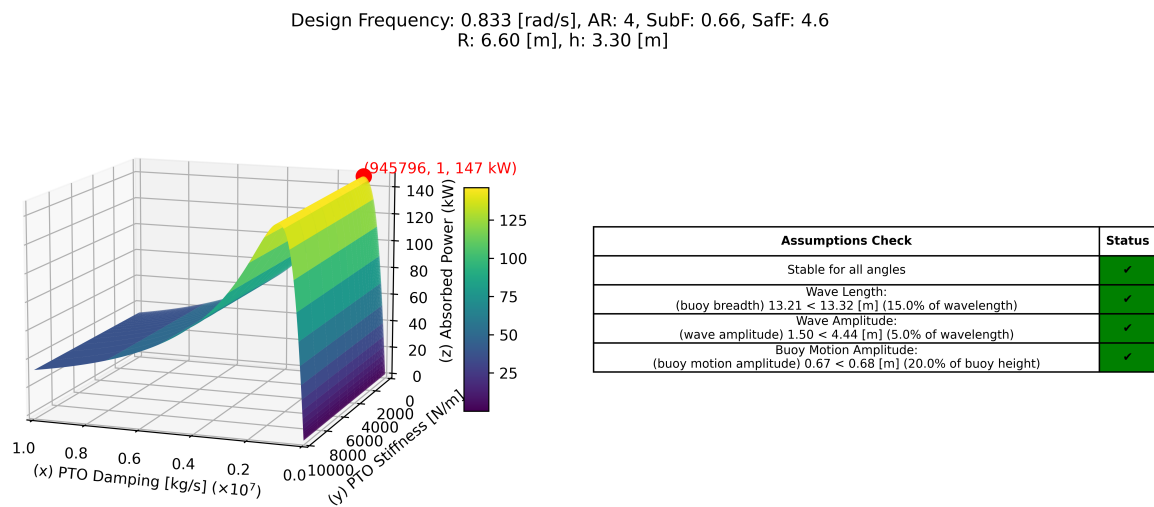
Figure 8.6a demonstrates that at low $\{SubF, SafF\}$, peak power is obtained at higher frequencies in the range $1.50\text{rad s}^{-1} < \omega < 1.75\text{rad s}^{-1}$. Higher power outputs can be found at lower frequencies with narrower bands focusing on the range $1.00\text{rad s}^{-1} < \omega < 1.25\text{rad s}^{-1}$. Therefore, by analyzing the non-monotonic behaviour shown in Figure 8.6b, higher SubFs lead to higher absorbed power. The design is frozen to $AR = 4.0, SubF = 0.66, SafF = 4.6$ optimized for $\omega = 0.8331\text{rad s}^{-1}$ since the lines corresponding to higher power all violated pre-established assumption violations and therefore cannot be selected with confidence.

8.2.4 Tuning for Maximum Power

Power tuning consists of running a logarithmic space of PTO damping and stiffness coefficients until a region of interest is defined. A linear space may then be used to zoom into the power peak to un-

derstand the local behaviour at a higher resolution. However, the WECSolver software automatically returns the global maxima. Generally speaking, low stiffness values are witnessed which are positive markers indicative of the proximity to resonant buoy motion. Poor sizing would require high stiffness to bring the system to an (optimal) resonant frequency. A drop-off in performance of overdamped systems is to be expected, which highlights the importance of tuning the damping coefficient accordingly. Simultaneously, a dynamic window returns assumption checks on the buoy diameter relative to the wavelength, the buoy height relative to the amplitude of the buoy motion, the wave amplitude relative to the wavelength, and ensuring that the body does not tip over before the set rolling and pitching angle limit. Although the input space has already undergone a verification of certain assumptions, an overview of all tests guarantee a trustworthy result along with printed absolute values.

Tuning the PTO damping and stiffness values for the $AR = 4.0$, $SubF = 0.66$, $SafF = 4.6$ at $\omega = 0.8331\text{rad s}^{-1}$ case resulted in a maximum absorbed power of 147 kW as shown by the peak in Figure 8.7. Therefore, it should be noted that the power requirements specified in *USR-REQ-1-1-WEC* and *USR-REQ-1-1-WEC-1* could not be satisfied; these limitations are induced by the aspects covered in Subsection 8.2.5.



107

Figure 8.7: Tuning of PTO Damping and Stiffness for $AR = 4.0$, $SubF = 0.66$, $SafF = 4.6$ at $\omega = 0.8331\text{rad s}^{-1}$

8.2.5 Results and Recommendations

To conclude, a buoy sized to $AR = 4.0$, $SubF = 0.66$, $SafF = 4.6$ optimized for $\omega = 0.8331\text{rad s}^{-1}$ was chosen, yielding an average power of 151.8 kW and a capacity factor of 63.2%. In order to calculate the average power, the area under a Gaussian distribution of the wave frequencies multiplied by the power curve is evaluated Figure 8.8. The power curve in Figure 8.8 is computed for the range of frequencies using the equations in Subsection 8.2.1 and the optimal PTO damping and stiffness values determined in Figure 8.7. The capacity factor is calculated by dividing the average power by the peak power. It should be noted that the lacking 36.8% from the capacity factor stems from the power curve yielding higher power at frequencies above the (median) design condition at $\omega_{0.50} = 0.8331\text{rad s}^{-1}$.

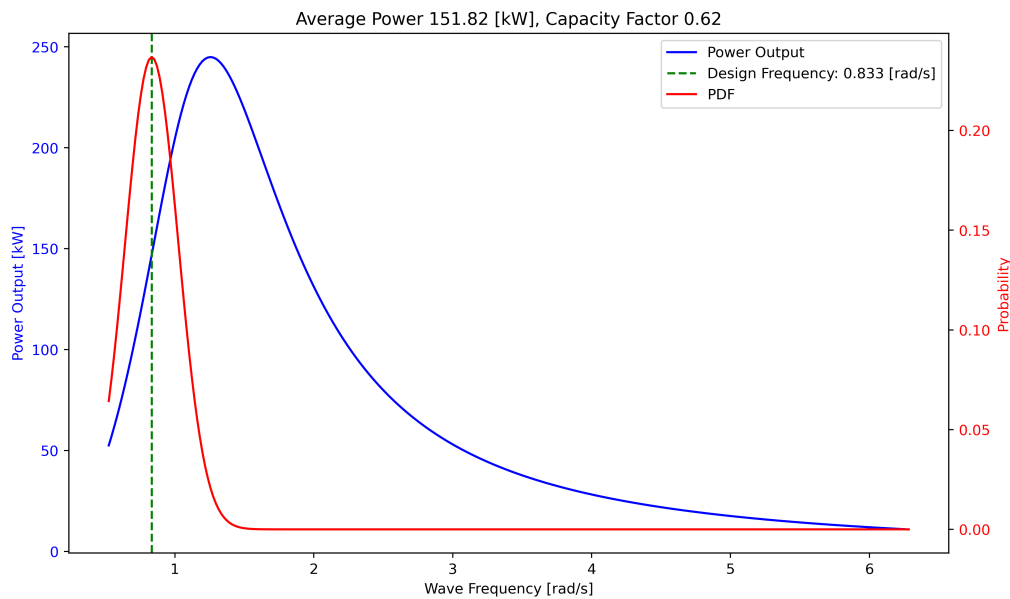


Figure 8.8: The power output of the WEC for different wave frequencies and the gaussian distribution of wave frequency probability that are used in computing the average power and the capacity factor.

At $SafF = 1.0$, the system is already inherently heavy at $62.5 \times 10^3 \text{kg}$ due to *USR-REQ-1-1-WEC-5*, which actually leads to a sub-optimal system because a margin of 3.6 times the buoy mass remains, suggesting that higher tether loads and increased AWES sizing could be supported.

Due to the 2.3 MW constraint set for the AWES segment, lower limits for buoy mass are directly set by the kite tether loads. Unfortunately, these system integration characteristics severely hinder the power output capacity of the WEC system; in essence, the buoy has to be heavily oversized in order to produce marginal power levels when existing market solutions can produce equivalent power with orders of magnitude less mass and volume. As a counter-measure, the aspect ratio (AR) and the submergence factor ($SubF$) are increased until the diameter of the buoy exceeds 15% of the wavelength of the wave environment due to limitations in the linearized potential flow theory, or when the buoy amplitude motion exceeds 20% of the buoy height. Wider bodies will begin to roll, pitch, and span several wave crests which requires advanced computational tools to account for. In general, point absorbers need to respect these constraints regardless provided that it relies on heaving motion for power generation unlike larger concepts (eg. line attenuators) that can span several wave crests.

Broader trends reveal that peak power outputs can be obtained for narrower frequency bands centered in the range $1.00 \text{rad s}^{-1} < \omega < 1.25 \text{rad s}^{-1}$, which currently lies outside the environmental conditions of the west coast of Ireland as given by $0.7241 \text{rad s}^{-1} < \omega_{env} < 0.9807 \text{rad s}^{-1}$, which would require alterations in the buoy shape for suitable alignment.

As a recommendation, the integrated design should cycle over a range of power budget ratios of both systems (P_{AWES}/P_{WEC}). Note that maximizing total power produced by the integrated system may not translate to a minimized LCOE. As it stands, $\bar{P}_{WEC}/\bar{P}_{total} = 6.19\%$. Furthermore, the current simulation pipeline considers a simple cylinder whereas an analysis of the effect of the buoy shape on the absorbed power would allow for a more efficient geometry. Lastly, an exploration of control strategies involving actively adjusting the PTO stiffness can help increase power output for frequencies other than the design $\omega_{0.50} = 0.8331 \text{rad s}^{-1}$. As a next step, simulating the performance of the buoy using validated and verified open-source numerical simulators such as WEC-SIM [70] can be used to confirm the results of this analytically-sized WEC and help achieve higher absorbed power, potentially reaching the *USR-REQ-1-1-WEC* target of 200 kW.

8.2.6 Stability of a Floating Body

It is also important to ensure that the WEC system is stable. In order to reduce the loads in the submerged body, it is important that the floating buoy is stable by itself. The stability of floating bodies might be counterintuitive since the stability mechanisms work differently than those of fully submerged bodies as described in Section 8.3.

Since the submerged volume of the body changes when there is angle changes, the stability is now dependant on the centre of gravity, the centre of buoyancy and the metacentre. In order for the the body to be stable, the metacentre has to always be higher than the centre of gravity, and as such, the metacentric height (MB), the difference between the metacentre and the centre of gravity has to be always positive. In order to calculate the metacentric height, one can use Equation 8.10 where MB is the difference between the metacentre and the centre of buoyancy, and GB is the vertical difference between the centre of gravity and the centre of buoyancy [71].

$$MG = MB - GB = \frac{1}{V_s} - GB \quad (8.10)$$

8.3 | Submerged Buoy (SB)

As mentioned in the a single-body system is used in order to reduce the complexity of the system. The SB will ensure that the forces applied by the PTO are transferred to a static system in order to generate power. Without a static SB the forces will not be transferred and as such no power would be generated. It should be noted that the SB will need to comply with *USR-REQ-1-1-WEC-5* to *USR-REQ-1-1-WEC-8* in order to give enough stability and compatibility with the floating body.

As seen in Figure 8.9 four main forces affect the SB. The buoyancy, which is always pointing in the opposite direction to the weight. The force applied by the PTO can be both upwards or downwards, and finally, the tension force that comes from the mooring lines attached from the sea bed to the SB. In order for the SB to be in equilibrium, the added forces must equal to zero. Two of those forces, the weight and the buoyancy are constant over time, while the tension and the PTO force are variable over time. *USR-REQ-1-1-WEC-8* implies that the SB shall not sink no matter the force applied by the PTO, and in order to do so, the volume of the buoyancy force needs to be bigger than all the other forces combined since that will be the extreme case for sinking such component. Knowing this, one can calculate the volume needed for this condition using Equation 8.11. m is the mass of the SB, g is the gravitational acceleration, F_{PTO} is the force applied by the PTO, T is the tension of the mooring lines in the vertical direction and ρ_w is the density of the sea water

$$V \geq \frac{mg + F_{PTO} + T}{g\rho_w} \quad (8.11)$$

One can also optimise the weight of the SB to have the most amount of volume possible with the least amount of weight for a given density and thickness of the outer shell. In Table 8.3 the table with the preliminary sizing for the SB can be seen given that the component is made of stainless aluminium and given a preliminary thickness of 10 cm. It is also important to note that ballast made out of wet sand is added to the bottom of the SB in order to reduce the weight of the steel and lower the centre of buoyancy of the SB. It is set that the ballast will cover 30% of the height of the SB. If such values are used to design the SB and the moring is always kept in tension, the SB should be stable, meaning that *USR-REQ-1-1-WEC-6* would be passed since its acceleration would be 0 m s^{-2}

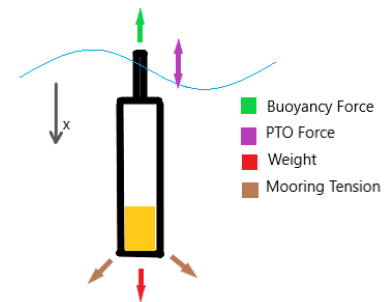
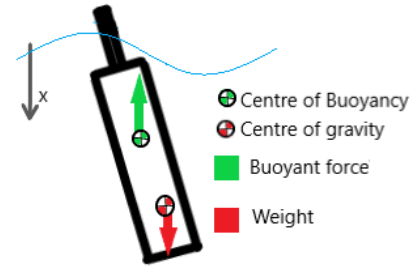


Figure 8.9: FBD of the submerged body

Table 8.3: SB Sizing

F_{PTO} [N]	ρ_{steel} [kg m ⁻³]	t_{shell} [m]	m_{steel} [kg]	D [m]	L [m]	V [m ³]	Height Factor [-]	ρ_{sand} [N]	m [kg]
527430	2400	0.2	6877	5.285	5.285	116	0.3	1682	58093.29

It is also important to verify the stability of the SB since a non-stable SB will lead to lower performance of the WEC and increased forces applied on the mooring lines. In order for a submerged body to be stable, its centre of gravity has to be lower than its centre of buoyancy, since in this case, the gravity force applies a restoring force into the system as seen in Figure 8.10. The centre of gravity of the SB with the ballast configuration shown in Table 8.3 is 1.654 m lower than the centre of buoyancy, meaning that the SB is stable. To add, mooring line tension and inertia will add extra stability meaning that USR-REQ-1-1-WEC-7 is passed.

**Figure 8.10:** Moment stability of a submerged buoy

8.4 | Mooring Subsystem

In order for the whole system to stay in place, a mooring system needs to be designed. Such a system is composed of two subsystems, the anchoring and the mooring lines.

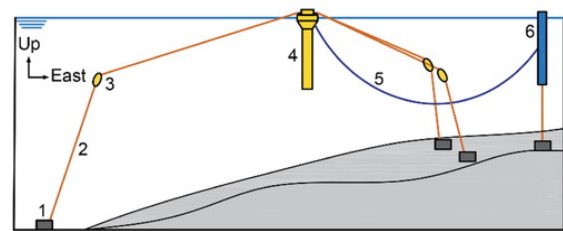
The mooring lines need to be able to support the maximum tension that SB exerts on them. The anchoring system needs to be able to withstand the loads that the mooring lines exert on the

Given the values shown in Table 8.3, the maximum and minimum vertical tension that the mooring lines will need to support will be 1.055 MN and 510 N and can be calculated by rearranging Equation 8.11 for upwards and downward force from the PTO, as seen respectively in Equation 8.12 and 8.13.

$$T_{v_{max}} = Vg\rho_w - mg + F_{PTO} \quad (8.12)$$

$$T_{v_{min}} = Vg\rho_w - mg - F_{PTO} \quad (8.13)$$

Considering only one mooring tension line, and a horizontal force applied by the kite deployment of 650 kN at an angle of 20 deg, this means that the biggest tension that the mooring line would support would be of 1.24 MN. It is worth mentioning that more studies in the mooring system would need to be performed in further stages of the project due to its complexity and importance. It is also important to note, that not only one mooring tension line can be used, but different arrangements of 3 or more mooring lines can be used as seen in Figure 8.11.

**Figure 8.11:** Three mooring line mooring system with a buoy taut system [72]

8.5 | Anchoring Subsystem

At the end of Section 4.2, the suction pile was chosen as the method of anchoring each WaveWings unit to the seafloor. The anchor is sized by the maximum vertical and horizontal capacities the suction pile withstands. This is governed by the maximum tether force of the AWES, which is estimated to have a maximum of 760 kN. This is multiplied by a safety factor of 4. This safety factor was chosen as the mooring is important to the operation of the unit and must be reliable. Thus, the mooring must be designed for 3040 kN, or 310 metric tonnes. To size the dry mass, a relation between vertical resistance

force (metric tonnes) to the anchor dry mass (metric tonnes) is given in the left graph in Figure 8.12. The dry mass sized by horizontal resistance is given in the right graph in Figure 8.12.

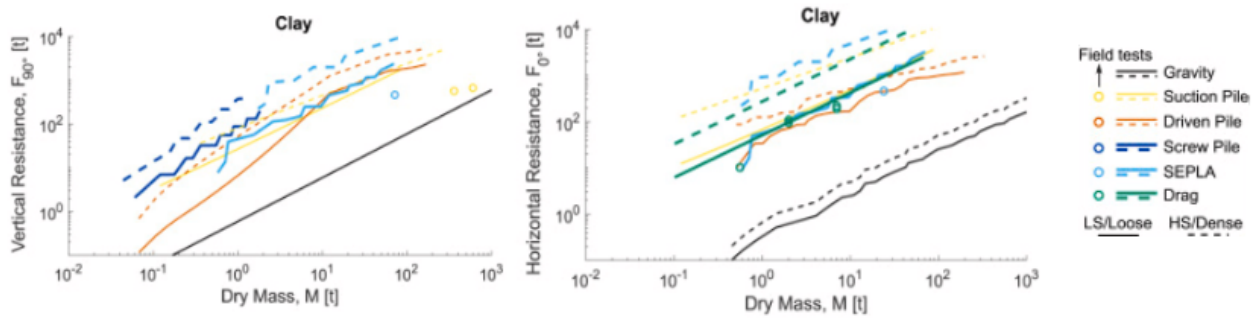


Figure 8.12: Anchoring vertical (left) and horizontal (right) resistance to dry mass ratios for different anchoring systems [18]

For the vertical resistance, the suction pile is assumed to hold the AWES load if the tether was aligned vertically above the buoy. Then, from the above graph, the suction pile dry mass is sized between 10-25 metric tonnes, depending on the characteristics of the clay. For the horizontal resistance, it is assumed that the maximum kite force acts 20° above the horizontal. It is also assumed that mooring line is attached to the pile at 150 m depth, and the buoy is displaced 25 m from the pile. Including the safety factor, this gives a horizontal resistance of 1772 metric tonnes. From the above graph, the suction pile dry mass is sized between 10 - 100 metric tonnes. Thus, the upper bound is taken, and the suction pile is 100 metric tonnes.

8.6 | Main Control Subsystem

The main control subsystem consists of the main control computer which is connected to the different sensors and actuators. The main sensors, which are relevant for all the different subsystems, are an anemometer, barometer and thermometer which are used for measuring the environmental conditions such as the wind speed for the AWES system. The GPS and IMU are sensors which provide the position and attitude of the whole buoy, cameras for inspection, and a hydrophone and microphone to measure the impact of the WaveWings system on the environment.

8.7 | Drum Subsystem

The drum dimensions are determined by the tether diameter and the $\frac{D_{drum}}{d_{tether}}$ ratio which equals 50 as explained in Section 7.6. Multiplying this ratio with the tether diameter results in a drum diameter of 2.8 m. The tether is wound around the drum in one layer to counteract abrasion of the tether. To avoid contact of the tether with itself when it is on the drum a tether spacing of 10% the tether diameter is used which results in a spacing of 5.6 mm. This results in a drum width of 7 m.

The drum is subjected to torsion, bending and compressive hoop stresses during operation. Torsion and bending only become a problem for long drums [73] thus the drum thickness is sized to resist the hoop stresses. Frictional effects between the drum shell and the tether are neglected and it is assumed that the pressure acting upon the drum is uniform, then Equation 8.14 [73] is used to calculate the thickness where Q_{tether} is the nominal tether tension that is equal to 613 kN and tether diameter d_{tether} is equal to 5.6 cm. The compressive hoop stress should not exceed 85% of the material yield stress according to the DNV standard [74]. Using CFRP with a yield stress of 570 MPa, the allowable compressive hoop stress σ_c is 485 MPa.

Table 8.4: Drum characteristics

Parameter	Values	Unit
Width	7	m
Diameter	2.8	m
Mass	4300	kg

$$t_{drum} = \frac{Q_{tether}}{\sigma_c \cdot d_{tether}} \quad (8.14)$$

The resulting thickness is 4.5 cm. The buckling of the drum shell is another problem that needs to be designed for. With Equation 8.15, the critical tension in the tether $Q_{critical}$ is calculated. The Young's modulus E of CFRP is 70 GPa.

$$Q_{critical} = \frac{E \cdot d_r \cdot t_s^3}{D_d^2} \quad (8.15)$$

The critical tension equals 46.2 kN which is 8% of the nominal tether force. This means that the drum will buckle instantly if no internal structure counteracts this buckling. That's why the radial piston pumps will be placed inside of the drum so they will resist the buckling. To connect the drum to the buoy structure a triangular structure is used. The triangular structure is made from the same material as the drum. The mass of the drum comes out as 4300 kg. Now the drum is designed and *USR-REQ-1-1-AWE-7-3* is fulfilled since the tether is retractable around a drum.

8.8 | Launch-Retrieval Tower

The launch-retrieval tower (LRT) is, as selected in Chapter 4, a telescopic launch mast mounted on the upper surface of the buoy Figure 8.13. Note that for illustration purposes, the winch and the drum are shown outside and on top of the buoy but in the actual model, they are stored within the buoy. During the retrieval of the kite, the guiding cable is reeled-in through a pulley at the top of the mast by a winch system simultaneously as the tether is reeled-in. This guiding cable secures the leading edge of the kite to the top of the mast. Next, the KCU activates the pumps in the kite to deflate the tubes. Once the kite is limp, the kite control unit, or KCU, begins the reefing process, reeling in the kite's bridle lines until the kite is completely folded upon itself into a 6.5 m³ volume. Simultaneously to the reeling-in of the bridle lines, the mast is retracted at a rate that allows the bridle lines to always be in tension, avoiding any tangled lines. The telescopic mast is now at its minimum height with the folded kite positioned at its top. To store the kite within the buoy for weatherproofing, the guiding cable is allowed to be reeled out at the same time as the drum reels in the tether line, lowering the folded kite into the storage area. In line with *USR-REQ-1-1-WEC-2*, the pool-cover-esque system closes the storage area in a waterproof manner, protecting the kite, drum, winch, and all systems other than the LRT environmental conditions. The launch-retrieval tower shall be equipped with warning lights to satisfy *USR-REQ-1-2-1-2*.

The launch mast is to a retrofitted marine telescopic boom crane typically used on ships. It must sustain:

1. 10 kN drag force perpendicular to mast meaning a 200 kN torque for a 20 m mast height.
2. The kite system's mass of approximately 500 kg means 5 kN of weight of kite parallel to mast.

The HTC1301-0220 telescopic marine crane model from MacGregor weighing 7.5 can lift loads of up to 2 tons to a height of 20 m¹. That is four times more than enough to lift the 500 kg kite system. A unit is estimated to cost EUR 100,000 but ordering in bulk for a whole WaveWings farm could, pending future negotiations, lead to approximately a 20% discount per unit. The full price is assumed in economic calculations of this paper. The selected model is designed for maritime applications and can thus be installed on top of the buoy without worry of salinity wear effects. Furthermore, retrofitting the crane to extend and retract only in the vertical direction will almost nullify the moment caused by the weight of the kite, this weight moment, however, is replaced by the moment caused by the drag of the kite during take-off.

The MacGregor crane is electrically powered, increasing its sustainability and allowing the crane to be powered by the wind and wave power onboard. At this moment in the design phase, it is assumed that

¹<https://www.macgregor.com/globalassets/picturepark/imported-assets/81999.pdf>

the power consumed by the LRT is minimal since the LRT is only active for a fraction of the mission time. Future iterations in the design need to consider the instantaneous power consumption of the LRT.

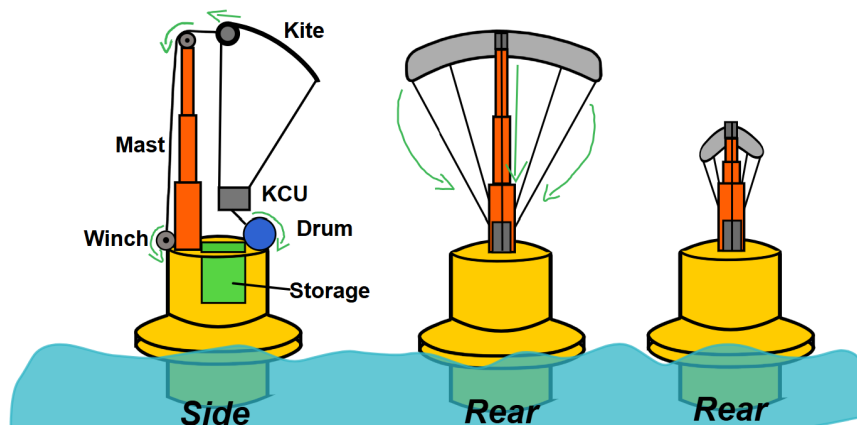


Figure 8.13: Launch Tower Concept. Not to scale. Winch and drum are located outside and on top of the buoy for illustration purposes only. They are actually stored within the buoy at all times.

8.9 | Power Subsystem Characteristics

8.9.1 Electrical Block Diagram

The Electrical Block Diagram is presented in Figure 8.14. The two systems that make up a WaveWings unit are the airborne system and the floating system. As defined in the concept configuration, the airborne system consists of the kite, tether, and KCU. This system does not generate power for the electrical grid. The airborne system has an onboard wind turbine, and this solely provides power to the sensors and components of the airborne system. This is illustrated in Figure 8.14, as no power is sent out of the airborne system. The floating system is designed to generate power for transmission to shore, as it contains the power subsystem with the AWES and WEC PTOs.

The two operational phases are the power-generating reeling-out phase and the power-consuming reeling-in phase. During reel-in, the AWES PTO requires power from either the WEC PTO, energy storage, or from the infield electrical infrastructure. This is shown in the diagram. The black arrow is flow of power regardless of phase. The floating system contains many black arrows, as the WEC PTO is operational regardless of reel-in or reel-out. Thus, the reel-in and reel-out arrows are applicable only to the AWES PTO.

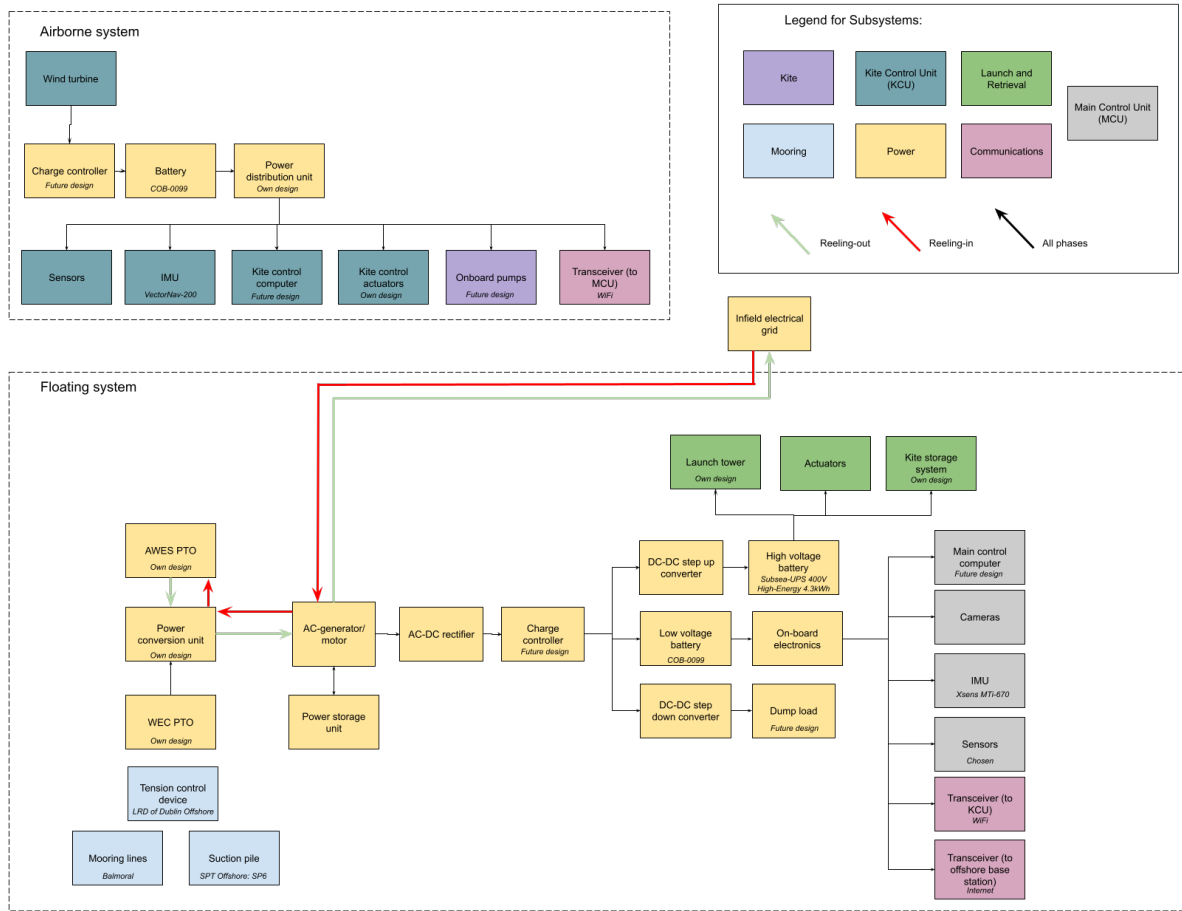


Figure 8.14: Electrical Block Diagram

8.9.2 Power Take-Off Subsystem

This section focuses on the Power Take-Off subsystem (PTO). The PTO converts the harvested wave and wind energy and converts this into electricity. For both energy sources, hydraulic based power take off units have been selected. This is already standard practice for WEC, hydraulic PTOs are the most widely used PTO choice for WEC systems [75]. For AWES, however, the current industry uses mechanical gearboxes for the PTO. Yet, mechanical PTO subsystems are expected to have trouble integrating with kites of larger sizes [76]. [77] has thus presented a possible solution to this up-scaling issue - using hydraulic PTO subsystems for large AWES. This section uses a similar approach to find the sizing, life cycle assessment, and performance as the predecessor to [77], [78]. Since both energy sources use hydraulic PTO subsystems, a consideration to combine the PTO subsystems into one, large, interconnected hydraulic system was made. It was hypothesized to reduce mass and costs, since the amount of generators and motors could be coupled. This is however not a current possibility due to limitations in current hydraulic motor capabilities, no single hydraulic motor can provide the required power. Having a single generator also increases the cost of it failing, all power production is halted once it fails. Having multiple generators will only see this problem in the unlikely event that all generators fail simultaneously. It is thus decided to opt for separate hydraulic systems, only being interconnected to provide power in the case of failure. This report uses existing components as guidelines for sizing, also when the requirements do not match the components exactly.

Hydraulic PTO Systems

Before the hydraulic PTO subsystems are described and presented, a general overview of hydraulic PTO systems is provided in this section. A hydraulic PTO requires a pump to convert mechanical energy into hydraulic energy. This can for example be a radial piston pump or a cylinder. Hydraulic subsystems are connected to each other with pipes, which transport the pressurized hydraulic fluid from component to component. Since hydraulic fluid is prone to leaking out of subsystems, the hy-

hydraulic fluid that is considered for this project is biodegradable. This already exists, and has been used in, among others, the maritime industry. To ensure a constant pressure in the pipes, accumulators are present in the hydraulic system. Accumulators store hydraulic fluid at high pressures, releasing fluid once the pressure in the hydraulic system drops below nominal operating conditions. Accumulators can also be charged, accumulating fluid at times when the pressure is above nominal operating conditions. An accumulator is comprised out of piston accumulators and gas cylinders which are filled with Nitrogen gas. The high pressure in the pipes are fed into a hydraulic motor, which converts the hydraulic energy into mechanical energy, that is put into an electrical generator. This is the whole process of a hydraulic PTO subsystem. The electricity produced is then put into a transformer, which is described in Section 10.5. For the whole hydraulic PTO subsystem, a working pressure of 350 bar is used.

WEC PTO

The WEC is required to provide a power of 200 kW. This means that the WEC generator generates 200 kW at rated conditions. Assuming an efficiency of 95% for both the pump and the motor, the power absorbed by the pumps has to be $200 \cdot 0.95^{-2} = 221.6 \text{ kW}$. Note that this efficiency is extremely high, but using a more accurate efficiency leads to issues in sizing other subsystems. It is a recommendation to take this efficiency into account in future research. The pump is made out of three hydraulic cylinders, moving with the heaving of the buoy. Check valves ensure the direction of the flow. The accumulator needs to store the energy so that the hydraulic motor can provide a constant rpm to the generator and enough energy to extend the telescopic boom when the kite is launched. In the case of a failure occurring in the AWES accumulator, the WEC generator is cut off, and all the hydraulic power generated by the WEC is diverted to the AWES, to save the kite. Cutting off the WEC generator is also required when extending and retracting the telescopic boom, it can be done with the use of the WEC hydraulic system. Hydraulics are also able to be used to control the heaving of the buoy, as a potential method to tune and detune the heaving of the buoy.

AWES PTO

The AWES provides a power of 2300 kW. This means that the AWES generator will generate 2300 kW at rated conditions. Like in Subsection 8.9.2, an efficiency of 95% for both the pump and the motor was assumed. The peak power production of the AWES system, mentioned in Section 7.5, is 3.6 MW. This means that the rated power for the hydraulic motor-pump needs to be $3600 \cdot 0.95^{-2} = 3249 \text{ kW}$. The AWES uses two pumps, so a failure in one does not lead to the loss of the kite. How this is done is explained in Table 8.9.2. The phases of the AWES are defined in Section 7.5, the reel-out phase takes 126 s and the kite produces 3600 kW at a speed of 20 rpm. The reel-in phase takes 43 s, the kite requires 210 kW, and is at a speed of 47 rpm. The AWES system produces 3017 kW during reel out and 200 kW during reel in, averaging the required 2300 kW.

The pumps that the AWES PTO system use are radial piston pump motors, this type is good at handling high torques and low speeds (rpm), and can function as pumps or motors. The mass for the pump motor is estimated using a catalogue of Bosch-Rexroth ², note that the requirements of the pump motor do not relate to a specific unit in the catalog. A mass of 10 000 kg is assumed for both motor-pumps. The pump motor must be able to reverse its outputs and change speeds when the system switches from reeling out to reeling in and vice versa. During the sizing and mass estimations an assumption is made that the components are scalable, a unit of half the capacity is half the mass of a unit with whole capacity.

The accumulators are the energy storage devices in a hydraulic PTO. Accumulators are massive devices, when a requirement for the accumulator requires it to provide enough power to the generator to produce 2300 kW and to reel the kite back in at the same time, it has proven to be too heavy. For this reason, the accumulators are sized so the mass of the PTO does not exceed 20 000 kg. For this mass budget, the AWES produces 200 kW during the reel in of the kite. The power required to reel the kite back in is 210 kW, this power is going through the pump and accumulator twice so the efficiencies

²<https://www.valin.com/sites/default/files/asset/document/Bosch-Rexroth-Hagglunds-CBM-Brochure.pdf>, accessed on June 25 2024

are applied twice. The accumulators are thus required to store $\frac{(200+210) \cdot 43}{0.95^{-2}} = 19.5 \text{ MJ} = 5.42 \text{ kWh}$. The sizing procedure for the accumulators followed a similar procedure as in [78]. Equation 8.16 and Equation 8.17 are used to find the volume required for the accumulators and the cylinders. Note that providing a constant power output for all the phases would result in an accumulator that is too massive. The result of this is that the power production of the entire unit will be 3.21 MW at reel-out and 400 MW at reel-in.

$$E_{acc} = \frac{p_0 \cdot V_0}{n-1} \left(\left(\frac{p_0}{p_{max}} \right)^{\frac{1-n}{n}} - 1 \right) \quad (8.16)$$

$$p_0 = \frac{p_{max} \cdot V_{min}}{V_0} \quad (8.17)$$

Where p_0 is the pre-charge pressure at V_0 , V_0 is the total volume, the sum of the volumes of the accumulator and gas cylinders, V_{min} is the volume when all the of the working volume in the piston is compressed so only the gas cylinder volume, p_{max} is the working pressure, 350 bar in Pa, n is the ideal gas constant for isentropic processes (1.4), and E_{acc} is the total energy stored in the accumulators. Assuming a V_0 of 3 m³ and a V_{min} of 2 m³ leads to a p_0 of 233.33 bar. The volume stored in the accumulator, V_{acc} is 1 m³. This equation assumes adiabatic compression.

The mass of the piston accumulators is determined by using a catalog made by Parker as a guide ³. Taking a V_{acc} of 1000 L, 1 accumulator of 1000 L with a mass of 6037 kg is used. This equates to a mass of 6037 kg. Each accumulator is held in place with a frame, the 1000 L accumulators have a frame of 500 kg. This leads to a total frame mass of 500 kg.

To calculate the mass of the gas cylinders, cylinders of 75 L are considered. Dividing the volume stored in the cylinders 2000 L by 75 L results in a total of 26.67 gas cylinders. Each cylinder has a mass of 133 kg, resulting in a total mass of 3546.67 kg. The cylinders are held in place using frames, each frame weighs 23.67 kg. This leads to a total frame mass of 631 kg.

The mass of the nitrogen gas was calculated using the ideal gas formula, Equation 8.18.

$$pV = nRT \quad (8.18)$$

Where p is the pressure, V is the volume, n is the number of moles, R is the gas constant, and T is the temperature. Using 350 bar as the pressure, V is 2 m³, R is 8.3145 J K⁻¹ mol⁻¹, T is 288 K. This results in a value of n of 29.2 kmol. This translates to a mass of 864 kg.

The pipes in [78] are made out of a synthetic rubber and low alloy steel combination, to allow for the rotation of the AWES. This is not a function for the WaveWings system, but for ease and compatibility, the same piping is used. The specific mass of this piping is 2.6 kg with a total length of 250 m results in a total mass of 650 kg

The hydraulic energy is converted to rotational energy by two hydraulic motors, which produces sufficient rpm for the generators to produce the constant required 2.3 MW. The motors have a combined mass of 700 kg. This value was calculated using data from [78].

The hydraulic motors are connected to generators, which take the mechanical rpm from the motors and converts it into electricity. The generators from [78] are scaled to the power requirements of the WaveWings system, which results in a mass of 7000 kg.

[78] does not take the mass or type of hydraulic fluid into account. For this, an estimate of 1500 L was assumed, this based on the fact that the accumulators require 1000 L. With a specific gravity of 0.9250 [79], this results in a mass of 1388 kg.

The characteristics of the AWES hydraulic PTO is mentioned in Table 8.5. The materials used is taken from [78].

³<https://www.parker.com/literature/Accumulator%20&%20Cooler%20Division%20-%20Europe/Accumulator-Catalogue.pdf>, accessed on June 24, 2024

Table 8.5: Overview of the PTO used by the AWES

Part	Characteristic	Value	Unit
Bi-directional motor pump (combined)	Reel-out power	3249	kW
	Reel-out speed	20	rpm
	Reel-in power	210	kW
	Reel-in speed	47	rpm
	Material	50% Cast iron 50% Chromium steel	-
	Efficiency	95	%
	Mass	10000	kg
Accumulator (combined)	Energy stored	20.6	MJ
	Material	Pistons: Carbon steel Gas cylinders: Carbon steel Frames: Section steel Gas: Nitrogen	-
	Pressure	p_{max} : 350 p_0 : 233.33	bar
	Efficiency	95	%
	Mass	Pistons: 6037 Gas cylinders: 3547 Frames (pistons + cylinders): 500 + 631 Gas: 864	kg
	Volume cylinder	2000	L
	Volume accumulator	1000	L
Pipe	Material	50% synthetic rubber 50% low alloy steel	-
	Specific mass	2.6	kg/m
	Length	250	m
	Mass	650	kg
Hydraulic motor (combined)	Material	50% Cast iron 50% Chromium steel	-
	Efficiency	95	%
	Mass	700	kg
Hydraulic Fluid	Type	Biodegradable	-
	Specific gravity	0.9250 [79]	-
	Mass	1388	kg
Generator	Mass	7000	kg

Such a detailed table is not produced in Subsection 8.9.2 due to the lack of previous research. One can assume, however, similar accumulators, pipes, hydraulic motors, and hydraulic fluids are used after scaling the WEC to AWES appropriately.

Integrated PTO

The assumed mass of the entire PTO is 1.2 times the mass of the AWES PTO. This is due to the lack of a worked out WEC PTO. Scaling the mass of the WEC to the power requirements would result in a smaller factor than 0.2, so the total mass estimation is conservative. The total mass of the PTO is roughly 36 000 kg.

As mentioned in the introduction of Subsection 8.9.2, the AWES and WEC will be connected in case of failures. This is in the case of a failure in one of the AWES PTO systems, either the hydraulic accumulator subsystem or the motor pump. Without this connection, the unit is unable to reel the kite back in due to an insufficient energy storage, resulting in the loss of the kite. With the connection, the WEC can provide additional power to the still operating AWES pump. It is assumed that the power provided by the system in this case is zero. Once all the accumulators in the AWES PTO are empty and the kite is still airborne, the kite will be reeled back in by wave energy alone. The hydraulic system of

the WEC also operates the telescopic boom, being able to extend it using hydraulic energy produced by the waves. This is clearly shown in Figure 8.15, which is inspired by various existing hydraulic diagrams [80], [81], [82].

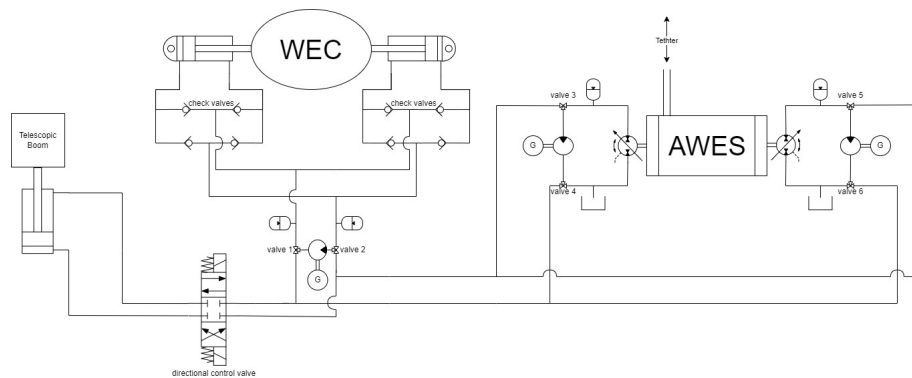


Figure 8.15: Hydraulic PTO of the unit

Note that essential elements such as pressure relief valves and temperature regulating equipment is not represented on Figure 8.15, as it is a simplified PTO layout. It should also be noted that different levels of details are present for the WEC, AWES, and telescopic boom system as different sources are used for each. This diagram should be interpreted as a diagram that highlights the possibility of interaction, not a detailed hydraulic PTO diagram.

During normal operation, the valves 1 and 2 are opened such that flow only goes to the hydraulic motor. This isolates the WEC PTO. Valves 3, 4, 5, and 6 are open such that flow only goes in the AWES PTO subsystem. When the telescopic boom needs to be extended, the valves 1 and 2 on the junctions to the WEC motor cut flow off to the WEC motor, and the directional control valve in between the WEC and the Hydraulic boom allows flow to the pistons operating the extension of the boom. When the boom is retracted, the directional control valve changes configuration to allow for the flow of hydraulic fluid. In the event of a failure in the AWES hydraulics system, valves 1 and 2 cut off flow to the WEC motor, and the corresponding valves in the failed part of the AWES (valves 3 and 4 or 5 and 6) are opened to allow for the WEC to contribute power to reel the kite back in.

The possibility of not harvesting wave energy is also considered. In this situation, the WEC valves 1 and 2 will be closed and electricity is required to power the hydraulic system in the AWES part. Valves 3 and 4 or 5 and 6 will allow flow to the telescopic boom, making it possible for the kite to launch. In this situation, the units are energy consuming.

8.10 | Material Selection

Although still no detail structures have been designed it is important to, at this stage of the project have a general outline of the materials that will be used to make build the floating system. In order to do so, literature was researched to have an estimate of the materials that industry uses for general parts of the system, and some material choices were done. According to [83] states that the CorPower Hiwave 5 device is made out of 83% steel while a smaller portion of 12% is made out of fiber glass. [84] has similar conclusion where 81 % of the weight is made out of steel. In the other hand, the other biggest contribution is cement as an 18% due to their use for it as a ballast. In the WaveWings unit the ballast is included on the SB unit, which is made out of 10.58% steel and 89.5% sand. The sand chosen is Coal mine overburden sand due to its low environmental impact.

Regarding the mooring system, while further studies will be performed in the future, there is two plausible options, either a catenary or a semi-taut system will be chosen. If a semi-taut system is chosen the mooring lines will probably be made out of nylon or steel[85]. If suction pile anchors are chosen, they will probably will be made out of steel due to their reusability and availability in the market. In [78] it was assumed that the drum will be made out of carbon fibre-reinforced polymer,

due to its high performance in the load cases required. The telescopic boom will probably be made out of steel and the material selection for the PTO system was discussed in Section 8.9.

8.11 | Communications and Data-Handling

There are several aspects concerning communications and data-handling. First, the architecture on the airborne system and on the floating system are discussed in Subsection 8.11.1. Afterwards, the architecture on the farm-level is described in Subsection 8.11.2. The Communications and Data-Handling (CDH) diagram is presented at the end of Subsection 8.11.2.

8.11.1 On the Subsystem-Level

Firstly, the antenna directivity is important for component selection. In the case of the floating body, a high-gain unidirectional antenna is more sensible as it maximises range and signal strength. Placement of this antenna must be on the drum and aligned along the tether line such that it is always pointing in the general area where the kite is flying. In the case of the airborne system, the movement of the kite makes an omni-directional antenna more sensible. This hybrid configuration brings advantages for more reliable communication regardless of the kite dynamics. Secondly, the components must be water-proof and corrosion-resistant. For proper selection, the IP ratings of antennae must also be investigated. These components must be IP65 rating or better, meaning it must at least withstand low jets of water from all directions. Thirdly, sustainability must be addressed. Unfortunately, lead is predominantly used in telecommunications components and is not sustainable. It is highly toxic to humans and wildlife with exposures mainly through inhalation or ingestion. Lead that enters the human body causes organ damage or can accumulate in the bones to linger for decades [86]. Lead is still used in telecommunications as it is malleable and stable such that it has high corrosion-resistance. However, the antenna options that do not contain lead are not as vast as the options containing lead. Lead-containing antennae often have better performance, especially in the corrosive offshore environment. Despite its toxicity, lead-containing antennae will be considered, but the appropriate precautions will be taken for workers during production, installation, maintenance, and decommissioning. Considering these, the selection for the airborne system and floating system are presented in Table 8.6. For compatibility, both antennae have similar frequency ranges, gain, and are the same connector type. This gives compliance to *USR-REQ-4* and *USR-REQ-4-1*. The IP ratings are also given for both, and are in compliance with *USR-REQ-4-3*. The Weidmüller 1367130000 is equipped on the airborne system, and the Phoenix Contact 2701186 is equipped by the drum on the floating system, aligned with the tether to point to the kite.

Table 8.6: Specifications for the communications subsystem on each WaveWings unit

Antenna Model	RF Protocols	Directivity	Gain	Frequency Range	IP Rating	Connector Type
Weidmüller 1367130000	WiFi	Omnidirectional	8dBi	2.4 - 5.935 GHz	IP67	N Type Female
Phoenix Contact 2701186	WiFi	Unidirectional	9dBi	2.4 - 5 GHz	IP67	N Type Female

8.11.2 On the Farm-Level

Typically in offshore wind turbine farms, telemetry and communications are done by means of a very high frequency (VHF) band and using terrestrial trunked radio (TETRA)[87]. This has been used for the past decade. However, there is an increasing trend of the use of 4G/5G networks for offshore renewable farms. Cellular communication is suitable because of its ability to generate high throughput at low latency, inherent security and architecture, and high-density connections[87]. A complete shift away from TETRA is expected after 2-3 years[87]. As the WaveWings farm is projected to begin installation in 2028, this shift away from TETRA will have already occurred.

For the farm, a 4G/5G network will be implemented. This will be installed by Vilicom, a Marine Advanced Technology Products & Services Company based in Dublin, Ireland. They are known for

partnering with Vodaphone in order to implement a 4G network into the world's largest offshore wind farm in operation, Hornsea 2, 55 miles off the Yorkshire coast in England[88]. Although a private network has many advantages, a microwave link to shore in the form of a subsea fiber optic cable must be installed for redundancy[87]. The 5 offshore substations will operate in a frequency range of 2.4 - 5 GHz just like the individual WaveWings units, such that it is in compliance with *USR-REQ-4-5*.

A centralised control station will be placed onshore, with the necessary network equipment and control consoles if commands must be sent to one of the 400 units. It will also operate in the frequency range of 2.4 - 5 GHz. This allows for compatibility between the onshore substations and the farm, giving compliance to *PGO-REQ-3-1*. Should this fail, the 5 onshore substations are linked to the 5 offshore substations via fiber optic subsea cables for for compliance to *USR-REQ-4-4*. The offshore substations are also equipped with 4G/5G. Certain units will also have 4G/5G, with other units simply having repeaters for extended coverage. Each star will have its own Local Area Network (LAN) for local data collection and initial processing. For this, there must be Ethernet switches and WiFi access points. All units and offshore substations have antennae and necessary modems. The communications and data-handling diagram is visualised in Figure 8.16. The subsystems involved are specified in the legend, and the handled data variables are in dashed boxes.

As this design project is tasked on the unit, the team has left a deeper analysis on the farm-level for future study. A complete layout for communications architecture can be optimised using models, adjusting placement, signal strength of devices, and use of extensions accordingly. However, the details provided in this section are asked to be considered.

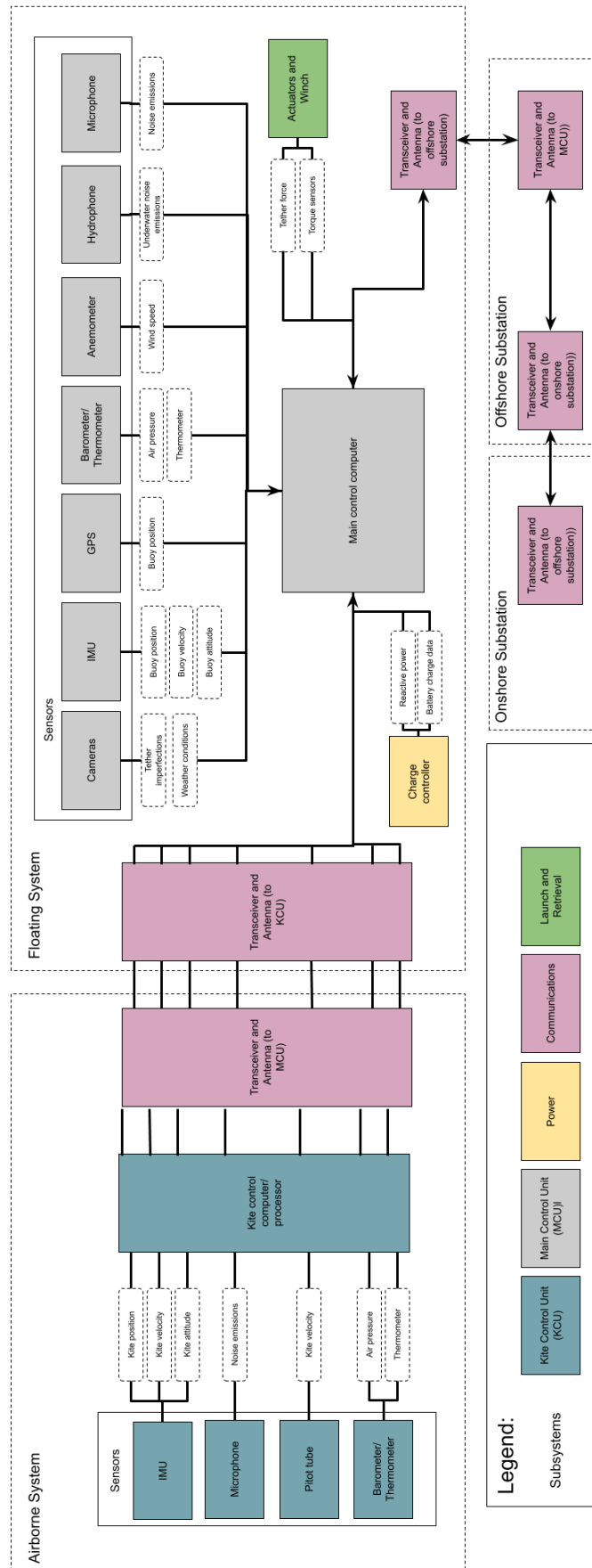


Figure 8.16: Communications and Data-Handling Diagram

9 | Control System

The control system is crucial in combining the operations of the AWES and the WEC systems. The goal of the control system is to maximize the electricity generation, all while respecting operational constraints, such as structural limitations and stability requirements. Specifically, this chapter explores strategies to create synergy between the AWES and WEC systems using control, thus exceeding the performance of separate AWES and WEC systems. After a review of the control system requirements, the operations of the WaveWings units are analyzed, a control architecture is proposed and the sub-system control is shortly introduced, before possible control strategies of the combined system are explored.

9.1 | Control System Requirements

In the first phase of the WaveWings project, a set of requirements were devised. Those relating to the control system are presented in Table 9.1. These requirements constitute the basis of the design of the control system.

Table 9.1: Requirements for control subsystem

Identifier	Requirement
USR-REQ-1-1-AWE-5	The AWES shall be controlled to perform the mission.
USR-REQ-1-1-AWE-5-2	The control system shall measure weather conditions.
USR-REQ-1-1-AWE-5-3	The kite shall be controllable.
USR-REQ-1-1-AWE-5-3-1	External experts shall be contacted for use of relevant control simulation software.
USR-REQ-1-1-AWE-5-3-2	Stability analysis shall be done to verify AWES behaviour.
USR-REQ-1-1-AWE-5-4	The AWES shall perform reel-in operation.
USR-REQ-1-1-AWE-5-5	The AWES shall perform reel-out operation.
USR-REQ-1-1-WEC-2-5	The WEC shall be controllable.
USR-REQ-1-1-1	The AWE and WEC shall perform better than the two systems individually.
USR-REQ-1-1-1-1	A literature study and simulation shall be performed to ensure the synergy feasibility.

9.2 | Operations Overview

To generate electricity from a combined AWES and WEC system, the operations are subdivided in different phases. These are described in this section, and looking ahead to possible control strategies, for each phase, a discussion will be included on the impact of buoy movement and flight stability on the different operation phases.

9.2.1 AWES Launch

The first main phase for the AWES subsystem is the launch of the kite, which is performed when suitable wind conditions are predicted. For this, it is required to first extract the kite from the storage, inflate the leading edge and get the kite to the top of the launch tower, as explained in Section 8.8. After the detachment of the kite from the launch tower, it ascends to the operating height. During this phase, the kite is close to the buoy and the water surface, thus precise manoeuvring and low disturbances are required. A control strategy that offers stability and predictability is thus required. After the launch of the AWES, the nominal energy harvesting operations, consisting of a reel-out and reel-in phase, begin.

9.2.2 AWES Reel-Out

During the reel-out phase, *USR-REQ-1-1-AWE-5-5*, energy is generated by the kite flying figures of eight. This phase offers the most possibilities for optimization as flight stability constraints are relaxed because the kite is far away from the water surface and flying near nominal aerodynamic conditions. It is also the phase in which the kite spends the most time, approximately 70% during active operations, as computed in Subsection 7.5.2, thus it is the most important phase to optimize.

9.2.3 AWES Reel-In

When the maximum tether length is reached during reel-out, the operations switch to the reel-in phase, *USR-REQ-1-1-AWE-5-4*. During this phase, the tether is reeled in with a force as small as possible. This means that the aerodynamic force produced by the kite should be small. Due to the choice of using a leading-edge kite (LEI), there exists a minimum lift-over-drag ratio that needs to be flown to ensure structural stability of the kite. The angle of attack of the kite thus needs to be tightly controlled by the control system in this phase. Once the minimum tether length is reached, the operations switch to the reel-out phase again.

9.2.4 AWES Retrieval

During the operation of the AWES system, it is important to monitor the weather conditions. If heavy storms are predicted, or on the contrary, the wind speed drops too low for power generation, the kite needs to be retrieved. Retrieval is also necessary if any of the AWES components are damaged. The kite is reeled in towards the launch mast, thus, similar considerations to the AWES launch apply and the control system should provide precise manoeuvring.

9.2.5 WEC Energy Harvesting

The WEC part of the WaveWings system is almost continuously in operation, harvesting energy in a single phase. During this phase, the movement of the floater is controlled in order to generate a maximum of power.

9.2.6 WEC Storm-Safe Mode

During extreme weather conditions, accompanied by large wave amplitudes, it is necessary to stop the WEC energy harvesting operations to protect the structure from damages due to large displacements and forces. In this phase, called the WEC storm-safe mode, the control system needs to counteract the incoming excitation force in order to reduce the motion of the floater.

9.3 | Control Architecture

The control architecture, illustrated in Figure 9.1, is an overview of the different components of the control system and their relative hierarchy. Each layer is connected with its neighbours, thus data and control decisions can flow both ways. The system & environment block represents the physical world, thus encompassing all kinds of environmental effects, like the wind and wave conditions, but also the dynamics of the physical WaveWings system. One level higher, the sensors and actuators are responsible for interacting directly with the environment, gathering data, such as weather conditions, *USR-REQ-1-1-AWE-5-2*, and executing control decisions. The individual

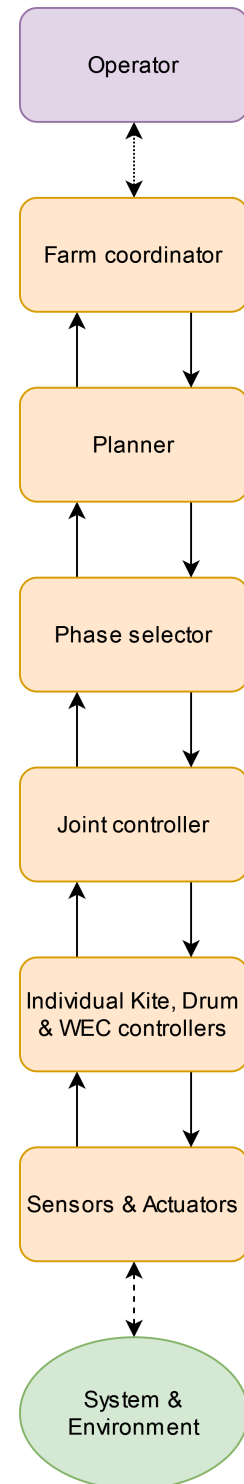


Figure 9.1: Control Architecture of the WaveWings system.

subsystem controllers, namely the kite, drum & WEC controller, are responsible for generating the actuator instructions based on the set-points generated by the joint controller. This layer is responsible for identifying a strategy to combine the individual subsystems. On a higher level, the phase selector chooses the appropriate operations phase, which have been presented above. The planner is responsible for predicting future conditions, for example the wind and wave forecast. The farm coordinator deals with integrating the individual WaveWings units into a coherent farm strategy, considering possible interference and scheduling the power delivery phases. The farm is connected to the outside world through the operator, which is the company managing the farm and setting goals such as electricity targets or maintenance schedules.

The focus of this project is to explore the possibility of synergy between the AWES and WEC system, as specified by *USR-REQ-1-1-1*. Thus, first, the logic of the subsystem controllers is examined individually, and then possible strategies implemented by the joint controller are investigated.

9.4 | Subsystem Control

The actual hardware belonging to the central control system has been described in Section 8.6. Before devising strategies to combine the control of the AWES and WEC, however, it is important to first consider the subsystems individually. The three main controllable subsystems, the kite, the drum and the WEC are shortly introduced, with a focus on the connection of the control logic to the physical actuator. Additionally, conventional control strategies for individual optimization of the subsystems are presented as well as some background information necessary to develop the combined control strategies in the next section.

9.4.1 Kite

As prescribed by *USR-REQ-1-1-AWE-5-3*, the kite is controllable, which is ensured by the KCU, which has been sized in Section 7.7. During the reel-out phase, the kite flies in figures of eight. The figure-eight trajectory is usually defined in terms of attraction points to be followed by the kite controller [89]. By moving the attraction points, the length of the trajectory, and thus the time taken by the kite to fly a single figure eight, can be changed [7]. The following of the trajectory defined by the attraction points can be performed by a simple PID-controller [6, p.137-163], but also more advanced control techniques such as nonlinear dynamic inversion can be used [89]. The attraction points are usually constant and defined in spherical coordinates, thus the length of the trajectory increases with increasing tether length. By expressing the attraction points in a Cartesian coordinate system, or by continuously changing the attraction points during the reel-out phase, a constant trajectory length can be achieved.

9.4.2 Drum

The drum, to which the tether is attached, is the second subsystem which can actively be controlled. Specifically, the rotational velocity of the drum can be regulated. There are two conventional control modes for the drum, however, more complicated ones can be envisioned if necessary. During constant-force operations, the rotational velocity is adapted in order to maintain a constant tether force. This regime is physically relevant, the natural response of the drum to the torque produced by a change in tether force is the corresponding change in rotational velocity. During constant-velocity operations, the goal is to keep the rotational velocity of the drum constant. This requires rapid adaptations of the resistance to rotation by the drum control actuator. Proportional controllers can be used for the drum [6, p.137-163]. The drum being part of the AWES PTO, it is controlled by hydraulics, Subsection 8.9.2. Any oscillations in the mechanical energy are stored in accumulators, thus allowing the electrical generator to run at constant electricity output, thus increasing the conversion efficiency. The choice of this PTO thus enables allowing for more mechanical energy oscillations of the AWES, increasing the design space for possible combined control strategies.

9.4.3 WEC

Control of WECs is based on the *Optimal phase condition*: The instantaneous phase of the floater velocity is synchronised with that of the wave excitation force [90]. The actuators of the WEC control system are usually integrated in the PTO, Subsection 8.9.2, thus fulfilling *USR-REQ-1-1-WEC-2-5*. Proper control of the WEC can play an important role in increasing the power output of a WEC, an increase of up to five times when considering the annual power production [91].

9.5 | Control Strategy

Different control strategies to combine the AWES and WEC systems are possible. First, a baseline strategy will be presented, which focuses on decoupling the performance of the AWES and WEC. Afterwards, a WEC-amplifying strategy is developed, showing the potential to exploit synergy. Both of these strategies are modelled using simulations. Finally, some further considerations related to the combined control are briefly discussed.

The focus of this section are strategies to combine the control of the AWES and the WEC. The detailed low-level control of the individual systems is not of interest here, it is assumed that the appropriate set-points / trajectories can be followed with sufficient accuracy.

9.5.1 Simulation Approach

Following *USR-REQ-1-1-1-1*, simulations have been performed along with the literature study and expert consultations, *USR-REQ-1-1-AWE-5-3-1*, in order to develop and present the different strategies. A floating AWES simulation from literature [6, p.137-163] is used for this purpose. The combination of AWES and WEC systems being a recent development, there does not exist a simulation tool for this purpose in the literature yet, and custom developing such a tool would have exceeded the scope of this project. Therefore, a floating AWES simulation has been chosen. The displacement of the floating platform has been chosen as a proxy for the WEC power output. The WEC not being modelled, it is well established that the WEC power output is a monotonically increasing function of the displacement.

In order to simplify the computations, the kite and floater model that is used as a standard in the simulation is used for all demonstrations. Implementing the kite and floater as designed in previous sections of this report would induce significant additional work, especially hydrodynamic coefficients need to be recomputed using numerical solvers for each change in geometry. Since the goal is to develop a generalizable control strategy, using a model that does not represent the exact WaveWings unit does not constitute a major issue. Only the reel-out and reel-in phases of the AWES operations can be simulated, launch and retrieval exceed the capabilities of the simulation tool.

9.5.2 Baseline Strategy

As a baseline strategy, decoupling the AWES and the WEC system as much as possible is used. The goal of this strategy is to keep the tether force constant during an operations phase, or, if the operation demands a change in tether force, keep the speed of the tether force change low. As such, the tether force acts as a (quasi-)static force on the buoy/kite, thus the dynamics of the buoy and kite are decoupled. The control of the WEC and the AWES can thus individually be optimized, with the only difference compared to a conventional WEC being the constant, large magnitude tether force acting on the floater.

In the simulation, this strategy can be modelled by imposing a constant tether force requirement on the drum. Figure 9.2 presents the floater movement with and without an attached kite force, as well as the tether force with and without a moving platform. It can be observed that adding the kite force to the floater, Figure 9.2b only slightly increases the movement of the buoy, compared to when no tether force acts on the buoy in Figure 9.2a, mainly in the y-direction where a slow oscillation with an amplitude of ± 5 m develops. When observing the tether force of a kite with an immobile platform, Figure 9.2c, a slight oscillation can be seen, which is caused by the figure eight trajectory of the kite. Adding the motion of the buoy in Figure 9.2d only slightly increases the amplitude of the tether force

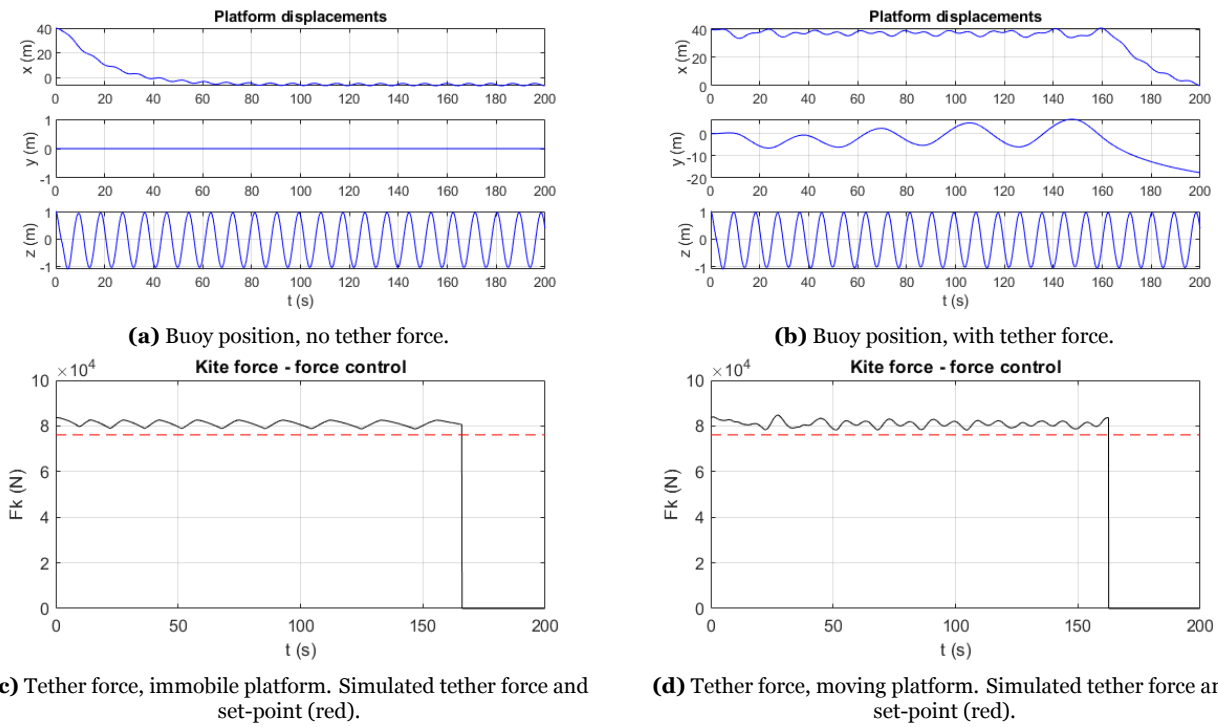


Figure 9.2: Baseline control strategy. Waves with a period of 9s and a height of 2m. Reel-out phase (0-160s) and reel-in phase with zero tether force (160-200s).

oscillations. The controller is thus successful in implementing the baseline strategy.

Based on the requirements for the different operation phases discussed earlier in this chapter, the baseline strategy is the appropriate strategy to be chosen during launch and retrieval of the airborne system, as well as during reel-in, in order to guarantee maximum stability and predictability of the dynamics. During reel-out, which is the energy-generating phase, this strategy may also be employed, allowing for individual optimization of the AWES and WEC power output.

9.5.3 WEC Amplification Strategy

The baseline strategy decouples the dynamics of the AWES and the WEC as much as possible, thus it also does not allow for any control synergy. If amplification of the energy output as a result of having both the AWES and WEC combined in a single unit is desired, an alternative control strategy needs to be considered. One possible adapted strategy is presented in this section.

This strategy is based upon previous work performed on floating AWES systems [6, p.137-163], and the interaction between the kite and the platform for such a system [7]. The objective is to amplify the movement of the floater using the tether force oscillations (TFOs) of the AWES system. This requires the drum controller to be set to follow a constant reel-out velocity, as introduced in Subsection 9.4.2, the TFOs are then transmitted to the platform, in this case the floater. The frequency of these TFOs, which can be controlled, as explained in Subsection 9.4.1, can be close to the resonant frequency of a floating AWES platform [7]. Considering the symmetry of the figure eight,

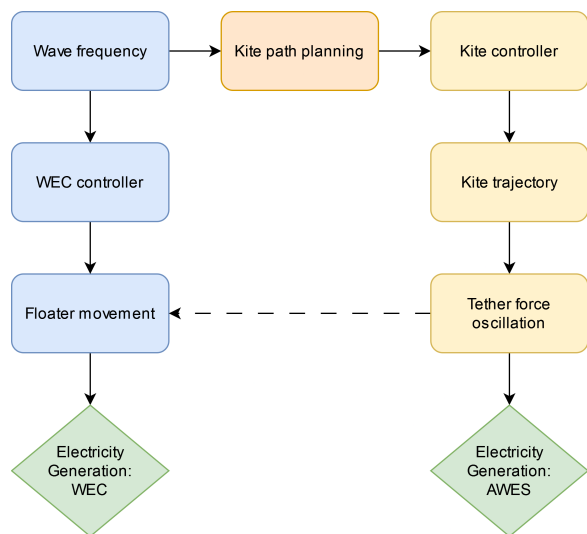


Figure 9.3: WEC-amplification strategy, control flow diagram. Controlled kite trajectory leads to amplified floater movement, and thus increased WEC power output.

the TFO period is half the period of the complete trajectory. For the case of the WEC, the subsystem control effectively tunes the resonance of the buoy to match the incoming wave period, as presented in Subsection 9.4.3. As such, the TFOs may be transmitted to the floater and thus induce significant displacements of the platform. The proposed strategy consists thus of matching the period of the TFOs with the wave period of the buoy in order to amplify the displacement magnitude of the buoy, to be harvested by the PTO of the WEC. This strategy is illustrated in Figure 9.3.

This strategy offers several advantages compared to the baseline strategy, with the main goal being to increase the WEC power output. However, there are also some disadvantages present, which are difficult to quantify but do require consideration.

Advantages

- Increased WEC Power Production
- Use of established AWES control strategies
- No additional tether lifetime impact, because the tether is limited by bending fatigue

Disadvantages

- Increased fatigue of buoy mooring
- Sub-optimal kite trajectory might lead to decreased AWES power generation
- High kite turning rate required for optimal period matching

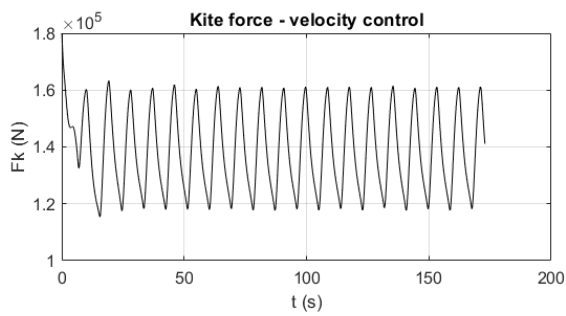
This strategy is only suited to be employed during the reel-out phase of the operations, as it induces considerable motion and quickly varying forces, which is sub-optimal for all other operations phases as discussed before.

Using the simulation approach introduced before, the WEC amplifying strategy was implemented. A reel-out velocity of zero was used in order to keep the TFO period constant over time. This resulted in a TFO period of 9 s. All waves are simulated with a 2 m significant wave height and the phases of the kite trajectory and waves are aligned. Since the turning rate of the kite significantly restricts the trajectories available to the control system planner, two different wave period regimes are explored. The TFO period is fixed at 9 s for simplicity of simulation, and the wave period is set at 9 s and 3 s, in order to simulate the conditions when the trajectory period is 1 or 3 times the wave period. It is crucial that the wave period is an odd multiple of the TFO period, such that the tether force can have an overall constructive impact. The results are shown in Figure 9.4.

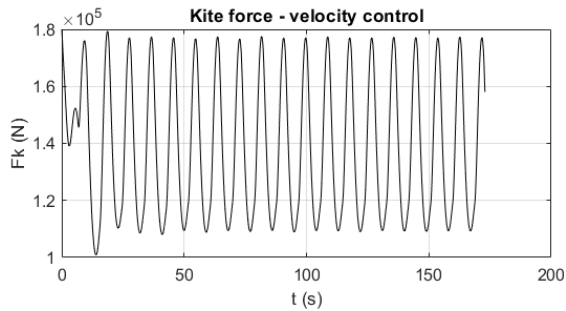
It may be observed that the magnitude of the TFOs is increased for a wave period of both 3 s and 9 s, Figure 9.4e and Figure 9.4c, compared to the case of no waves, Figure 9.4a, the average stays constant however, thus promising equal power output. Compared to the baseline strategy, the TFOs are significantly increased in all cases.

When considering the buoy position, it can be seen that applying the varying tether force, Figure 9.4d, induces significant oscillations in the horizontal plane compared to the case where no tether force is applied, Figure 9.4b. However, the position in the vertical axis is not affected significantly. This is due to the high stiffness of the buoy system in this direction because of the buoyancy force of the big and heavy buoy. For the case where the TFO period is 3 times the wave period, Figure 9.4f, it can be observed that there is still significant motion in the horizontal plane, although at a slightly reduced magnitude. The motion of the buoy in the vertical direction because of the wave excitation is also reduced in magnitude, probably because of the resonance mismatch between the uncontrolled floater of the simulation and the wave period.

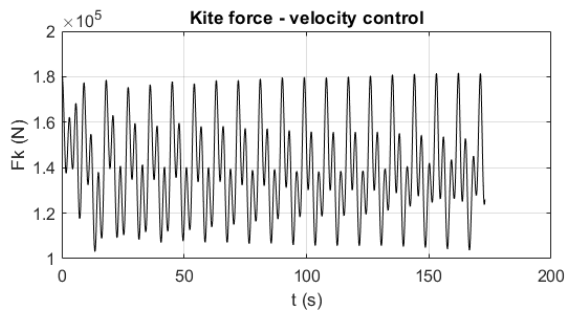
WEC PTO systems usually harvest the energy of the vertical motion of the floater. The vertical motion is not amplified, however, thus there is no additional power output to be gained. The WaveWings unit is not aligned vertically though, because of the significant side-wards force applied by the tether, the elevation angle of the WaveWings kite during reel-out is 30° , thus the buoy will be in an oblique position during reel-out operations. Resulting of the design of the floating system, the PTO is aligned with the major axis of the floater, thus the PTO will also be inclined and is thus able to harvest the horizontal motion induced by the TFOs.



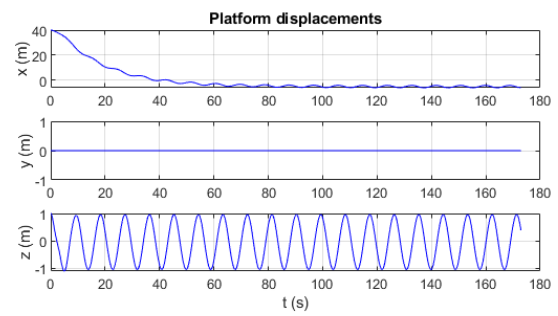
(a) Tether force, no waves.



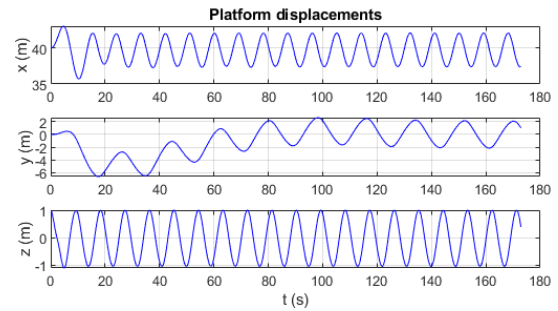
(c) Tether force, waves with a 9 s period.



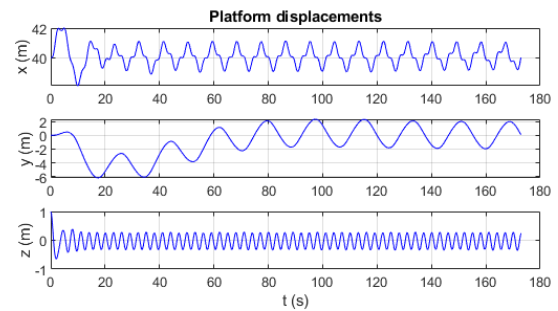
(e) Tether force, waves with a 3 s period.



(b) Buoy position, no applied tether force, waves with a 9 s period.



(d) Buoy position, waves with a 9 s period.



(f) Buoy position, waves with a 3 s period.

Figure 9.4: WEC amplification control strategy. Waves with a height of 2 m.

9.5.4 Further Considerations

Ground-generating airborne wind energy systems usually operate in pumping cycles, which means there are clearly distinguishable reel-in and reel-out phases. However, alternative operating modes have been proposed, for example rapid switching of reel-in and reel-out during a single figure-eight trajectory [89, p.345]. The tether length is thus almost constant. A possible control strategy for this mode could be similar to the previously proposed WEC amplification strategy. The reel-in and reel-out could be synchronized with (a multiple of) the WEC period. By performing the reel-out and reel-in aligned with the TFOs, amplified by the floater movement, overall power output can increase. Specifically, peaks in tether force would increase the power produced during reel-out and minima in tether force would lead to reduced energy consumption during reel-in. Due to this operating mode not having been simulated, this strategy could not be tested in this phase of the project.

A different effect worth noting is the action of the buoy as a damper. Sudden, large loads on the kite, for example as the result of gusts or turbulence, lead to large increases in the tether force. The floater not being fixed, in contrast to conventional AWES platforms, can respond with movement to this impulse, thus decreasing the tether load.

10 | Farm Design

The integration of the 400 units into a farm is a complex task. A farm design is often governed by characteristics of the electrical infrastructure. Firstly, the requirements associated with the farm design are listed in Section 10.1. Next, the strategy and important criteria are presented in Section 10.2. Then, then types of configurations are described in Section 10.3. Afterwards, the source type and transmission to shore are presented in Section 10.4. The power electronics are described in Section 10.5. Finally, the methodology for the determination of the layout is presented in Section 10.6. It must be stated that the layout presented at the end is subject to change after analysing budgets in Chapter 16.

10.1 | Requirements

Table 10.1: Requirements for the farm design

Identifier	Requirement
USR-REQ-1-2	The farm shall consist of 400 units.
USR-REQ-1-2-1	Individual units shall operate in a specified control area.
USR-REQ-1-2-1-1	The clearance between units shall be the maximum tether length with an applied safety factor.
PGO-REQ-3	The farm shall be connected to an onshore electrical grid.

10.2 | Strategy

There are several criteria to the decision-making for the farm layout, namely reliability, cost, and sustainability. Reliability of a cable layout is determined through a reliability block diagram, which depicts the flow of power when certain cables fail. Since an offshore farm receives less maintenance and is in a harsher environment than an onshore farm, reliability becomes a paramount consideration in order to mitigate the impact of a cable failure. Reliability of cable types are quantified by the International Electrotechnical Commission (IEC) rating they receive. All submarine power cables installed must at least be in compliance with the international standard IEC 60288 [92] However, higher IEC ratings are awarded for higher voltages carried or better insulation[93].

Cost is also important to the strategy for an offshore farm. It is most dependent on the length of the cable and the voltage the cable is designed to carry. It becomes evident that in order to minimise cost, it is an optimisation problem for minimising the cable length in the layout. Subsea cables can be €1M/km to over €2.5M/km[92]. Cables designed for the higher voltages are more expensive than the medium voltage (MV) inter-array cables. Thus, the length of the high voltage (HV) cables specifically must be minimised in length.

Finally, sustainability is an important aspect. One way to consider sustainability is by minimising the enclosed area of the farm. Different configurations lead to a different total farm areas, and this must be investigated. Also, another consideration for sustainability is preservation of seafloor architecture such that the subsea cables are placed around potential obstructions. This is often done by first deploying vessels that scan and produce geo-data of the seafloor contour and architecture. Then during cable laying, an underwater Remotely Operated Vehicle (ROV) is deployed for visual inspection of the seafloor, and the cable layout is adjusted accordingly. It must be noted that this aspect is unable to have a complete analysis at this stage of the project, however the sustainability potential of the following configurations can still be assessed.

The power flow through the farm to shore is complex. Firstly, the configuration must be chosen. The configurations are given in Section 10.3. The inter-array cables must have a specified voltage, and be chosen to be either AC or DC. Next, radial feeder cables join the configurations (either strings or stars) and join them to the offshore collection point(s). Then, the source type for electricity and the power transmission to shore are explained in Section 10.4. Power electronics are described in Section 10.5,

and their placement either on-or-offshore is discussed. Finally, the power is reached by the onshore station(s). The overview of the decision-making is given in Figure 10.1.

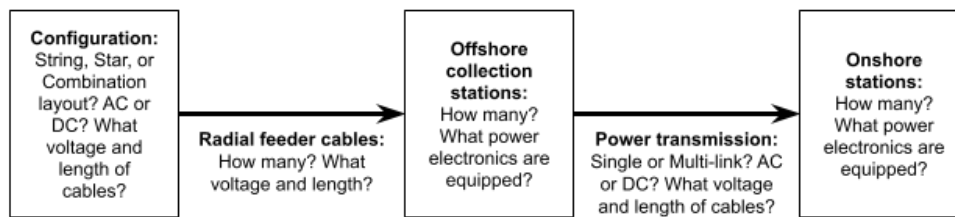


Figure 10.1: Farm Overview

10.3 | Types of Configurations

Now that the three criteria for a complete farm layout are known, types of configurations can be explored and assessed relating to these criteria. The configurations are constructed with medium voltage (MV) inter-array cables. Medium voltage cables carry anywhere between 1kV to 50 kV, but typically 22 kV or 34 kV are used for inter-array cables. Only regular (patterned) configurations are used in this analysis, as an irregular layout is an optimisation problem that requires geo-data from seafloor mapping.

10.3.1 String Layout

A common configuration for offshore wind is the string layout. It comprises of units in a line or string. A simple single string is shown in Figure 10.2a. In the diagram, individual units are equipped with a transformer and a generator. Coinciding circles depict a transformer, and the circle with a G is a generator. Notice that a cable failure is more catastrophic the closer it is to shore, as more units behind the cable failure are not able to transmit power. Thus, reliability is limited for the units in series. In the case of a large farm, two or more strings are joined using a radial feeder cable. The radial feeder cables join to This layout is considered a regular layout as it is patterned. Cost-wise, string layouts are cheaper than the other configurations due to their simple structure and quicker installation time.

10.3.2 Star Layout

Another configuration for offshore wind is the star layout. It consists of units arranged in a star, and inter-array cables connect each unit to the star's center. Notice that a cable failure between the unit and the center junction only removes that unit from power transmission. This greatly improves reliability. This layout is typically more costly than a string layout due to its greater complexity. A star layout is depicted in Figure 10.2b. This layout is also considered regular.

10.3.3 String-and-Star Combination

As each of the above configurations has their advantages and disadvantages, a combination of the two can find a balance. In this layout, two or more stars are joined through a radial feeder cable. This is more practical for a large farm, as there high number of stars can converge to the smaller amount of offshore collection stations. These junctions are needed before reaching the offshore collection station(s). A simple combination layout is depicted in Figure 10.2c. This layout is also regular if the number of units to a star is the same, and the farm itself is symmetrical.

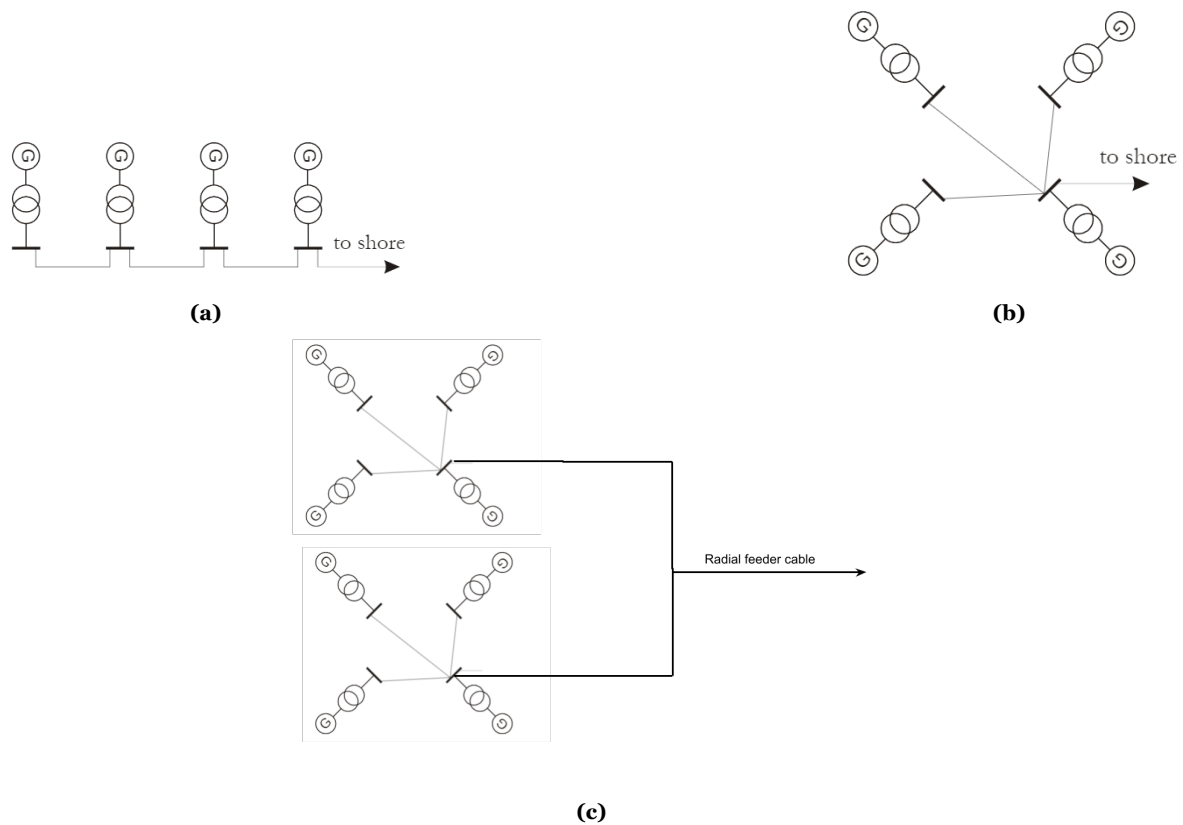


Figure 10.2: String layout (a) star layout (b) and combination layout (c) [94]

10.4 | Source Type and Transmission to Shore

Firstly, it must be distinguished that the power transmission to shore requires high voltage (HV) sub-sea cables. These cables carry voltages greater than 50 kV, but typically 66 kV, 132 kV, and 275 kV cables are used for transmission in the offshore farm application. The two means of power transmission from the farm to onshore are either AC or DC source. The choice is most dependent on the distance for shore and cost. As determined in Chapter 11, HVAC is more cost effective for power transmission at a 70 km distance to shore. As HVAC is used, inter-array cables and other MV cables are all AC, as this requires no converters. All cables are 3-phase AC and made of cross-linked polyethylene (XLPE). All the cable voltages are specified at the end of Section 10.6.

10.5 | Power Electronics

The placement of the power electronics on-or-offshore is another consideration in the farm layout. Power electronics have one of the highest failure rates in a system, and thus, there is more effort to place them onshore where they are more easily accessible for maintenance or repair [95]. Power electronics is a broad umbrella term, under which encompasses converters, transformers, power sensors, and power semiconductors. However, as the individual units transmit in AC, and onshore grids take AC, no converter is needed. A transformer comes in the form of a back to back (B2B) converter, where the AC source power is stepped to the power compliant to the onshore grid. This is done by converting AC-DC-AC. The placement of transformers will be onshore to decrease maintenance and repair costs. Power sensors are inevitably in the offshore environment, and are deployed on each individual unit. The power data from these sensors is sent to the nearest offshore collection station. Finally, the power semiconductors comprise of diodes, thermistors, and transistors, however these are not present in the farm layout.

10.6 | Layout Determination

In this section, first the layouts are tested using Python in Subsection 10.6.1. Then, the final layout is presented in Subsection 10.6.2.

10.6.1 Testing of Configurations

In order to select a configuration, Python was utilised for testing. It must be stated that only string-and-star combination layouts were tested. In the farm application, stars must be combined with strings, otherwise, there is a multi-link transmission to shore in the form of 10+ 70 km cable lines. Thus, a star-only configuration is not feasible in the farm design. Although a string-only layout is feasible, the layout is inherently less reliable than a combination layout, and thus was not tested.

It must be stated that the farm layout, for simplicity, was taken as a regular layout ie. the farm is symmetric. All the tested configurations had the same number of WaveWings units within them. Irregular farm layouts have the potential to increase power generation. However, this is an optimisation problem often using artificial intelligence that requires geo-data on the contour and architecture of the seafloor. This task is left for future study.

For the string-and-star combination layout, the Python code first finds the potential star configurations by finding the factors of 400. This complies with *USR-REQ-1-2*, as the configuration then contains 400 units. From literature, the number of units within a star is typically not over 10[96]. Then, the code spaces the individual units by at least 2000 meters of each other such that the code complies with *USR-REQ-1-2-1*. This operational window is constrained by the maximum tether length used in operation of the AWES with a safety factor applied. It determines the length of the MV cables within the star and multiplies this by the number of stars in that given configuration to give the total MV cabling length. Finally, the code arranges the stars such that the farm is enclosed in a box, so that the total farm area is given. Concerning sustainability, it is necessary to minimise the farm area in order to mitigate the impact on the marine environment. This is summarised in Table 10.2.

Table 10.2: String-and-star configurations

No. Units in a Star	No. Stars in a Farm	Total Length of MV Inter-Array Cables in Farm [km]	Enclosed Area [km ²]
4	100	452.5	256
5	80	544.4	204.8
8	50	836.2	128
10	40	1035.5	102.4

Configurations with lesser number of units within a star require a more extensive network of radial feeder cables. As radial feeder cables are at a higher voltage than the MV inter-array cables, they are more costly per km, and drive up the cost of the cabling. As a result, the first two rows are not as suitable. Concerning enclosed area, the option with 8 units to a star already halves the enclosed area of the farm. The 10 units to a star is also suitable, however, the enclosed area is not much lower, yet the total length and cost of the inter-array cables increases.

10.6.2 Final Layout

It is found that the best string-and-star combination layout is 50 stars each with 8 units, using 22 kV inter-array cables within the star. At the center of each star is an offshore transformer that steps up the 22 kV to 66 kV. These transformers are placed on a floating platforms at the center of each star. Then, there are 25 radial feeder cables at 66 kV each connecting two star groups. The 25 radial feeders will be split into 5 main radial feeders of 66 kV that join to 5 offshore collection stations of the farm. The farm has a multi-link power transmission to shore using 5 links. There are five onshore stations each with a back to back converter (B2B) step the voltage to the onshore grid-compliant power by being placed in series to each multi-link. This gives compliance to *PGO-REQ-3*. Aside from these B2B transformers onshore, each WaveWings unit houses its own transformer. The power transmission to shore is presented in Figure 10.3, with cable voltages, source, and transformers specified. The section before an offshore collection station (one-fifth of the farm) is presented in Figure 10.4, with cable voltages specified. Five of these diagrams becomes the 400 unit farm. The cable types are XLPE (cross-linked polyethylene) which are rated for the subsea application, and they are often embedded

a few meters below the seafloor[94]. It must be stated that this proposed layout is subject to change after analysing the budgets in Chapter 16.

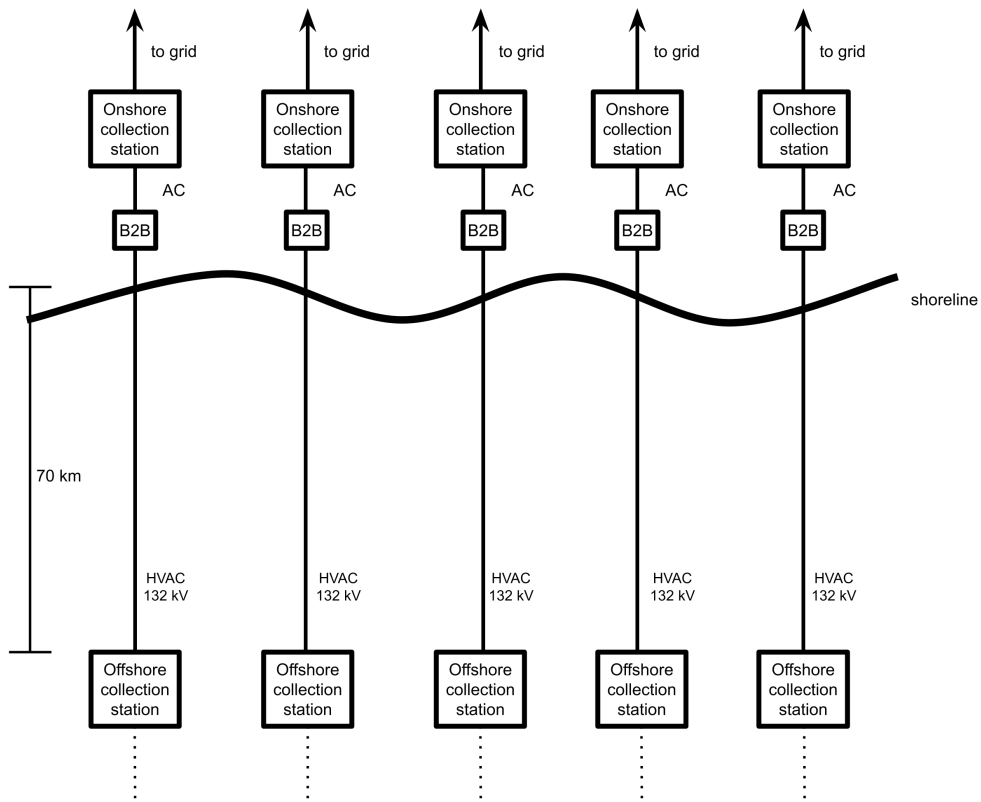


Figure 10.3: Power transmission from the offshore collection stations to shore

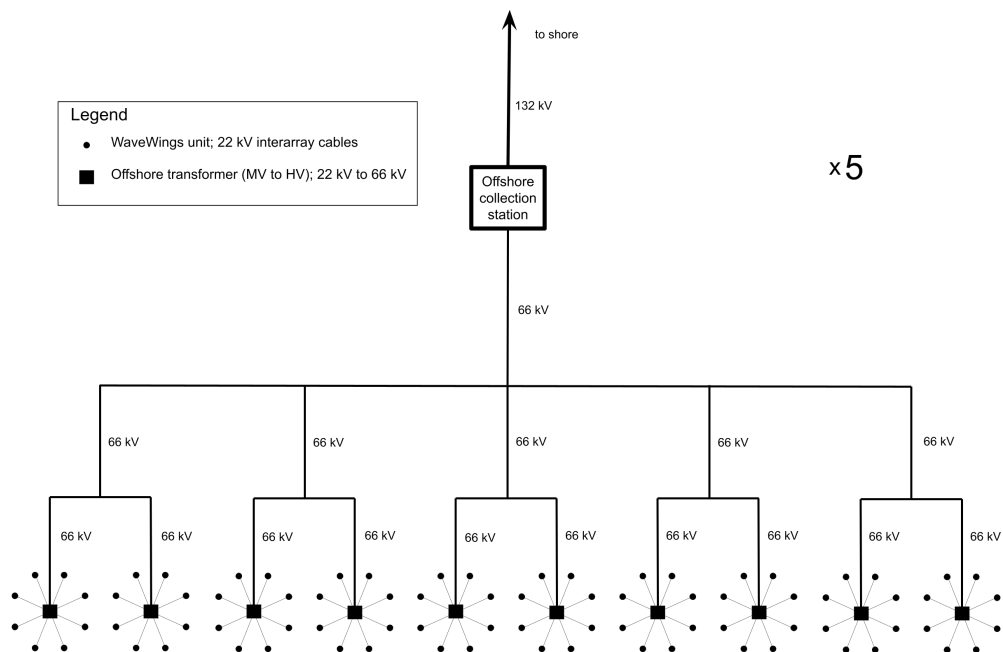


Figure 10.4: One fifth of the final farm layout

11 | Financial Analysis

This section describes the methods and tools developed to carry out an in-depth analysis of the financial aspects of the WaveWings project. First, an overview of the requirements related to the section. Then, the economic model developed for the project and assumptions made is provided in Section 11.2. After this, the results are discussed in Section 11.3. Finally, to further analyze the economic model and the effects of changing input parameters, a sensitivity analysis is carried out in Section 11.4, where a map of LCOE values for the chosen farm location is included.

11.1 | Requirements

Table 11.1 mentions all the requirements related to the financial and economic performance of the project. These are taken into account when drawing conclusions in this section.

Table 11.1: Requirements for financial and economic aspects

Identifier	Requirement
USR-CON-1	The farm shall provide a 50-80% LCOE reduction compared to other off-shore renewables.
USR-CON-1-1	The farm shall provide total cost savings of 40% compared to individual deployment of airborne wind and wave energy systems.
USR-CON-1-2	Each unit shall provide a 25-30% manufacturing cost reduction compared to separate corresponding units of airborne wind energy and wave energy generation.
USR-CON-1-3	Detailed cost estimations shall be carried out for all components of the system, both for a single unit and for a 1 GW farm.
USR-CON-1-5	The system shall have a mission lifetime of 20 years.

11.2 | Economic Model Description

The economic model developed for the WaveWings project is written in Python and makes use of open-source libraries such as geopandas and shapely to handle geographic data. It consists of three main modules: the AWES module, WEC module and infrastructure module. Each of these makes use of analytical and empirical relationships collected from various sources, and calculates specific components of the capital and operational expenditures. These costs are then combined to estimate several key performance indicators (KPIs) and to generate graphics of the cost breakdown structure. An overview of the architecture of the program is shown graphically in Figure 11.1. Each module is enclosed in a box, with a heading indicating the source of the cost relationships used. Each module is described in more detail in the following sections.

It is important to note that the actual cost of individual WaveWings devices is not simply a summation of the components required for the AWES and WEC systems individually, since some subsystems, such as the PTO, relate to both the AWES and WEC. Furthermore, according to the system definition (Section 4.4), AWES and WEC are not identified as individual systems since in the case of WaveWings these concepts are very closely interconnected. Instead, an airborne and floating system are defined. However, due to the complexity of modelling this interconnection and the lack of existing information on similar devices, it is assumed that the AWES and WEC cost components may be added together.

The economic model takes over 50 individual inputs, ranging from general pa-

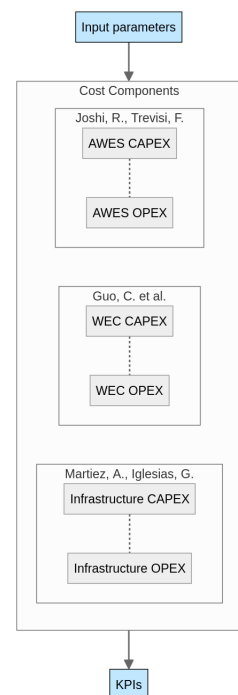


Figure 11.1: Architecture of the WaveWings economic model

rameters, such as the project lifetime, to component-specific parameters, such as the surface area of the kite. Each module has its own specific set of inputs, and is described in the corresponding sections below.

11.2.1 AWES Module

The AWES module makes use of *Reference Economic Model for Airborne Wind Energy Systems*, [97] which has been developed with both onshore and offshore airborne systems in mind. The module breaks up cost components into three sections: kite, tether and ground station, and takes the following inputs:

- n_dev number of devices
- S projected wing area
- LF loading factor
- L_str_soft kite lifetime
- N_y lifetime of project
- P_rated_obgen KCU generator power
- P_rated_gen main generator power
- l_tether tether length
- mat_winch winch material
- τ winch peak torque
- E_rated_hacc hydraulic accumulator rated energy storage

Figure 11.2 shows a graphic representation of the component costs estimated by the model. In the figure, cells highlighted in red indicate that they have not been fully implemented in the economic model due to lack of data, or are not relevant for this project. For example, electrical drivetrain costs from the original source have been omitted since a hydraulic drivetrain is used instead. For conciseness, the balance of system and balance of plant cost components from the original source are not included in this diagram as they are also not implemented (these costs are accounted for in the infrastructure module - Section 11.2.3). In addition, the relations given by the original source have been extended to also consider the costs of the Launch & Landing system, which is an important component of the WaveWings devices.

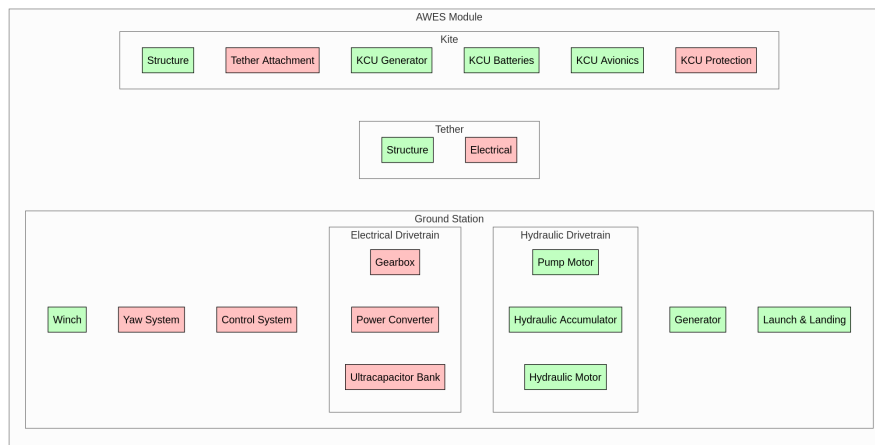


Figure 11.2: Cost components estimated by the AWES module

Kite structure CAPEX (capital expenditures) are estimated based on the projected wing area, with the frequency of replacement based on an assumed kite lifetime of 0.75 years and operational parameters of the devices. With these values, the OPEX (operational expenditures) is estimated based on the required replacement rate.

The CAPEX of the generator and batteries required for the KCU are estimated based on their rated power, which has been calculated to be 23 kW. In addition, the cost of KCU avionics have an assumed fixed cost of €30,000, as given by [97]. OPEX costs are not estimated for these components due to lack of available data.

One of the largest contributors to the final costs of the project is the tether component of the airborne system. The CAPEX of this component has been adjusted from the original source to depend on length,

making use of the specific weight of the selected tether material (Dyneema SK78). The lifetime of the tether is assumed to be the same to that of the kite. To calculate the replacement rate, this is taken into account along with the average loading factor of the kite. Additionally, the replacement costs are also adjusted such that only 70 m of the tether (stroke of the tether, as discussed in Section 7.6) has to be replaced at a time. This is due to the fact that the part of the tether that deteriorates most rapidly is the one that is being constantly spooled in and out of the drum. This means that during maintenance, the tether is split in two, with the part closest to the kite being spooled around the drum, and a new tether section being connected to it and to the kite. With these assumptions in mind, the OPEX of the tether is calculated based on this replacement rate and replacement fraction.

The winch component CAPEX is estimated based mainly on material costs. For this, the specific costs (with respect to mass) of various materials are implemented in the economic model. For the case of WaveWings, CFRP is assumed. An important consideration to keep in mind when analyzing the results of the economic model is that manufacturing and post-production costs (i.e. special treatments), are not considered. The OPEX is not modelled due to lack of available data.

Hydraulic drivetrain costs, including the generator, are driven by the rated power and rated energy (hydraulic accumulators) of the subsystem. The OPEX of each of these components is estimated based on an expected lifetime and replacement rate. Furthermore, the effect of learning rates and increasing product maturity are not considered, as it is assumed that the devices are manufactured as part of a single batch.

Specifically, for the pump-motors, a yearly replacement rate of 0.125 is assumed, resulting in 3 replacements throughout the project lifetime. Hydraulic accumulators are assumed to have a yearly replacement rate 0.1, and hydraulic motors 0.08 [97], resulting in 2 replacements over the project lifetime for each of these components.

The final component considered in this module is the launch and landing system. For this, a commercial off-the-shelf option is selected, as discussed in Section 8.8. As such, a fixed cost of €100,000 is assumed. OPEX of this component is also not modelled due to lack of available information.

11.2.2 WEC Module

The WEC module makes use of *Estimating the Cost of Wave Energy Converters at an Early Design Stage: A Bottom-Up Approach* [98]. This source estimates costs of various WEC components primarily from raw material and manufacturing costs. Specific values for the masses of each component are estimated from the detailed design sizing and the CAD model. As such, the input parameters for this module are the following:

- | | | |
|--|--|---------------------------------------|
| • n_dev number of devices | • m_hull_supporting supporting component mass | cast iron mass |
| • m_hull_steel hull steel mass | • m_mechanical_hpsteel high precision steel mass | • m_mechanical_bearings bearings mass |
| • m_hull_ballast ballast mass | • m_mechanical_lpsteel low precision steel mass | • m_mechanical_shaft shafts mass |
| • m_hull_reinf_concrete reinf. concrete mass | • m_mechanical_cast_iron | • pto_type PTO type |
| • m_hull_fibreglass fibreglass mass | | • P Rated WEC rated power |

A graphical overview of the components calculated by this module is shown below in Figure 11.3. Again, components highlighted in green are implemented by the economic model, and those highlighted in red are not omitted for the same reasons described in Subsection 11.2.1. It is important to point out that mooring and installation costs are omitted here as they are estimated as part of the infrastructure module (Subsection 11.2.3).

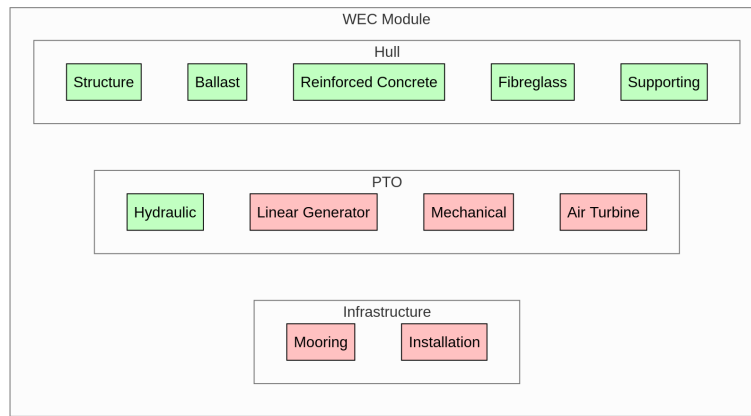


Figure 11.3: Cost components estimated by the WEC module

For this module, no modifications have been made to the relations provided by the original source, other than omitting irrelevant components.

11.2.3 Infrastructure Module

The infrastructure module primarily makes use of a model developed for the analysis and mapping of the LCOE of floating offshore wind in the Mediterranean Sea [36]. Several adaptations are made to it, as proposed by [8], to adapt the model for use in the chosen farm location off the western coast of Ireland. As such, the following are the input parameters to this module (for conciseness, less important inputs are left out).

- `n_dev` num. of devices
- `n_mooring_lines` num. of mooring lines
- `n_ex_cab` num. of export cables
- `n_off_sub` num. of offshore substations
- `n_on_sub` num. of onshore substations
- `n_dev_trip` num. of devices per trip
- `t_inst` installation time
- `v_boat` boat velocity
- `c_boat` boat cost
- `c_anchor` anchor cost
- `c_mooring_line` mooring line cost
- `c_chain` chain cost
- `c_ex_cab` export cable cost
- `c_off_sub` offshore substation cost
- `c_on_sub` onshore substation cost
- `c_inter` inter-array cable cost
- `n_array` grid lambda (num. of devices in each row/column)
- `d_port` distance to port
- `d_shore` distance to shore
- `depth` water depth
- `p_rated` rated power
- `N_y` project lifetime
- Kite operational window

For most of the inputs, values used by the original source and adapted version for the Mediterranean coast are assumed. However, it is important to keep in mind that these values are specific to offshore wind turbine farms.

Using these inputs, the model breaks down the infrastructure costs even further into four parts: development and consent, installation, component costs and end-of-life costs. This is shown visually in Figure 11.4.

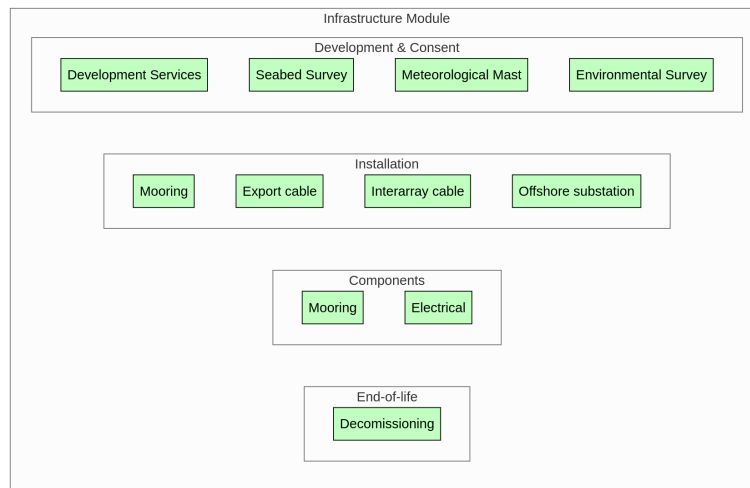


Figure 11.4: Cost components estimated by the infrastructure module

As can be seen by the highlighted green cells, all proposed components from the original paper are implemented for the economic model. Furthermore, mooring and installation costs proposed by [98] for the WEC Module are instead implemented here, according to the corresponding costs for offshore wind turbine projects.

In Figure 11.4 the development and consent costs include environmental, meteorological station and seabed station surveys, project management and development services. These are estimated in the original source by extrapolating data from bottom-fixed offshore wind. Furthermore, the end-of-life costs involve carrying out a reversed installation process. Typically, the estimation of the decommissioning costs is made as a percentage of the installation costs. However, in this case, for simplicity and due to difficulties modelling the process accurately, a fixed value is assumed. Details about this can be found in the original source.

The three largest contributors to the overall infrastructure costs are installation, electrical and mooring costs. A simplified relation for each of these costs is shown in below in Equation 11.1, Equation 11.2 and Equation 11.3 respectively.

$$\text{CAPEX}_{\text{inst}} \propto d_{\text{port}} \quad (11.1) \quad \text{CAPEX}_{\text{elec}} \propto d_{\text{shore}} \quad (11.2) \quad \text{CAPEX}_{\text{mooring}} \propto \text{depth} \quad (11.3)$$

As can be seen from these relations, the three variables contributing the most to the infrastructure costs are the distance to port d_{port} , the distance to shore d_{shore} and the sea floor depth depth at the farm location. As mentioned in Chapter 5, the selected port is Rossavel, and is located approximately 70 km away from the farm, and approximately 40 km from shore. The sea floor depth at this location is 150 m.

Tied to these are operational expenditures, which are estimated based off of offshore HAWT projects, but scaled to the power output of the WaveWings 400 unit farm.

11.2.4 Key Performance Indicators

A set of financial KPIs are implemented to allow for a better understanding of the economic performance, efficiency and effectiveness of the project. These indicators are also used in the market analysis (Chapter 6) to compare the WaveWings project with competitors in the relevant markets. The indicators implemented in the economic model are:

- Weighted average cost of capital (WACC)
- Annual energy production (AEP)
- Capital expenditures (CAPEX)
- Operational expenditures (OPEX)
- Levelized cost of electricity (LCOE)
- Levelized revenue of electricity (LROE)
- Net present value (NPV)
- Internal rate of return (IRR)

The most commonly used metric in the renewable energy industry is the LCOE, which is calculated with the following formula:

$$\text{LCOE} = \frac{\sum_{y=0}^{N_y} \frac{\text{CAPEX}_y + \text{OPEX}_y}{(1+r)^y}}{\sum_{y=0}^{N_y} \frac{\text{AEP}_y}{(1+r)^y}} \quad (11.4)$$

where r is the discount rate, AEP is the annual energy production, y is the specific year, and N_y is the project lifetime [97]. In the case of the WaveWings project, the CAPEX is assumed to be entirely expended in the first year and the OPEX and AEP are assumed to be constant throughout the operational years. Furthermore, EOL decommissioning costs are assumed to be expended entirely in the final year.

The final discount rate may be approximated by the weighted average cost of capital (WACC), which represents a project's average after-tax cost of capital from all sources, including stock, bonds, and other forms of debt. As such, WACC is the average rate that a project must be able to pay in order to finance itself. This is also a common way to determine the required rate of return as it expresses the return that shareholders and money-lenders expect. The WACC (discount rate, r) is calculated with the following formula:

$$r = \frac{1}{1+q} r_e + \frac{q}{1+q} r_d (1 - T_C) \quad (11.5)$$

where q is the debt-to-equity ratio, r_d is the cost of debt, r_e is the cost of equity and T_C is the tax rate for corporations [97]. For this, typical values for wind energy projects are assumed: $q = 70/30$, $r_d = 0.08$, $r_e = 0.12$, and $T_C = 0.25$.

In addition to this, the net present value (NPV) and the internal rate of return (IRR) are indicators that allow for the quantification of the profitability of a project. Specifically, NPV is the difference between the present value of future cash inflows and the present value of future cash outflows over a given period of time (in this case, the project lifetime, 20 years). It can be calculated with Equation 11.6.

$$\text{NPV} = \sum_{y=0}^{N_y} \frac{(p_y + \text{subsidy}_y) \text{AEP}_y - \text{CAPEX}_y - \text{OPEX}_y}{(1+r)^y} \quad (11.6)$$

The IRR determines the efficiency of a project in generating profits, and can be calculated by finding the break-even point of the NPV. In other words, the discount rate at which the NPV is zero, which translates directly to a rate at which returns must be generated to cover expenses.

To determine the financial viability and profitability of a project, the WACC and IRR can be compared. The general decision rule to do this is:

- If $\text{IRR} > \text{WACC}$, the project is expected to generate returns greater than the cost of capital, suggesting it will add value to the company and should be accepted.
- If $\text{IRR} < \text{WACC}$, the project is expected to generate returns less than the cost of capital, suggesting it will destroy value and should be rejected.
- If $\text{IRR} = \text{WACC}$, the project is expected to generate returns equal to the cost of capital, suggesting it will neither add nor destroy value.

To contrast with this, the return on investment (ROI) typically focuses on the initial investment made in the project and the end profit. However, it is decided to use the IRR in place of this indicator, as it takes into account irregular cash flows over time. This better captures the finances of the project.

Some additional, less commonly used, KPIs are also implemented in the economic model. Among these are the levelized revenue of electricity (LROE) and levelized profit of electricity (LPOE). These are described in more detail, along with formulas for each, in [97].

11.3 | Economic Model Results

Using the economic model described above with the appropriate inputs for the 400 unit farm yields the following results. First, Figure 11.5 shows two pie charts, indicating the proportion and actual cost of each category. Note that the amounts indicated on the charts refer to the entire 400 unit farm over the 20 years of operation. The chart on the left displays the cost breakdown with respect to each module (AWES, WEC and infrastructure). The pie chart on the right displays the cost breakdown of specific components from all modules. Components with a contribution of less than 10% are combined into the category "Other".

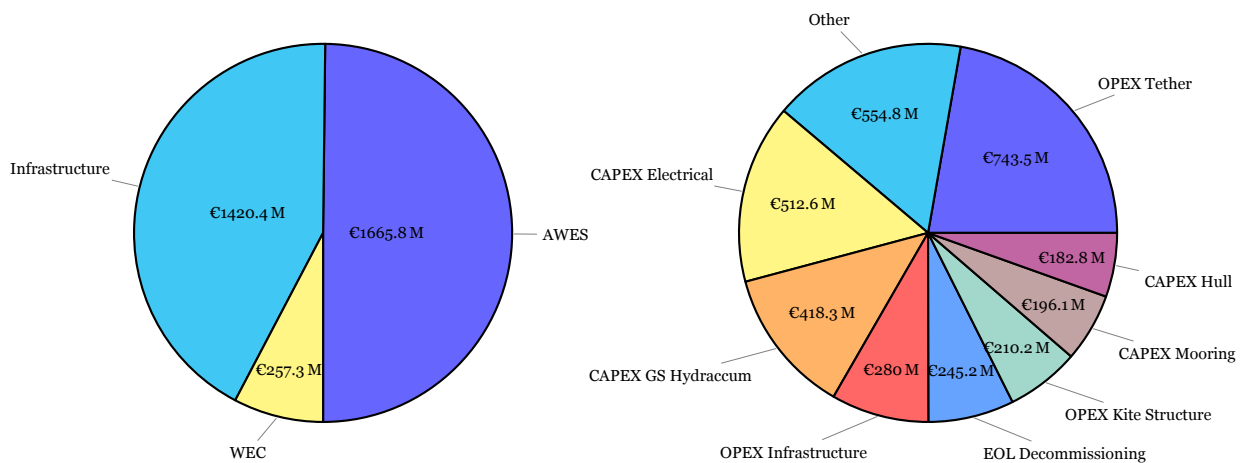


Figure 11.5: Cost contribution breakdown, along with the cost of each component in millions of euros

First, the cost breakdown illustrated in Figure 11.5 shows that the AWES module represents the largest cost component, contributing to 49% of the total cost with an expenditure of nearly €1.7 billion. The primary driver behind this significant cost is the OPEX associated with the tether, which is to be expected given the high specific cost of Dyneema SK78, and the yearly replacement rate of nearly 1. As described in Figure 11.2, a replacement technique is implemented for which only a portion of the tether (equal to the tether stroke) must be replaced. It is important to note that with this replacement technique implemented, the tether cost is decreased from €1.3 billion to €743.5 million. However, as this is still such a large contributor, the tether's maintenance and replacement are crucial factors influencing the overall economic viability of the device.

In addition to the tether costs, it can be seen that CAPEX of the ground station hydraulic accumulator (relating to the AWES PTO) makes up 12.5% of the total costs, by contributing a total amount of €418.3 million. These hydraulic accumulators must store energy temporarily, as explained in Subsection 8.9.2. Given the large power requirement for the AWES PTO of 2.5 MW, these large costs are also expected.

Other than AWES costs, infrastructure costs also have make up a large portion of the total project expenditures. Overall, these contribute a total of €1.4 billion, making up 42.5% of the total project costs. The two largest components of this are the electrical infrastructure CAPEX (15.3% at a cost of €512.6 million) and the infrastructure OPEX (8.37% at a cost of €280 million). The reasons behind this are likely due to the large number of devices present in the farm, and the need to travel back and forth to the farm, increasing the costs of transporting components via vessels. However, to more accurately

determine the driving factors behind infrastructure costs, a sensitivity analysis of the infrastructure module is carried out in Section 11.4.

In addition to this cost breakdown, the KPIs described in Subsection 11.2.4 are also calculated, and provide a comprehensive overview of the project's profitability and efficiency. These are shown below in Table 11.2.

Table 11.2: Financial key performance indicator results from the economic model

Parameter	Value
WACC (%)	7.8
AEP (MWh)	4725147
CAPEX (M€)	1861.01
OPEX (M€)	1237.41
LCOE (€/MWh)	49.4
LROE (€/MWh)	84.2
LPOE (€/MWh)	34.8
NPV (M€)	1693.26
IRR (%)	22.5

As mentioned in Subsection 11.2.4, the WACC and IRR can be compared to determine the financial viability and profitability of a project. To look into this in more detail, the discount rate can be plotted against the NPV, as shown below in Figure 11.6.

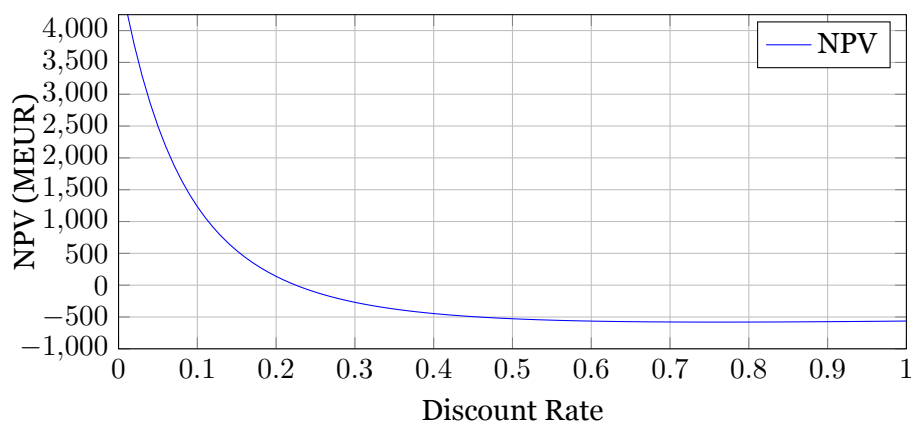


Figure 11.6: NPV plotted against discount rate

The discount rate at which the NPV breaks-even indicates the IRR. In this case, the WACC is 7.8%, and the IRR is 22.5% (as seen in Figure 11.6), which significantly exceeds the WACC. This suggests that the project is expected to generate returns well above the cost of capital, indicating strong profitability.

Finally, looking at the LCOE, which is a crucial indicator for comparing renewable energy technologies, it is determined that the WaveWings project achieved a value of 49.4 €/MWh. This fits within the requirements stated for the project, which leads to the conclusion that the concept described in this report is in fact viable.

11.4 | Sensitivity Analysis and LCOE Mapping

In addition to the results obtained above, a sensitivity analysis is also carried out to determine which inputs have the most significant effect on the financial parameters. For this, the focus is shifted to the farm placement, as this is a factor that is likely to change (within the selected region of the western

Irish coast) as the project develops ¹, and makes up a large contribution of the total project

expenditures. As such, the infrastructure module is tested for a wide range of farm location inputs. Specifically, the installation, electrical infrastructure and mooring costs are varied, since these correlate on location-dependent parameters, namely, d_{port} , d_{shore} and $depth$, respectively. This is shown by relations Equation 11.1, Equation 11.2 and Equation 11.3.

It is not realistic to vary these inputs individually, as they are coupled. That is, for a given location off the Irish coast, there is a corresponding shore distance, port distance and sea floor depth. As a result, the economic model has been extended to support these calculations.

To estimate the minimum straight-line shoreline distance, the `geopandas` and `shapely` Python libraries are used. The shoreline is taken from NOAA [99], and re-projected to from `ESPG:4326` to `ESPG:3857` in order to find distances in an appropriate unit. With this, the minimum, straight-line distance to shore from an arbitrary point may be calculated.

However, it is important to note that this is only a good estimation when the distances are relatively small, as effects due to the curvature of the Earth are not accounted for correctly.

In addition, to estimate the minimum distance to port, it is not sufficient to find the minimum straight line distance as done previously. This distance should represent the path vessels must take in order to reach the farm for activities such as installation or maintenance. As such, the A* path finding algorithm is used to estimate the optimal trajectory of vessels from a given location to the port of Rosaveel. An example image of these optimized paths is shown in Figure 11.7. As can be seen, a silhouette of the Irish coastline has been projected onto a discrete grid where white spots indicate ocean and black spots indicate land. The algorithm is used to avoid these obstacles and travel in an efficient line to the endpoint (in this case, the port).

Finally, bathymetry contours are obtained from SEAI [45]. For each sample point, the sea floor depth may be estimated by simply finding the corresponding depth level.

With this data, the individual contributions of the installation, electrical and mooring CAPEX may be plotted, for a discrete set of locations off the Irish coast. These are shown in Figure 11.8 as heatmaps, with the colour indicating the CAPEX at that specific location.

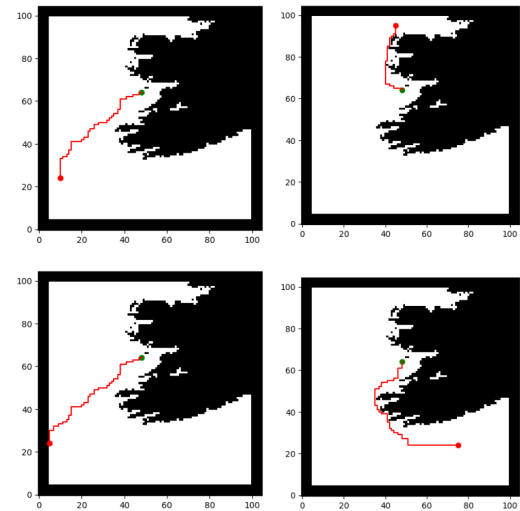


Figure 11.7: A* search algorithm optimal path estimation for vessels travelling to and from an arbitrary location

¹Although individual device costs are also likely to change, they are not considered as part of this sensitivity analysis since a simple evaluation of the largest costs is deemed sufficient to establish which cost contributors are most important.

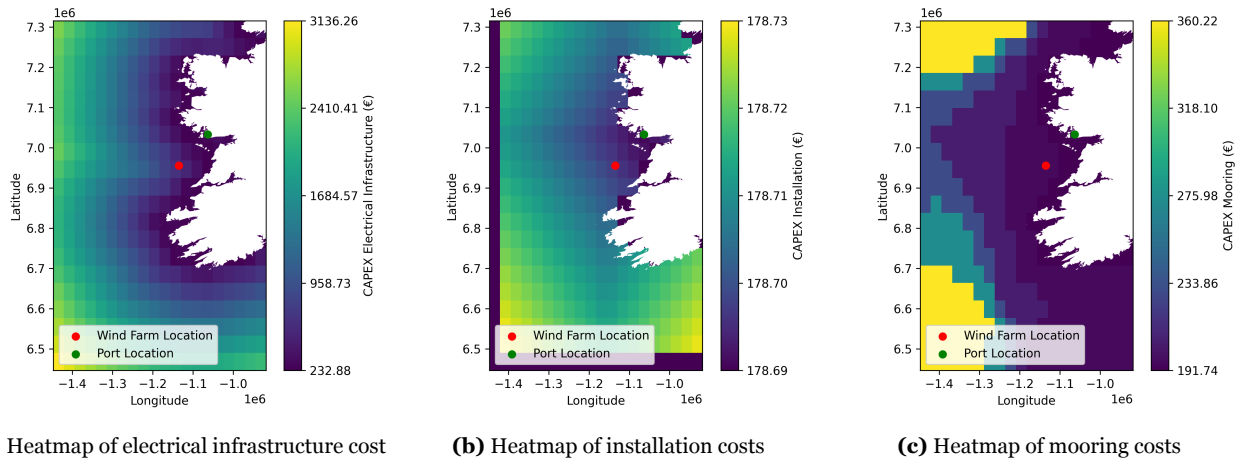


Figure 11.8: Heatmaps of individual components of the infrastructure CAPEX for the offshore wind farm

Note that the dark edges around the edges the coastline in Figure 11.8b are side-effects of discretization the shoreline geometry. This could be mitigated by increasing the sample point resolution (use more points per km^2). However, this is not done due to time constraints, and is not considered to have a large effect on the results of this section.

As can be seen from the figures, electrical infrastructure costs increase sharply from a base value of €512 million to over €2 billion by moving the farm eastwards. A similar effect can be seen from the installation costs. On the other hand, it can be seen that a region of low mooring costs is present around the Irish coastline, up until around 200 km away from the shore. This, together with the fact that electrical infrastructure makes up one of the largest components of the project expenditures, as mentioned in Section 11.3, leads to the conclusion that this farm location is crucial to the viability of the project. Moreover, the project is likely to benefit from a reduction in LCOE and increased IRR if the farm location is further optimized to reduce these costs.

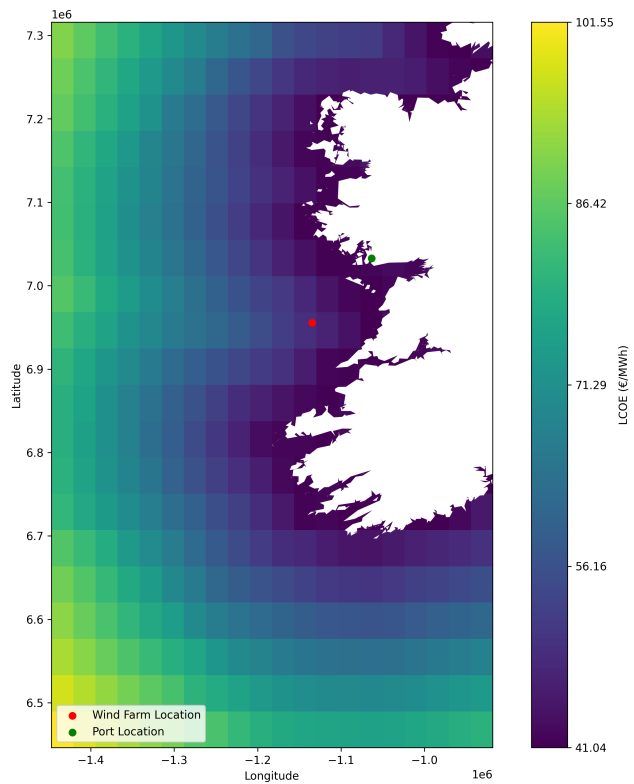


Figure 11.9: LCOE Map

To look into this in some more detail, the individual electrical infrastructure, installation and mooring costs can be set as inputs to the economic model to calculate the LCOE at discrete points in the map, and plot it again as a heatmap. This is shown in Figure 11.9. As can be seen, it is still possible to further reduce the LCOE of the WaveWings farm by either moving closer to the shoreline, or to a location such as the one south-west of the current location, where a low-LCOE region extends further offshore.

12 | Risk Analysis

In order to ensure the reliability, predicted functionality, and safety of an integrated WaveWings system, a risk analysis is carried out. Given that the field is currently in development, these concepts are inspired from the petroleum industry, knowledge on floating offshore platforms and wind turbine technologies, and studies carried out by start-up’s and researchers in the field of AWES. Firstly, a SWOT diagram indicates the strengths (helpful internal aspects), weaknesses (harmful internal aspects), opportunities (helpful external aspects), and threats (harmful external aspects). By identifying these aspects early in the product development phase, unforeseen limitations are eliminated. Additionally, it serves as a review of the additional requirements that are needed in reducing weaknesses and threats identified through the novelty of the technology whilst enhancing strengths and opportunities found in the synergy of wave and wind power. Secondly, the technical risk assessment outlines risks, consequences, and mitigation strategies for all key subsystems, namely: Kite, Kite Control Unit, Buoy, Mooring, Communications, and Power. By tabulating these elements, a Failure Mode and Effects Analysis (FMEA) procedure is replicated to thoroughly identify relevant issues that can arise. Consequently, risk and post-mitigation risk maps are displayed for a visual summary of the findings. A Fault Tree Analysis (FTA) shall be presented from a high-level system integration perspective to understand the interactional failure modes between the AWES and WEC components. In essence, a preliminary Common Mode Analysis (CMA) framework is established because the interaction of these technologies in a single platform has yet to be realized in industry.

Throughout the assessment, definitions for probability and severity bands should be considered in Table 12.1 and Table 12.2, respectively. These are used when generating the risk maps shown in Figure 12.1 and Figure 12.2.

Table 12.2: Severity Bands

S Value	Definition	Harm
1	No Impact	No harm
2	Very Minor	Maintenance
3	Minor	Harm to environment
4	Moderate	Limited efficiency reduction without impact to long-term functionality, temporary down-time (eg. software failure)
5	Critical	Functionality of product in energy-harnessing phase impeded, short-term reliability of system cannot be assured
6	Catastrophic	Grid-level impact of integrated system failure, independency of system failure not assured

Table 12.1: Probability Bands

P Value	Definition
1	Extremely Unlikely
2	Remotely Likely
3	Occasional
4	Reasonably Likely
5	Frequent

12.1 | Requirements

Requirements for this section are limited, stemming from guidelines on the methods that should be used when carrying out a technical risk assessment, as shown in Table 12.3.

Table 12.3: Requirements for Technical Risk Assessment

Identifier	Requirement
USR-CON-3	The design shall include a high-level FMEA and FTA.

It should be noted that the Fault Tree Analysis (FTA) could not be carried out due to limited understanding of the system’s behaviour without the access to a prototype, testing facilities, and a thorough investigation into failure modes with a quantified probability. R. Schmehl, V. Salma, and F. Friedl [100] do present relevant AWES FTA whilst literature on FTA’s for WEC are lacking. Nevertheless, the FMEA shall serve as a robust framework to explore relevant failure modes.

12.2 | SWOT Analysis

Table 12.4: SWOT diagram

	Helpful	Harmful
Internal	<p>Strengths</p> <ul style="list-style-type: none"> Combining AWES and WEC technologies can lead to a lower LCOE than conventional wind turbines since they share the same infrastructure and the power production is increased compared to individual systems. The associated requirements are USR-CON-1 and USR-CON-1-1. AWES can extract energy from more reliable and powerful winds at high altitudes. The associated requirements are USR-REQ-1 and USR-REQ-1-1. Combining AWES and WEC leads to a design that uses less material than an individual WEC or AWES and less material than a conventional wind turbine. The associated requirement is USR-CON-1-2. 	<p>Weaknesses</p> <ul style="list-style-type: none"> AWES is a relatively new technology and WEC is not widely commercialised yet. Combining both technologies into a single platform has never been done before. This ambition is translated to requirements DEV-CON-7 and USR-CON-1-1-CTR-1. Control strategies are more complicated than with conventional wind turbines, which requires both robust and reliable software as well as suitable risk management. This is reflected in requirements USR-REQ-2-3-AWE-1 and USR-REQ-2-3-AWE-2.
External	<p>Opportunities</p> <ul style="list-style-type: none"> As shown by the surge in fossil fuel prices due to the Russian-Ukrainian war, Europe needs to build energy self-sufficiency. The EU is investing more than €210 billion forenergy efficiency and renewable energy by 2027 for this purpose [54]. The 2012 global primary power demand is 18TW. High altitude off-shore wind resources worldwide have an 1800 TW power production potential whereas lower altitude winds that wind turbines extract energy from only have 400TW of power production potential; wind energy extraction is not limited by geophysical limits [55]. 	<p>Threats</p> <ul style="list-style-type: none"> Shipping routes, fishing industry, oil and gas exploration, and military use of off-shore areas can hinder the approval of an off-shore wind-wave farm [56]. Natural areas would prohibit the installation of a farm. Requirements ENV-CON-4 and ENV-CON-5 stem from this.

12.3 | Technical Risk Assessment

According to S. Ambühl [101], the failure probability threshold required by manned and unmanned systems are 3×10^{-5} and 5×10^{-4} , respectively. Therefore, it is inherently beneficial to develop unmanned platforms pushing for full offshore autonomy due to minimized risks for human life. Inevitably, however, maintenance crews need to be aware of the risk of operating near dynamic systems but will traditionally intervene during static states, that is, before or after failure events. Nevertheless, financial risks remain provided that systems with autonomy require high reliability to avoid severe failure modes and limit the movement of maintenance crews to locations far away from the coast. In a grid setting, where the failure of a single unit may impact the functionality of neighbouring units, a Zonal Safety Analysis (ZSA) is recommended in conjunction with existing grid layout (highly-dispersed units are at lower risks of interfering with one another).

Acknowledging the fact that AWES and WEC technologies are up-and-coming technologies with relatively low TRLs, the exact failure probability of all components cannot always be modelled with existing knowledge. Therefore, in this risk assessment, risk shall be approximated as a product of relative probability and severity levels and, when possible, be supported with existing statistical models. Risks are ordered by subsystem with the exception of the “Grid” that has high-level implications across all subsystems and the integration of the unit. Identifiers are “GRD” for Grid, “AWE” for Kite, “KCU” for Kite Control Unit, “MOR” for Mooring, and “PWR” for Power. Probability and severity value are defined as shown in Table 12.1 and Table 12.2, respectively. These are to be used to construct the risk map shown in Figure 12.1.

For AWES, R. Schmehl, V. Salma, and F. Friedl [100] present an approach to improving reliability and safety through the use of an FMEA; several of these concepts are translated into risks tabulated in Table 12.5. Similarly, for WEC, risks involved with the use of hydraulic PTOs were identified [102] whilst Sandia National Laboratories [103] confirm that hydraulic, high-voltage electrical, and instrumentation systems are high-priority subsystems in an FMEA. Additionally, it is suggested that failure log of a deployed system should be compared to the original FMEA whilst a failure mode analysis should be used in numerical modelling and experimental testing to confirm the fatigue analysis and extreme response analysis when optimally designing a WEC system [102]. However, the scope of the study presented below shall remain limited to aspects that apply to all hydraulic PTO WEC systems and that are integrated with an AWES. Coupled effects, subsystem or grid level, will be reflected in the analysis to demonstrate inter-dependencies that may not be apparent in decoupled systems.

Table 12.5: Technical Risk Assessment

Risk ID	Risk	Consequence	Mitigation Strategy
TR-GRD-1	Deep offshore placement of systems leads to limited accessibility for maintenance crew, requires sustained reliability and autonomy to limit costs of downtime	Costly failure events, increased LCOE, disruption in electrical grid, trust and reliability in system as a primary source of energy damaged	Use of support vessel to limit times made in displacement, especially in testing phases of the product
TR-GRD-2	Failure of electrical infrastructure (cabling, substations)	Abrupt loss of power, heavy costs, electrical grid maintenance crew required	Installation by certified electrical engineers, back-up sources from primary nation-wide grid
TR-GRD-3	Tangling of tethers of kites in grid	Re-design/re-mooring may be required, disruption of local or domino-effect flight capabilities of AWES component	Small-scale grid testing to check for interferences
TR-GRD-4	Ship routes interfering with grid	Entire grid at risk of damage, WEC systems close to shipping routes may be inefficient due to locally-induced waves	Location survey, clear communication with local maritime authorities
TR-GRD-5	Grid placed in high-activity marine ecosystems	Migrations and movement of large marine wildlife causing damage to the grid and harm to the wildlife	Location survey, clear communication with local maritime authorities
TR-AWE-1	Fatigue-induced bridle line failure	Reduced controllability leading to power output losses, loss of kite, loss of partial grid capabilities due to moving projectile	Safety factor of 3 applied to nominal bridle loads
TR-AWE-2	Deflation of the structural members (tubes) on the kite; decreased controllability and aerodynamic efficiency	Water landing likely, submerged AWES cannot be recovered autonomously, can sink with time leading to loss of kite, replacement and displacement of maintenance crew required	Installation of pumps to compensate for pressure losses, designing kite to have compartments to limit spread of leak
TR-AWE-3	Ruptured tether due to loads exceeding nominal conditions during extreme events with failure in retrieval protocol; premature rupture in tether due to underestimated fatigue cycles before end-of-life	Loss of kite, loss of partial grid capabilities due to moving projectile, tether backlash leading to damage of neighbouring equipment	Safety factor of 3 applied to nominal tether loads

TR-AWE-4	Dirty kite surfaces leads to added mass	Decreased aerodynamic efficiency	Spray nozzles integrated into launch tower to regularly get rid of accumulated salt, dirt, and bird excrements
TR-AWE-5	Rupture of the kite sail due to adverse weather conditions (lightning, hail, bird strike, hard landings)	Loss of kite, replacement and displacement of maintenance crew required	Patches/strips of Kevlar placed onto the sheet as reinforcements
TR-KCU-1	Poor KCU characteristics and synchronization with launch tower elements leading to water landing	Submerged AWES cannot be recovered autonomously, can sink with time leading to loss of kite, replacement and displacement of maintenance crew required	Onboard inflatable elements with CO2 cartridges for fast inflation, synchronized tether reel-in to avoid drifting
TR-KCU-2	Wind turbine failure	Loss of power to KCU, loss of control	Robust testing programme and determination of durability of turbine
TR-KCU-3	Software issues originating from flight or system state controllers	Incorrect representation of flight state, highly likely kite will crash whilst minimizing power generation	Robust testing programme in isolated environment, pushing software to limit of flight envelope, implementing software fixes
TR-KCU-3	Primary CPU hardware failure	Measurements fed to logic block cannot be processed, kite no longer subjected to any control strategy	Robust testing programme in isolated environment, pushing software to limit of flight envelope, implementing software fixes
TR-KCU-4	KCU electrical malfunction (short-circuit, fire)	Submerged AWES cannot be recovered autonomously, can sink with time leading to loss of kite, replacement and displacement of maintenance crew required	Design methodology needs to consider reliability, robustness, and requires substantial on-site testing with similar environments
TR-MOR-1	Mooring line failure; overloaded tension, whales, internal cracks, superficial corrosion leading to crack growth	Floating platforms start to drift, collisions with neighbouring units, tether lines will tangle if kites are not reeled-in during detection of this event	Regular inspections are performed, create digital twin (analytical model) to estimate repair needs
TR-MOR-2	Anchor failure; becomes loose, starts tilting, platforms will start to drift	Decrease in power output, floating platforms start to drift, collisions with neighbouring units, tether lines will tangle if kites are not reeled-in during detection of this event	Execute anchoring and monitor with care and effort
TR-MOR-3	Loss of pre-tension	Disturbance of mooring pattern in grid limited	Satellite monitoring of mooring patterns in grid and adequate installation protocol
TR-PWR-1	Wave conditions that deviate from nominal design conditions will lead to over-extension of PTO; WEC platform heaves past stopper limit	Heavy damage to integrated unit, maintenance crew required for replacement	Design storm-mode for system to submerge during extreme weather or to shut PTO system securely to constrain moving parts
TR-PWR-2	WEC hydraulic PTO leakage due to overpressure; environmental damage	Decrease in power output and durability, maintenance crew required	Monitor health closely, use biodegradable hydraulic fluids
TR-PWR-3	WEC hydraulic PTO water ingress	Decrease in power output until maintenance crew required	Robust design isolating PTO system, suitable seals if needed
TR-PWR-4	Seizure of WEC hydraulic PTO due to fatigue, buckling of piston rod, bearing failure, and leakages from worn-out bores and seals	Low volumetric efficiency, overheating of motor leading to loss of lubrication through leakages, additional wear/friction, and damage	Health monitoring through use of probe for (coolant) temperature and pressure
TR-PWR-5	Loss of control, flow energy, induced unsteady discharge rates, and increased contamination risks of hydraulic fluid due to failure of pressure lines, shut-off valves, check valves, flow control valves, pressure relief valves, and accumulators	Pressure spikes, environmental pollution, overheating of motor, vibrations	Health monitoring through use of probe for pressurized lines, flow directions, and fluid temperature and colour

TR-PWR-6	Failure of electric generator as induced by shorting of circuit windings, abnormal connection of stator windings, eccentricity of rotor dynamics, broken rotor bars, cracked end rings, and increased torque pulsations	Low to no conversion efficiency, pulsating/intermittent conversion	Monitoring of leakage, temperatures, and vibrations of stator-rotor-gearbox-motor assembly
TR-PWR-7	Generator rotor failure	Maintenance crew required, substantial costs due to replacement of integrated unit required	Design methodology needs to consider reliability, robustness, and requires substantial on-site testing with similar environments
TR-PWR-8	Fire induced by saline environment or structural integrity of buoy	Catastrophic event impacting operation of WaveWings unit and significant financial damages	Consideration of Ultimate Limit States, Fatigue Limit States, Accidental Limit States, and Serviceability Limit States; electrical components should be as isolated and waterproof as possible
TR-PWR-9	WEC hydraulic motor failing to convert hydraulic energy of fluid to rotational energy of shaft due to motor losses, low fluid energy flow, and unsteady or obstructed energy conversion	Low to no shaft torque, low to no power generation, unsteady power delivery, high temperatures, increased vibrations and noise	Measurements of fluid state and power

Note that for the majority of items, no known probability distribution is known. However, with the use of research by R. Schmehl, V. Salma, and F. Friedl [100], probability distributions could be calculated for the items shown in Table 12.6.

Table 12.6: Known Probability Distributions

Risk ID	Probability Distribution
TR-KCU-2	Weibull($\eta = 50000, \beta = 1.2, \gamma = 0$)
TR-KCU-3	Constant($q = 0.001$)
TR-COM-1	Weibull($\eta = 100000, \beta = 1.0, \gamma = 0$)
TR-KCU-3	Weibull($\eta = 25000, \beta = 0.7, \gamma = 0$)
TR-COM-2	Constant($q = 0.001$)

12.4 | Risk Maps

Risk maps shown in Figure 12.1 and Figure 12.2 provide a visual overview of the risks identified where the normalized product of risk and probability yields higher risk level tending to the top right corner whilst lower risk levels tend to the bottom left corner. By applying the risk mitigation strategies that were established in Section 12.3, all items in Figure 12.1 will shift left-bound to lower probability levels or to lower risk levels if there lowest probability level has already been attained; results are tabulated in Figure 12.2.

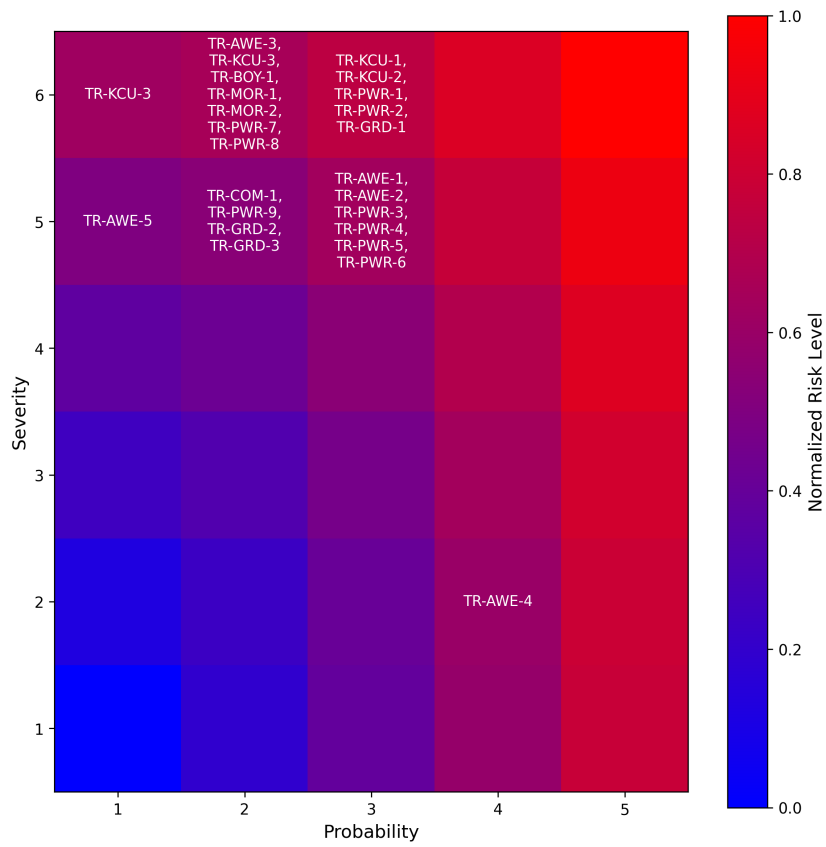


Figure 12.1: Risk Map

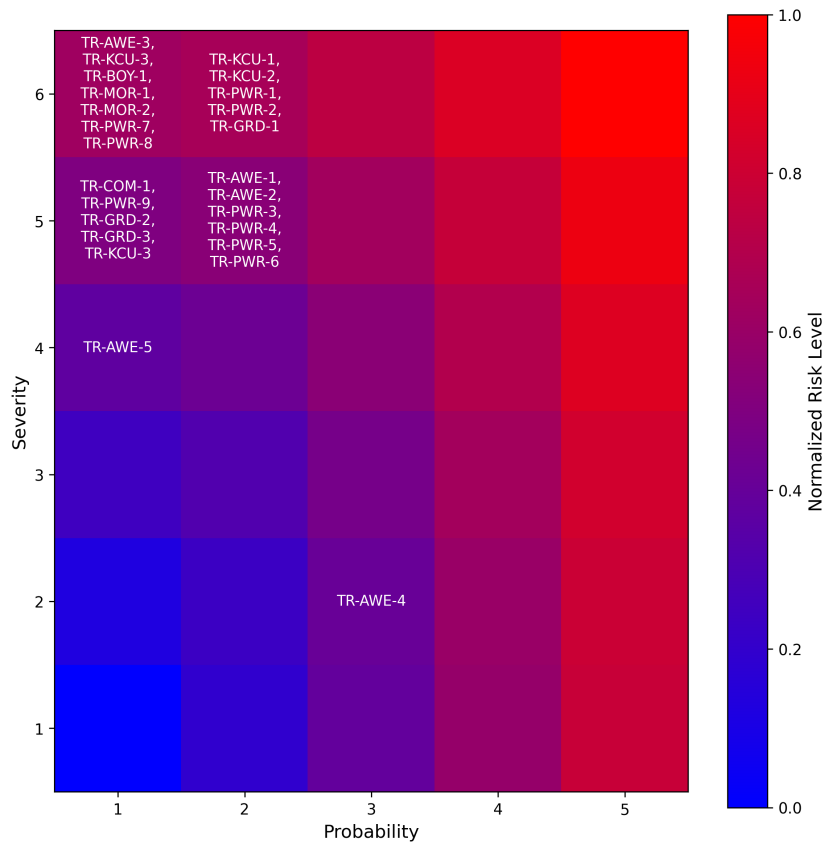


Figure 12.2: Risk Map, Post Implementation of Mitigation Measures

13 | Sustainability Evaluation

The following section will discuss the sustainability performance of WaveWings devices and the farm's environmental impact. The environmental impact of the wave wing devices will be done by performing an LCA analysis of the impact of a singular WaveWings unit in the installation of the farm. Apart from the possible environmental impact is evaluated by looking into the marine ecological importance areas in the farm location and by looking at the possible effects of a farm on such a location.

13.1 | Requirements

Table 13.1 shows the requirements related to the sustainable performance of the project. These are evaluated at during the section.

Table 13.1: Requirements for sustainability of the farm and individual units

Identifier	Requirement
USR-CON-2	The farm shall provide a 70-95% reduction GWP compared to the current average electricity generation.
USR-CON-2-1	The farm shall save 1.34 million tons of CO ₂ per year compared to average emissions for electricity generation in 2023.
USR-CON-2-2	Each unit shall use 90% less material than a comparable floating HAWT.
USR-CON-4	The farm shall adhere to Irish environmental laws.
USR-CON-4-6	The system shall use non-toxic materials.

13.2 | Life Cycle Assessment

A Life-Cycle Assessment (LCA) of a product is an essential component for sustainable engineering. The LCA shows the impact of the construction, operation, and decommissioning of the product on the environment, it is a quantification of environmental burdens of a product over its whole life-cycle. The WaveWings GWP is predicted to be 17.97 kgCO₂/MWh. An LCA consists out of four phases. The first phase, Subsection 13.2.1, is a goal and scope definition which defines the research objectives, intended applications, target audience, and the aspects required for validation and comparison of the work. This includes the methods, assumptions, and boundaries that are applied in the analysis. The functional unit is also defined in this section. The second phase, Subsection 13.2.2, is the inventory analysis (LCI) which outputs the bill of materials, all the materials used in the product. The third phase, Subsection 13.2.3, is the impact assessment (LCIA) which uses the bill of materials to find the impact of the product. Lastly, the fourth phase, with the LCA of the WaveWings unit complete, the results are compared to an LCA of a floating offshore wind turbine in Subsection 13.2.4.

All the four phases of an LCA influence each other, as shown in Figure 13.1.

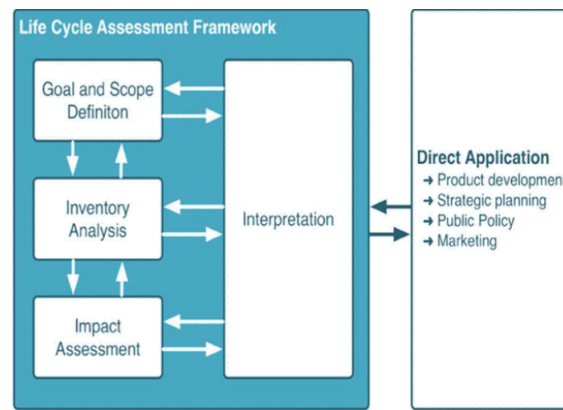


Figure 13.1: LCA Phase Interrelations [104]

13.2.1 Goal and Scope Definition

This is the first phase of an LCA.

Goal Definition

The purpose of the LCA is to assess the environmental burden of the production of one functional unit, which is 1 kWh, using the WaveWings energy unit. The LCA will highlight environmental weak points in the WaveWings life cycle. The impact category that the LCA focuses on is Global Warming Potential (GWP), expressed in kgCO₂eq/MWh.

Applications

This LCA is a preliminary estimate for the environmental impact, in specific, the global warming potential, that one WaveWings device has. Such insight can help in further stages of the project to know where more work should be performed in order to reduce the environmental impact of the WaveWings devices. Also, knowing the environmental impact of the devices might help in order to convince the stakeholders of the low environmental impact of the units when compared to other energy production systems.

Assumptions

Assumptions made during the LCA are listed below. These assumptions are based on requirements or engineering intuition.

- The WEC and AWES provide 200 kW and 2300 kW respectively
- GWP from literature can be scaled according to mass or dimensions to find the GWP of the WaveWings application
- The installation time is assumed to be twice as long as CorPower, due to the larger systems and larger depth
- Operation and maintenance is four times as high as CorPower, due to the relative higher number of systems
- Disposal time is assumed to take as long as installation time
- The telescopic mast production is assumed to emit 15 000 kgCO₂eq

Boundaries

The boundaries of the LCA are the life-cycle stages that are looked at in detail. A so called 'Cradle-to-grave' view is taken, with the recycling stage considered in less detail. The life stages are thus: Materials and Manufacturing, Installation, Operation, and End-of-life.

Methods

An LCA can be performed with two main methods. A detailed system architecture, Installation and Transport (I&T), Operation and Maintenance (O&M) and End-of-Life can be used in order to calculate the actual environmental impact. Alternatively, an early design analysis can be performed based on existing literature to perform a preliminary estimate. The main drivers of the environmental impact of products are the material they are constructed from and the method they are constructed with. The main driver for the installation of the systems will be the distance from the manufacturing site to the installation point, and the method of transport. O&M impact of offshore systems is mainly determined by the distance from shore the maintenance rate and the method of transport. Finally, the End-of-Life impact will be determined by the disposal methods used, such as recycling, reusing, or disposing. Existing LCA programs and tools exist in order to perform accurate LCA, however, due to the preliminary design of the project and time constraints, using such systems would decrease the accuracy of the results, and as such the second approach of using preliminary estimates based on literature will be used. Using one of the programs, such as Open LCA, is a recommendation for a future report.

In this report, the LCA consists out of the combination of existing LCAs of WEC and AWES and comparing it to an LCA of a floating horizontal axis wind turbine. The AWES LCAs that are used are [78] and [105]. The WEC LCAs that are used are [83] and [84]. [83] performs an LCA on a 10 MW array of 28 buoys of CorPower Hi-Wave-5 point absorber WEC on the coast of Aguçadora, Portugal. [84] performs an LCA on for the WEPA system on the town of Porto Conte in the North-West coast of Sardinia. The average estimation of the GWP for the CorPower array is 35.15 gCO₂eq/kWh, and the average GWP of the SEPA device is 448.98 gCO₂eq/kWh. Such a difference comes mainly from the location chosen for the systems, since annual energy production of the SEPA systems is much lower since the average mean wave power is only 2 kW m⁻¹ compared to 65 kW m⁻¹.

Subsection 13.2.2 consists out of lists of components that are included in an AWES and a WEC, while considering all the life phases. Subsection 13.2.3 computes the impact or GWP of each component in the lists. Subsection 13.2.4 compares the LCA of floating horizontal HAWT farm to the WaveWings farm.

Limitations

It is important to know the limitations of the LCA performed. As explained in Subsection 13.2.1 the LCA is based on literature and not on actual data from manufacturing, materials, and real-life lifetime operations. This is done in order to have a preliminary estimation of the LCA based on the design parameters that are known. While not accurate it gives a good estimate of the environmental impact that can be expected.

Another limitation of the analysis is that some of the parameters used for the analysis are based on estimation themselves, which by itself also reduces the accuracy of the analysis.

13.2.2 Inventory Analysis

This is the second phase of an LCA. This section delves into all the components that the WaveWings unit consists out of. Relevant information in other life stages is also mentioned.

Materials & Manufacturing

AWES: The AWES consists out of a kite, a KCU, a tether, a drum/winch, and a telescopic boom.

The kite has a surface area of 360 m². The kite is made out of ALUULA Vaepor.

The KCU will control the kite, and was assumed to be sized proportionately to the size of the kite.

The tether is created out of Ultra High Molecular Weight PolyEthylene (UHMWPE), created by Dyneema DSM. The dimensions for the tether are 1150 m in length with 5.6 cm in diameter. The mass of the tether is 1872 kg. The tether is the component that is to be partially replaced annually.

The drum is made out of carbon reinforced fibre polymer (CFRP). The diameter of the drum is 2.8 m, length is 7 m, and the thickness is 4.5 cm. Taking a density of 1.55 g cm⁻³, relates to a mass of 4295 kg.

The telescopic boom is assumed to be made out of steel. The GWP to make the boom is assumed to be 15 000 kgCO₂. This assumption is based on the GWP of the other components.

WEC: A clear mass distribution of the buoy system is still not clear since no detailed design has been

performed so far. Since the total mass of the WEC system is known, one can scale the mass decomposition of the WaveWings device based on literature. Both articles imply that the total mass distribution from buoy is mainly composed by steel ranging from 81-83% of the total buoy mass. As such steel will be the main driver regarding material consumption for the buoy.

It is known that the total weight of the buoy considering all of the components, has to be equal to 4.6 the tether force. Although no exact detailed design on the buoy and components has been performed yet, some preliminary weight definitions has been done. Subtracting the weight

Ballast: Using the values expressed in Section 8.3 the preliminary mass distribution for the SB can be performed. The SB is composed out of 6877 kg of steel and 58 093.293 kg of coal mine overburden sand (OBS). Using this type of sand decreases the impact in GWP since it can be processed using more sustainable practices. Also such sand does not require extra impact since it is extracted from already open mines. Such characteristics can also reduce the impacts in other categories not assessed in this LCA [106].

Shared: The shared component of the WaveWings unit is the PTO. The PTO consists out of cylinders, pumps, pipes, accumulators, motors, and generators. Subsection 8.9.2 discusses the PTO in detail, however the information about the specifics of the WEC PTO and AWES PTO is not at the same maturity. Because of this, the masses of the AWES PTO are multiplied by a factor of 1.1 to find the total mass of the PTO of the WaveWings unit. For a future report, an in-depth analysis of the WEC PTO also needs to take place. Taking an AWES PTO mass of 31 500 kg, the factor multiplication approach results in a total PTO mass of 34 650 kg.

Installation

While the main device is built and assembled in the harbour of Roseville, parts of the system will be manufactured by different suppliers, and as such, they will be transported to Roseville. In [83] it was considered that the 38.1% of the total mass was built by the manufacturer (CorPower) and 28.4 % by the local market in Portugal. As such it can be assumed that for the WaveWings project, 66.5% of the total mass will be built and produced in Ireland, meaning that only 33.5% comes from other suppliers from Europe. In [83], it was also assumed that in order to install the cables, anchor and buoy, a total of 1.58 days are needed per system, meaning that a total of 15 216 L of fuel were required per day. Considering the higher depth of the installation project for WaveWings and the bigger distance to the harbour, it can be assumed that the amount of time per installation phase is 1.5 times higher, meaning that the total amount of installation time per device is 3.1 days, with a total fuel consumption of 30 432 L.

Operations & Maintenance

The required Operation & Maintenance of the WaveWings device is still uncertain due to the novelty of such design. Articles [83] and [84] present different strategies for the required amount of instances of maintenance. While [84] considers that inspection will only need to be performed once every year for a total amount of 20 h with a consumption of 800 L of fuel per instance, [83] assumes that more inspections and maintenance operations will need to be performed with a total year fuel consumption due to such maintenance operations of 6428 L of fuel. Considering the higher complexity of the system and the higher distance to shore, it was assumed that the required amount of fuel for the O&M operations would be 4 times larger than the required for the CorPower array. This means that a total of 25 700 L of fuel are required per year in order to do O&M operations of a single WaveWings device. Due to the uncertainty of the parts that will need to be replaced, the impact of such replacement is not considered. The exception to the rule is the other kite since correct models of the wear of such tethers have been developed.

The tether is the component of the AWES that will be replaced the most often. This needs to be replaced every 1 year. Additionally, a planned maintenance schedule of 6 visits per year is assumed per unit.

End-of-life

At the end of the operational life, the decommissioning activities are mainly related to the disconnection of the WaveWings system, their transport back to land and the reusing, recycling or disposal of the components. It is assumed that the site can and will be re-energised and so no further impacts are considered from the decommissioning of subsystems, like anchors, electrical cables or substations [83]. As such, fuel used for decommissioning will be 6828 L, which is the same as the fuel used for the installation of the floating buoy and mooring. It is assumed that at the end of life, 15% of the steel of the buoy has been corroded, meaning that only a total of 178.5 t can be recycled [84].

13.2.3 Impact Assessment

The third phase of the LCA is the impact assessment. This quantifies the impact of every component and visualizes it in multiple graphs. The GWP values are attained by using Equation 13.1 and Equation 13.2.

$$kgCO_2eq_{WW} = GWP_{lit} \cdot AEP_{lit} \cdot t_{lit} \cdot \frac{x_{WW}}{x_{lit}} \quad (13.1)$$

$$GWP_{WW} = \frac{kgCO_2eq_{WW}}{AEP_{ww} \cdot t_{ww}} \quad (13.2)$$

Where the subscript *WW* means that it relates to the WaveWings unit, while *lit* indicates the relationship to the sources mentioned in the Subsection 13.2.1. *kgCO₂eq* indicates the amount of carbon dioxide equivalent emitted per component in kilograms, *AEP* is the annual energy production, *t* is the lifetime of the unit in years, and *x* is either the mass or the size of the component, depending on the type of information available.

The components mentioned in Subsection 13.2.2 are analysed and the GWP is assessed. It is estimated that the total *CO₂eq* emissions of a single unit deployed in the array configuration is 4 271 858 kgCO₂eq, meaning that the total emissions of the farm is 1708 MteqCO₂. The final GWP of the WaveWings unit is 17.97 kgCO₂eq/MWh. In Figure 13.2 the distribution of the contributions to the GWP can be seen. The biggest contributor to the GWP is the O&M holding a 35.23 % of the impact. This is due to the high maintainability of the tether, and the conservative approach taken in this report where it is assumed that due to the novelty of the design there will be more maintenance trips required. The second biggest contributor are components and manufacturing of the buoy due to the high mass of the buoy holding a 31.79 % of the impact. Due to the depth of 150 m and the high forces experienced by the system the impact of the mooring is bigger than compared to other literature like [83].

In Figure 13.3 the breakdown for the component section is shown. As expected, the buoy was the highest contributor holding 58.33 % of the impact. However, the big impact of the drum was not expected due to its small size, when analyzing more in depth that such an impact is directly related to the high GWP impact that the CRFP used in the drum has. Another possible explanation is that [78] does not use calculations for its LCA, but is assumptions based.

In Figure 13.4 the electronics contributions can be seen. It is evident that the array cables and transformers are the largest contributors in the electronics section.

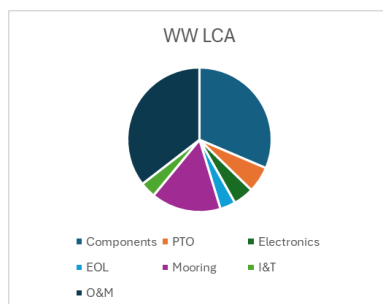


Figure 13.2: Contribution of each section in GWP

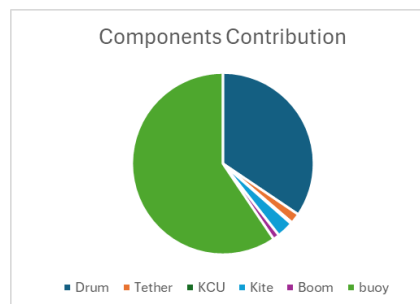


Figure 13.3: Breakdown of component contribution to GWP

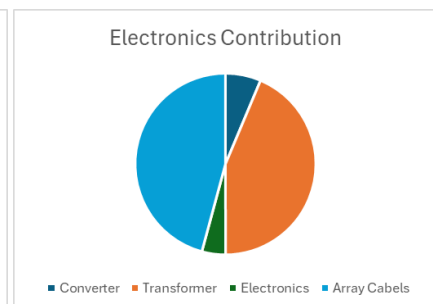


Figure 13.4: Breakdown of electronics contribution to GWP

A sensitivity analysis is performed in order to verify the results shown in the previous paragraphs.

Such analysis was focused on the change of the component's impact and the O&M impact since they are the biggest contributors to the GWP. Table 13.2 shows the results of the sensitivity analysis. In the table, the $kgCO_2eq$ and total percentage for different components can be seen when the impacts of one of the components is varied by $\pm 5\%$. It is clear when analysing the results that even when the impact of the O&M or the Components is increased or decreased by 5%, the results of the LCA do not change. As such it is clear that the biggest impacts come from the O&M and the Components. For further developments, more sustainable practices could be used in order to manufacture the parts, such as using recycled materials, reusing existing systems, or using sustainable manufacturing processes. In order to further reduce the impact of the O&M, more sustainable methods of transport could be used and better planning could be performed.

Table 13.2: Sensitivity analysis LCA

	kg eq CO ₂	[%]	kg eq CO ₂	[%]	kg eq CO ₂	[%]	kg eq CO ₂	[%]	kg eq CO ₂	[%]
			-5% O&M	-5% O&M	+5% O&M	+5% O&M	-5% Comp	-5% Comp	+5% Comp	+5% Comp
Components	1356653	31.79183	1356653	32.36198	1356653	31.24142215	1424485	32.8591	1288820	30.69009
PTO	247870.6	5.808606	247870.6	5.912777	247870.6	5.708042549	247870.6	5.717718	247870.6	5.902431
Electronics	194072	4.547887	194072	4.629449	194072	4.469150259	194072	4.476726	194072	4.621348
Mooring	664590.6	15.57403	664590.6	15.85334	664590.6	15.30440089	664590.6	15.33034	664590.6	15.8256
I&T	150486.2	3.526497	150486.2	3.58974	150486.2	3.465442679	150486.2	3.471317	150486.2	3.583459
O&M	1503620	35.23587	1428439	34.07439	1578801	36.35712133	1503620	34.68452	1503620	35.80502
EOL	150007.5	3.51528	150007.5	3.578323	150007.5	3.454420142	150007.5	3.460276	150007.5	3.572061
Total	4267300	100	4192119	100	4342481	100	4335132	100	4199467	100

The total mass of the buoy is 640.7 t. A breakdown of the mass is provided in Section 16.2

13.2.4 Comparison to Floating HAWT

This section compares the WaveWings characteristics to characteristics of a floating offshore wind turbine.

Floating offshore wind has a GWP of between 25.6 and 45.2 kCO_2eq/MWh [107]. Compared to the Wave Wing's GWP of 17.97 kCO_2eq/MWh , WaveWings has a reduced GWP of 30-60%. Requirement *USR-CON-2* is thus not met.

The mass of a floating offshore wind turbine is 9791 t, depending on the type of floater used [107]. This is a wind turbine with a rated power of 6 MW. Compared to the WaveWings unit's mass of 643 t which is determined in Section 16.2, normalizing the power produced results in the WaveWings in having a reduced mass and material use of 84.2%. Requirement *USR-CON-2-2* is thus not met.

13.3 | Additional Evaluation Criteria

Looking at the energy balances ¹, Ireland gets 55% of its electricity from natural gas, 22% from coal, 10% from oil products, and 13% from biofuels and renewables. The WaveWings farm produces a total energy of 96.4 Wh in its 20 year lifetime. It is assumed that this extra energy produced in Ireland will be subtracted from the coal, natural gas, and oil production. This translates to a reduction of 24.33 Wh of coal production, 10.58 Wh of oil product production, and a 61.48 Wh of natural gas production. [108] states the emissions of each of these sources in gCO_2eq/kWh , namely 820 for coal, 600 for oil, and 490 for natural gas. The WaveWings unit has an emissions value of 17.97. Comparing the million tonnes of equivalent CO_2 emitted by non-renewables and the WaveWings unit, using a 1 GW farm of Wave Wing units will save 54.67 million tonnes of CO_2 equivalent, equating to 2.73 million tonnes of CO_2 equivalent annually. Requirement *USR-CON-2-1* is thus met.

Another method to assess the environmental impact on GWP is to assess the energy payback time (EPBT) of the energy. To do so, Equation 13.3 can be used, where the total emissions of the farm are related to the global warming potential difference between conventional energy methods and the WaveWings farm, times the total amount of energy produced.

¹<https://unstats.un.org/unsd/energystats/pubs/balance/>, accessed on June 25, 2024

$$EPBT = \frac{kg - eq - CO_{2_{WW}}}{(GWP_{conv} - GWP_{WW}) * AEP_{WW}} \quad (13.3)$$

In conclusion, it estimates the amount of time that the farm takes to pay back the amount of emissions emitted. Compared to Ireland's energy market, The EPBT is 0.15 years.

Other sustainable requirements that can not be asses with an LCA also need to be discussed. One of such impact is the influence on the ecology in the region where the farm is placed. By ensuring that the farm location is not placed in any region of ecological importance a better estimate of the ecological impact can be known. In Figure 5.6 the areas of ecological importance for the specific location in the West coast of Ireland were shown, showing the zones of abundance of different animals. It is clear from the image that the farm is placed outside of any region of ecological importance. It is important to note that while the farm is placed outside such regions, more evaluation would need to be performed in order to ensure the low impact of the region. As such, the requirement ENV-CON-4-3 from the stakeholder's requirements can be said to be satisfied. It is also interesting to consider the "reef effect" that the farm could have. Since no constant ship traffic or fishing would be allowed in the area; fauna could find in the region of the farm a marine oasis which could boost biodiversity.

Finally, in further stages of the project, impacts on fauna like electric and electromagnetic field disturbances, water pollution, or noise will need to be assessed. Disturbances in the Earth's magnetic fields can disorientate species that depend on the latter for orientation. Disturbances on the electric fields can disturb the hunting or behavioural behaviours of species that depend on the electric fields for socializing or hunting. Species that depend on hearing for survival might be affected by constant and punctual noise sources, and as such noise levels should not surpass 90 dB constant and 100 db punctual, complying with *USR-CON-4-1* [9, 109]. If such impacts of the design are too disturbing for the fauna, the final location or the design of the system must change to respect the ecology of the area. Only now are we starting to scratch the surface of the impact that human activities have on marine ecosystems and, as such, great care should be taken to prevent further harm to ecosystems.

14 | Verification & Validation

Verification and Validation procedures seek to acknowledge the suitability, accuracy, and assumptions taken when generating models; these can be pre-existing from literature or can be made in-house by the WaveWings team. In reality, due to time constraints, fully validating softwares — especially complex ones — can be difficult. Therefore, the majority of softwares are verified in terms of relevance to the design goal, interpretation of results, and robust checks that do not violate assumptions. Firstly, a compliance matrix is presented in Section 14.1 to inform the reader on the extent to which requirements could be met throughout this conceptual design study. Secondly, V&V procedures for WEC and AWES are presented in Section 14.2. A sensitivity analysis is not included in this chapter since it is very difficult to do system-wide. Sensitivity analyses are performed per subsystem in their respective section.

14.1 | Compliance Matrix

The compliance matrix shows compliance with all the requirements. When the design complies with the requirement a checkmark is placed next to the requirement and the section where it is discussed is shown. If the design does not comply with the requirement a cross is placed next to it and the section where it is discussed is shown. Some requirements were not proved or investigated in this report and will need to be proven in future detailed designs. These requirements are marked in orange with a horizontal dash.

Table 14.1: Compliance matrix (part 1)

Identifier	Requirement	Pass	Explanation
USR-REQ-1	The farm shall produce 1 GW of rated electrical power.	✓	Discussed in Chapter 16
USR-REQ-1-1	One unit shall produce 2.5 MW of rated electrical power.	X	USR-REQ-1-1-WEC not satisfied
USR-REQ-1-1-AWE	The AWES part of one unit shall produce 2.3 MW of rated electrical power.	✓	Discussed in Subsection 7.5.5
USR-REQ-1-1-AWE-1	The unit shall operate at a location with a mean surface wind speed of 11 m/s.	X	Discussed in Subsection 5.3.2
USR-REQ-1-1-AWE-2	The AWES shall produce a maximum of 3.6 MW of power during reel-out.	✓	Discussed in Subsection 7.5.5
USR-REQ-1-1-AWE-2-1	The AWES shall maximise CL^3/CD^2 for peak power generation.	X	Discussed in Subsection 7.3.5
USR-REQ-1-1-AWE-3	The AWES shall convert harvested energy to electrical.	✓	Discussed in Subsection 8.9.2
USR-REQ-1-1-AWE-4	The AWES shall survive operational environmental conditions.	-	To be proven in future detailed design
USR-REQ-1-1-AWE-4-1	The kite shall have a system to absorb lightning strikes.	-	To be proven in future detailed design
USR-REQ-1-1-AWE-4-2	The AWES shall resist hail of size 3 centimetres.	-	To be proven in future detailed design

Table 14.2: Compliance matrix (part 2)

Identifier	Requirement	Pass	Explanation
USR-REQ-1-1-AWE-4-3	The AWES shall endure 32000 hours of UV radiation.	-	To be proven in future detailed design
USR-REQ-1-1-AWE-4-4	The kite shall survive a soft landing in the water.	-	To be proven in future detailed design
USR-REQ-1-1-AWE-4-5	The AWES shall operate between -15°C to 35°C.	-	To be proven in future detailed design
USR-REQ-1-1-AWE-4-7	The AWES connection between the tether and the buoy shall withstand a maximum force of 920 kN.	-	To be proven in future detailed design
USR-REQ-1-1-AWE-4-8	The AWES structures shall not resonate with waves.	-	To be proven in future detailed design
USR-REQ-1-1-AWE-4-9	The AWES shall be modelled with control simulation software for tether fatigue.	-	To be proven in future detailed design
USR-REQ-1-1-AWE-4-10	The kite shall withstand aerodynamic forces at maximum velocity.	-	To be proven in future detailed design
USR-REQ-1-1-AWE-4-11	A fatigue analysis shall be carried out on the AWES structures under cyclic loading.	-	To be proven in future detailed design
USR-REQ-1-1-AWE-4-12	The tether shall resist the tension force of the nominal tether force times the tether safety factor.	✓	Discussed in Section 7.6
USR-REQ-1-1-AWE-5	The AWES shall be controlled to perform the mission.	✓	Discussed in Chapter 9
USR-REQ-1-1-AWE-5-2	The control system shall measure weather conditions.	✓	Discussed in Section 9.3
USR-REQ-1-1-AWE-5-3	The kite shall be controllable.	✓	Discussed in Subsection 9.4.1
USR-REQ-1-1-AWE-5-3-1	External experts shall be contacted for use of relevant control simulation software.	✓	Discussed in Subsection 9.5.1
USR-REQ-1-1-AWE-5-3-2	Stability analysis shall be done to verify AWES behaviour.	-	To be done in future detailed design
USR-REQ-1-1-AWE-5-4	The AWES shall perform reel-in operation.	✓	Discussed in Subsection 9.2.3
USR-REQ-1-1-AWE-5-4-3	The AWES PTO shall be capable of handling 3.6 MW power.	✓	Discussed in Subsection 8.9.2
USR-REQ-1-1-AWE-5-5	The AWES shall perform reel-out operation.	✓	Discussed in Subsection 9.2.2
USR-REQ-1-1-AWE-6	The AWES shall launch the system.	✓	Discussed in Section 8.8
USR-REQ-1-1-AWE-6-1	The AWES shall have a launch velocity of 5 m/s or slower.	✓	Discussed in Subsection 7.5.3
USR-REQ-1-1-AWE-6-3	The AWES shall launch the kite in 5 minutes.	-	To be proven in future detailed design

Table 14.3: Compliance matrix (part 3)

Identifier	Requirement	Pass	Explanation
USR-REQ-1-1-AWE-7	The AWES shall retrieve the system.	✓	Discussed in Section 8.8
USR-REQ-1-1-AWE-7-1	The AWES shall retrieve the kite in 5 minutes.	-	To be proven in future detailed design.
USR-REQ-1-1-AWE-7-3	The tether shall be retractable around a drum.	✓	Discussed in Section 8.7
USR-REQ-1-1-AWE-8	The AWES part shall produce maximum power at 12.5 m/s rated wind speed.	✓	Discussed in Subsection 7.5.2
USR-REQ-1-1-AWE-9	The kite shall be able to turn with a maximum turning radius of 100 m during operations.	✓	Discussed in Subsection 7.3.2
USR-REQ-1-1-WEC	The WEC part of one unit shall produce 0.2 MW of rated electrical power.	X	Discussed in Subsection 8.2.4
USR-REQ-1-1-WEC-1	The WEC system shall operate 70 kW/m.	X	Discussed in Subsection 8.2.4
USR-REQ-1-1-WEC-2	The WEC shall survive operational environment conditions.	✓	Discussed in Section 8.8
USR-REQ-1-1-WEC-2-1	The WEC shall withstand a salinity of 35 grams per litre.	-	To be proven in future detailed design
USR-REQ-1-1-WEC-2-2	The WEC shall operate between 9.5°C to 34.5°C.	-	To be proven in future detailed design
USR-REQ-1-1-WEC-2-3	A fatigue analysis shall be carried out on the oscillator of the WEC system.	-	To be completed in future detailed design
USR-REQ-1-1-WEC-2-4	The buoy shall float.	✓	Discussed in Figure 8.2.2
USR-REQ-1-1-WEC-2-5	The WEC shall be controllable.	-	To be proven in future detailed design
USR-REQ-1-1-WEC-2-6	The WEC shall be waterproof.	✓	Discussed in Section 8.8
USR-REQ-1-1-WEC-2-7	The WEC shall be fully submersible.	-	To be proven in future detailed design
USR-REQ-1-1-WEC-3	A unit shall be transportable back to shore.	-	To be proven in future detailed design
USR-REQ-1-1-WEC-4	The system shall be anchored to the seafloor.	✓	Discussed in Section 8.4
USR-REQ-1-1-WEC-5	Buoy weight shall be at least the induced peak tether load.	✓	Section 8.2
USR-REQ-1-1-WEC-6	The SB shall have a maximum acceleration of $0.06m/s^2$	✓	Discussed in Section 8.3
USR-REQ-1-1-WEC-7	The SB shall be stable	✓	Discussed in Section 8.3
USR-REQ-1-1-WEC-8	The SB shall provide more buoyancy than its weight plus the PTO force combined.	✓	Discussed in Section 8.3

Table 14.4: Compliance matrix (part 4)

Identifier	Requirement	Pass	Explanation
USR-REQ-1-1-1	The AWES and WEC shall perform better than the two systems individually.	-	Not yet known, discussed in Subsection 9.5.3
USR-REQ-1-1-1-1	A literature study and simulation shall be performed to ensure the synergy feasibility.	✓	Subsection 9.5.1
USR-REQ-1-2	The farm shall consist of 400 units.	X	Discussed in Chapter 16
USR-REQ-1-2-1	Individual units shall operate in a specified control area.	✓	Section 10.6
USR-REQ-1-2-1-1	The clearance between units shall be the maximum tether length with an applied safety factor.	✓	Section 10.6
USR-REQ-1-2-1-2	The WEC shall be equipped with warning lights.	✓	Section 8.8
USR-REQ-1-2-1-3	The AWES shall be equipped with warning lights.	✓	Discussed in Section 7.7
USR-REQ-2	The farm shall have a capacity factor between 50% and 60%.	✓	Subsection 7.5.4 and Subsection 8.2.5
PGO-REQ-3	The farm shall be connected to an on-shore electrical grid.	✓	Discussed in Chapter 10
PGO-REQ-3-1	The offshore substation and onshore substation must be compatible.	✓	Discussed in Chapter 10
USR-REQ-4	The system shall be able to communicate between the different systems and subsystems.	✓	Discussed in Section 8.11
USR-REQ-4-1	The communications subsystem of the airborne system and the floating system must be compatible.	✓	Discussed in Section 8.11
USR-REQ-4-2	The communications subsystem of the floating system must have a rating of IP65 or higher.	✓	Discussed in Section 8.11
USR-REQ-4-3	The communications subsystem of the airborne system must have a rating of IP65 or higher.	✓	Discussed in Section 8.11
USR-REQ-4-4	The communications subsystem must be redundant in case internet connection fails.	✓	Discussed in Section 8.11
USR-REQ-4-5	The communications subsystem and the offshore substation must be compatible.	✓	Discussed in Section 8.11
USR-CON-1	The farm shall provide a 50-80% LCOE reduction compared to other offshore renewables.	✓	Discussed in Chapter 11
USR-CON-1-1	The farm shall provide total cost savings of 40% compared to individual deployment of airborne wind and wave energy systems.	-	To be proven in future detailed design

Table 14.5: Compliance matrix (part 5)

Identifier	Requirement	Pass	Explanation
USR-CON-1-2	Each unit shall provide a 25-30% manufacturing cost reduction compared to separate corresponding units of airborne wind energy and wave energy generation.	-	To be proven in future detailed design
USR-CON-1-3	Detailed cost estimations shall be carried out for all components of the system, both for a single unit and for a 1 GW farm.	✓	Discussed in Chapter 11
USR-CON-1-5	The system shall have a mission lifetime of 20 years.	✓	Discussed in Chapter 11
USR-CON-1-5-1	After 20 years the farm shall have a power output of 70% of its initial.	-	To be proven in future detailed design
USR-CON-2	The farm shall provide a 70-95% reduction in GWP compared to the current average electricity generation.	X	Discussed in Subsection 13.2.4
USR-CON-2-1	The farm shall save 1.34 million tons of CO ₂ per year compared to average emissions for electricity generation in 2023.	✓	Discussed in Subsection 13.2.4
USR-CON-2-2	Each unit shall use 90% less material than a comparable floating HAWT.	X	Discussed in Subsection 13.2.4
USR-CON-3	The design shall include a high-level FMEA and FTA.	X	Discussed in Chapter 12
ENV-CON-4	The farm shall adhere to Irish environmental laws.	-	To be discussed in further stages of the project
ENV-CON-4-3	The farm shall not be placed in a marine protected area.	✓	Discussed in Chapter 5
ENV-CON-4-4	The farm shall not be placed in a sea-life migrating route.	✓	Discussed in Chapter 5
ENV-CON-4-5	The farm shall consider migratory routes of birds.	✓	Discussed in Chapter 5
ENV-CON-4-6	The system shall use non-toxic materials.	-	To be proven in future detailed design
DEV-CON-5	The design phase shall not take longer than 10 weeks with 10 people.	✓	The design was finished with a team of 10 people in 10 weeks.
GOV-CON-6	The farm shall be positioned 25 km or more from shore.	✓	Discussed in Chapter 5
USR-CON-7	The AWES subsystem shall use the soft kite pumping concept.	✓	Discussed in Subsection 4.1.1
GOV-CON-8	The farm shall be placed in the EU.	✓	Discussed in Chapter 5
USR-CON-9	The farm shall be placed where the sea is deeper than 60 meters.	✓	Discussed in Chapter 5

14.2 | Model Validation & Code Verification

Following from the requirements matrix, this section describes the verification and validation procedure for all code written throughout the project.

14.2.1 WEC Simulation

As explained in Section 8.2 the WEC performance was simulated using the open-source, widely verified and validated BEMSolver and the WECSolver which was developed by the authors of this text. Only the latter requires V&V procedures to be performed to ensure confidence in the presented results. The code is fully written in Python so unit tests are performed in Python to verify that each function works as intended. A subclass of Python's `unittest.TestCase` is made in Python with methods made corresponding to different tests for each function in the main code. Checks include using `assertTrue` and `assertFalse` to verify assumption checks, and `assertEqual` to verify computation checks. For example, theoretically, a $K_{PTO} = 0$ would mean that no energy is extracted from the waves by the buoy and thus power absorbed should be zero when using the power calculation function in WECSolver. As a system test, calculations of the absorbed power of the buoy are verified using manual calculations in Excel. System tests successfully led to the discovery of an indexing mistake in the function that reads hydrodynamic coefficient data from tab-separated files. The analytical equations used to compute the absorbed power are borrowed from peer-reviewed literature where numerical results were used for validation. Thus the equations can be used with confidence, although further numerical and experimental results would be needed to validate the results before full-scale manufacturing of the system.

14.2.2 Floating AWES Simulation

The floating AWES simulation has been used in the design of the control strategies in Chapter 9. The tool has been developed by A. Cherubini et al. [6, p.137-163] and published as peer-reviewed research. It can thus be assumed that code verification has been performed by the authors, and it is thus not necessary to evaluate the entire code base in the scope of this project. Validation using experimental data is not possible, since there does not exist any physical floating AWES systems yet, so far they are only researched on a theoretical basis. Thus validation can best be performed by comparing to other simulation models. The simulation model developed by S. Trombini et al. [7] also simulates floating AWES systems. The simulation tool used in this project was able to reproduce the results presented by S. Trombini et al. [7] in Subsection 9.5.3. Since the floating AWES simulation is not used to accurately size any (sub-)systems, but to demonstrate possible control strategies and propose future development options, this level of validation is sufficient. For future design of actual control code, further model validation will be necessary.

14.2.3 Economic Model

The economic model implements relations from three separate sources, as discussed in Chapter 11. These relate specifically to the AWES, WEC and infrastructure modules of the codebase. Due to limited available data, not all modules could be verified to their fullest. However, the infrastructure module of the code has been verified by comparing the outputs of the relevant functions to a case study specific to the Irish coast [8]. This provides good confirmation and an increased level of confidence with this part of the economic model. In addition to this, some individual costs of the AWES module have been verified by comparing costs to existing off-the-shelf components.

15 | Implementation Plan

Following is the chapter about the implementation plan. The main goal is to give a clear overview of the steps after the design process. The first section summarizes these phases. After that a RAMS analysis is presented. Continuing is the production plan and finally the logistics description and future developments are reported.

15.1 | Implementation Summary

The following phases were defined along with their work packages. An estimated duration was given based on offshore wind farm deployment, as grid installation and mooring are similar. Phase 1 must be done first as it is paramount for the involvement of stakeholders and their receiving their feedback. Also, it must be noted that there is a possibility to do Phase 3 and 4 concurrently. This makes the total implementation plan have a duration of

Table 15.1: Implementation plan

Phase	Workpackages	Duration
Phase 1: Small-scale tests	<ul style="list-style-type: none"> Smart Bay is consulted for testing of a smaller system in their sub-sea observatory. Note that only the WEC can be tested indoors. Verification of requirements takes place by test, demonstration, analysis, and inspection. Smart Bay also aids in testing the mooring configuration [49]. 	Estimated to be 1 year [110].
Phase 2: Secure supply chain	<ul style="list-style-type: none"> Order the off-the-shelf components. This includes the tether, drum, KCU, PTO, transmitters, receivers, and sensors. Arrange the production facilities, management, and assembly line personnel. Permits for the farm site as well as certification for the device must be drafted and requested already. 	Estimated duration is 1 year. Regular contact with stakeholders must be established within 10 business days. Scheduling for verification during subsequent phases must be done at least two months in advance. This is crucial as it is assumed stakeholders may be from other European countries or worldwide. Gathering of more stakeholders can occur concurrently, but ultimately within a year all necessary stakeholders must be contacted and scheduled with. Permits have long and unpredictable process times, thus it is best to send it in during this phase.

Table 15.1: Implementation plan (continued)

Phase	Workpackages	Duration
Phase 3: Part manufacturing, system assembly and offshore testing	<ul style="list-style-type: none"> • Manufacture all components that are not off-the-shelf. A batch-style production with an assembly line is efficient. • Assemble all manufactured components and off-the-shelf components with the electronics and motor systems. • Random checks are conducted by quality management during part manufacturing and assembly to ensure adherence to quality policy. • Test individual units at the site location. Assess unit performance and mooring configuration. • Permits and financial closure of the project is carried out to conclude pre-construction phase. 	Estimated to be 4 years [110]. Delivery interval can be minimised by an assembly line. Organisation of permits and financial closure takes time to process [111].
Phase 4: Offshore installation of mooring subsystem	<ul style="list-style-type: none"> • Smart Bay is consulted for pre-deployment planning and preparation, vessel provision, maintenance planning, and discussing device decommissioning at mission end [49]. • Arrange and embed all suction piles per unit at their coordinates of the farm using vibrational hammers. • Arrange the mooring lines. • Adhere to sustainability goals: no waste left behind, safe and non-destructive removal, and mitigate noise emissions. 	Estimated to be 1 year [110]. Duration is minimised by the nearness to Rossaveel.

Table 15.1: Implementation plan (continued)

Phase	Workpackages	Duration
Phase 5: Installation of electrical infrastructure	<ul style="list-style-type: none"> • Smart Bay remains involved for vessel provision and consulting of specialists for electric grid installation. • Install electrical grid on the seabed, ultimately connecting the offshore farm to the onshore grid. • Adhere to sustainability goals: no waste left behind, safe and non-destructive removal, and mitigate noise emissions. • Vilicom is consulted for the development of a 4G/5G communications network 	Estimated to be 1 year [110]. Duration is minimised by nearness to Rossaveel and proper planning with Smart Bay[49].
Phase 6: Deployment and testing of whole farm	<ul style="list-style-type: none"> • Transportation of the assembled system to the coast. • Smart Bay remains involved for vessel provision. Load system on boats for transportation to the site location. • The connection of each unit to the main grid must be verified. 	Estimated to be 1 year [110]. Duration is minimised by the nearness to the port Rossaveel and proper planning with Smart Bay[49].
Phase 7: Operation and Maintenance	<ul style="list-style-type: none"> • Personnel to assess performance and suggest optimisations: this includes the software for the smoothing of energy transfer to the main grid as well as updates to control software for AWES and WEC. • Maintenance detection through sensors, distress call when necessary, vessel provision to malfunctioning unit(s). 	Estimated to be 20 years [112]. Offshore wind turbines typically have an operational lifetime of 25-30 years. However, this was after the technology was better developed. WaveWings has an operational lifetime of 20 years as this is a new combined technology.
Phase 8: Decommissioning	<ul style="list-style-type: none"> • Consult specialists for the removal of the units, the suction piles / mooring lines, and the electrical grid. • Adhere to sustainability goals: no waste left behind, safe and non-destructive removal, and mitigate noise emissions. 	Estimated to be 1 year [110].

This table gives a great insight in the different future steps that need to be taken in the future after finishing the design process. It however does not give an insight yet off how the phases can be done simultaneously. This is shown by Figure 15.1.

	Year 1				Year 2				Year 3				Year 4				Year 5				Year 6				Year 7				Year 8						
	Q1	Q2	Q3	Q4	Q1	Q2	Q3	Q4	Q1	Q2	Q3	Q4	Q1	Q2	Q3	Q4	Q1	Q2	Q3	Q4	Q1	Q2	Q3	Q4	Q1	Q2	Q3	Q4	Q1	Q2	Q3	Q4	Q1	Q2	Q3
Small scale tests	█																																		
Securing supply chain					█																														
Manufacturing									█				█				█																		
Mooring installing									█				█																						
Electrical grid installing													█				█																		
Deployment and testing																					█				█										
Integration testing																									█				█						

Figure 15.1: This is a gantt chart of the phases. As shown some of the phases are parallel to each other to be time efficient.

As shown there are a lot of overlapping phases. Mainly during the manufacturing there need to be overlapping tasks, because otherwise the integration takes to long. Also, it is important to start the deployment before the manufacturing is finished, because otherwise there is a lot of storage room there needs to be provided for. The mooring and electrical grid installation can also be done simultaneously during the manufacturing. They should not however start at the same time to not get in each others way. The testing however needs to be finished to start any other phase.

Notice how a communications network is developed before the deployment of the WaveWings units. This ensures better communication to shore during its installation. Also, productivity of workers is increased when they have a strong connection, overall decreasing the installation time and cost.

The development and testing protocol for ocean technology is given in [113] and is applicable to WaveWings. This protocol specifies 5 phases: validation model, design model, process model, prototype, and unit demonstration. Table 15.2 shows the protocol and the characteristics of each phase.

Table 15.2: Protocol in the future development[113]

DEVELOPMENT	PHASE 1: Validation Model (lab)			PHASE 2 Design Model (lab)	PHASE 3 Process Model		PHASE 4 Prototype	PHASE 5 Demonstration
	Concept	Performance	Optimisation		Lab. Tests	Sea Trials		
Objectives / Investigations	Op. Verification Design Variables Physical Process Validate/Calibrate Maths Model Damping Effect Signal Phase	Real Generic Seas Design variables Damping PTO Natural Periods Power Absorption Wave to Devise Response Phase	Hull Geometry Components Configurations Power Take-Off Characteristics Design Eng. (Naval Architects)	Final Design Accurate PTO [Active Control] Mooring system Survival Options Power Production Added mass	Scale effects of Overall Performance PTO Method Options & Control Environmental Influences & Factors Inst. Power Absorption Characteristics Electricity Production & Quality Mooring & Anchorage Security		Ops Procedures Electrical Quality Grid Supply PTO Performance Control Strategy Survival	Grid Connection Array Interaction Maintenance Service Schedules Component Life Economics
Output/ Measurement	Vessel Motion Response Amplitude Operators & Stability Pressure / Force, Velocity RAOs with Phase Diagrams Power Conversion Characteristic Time Histories Hull Seaworthiness; Excessive Rotations or Submergence Water Surface Elevation Abeam of Devices			Motion RAOs Phase Diagrams Power v Time Wave Climates @ <i>head,beam,follow</i>	Incident Wave Field 6 D of F Body Motion & Phase PTO Forces & Power Conversion Seaworthiness of Hull & Mooring [Survival Strategies]		Full On-Board Monitoring Kit for Extended Physical Parameters	Service, Maintenance & Production Monitor, Telemetry for Periodic checks & Evaluation
Primary Scale (λ)	λ = 1 : 25 - 100 (∴ λ ₁ = 1 : 5 - 10)			λ = 1 : 10 - 25	λ = 1 : 10 - 15	λ = 1 : 3 - 10	λ = 1 : 1 - 2	λ = Full size
Tank	2 D Flume or 3 d Basin			3 - d Basin	3 - D Basin	Benign Site	Exposed Site	Open Location
Duration –inc Analysis	1-3months	1-3months	1 3 months	6 – 12 months	3 – 6 months	6 – 18 months	12 – 36 months	1 – 5 years
Typical No. Tests	250 - 750	250 - 500	100 - 250	100 - 250	50 - 100	50 - 250	Continuous	Statistical Sample
Budget (€000)	1 – 5	25-75	25-50	50 - 250	500 – 1,000	1,000 – 2,500	5,000 – 10,000	2,500 – 7,500
Model	Idealised with Quick Change Options Simulated PTO (0-∞ Damping Range) Std Mooring & Mass Distribution		Distributed Mass Minimal Drag Design Dynamics	Final design (internal view) Mooring Layout	Advanced PTO Simulation Special Materials	Full Fabrication True PTO & Elec Generator	Grid Control Electronics Emergency Res	First Fully Operational Device
Excitation / Waves	Monochromatic Linear (10-25Δf) (25-100 waves)	Panchromatic Waves (20min scale) +ve 15 Classical Seaways Spectra Long crested Head Seas		Deployment -Pilot Site Sea Spectra Long, Short Crested Classical Seas Select Mean wave Approach Angle		Extended Test Period to Ensure all Seaways inc.	Full Scatter Diagram for initial Evaluation Continuous Thereafter	
Specials	DoIF (heave only) 2-Dimensional Solo & Multi Hull	Short Crest Seas Angled Waves As Required	Storm Seas (3hr) Finite Regular As required	Power Take-Off Bench Test PTO & Generator	Device Output Repeatability Survival Forces	Salt Corrosion Marine Growth Permissions	Quick Release Connections Service Ops	Solo or Small Array (Up-grade to Generating Station)?
Maths Methods (Computer)	Hydrodynamic, Numerical Frequency Domain to Solve the Model Undamped Linear Equations of Motion		Finite Waves Applied Damping Multi Freq Inputs	Time Domain Response Model & Control Strategy Naval Architects Design Codes for Hull, Mooring & Anchorage System. Economic & Business Plan		Array Interaction Economic Model Electrical Stab.	Int Market Projection for Devise Sales	

The above table summarises the future development by presenting the important aspects at each phase, such as the estimated duration, scaling factor of the tested unit, the number of runned tests, characteristics of the model, the waves tested, and the math methods for analysis[113].

WaveWings requires an offshore test site near Ireland before a full scale farm deployment. This is a lengthy process involving permit applications as well as consulting airspace and marine regulations. Permits concerning AWES but are also applicable for WEC are the following:

- Archaeologist Report
- Dept Culture, Heritage And Gaeltacht
- Design Stage Report
- Discharge Documentation
- Environment Section
- Inland Fisheries Ireland
- Noise Impact Assessment
- Noise Monitoring Location Map
- Ornithology Assessment
- Photomontage
- Planning And Environmental Report Incl. Reinstatement Program
- Report On Existing Culvert
- Site Access Details
- Site Layout, Access Plan
- Traffic Management Plan
- Waste Management Plan

Figure 15.2: Documents necessary in the permitting process for a test site[50]

WaveWings has decided to outreach to SmartBay for their testing site. The above documentation is thus arranged between WaveWings and SmartBay and the Irish government. Additionally, SmartBay is partnered with the Marine Institute, which provides scientific and technical advice to the government to help adjust policy and to support the sustainability development goals[49].

15.2 | Reliability, Availability, Maintainability, and Safety (RAMS)

In this section, a RAMS analysis is presented. First, reliability is quantified or otherwise discussed in Subsection 15.2.1. Then, the availability of AWES and WEC are presented in Subsection 15.2.2. Next, the maintainability of the subsystems are given in Subsection 15.2.3. Finally, the safety protocol is stated in Subsection 15.2.4.

15.2.1 Reliability

Reliability is the probability that a device's performance will remain unchanged over time, after determining the conditions of use[114]. Reliability of components is either quantified in flight hours (FH) or in mean time to failure (MTTF) in hours. The kite is estimated to handle 6700 FH before a failure, and this was determined in Subsection 7.5.4.

Determining the reliability of the WEC involves a finite element analysis (FEM) as a prerequisite. However, as a FEM analysis has not been performed in this study for the WEC, instead, use is made of a study that provides a reliability assessment for point absorber WECs using hydraulic PTOs. The study makes use of Failure Mode and Effects Analysis (FMEA) in order to determine the Risk Priority Number (RPN). It is found that the hinge frame that connects to the piston has the highest RPN of device, followed by the generator[115]. The accumulators have the lowest RPN of the whole device[115]. As the hinge frame and the generator have the highest risk, they have the least reliability.

For reference, an analysis of a 10 kW point absorber WEC using a hydraulic PTO included a sensitivity analysis, where it was determined that wave force has the largest contribution of 58% on MTTF compared to other parameters. Thus, in the case of WaveWings, the reliability is most affected by the site location, which has a characteristic wave height of 4 meters. Storm conditions with much higher wave height and thus wave force shortens the MTTF, and thus WaveWings units have been designed to be fully submersible in such conditions.

15.2.2 Availability

Availability is the probability that a device's performance will be unchanged over time, after determining the conditions of use and assuming that any necessary external means are secured[114]. As such, availability is different from reliability in that it takes maintenance into account and improves as a result of its implementation.

Concerning the WEC, and that the components with the least reliability was the hinge frame of the pistons and the generator, the availability can be increased by proper sensors equipped for fault de-

tection. This can be done by equipping a vibration sensor on the hinge frame of the piston for fault detection, as well as equipping a KVAR meter to the generator to observe the reactive power.

15.2.3 Maintainability

Offshore wind turbine maintenance will be used for deciding the planned visits per unit per year for WaveWings. The Dutch Offshore Wind Innovation Guide suggests companies to plan one or two visits per turbine per year[116]. Hornsea, the world's largest offshore wind farm located in the UK, plans up to five maintenance events per turbine per year in order to remove marine growth and bird waste[117]; however, they comprise of 165 turbines. WaveWings is a more complex and unknown technology than wind turbines, and thus it warrants also to have a maintenance plan of 5 visits per unit per year. It must be addressed that WaveWings consists of more than double the amount of units than the world's largest wind farm, and planning so many visits per unit per year requires a higher work load and more personnel. For a more in-depth maintenance plan, one is provided per subsystem.

Kite

The kite requires replacement every year. However, it is useful to determine whether it needs replacement earlier than this constraint. Before WaveWings deployment, the frequency content of the kite must be studied during operational conditions to determine its mean and bounds. Then, during the WaveWings operational lifetime, microphones must be equipped on the kites. A fault in the kite can be detected through acoustics; it can be indicated by a shift in frequency peaks, sound pressures, and noise spectra[118]. If the microphone detects frequency content that greatly differs from typical behavior from kite acoustics, this might constitute to a fault in the kite, and thus a signal is sent out for kite maintenance or replacement. The tether is also replaced every year, and this is monitored by a camera pointed on the line to observe its status.

KCU

There are several methods for the maintainability of the KCU. Firstly, the software necessary for an update must be validated before being sent to the offshore systems. A bug has the potential to yield a system failure, as the KCU is central to operation of the airborne system. After the application of an update, the flight path must be observed, as done for a test flight, in order to assess the confidence in the performed maintenance. Also, When the airborne system is in retrieval, the KCU electronics must be protected from water leakage. For this, the KCU subsystem must be sealed in a compartment with a IP68 rating[119]. This rating ensures complete submersion in water at lower than 1 meter depth. Finally, the protective foam cover of the KCU is made of cross-linked polyethylene (XLPE) foam which is suitable in crash events and is water-proof. It is replaced after a crash event.

Launch and Retrieval

The launch tower is equipped with vibration sensors to detect loose components. Also, the speed at which the telescopic launch mast extends and retracts is monitored. Maintenance includes lubrication or replacement. The reel-in of the secondary winch is also monitored so that it is in the specified speed range. Lastly, the inside of the storage compartment must be visually inspected and cleaned.

Mooring

If the tension control device cannot keep the tension within the operational range, maintenance is called. Also the kite is retrieved to not risk AWES operation loads to damage the mooring. The faulty suction pile is removed and a new one is installed. The suction pile must be load tested for 30 minutes to assess the holding capacity. Once verified, it can be joined to the floating body.

Power

The power subsystem contains high risk components. This includes the hinge frames of the pistons as well as the generator. A need for maintenance is detected by the the vibration sensor or the KVAR meter. The hinge frame can be lubricated or replaced. The generator requires inspection. The motor is monitored by a thermometer to track its temperature. Thermometers, ammeters and volt meters are

also placed on other components such as the transformer, the energy storage, and the dump load. This way, the deterioration of components can be monitored. The subsea 3-phase AC cables of the farm layout must also be monitored. This is done by equipping thermometers, ammeters, and volt meters on the offshore collection stations. When a fault in a subsea cable occurs, a cables ship is mobilised. The faulty cable is either anchored out of the seabed and cut, or an ROV is deployed to cut the cable along the seabed. Cables ships are on 24-hour standby at strategic locations in the ocean[120].

Communications

There must always be a communications link between the units and the onshore site. If a signal is lost and not reestablished to the unit within 30 minutes, the kite is retrieved and stored until a vessel can be deployed to the unit for inspection and maintenance. It is not safe for the system to be operational without a communications link. If an offshore collection point loses connection with onshore for longer than 30 minutes, switch gears in the form of circuit breakers cut off the power transmission to shore. Note that the 4G network is the primary means of communications, and should this fail, there is a subsea fiber optic cable linked to shore. This redundancy provides increased availability.

Control

The control subsystem is maintained similarly to the KCU. Software updates are validated before being sent to the subsystem, as a bug has the potential for a system failure.

Structures

Monitoring of the structure comes in the form of vibration sensors by the drum, generator and gearbox of the AWES PTO for detection of loose components or to sense off-axis rotations. The drum must also be lubricated and this can be monitored by a oil analysis sensor. Pressure sensors in the hydraulic PTO of the WEC are equipped to detect leakages or overstressing of pistons.

15.2.4 Safety

As no humans are on the floating bodies during operation of the WaveWings farm, it can be reasoned that having a first aid kit on the floating body is not very necessary. However, placement of a first aid kit in the kite storage compartment is an easy-addition. Although vessels are required by law to have a first aid kit onboard, having one also on the floating body is handy in an emergency. This is not a large additional cost in relation to the overall cost of the farm, and thus a first aid kit will be placed on each floating body.

Anyone maintaining or repairing the system must have taken a first aid course, and be wearing safety shoes, glasses and proper clothes. Also, workers must be debriefed on the list of risks, mitigation, and contingency plans outlined in Table 10.2. Any workers maintaining the lead-containing antenna, must be wearing a mask and proper clothing. They must take a shower after maintenance is completed to limit lead exposure to themselves and others.

15.3 | Production Plan

In this section the production plan is presented. This will delve deeper into phase 3 of the implementation plan introduced in Table 15.1, mainly the manufacturing, assembly and integration of the systems and subsystems. At this stage, it is assumed that the design is completed and that off-the-shelf components and materials have already been acquired. The production plan in Figure 15.3 defines the parallel and sequential tasks for the manufacturing of the WEC and AWES systems separately before integration. Note each unit goes through the whole diagram such that when the first unit is finished, another unit is at the beginning of the process on the left of the diagram. Once enough units are finalized, batch installation is initialised to free up on-land storage space. Some tasks are within a series production line for better efficiency. Blocks in yellow represent off-the-shelf components that do not need to be manufactured. Green blocks represent the assembly and integration of subsystems. The flow diagram has three distinct sections, namely the AWES, WEC, and anchoring/mooring sections. These three sections combine in Y2 Q4 after which the final unit has been completed. So all in all, all 400 units are completed by Y2 Q4.

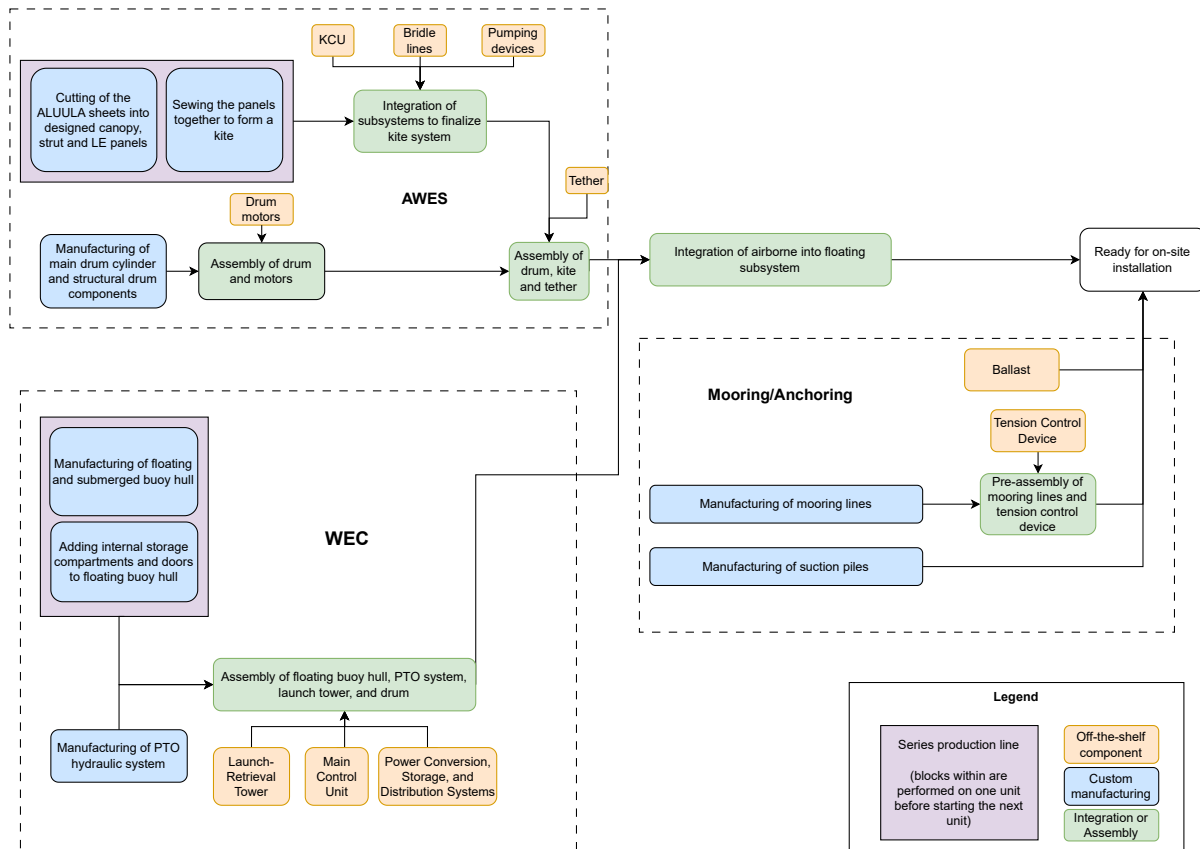


Figure 15.3: Production plan flow chart. The last unit is produced 4 years after the first unit.

15.4 | Logistics Description

Logistics description is a crucial aspect of project planning. It encompasses the strategies, processes and resources required in order to carry out the tasks of the implementation plan. A centered contact is SmartBay, located in Galway, Ireland. Besides using their indoor and outdoor sites for the testing of WaveWings at increasing scale sizes, they are also a consulting company. There are countless services that facilitate the deployment of WaveWings, namely: electrical infrastructure and cable laying, suction pile installation, mooring lines, communications network, vessel provision, and noise mitigation processes. Companies with potential off-the-shelf components are also necessary to contact.

SmartBay claims to cover these bases; however, it is advantageous to determine potential contacts beforehand. Vilicom is a communications company known for, with Vodaphone, installing a 4G network for Hornsea, the largest offshore wind farm in the world. They are based in Dublin, and thus not only does the company have impressive project, but they are near the WaveWings site location. Concerning the electrical infrastructure and cable laying, Seaway7 is a specialist with locations in the United Kingdom, the Netherlands, and several other countries. Van Oord of the Netherlands is also a specialist for offshore floating wind cable installation, having also an office in the United Kingdom. Both companies provide vessel provision as an additional service. Concerning the development of the WaveWings hydraulic PTO, Delta P Hydraulics Ltd is located in Carlow, and they specialise in hydraulic PTO systems. They have numerous off-the-shelf PTO systems and components that could prove useful in the development of the WaveWings hydraulic PTO. In addition, they provide maintenance services[121].

Sustainability has been a prevalent aspect that has been addressed in this project. Concerning the implementation plan, the suction piles require driving equipment before initiating suction. SPT Off-shore is a company based in the Netherlands specialised for suction pile installation[122]. Balmoral is a mooring line installation company based in Aberdeen[123]. However, although suction piles have a

silent suction process, their partial driving still has high noise emissions for the marine environment. Gentle Driving of Piles (GDP) is a new technology for the vibratory installation of tubular monopiles, making use of axial and torsional vibrations that greatly reduce noise emissions[124]. Its application has been verified by A. Tsetas et al. of the Faculty of Civil Engineering and Geosciences at the Delft University of Technology[125]. Vibrotwist is a company based in Delft that can be contacted and partnered with SPT Offshore for the application of GDP technology in the suction pile installation[124].

15.5 | Future Development

For the WaveWings project it is of great importance to keep improving. Thus, it is necessary to have a plan for the future. These developments for different criteria will be presented in this section.

Expansion and scaling

When the project is a success, it is important to keep developing. Expansion and scaling is one of the main fields that needs research. Firstly it is important to consider geological expansion. One development is increasing of the current site location. Another option is deploying to new locations, as done by Hornsea. Also the manufacturing and deployment capacity should be increased due to more demand. In the future this could make the production take less time. This also concludes further investigation in the supply chain. When the capacity of the WaveWings project gets bigger, new companies need to be contacted to keep up with the increased demand of material and to ensure the availability of high-quality material.

Technological advancements It is also necessary to keep the project technologically updated. Firstly, it is important that research is being done on the performance and reliability. This can be done by iteration; for example, the materials can be changed and then the control strategy is reevaluated. The monitoring systems that recognize failure should also be regularly updated to prevent unexpected risks. For the far future, it is also important to reevaluate the entire concept and investigate if newer different energy generating concepts have more advantages.

Environmental impact

Sustainability is a major aspect of the WaveWings project and should therefore be kept developed. Again, it is important to keep up to date with the material advancements, but the manufacturing and maintenance should also be updated and reconsidered. Next to that, innovative ideas have to be made about the recycling of the buoy.

Market and policy development

Finally the market and policy development must to be investigated thoroughly in the future. The WaveWings project is dependent on the market of sustainable energy. The need of this energy has a great effect on the development and the future of the project. Also the policy development has effect. If policies change some locations may not be available anymore for example.

16 | Budgets

The economics of the WaveWings project has been described in Chapter 11. To support the economic budgets, the mass and power budgets are defined in Section 16.1 and Section 16.2 respectively.

16.1 | Power Budget

The power budget is divided into the airborne and floating segments since the airborne segment, which consists of the kite and the KCU, generates and uses its own power while the floating segment which consists of all other systems use a fraction of the power that is generated by the WaveWings unit. In essence, the floating unit is the only one that generates a net positive power output. The airborne and floating power budgets are defined in Table 16.1 and Table 16.2 with the systems, their subsystems and their respective power used and power generated in kW with the net power in the airborne segment being 0 kW, and the net power for the floating segment being 2417 kW or 2.4 MW. This 2.4 MW is the power that leaves a unit toward the substation and then onward to shore and consumers. Note that 409 units would be required to produce 1 GW of power under the assumption that it is not consumed by supporting subsystems and that it is collected at the offshore substation directly.

However, in order to satisfy *USR-REQ-1*, power losses through the 70km HV subsea cable need to be accounted for such that the power provided onshore is 1GW. Existing literature estimates that there are 3 MW for a farm of 250 MW output [94], which corresponds to a 1.2% loss coefficient. Therefore, 419 units would be required – 19 additional units with respect to the original target – to account for these losses and the WEC system currently under-performing relative to the target set by *USR-REQ-1-1-WEC*. However, due to the conceptual scope of this project, a 20% margin will be imposed, bringing the grid requirement to 503 units. In order to preserve the grid configuration defined in Section 10.6 with stars of 8 units, the grid requirements shall be set to a value divisible by 8, namely 504 units. Therefore, the grid design exceeds the requirement set by *USR-REQ-1-2* but at the benefit of a decrease LCOE due to economies of scale. As outlined in Chapter 11, the LCOE for 400 units was at 49.40 EUR/MWh but with the up-scaling caused by the losses and margins, the LCOE for 504 units is at 46.65 EUR/MWh.

Table 16.1: Power Consumption and Generation for Airborne System Components

Subsystem	Component	Power Used [kW]	Power Generated [kW]
Kite	Onboard Pumps	21	0
KCU	Inertial Measurement Unit	0.0005	0
	Microphone	0.0005	0
	Barometer	0.0005	0
	Kite Control Actuators	2	0
	Kite Control Computer	0.0005	0
	Transceiver (to MCU)	0.0005	0
	Pitot Tube	0.0005	0
	Onboard Wind Turbines	0	23
SUM		-23.0	23.0
Net Power Output [kW]			0.0

Table 16.2: Power Consumption and Generation for Floating System Components

Subsystem	Component	Power Used [kW]	Power Generated [kW]
Mooring	Tension Control Device	10	0
MCU	Anemometer	0.001	0
	Barometer	0.001	0
	IMU	0.0005	0
	GPS	0.001	0
	Main control computer	0.005	0
	Cameras	0.005	0
	Hydrophone	0.001	0
	Microphone	0.0005	0
	Thermometer	0.0005	0
	Transceiver to KCU	0.0005	0
	Transceiver to offshore base station	0.002	0
Power	WEC PTO	0	2300
	AWES PTO	0	150
Launch & Retrieval	Launch tower	22	0
	Kite storage	1	0
SUM		-33.0	2450.0
Net Power Output [kW]			2417.0

16.2 | Mass Budget

The mass breakdown of the WaveWings unit is provided in Table 16.3. This includes every component of the unit.

Table 16.3: Mass breakdown of the WaveWings unit

Subsystem / Component	Mass [kg]
AWES PTO	30000
WEC PTO	6000
Transformer	7700
Drum	4300
Kite	408
Boom	7500
Tether	1872
KCU	100
Drum Structure	30000
Mooring	287441
Ballast	58095
Buoy Structure	209970
Total	643386

A total unit mass of 643 t is expected. The most massive subsystem in the unit is the Mooring subsystem, weighing 287 t. This is due to the large forces the suction anchoring system will have to sustain.

17 | Conclusion

The overarching theme of the WaveWings project is the combination of an Airborne Wind Energy System (AWES) with a Wave Energy Converter (WEC) system. In addition to the design of the subsystems, special considerations have thus been given to the integration of the two different modes of electricity generation. The design has been driven by the goal to improve over competitor technologies. The first competitor technology is AWES and WEC separately, this allows to evaluate the benefits of combining the two systems. The second competitor technology are floating Horizontal-Axis Wind Turbines (floating HAWT). Conventional HAWT are only reasonable in near-shore environments because of the need to anchor to the seafloor. In deep-offshore environments only floating systems are a reasonable choice, such as floating HAWT or the WaveWings project. This technology thus represents the closest competitor in a market environment which needs to be surpassed in terms of performance and cost, in order to have widespread success with a WaveWings-inspired system.

Observations relating to the combination of the system include a Levelised Cost Of Electricity (LCOE) reduction compared to existing renewable energy solutions to 49.40 EUR/MWh with 400 units but beneficially scaled to 46.65 EUR/MWh with 504 units due to considerations in losses and margins. As a comparison, a disintegrated farm with 400 standalone AWES and 400 standalone WEC systems along with additional infrastructure costs leads to an increased LCOE of 56.86 EUR/MWh, supporting the claim that an integrated solution is beneficial. Beneficial LCOE ranges can be attributed to reductions in material usage and infrastructure costs. Since the infrastructure costs constitute 42.5 % of the total project cost, a large savings potential can be obtained by increasing the power output of a single unit/of a single farm by integrating various electricity-generating technologies.

Looking closer into the costs, it can be observed that one of the major drivers is the yearly replacement of the AWES tether. For a more detailed design, this subsystem would thus be especially important to optimize, by using more accurate sizing methodologies or by reducing the tether load by changing the operational envelope. Another possibility would be to reduce the safety factors applied in the design by implementing advanced maintenance strategies for the tether, such as damage state estimation.

The large costs of the tether replacement are indicative of a larger trend relating to AWES systems. Compared to HAWTs, the material costs are relatively low, thus the capital expenditure (CAPEX) is low, however, due to the frequent replacement required, the operational expenditure (OPEX) is significantly increased. In the end, this results in a shift of the cost from the initial investment to the operational expenses. This might be advantageous for financial reasons because the system starts generating electricity, and thus revenue, with a low investment, the revenue can then be used to finance the operational expenses.

For the AWES system, simulation models have played an important role in sizing. Due to the lack of comparable kites, it is difficult to validate the results. Existing kites are order-of-magnitudes smaller, thus extrapolation can be uncertain. In general, the sizing of the airborne system includes large safety factors in order to account for the non-conservative idealized simulations. A more detailed design would require using more accurate modelling in order to reduce any safety factors in order to achieve a more optimal design.

Considering the WEC, there are major challenges related to the integration with the AWES. The large tether force and the requirement to fit all the AWES infrastructure into the buoy leads to a floater design that is far from the conventional design point for WEC of the same power generation capacity. These design challenges have led to a WEC system that has not been able to meet the power requirement. For future work, it is therefore of utmost importance to reevaluate the design of the WEC in order to consider possible ways forward in order to produce a sensible WaveWings system. Taking a step back, it might even be reasonable to make a study on the impact of the relative proportion of power generation by the AWES and the WEC subsystems. Due to the large degree of interconnection, a study on the impact of changing the relative sizing might lead to new insight into the optimal mixing of AWES and WEC.

One possible strategy towards synergy between the AWES and the WEC systems is the control system. Compared to individual optimization of the operations of the AWES and the WEC parts, using control strategies that combine the two systems offers the possibility for additional efficiency gains. After analyzing the operational phases of the WaveWings system, it was determined that for most operational phases it is best to decouple the AWES and the WEC in order to have maximum flight stability and control authority. The electricity-generating phase of the AWES system, however, offers the opportunity to integrate the control of the AWES and WEC. A WEC amplifying strategy has been proposed in order to increase the electricity output of the WEC part. This strategy has been argued using simulation results. However, the evidence of actual improvement of the baseline strategy of decoupling the AWES and WEC is still sparse. More extensive and accurate simulations are needed to fully quantify the impact of the proposed strategy. A more detailed analysis of the impact of the strategy on the fatigue of both the tether and the mooring is also needed in order to validate the assumptions taken and to decide whether potential power improvements outweigh the structural implications of the WEC amplification strategy. If a more extensive conceptual design is envisioned, additional potential strategies should also be considered. The analysis of this project has been focused on one strategy offering synergy potential, however, more strategies might be possible. A wide consultation of different engineers and researchers should be employed in order to generate a maximum of ideas for this new problem, which has not extensively been treated in the scientific literature before.

With regard to sustainability, special care has been taken during the site selection. This being a decision taken somewhat early in the design, while having a potentially big impact, it needed to be well-argued. The presence of shipping routes and other wind farms as well as the marine ecology was considered. A basic Life Cycle Assessment (LCA) was conducted to evaluate the impact of the whole WaveWings system. One of the major contributors to the Global Warming Potential (GWP) is the AWES drum made from carbon fibre. The choice for this material was taken because of weight consideration, however, the environmental impact is not good. In a further design iteration, the material choice might be reconsidered by trading off the environmental impact and the weight. For a more detailed design, the LCA can be significantly expanded in order to have a complete and accurate evaluation of the environmental impact of the WaveWings system.

References

- [1] Breukels, J., “An Engineering Methodology for Kite Design,” Ph.D. thesis, Delft University of Technology, 2011.
- [2] Loyd, M., “Crosswind Kite Power,” *Journal of Energy*, Vol. 4, 1980.
- [3] Ancellin, M., “Capytaine: a Python-based linear potential flow BEM solver,” , 2022. <https://capytaine.github.io/stable/index.html>.
- [4] Forbush, D., Grasberger, J., Husain, S., Keester, A., Leon, J., Ogden, D., Ruehl, K., Tom, N., Lawson, M., Michelen, C., Rij, J. V., and Yu, Y.-H., “WEC-Sim (Wave Energy Converter Simulator),” , 2024. <https://wec-sim.github.io/WEC-Sim/dev/index.html>.
- [5] Clara, T., De Laere, T., van Ginkel, D., van Vliet, L., Bredael, J., Dux, R., Leal, R., Matthé, J., Fernández-Nespral, G., and Güell Ybarra, M., “WaveWings DSE GitHub Repository,” , 2024. <https://github.com/TUD-AE/DSE2023-24-Q4-project05>.
- [6] Schmehl, R., *Airborne Wind Energy - Advances in Technology Development and Research*, 2018.
- [7] Trombini, S., Pasta, E., and Fagiano, L., “On the kite-platform interactions in offshore Airborne Wind Energy Systems: Frequency analysis and control approach,” *European Journal of Control*, Vol. 101065, 2024. <https://doi.org/10.1016/j.ejcon.2024.101065>.
- [8] Martinez, A., and Iglesias, G., “Site selection of floating offshore wind through the levelised cost of energy: A case study in Ireland,” *Energy Conversion and Management*, Vol. 266, No. 11502, 2022. <https://doi.org/10.1016/j.enconman.2022.115802>.
- [9] Comission, E., “Marine Strategy Framework Directive (MSFD) Common Implementation Strategy Setting of EU Threshold Values for continuous underwater sound,” Report, 1-12-2022 2022. <https://circabc.europa.eu/ui/group/326ae5ac-0419-4167-83ca-e3c210534a69/library/bc3ed92d-4c77-4d61-b92a-b906278236a9/details>.
- [10] Pietro Faggiani, R. v. d. V., Roland Schmehl, “Pumping Kites Wind Farm,” 2015. <https://doi.org/10.13140/RG.2.2.25280.64009>.
- [11] “SkySails Power,” , 2024. <https://skysails-power.com/>.
- [12] Thedens Paul, S. R., “An Aero-Structural Model for Ram-air Kite Simulations,” Ph.D. thesis, Delft University of Technology, 2023. <https://doi.org/10.3390/en16062603>.
- [13] Haug, S., “Design of a kite launch and retrieval system for a pumping high altitude wind power generator,” Ph.D. thesis, Delft University of Technology, 2012.
- [14] Bai, Y., and Jin, W.-L., “Offshore Soil Geotechnics,” *Wing Energy Engineering*, 2023.
- [15] “CorPower Ocean,” , 2024. <https://corpowersocean.com/>.
- [16] “Pelamis Wave Power,” , 2023. <https://www.emec.org.uk/about-us/wave-clients/pelamis-wave-power/>.
- [17] Energy, M., “Mocean Energy Technology,” , 2019. <https://www.mocean.energy/#>.
- [18] Cerfontaine, B., White, D., and Kwa, K., “Anchor geotechnics for floating offshore wing: Current technologies and future innovations,” *Ocean Engineering*, Vol. 279, 2023.

-
- [19] Sun, B., Zhang, Q., and Zhu, W., “Borehole Instability in Decomposed Granite Seabed for Rock-Socketed Monopiles during “Drive-Drill-Drive” Construction Process: A Case Study,” *Journal of Marine Science and Engineering*, Vol. 11, 2023.
- [20] Malhotra, S., “Selection, Design and Construction of Offshore Wind Turbine Foundations,” *Wind Turbine*, 2011.
- [21] J.F. Gaspar, e. a., “Power take-off concept for wave energy converters based on oilhydraulic transformer units,” 2016.
- [22] R. Ahamed, e. a., “Advancements of wave energy converters based on power take off (PTO) systems: A review,” 2020. <https://www.sciencedirect.com/science/article/pii/S0029801820302985>.
- [23] “The CorPower C4 set a new storm survivability record.”, 2023. <https://corpowersocean.com/corpower-c4-set-a-new-storm-survivability-record/>.
- [24] “CorPower Ocean features in ESB’s ‘Emerging Technology Insights’ report.”, 2023. <https://corpowersocean.com/corpower-ocean-features-in-esbs-insights-report/>.
- [25] Power, P. W., “Pelamis P-750 Wave Energy Converter,” 2014. <http://ctp.lns.mit.edu/energy/files/pelamisbrochure.pdf>.
- [26] Guo, C., Sheng, W., Silva, D. G. D., and Aggidis, G., “A Review of the Levelized Cost of Wave Energy Based on a Techno-Economic Model,” *Energies*, Vol. 16, No. 5, 2023.
- [27] “Mocean Energy lands £3m for next-gen wave machine,”, 2023. <https://www.powerengineeringint.com/renewables/marine/mocean-energy-lands-3m-for-next-gen-wave-machine/>.
- [28] “Mocean Energy Blue X wave machine completes sea trials,”, 2021. <https://www.mocean.energy/blue-x-device-removal/>.
- [29] Joensen, B., and Bingham, H. B., “Economic feasibility study for wave energy conversion device deployment in Faroese waters,” *Energy*, Vol. 295, 2024.
- [30] (GEBCO), G. B. C. o. t. O., “GEBCO Bathymetry,”, 2022. https://www.gebco.net/data_and_products/gridded_bathymetry_data/gebco_2022/.
- [31] Viré, A., “Fundamentals of Wind Energy I, Farm Layout,”, 2023.
- [32] Bertram, D. V., Tarighaleslami, A. H., Walmsley, M. R. W., Atkins, M. J., and Glasgow, G. D. E., “A systematic approach for selecting suitable wave energy converters for potential wave energy farm sites,” *Renewable Sustainable Energy Reviews*, Vol. 132, No. 110011, 2020. <https://doi.org/10.1016/j.rser.2020.110011>.
- [33] Thimm, L., “Wind Resource Parametrisation and Power Harvesting Estimation using AWERA - the Airborne Wind Energy Resource Analysis tool,” Ph.D. thesis, University of Bonn, 2023. <https://doi.org/10.5281/zenodo.7848071>.
- [34] Rusu, L., and Rusu, E., “Evaluation of the Worldwide Wave Energy Distribution Based on ERA5 Data and Altimeter Measurements,” *Energies*, Vol. 14, No. 2, 2021. ARTN39410.3390/en14020394.
- [35] Institute, M. C., “MPA Guide Marine Protection,”, 2024. <https://mpatlas.org/mpaguide/>.
- [36] Martinez, A., and Iglesias, G., “Multi-parameter analysis and mapping of the levelised cost of energy from floating offshore wind in the Mediterranean Sea,” *Energy Conversion and Management*, Vol. 243, 2021. <https://doi.org/10.1016/j.enconman.2021.114416>.

-
- [37] Commission, E., “EMODnet Human Activities, Energy, Wind Farms,” , 2024. <https://emodnet.ec.europa.eu/geonetwork/srv/eng/catalog.search#/metadata/8201070b-4b0b-4d54-8910-abcea5dce57f>.
- [38] Clara, T., Laere, T. D., Ginkel, D. v., Vliet, L. v., Bredael, J., Dux, R., Leal, R., Matthé, J., Fernández-Nespral, G., and Ybarra, M. G., “Baseline Report WaveWings (Group 5), Design Synthesis Exercise (AE3200),” Report, TU Delft, 2024.
- [39] Ireland, M. I., “Ireland Marine Atlas,” , 2024. <https://www.marine.ie/>.
- [40] O’Connell, R., de Montera, L., Peters, J. L., and Horion, S., “An updated assessment of Ireland’s wave energy resource using satellite data assimilation and a revised wave period ratio,” *Renewable Energy*, Vol. 160, 2020, pp. 1431–1444. <https://doi.org/10.1016/j.renene.2020.07.029>.
- [41] Cahill, B., “Characterizing Ireland’s wave energy resource,” *The Boolean: Snapshots of Doctoral Research at University College Cork*, 2011, pp. 21–25. <https://doi.org/10.33178/boolean.2011.5>.
- [42] Dalton, G. J., Alcorn, R., and Lewis, T., “Case study feasibility analysis of the Pelamis wave energy convertor in Ireland, Portugal and North America,” *Renewable Energy*, Vol. 35, No. 2, 2010, pp. 443–455. <https://doi.org/10.1016/j.renene.2009.07.003>.
- [43] Eireann, M., “CLI Storm Center,” , 2024. https://cli.fusio.net/cli/stormcenter/season_2021_2022.html.
- [44] Viré, A., “Fundamentals of Wind Energy I, Farm Layout,” , 2023.
- [45] “Sustainable Energy Authority of Ireland (SEAI),” , 2024. <https://www.seai.ie/>.
- [46] PWC, “Unlocking Europe’s offshore wind potential Moving towards a subsidy free industry,” Report, 2018. <https://www.pwc.nl/nl/assets/documents/pwc-unlocking-europes-offshore-wind-potential.pdf>.
- [47] GlobalData, “Ireland Wind Power Market Size and Trends by Installed Capacity, Generation and Technology, Regulations, Power Plants, Key Players and Forecast, 2021-2030,” Report, 2021. <https://www.globaldata.com/store/report/ireland-wind-power-market-analysis/>.
- [48] Offshore, I., “Harnessing Ireland’s unmatched offshore wind potential,” , 2024. <https://inis.offshorewind.ie/>.
- [49] “Smart Bay Facilities,” , 2023. <https://www.smartbay.ie/facilities>.
- [50] Petrick, K., “Airborne Wind Energy Country Mapping The situation for Airborne Wind Energy development in selected European countries in terms of resources, policies, stakeholders and opportunities,” Report, 2022. <https://airbornewindeurope.org/wp-content/uploads/2023/03/AWE-Country-Mapping.pdf>.
- [51] Innovation, E. C. D.-G. f. R., *Study on challenges in the commercialisation of airborne wind energy systems*, Publications Office, 2018. <https://doi.org/10.2777/87591>.
- [52] Fagiano, L. M., “Control of Tethered Airfoils for High-Altitude Wind Energy Generation - Advanced control methods as key technologies for a breakthrough in renewable energy generation,” Ph.D. thesis, Politecnico di Torino, 2009.
- [53] Ireland, W. E., 2024. <https://windenergyireland.com/>.
- [54] Bank, E. I., “Energy Overview 2023,” , 2023. <https://www.eib.org/en/publications/20220286-energy-overview-2023>.

- [55] Marvel, K., Kravitz, B., and Caldeira, K., “Geophysical limits to global wind power,” *Nature Climate Change*, Vol. 3, No. 2, 2013, pp. 118–121. <https://doi.org/10.1038/Nclimate1683>.
- [56] “Europe’s onshore and offshore wind energy potential - An assessment of environmental and economic constraints,” Report, European Environment Agency, 2009. https://www.eea.europa.eu/ds_resolveuid/58683b10a5ec519d1384c3e4a2c82168.
- [57] Ahrens, U., Diehl, M., and Schmehl, R., “Airborne Wind Energy,” , 2013. <https://doi.org/10.1007/978-3-642-39965-7>.
- [58] Fechner, U., “A Methodology for the Design of Kite-Power Control Systems,” Ph.D. thesis, Technical University of Delft, 2016. <https://doi.org/10.4233/uuid:85efaf4c-9dce-4111-bc91-7171b9da4b77>.
- [59] Salman, H. Y., Pitt, M., and A.D., “Drag correlations for particles of regular shape,” *Advanced Powder Technology*, Vol. 4, 2005. <https://doi.org/10.1163/1568552054194221>.
- [60] “Ocean Rodeo Flite: Dacron vs. Aluula Comparison,” , 2020. <https://www.realwatersports.com/blogs/news/aluula-vs-dacron-comparison>.
- [61] “ALUULA VS. DACRON: WHY ALUULA ALWAYS WINS,” , 2024. <https://oceanrodeo.com/blogs/news/aluula-vs-dacron>.
- [62] Roland, S., and Mikko, F., “AWESCO Deliverable D1.2 Improved Kite Design,” Report, 2018.
- [63] Roland, S., “Performance analysis of an airborne wind energy system,” , 2023. <https://github.com/awecourse/resources/tree/main>.
- [64] Gaunaa, R. S., Rodriguez, M., Ouroumova, L., and Mac, *Airborne Wind Energy for Martian Habitats*, Springer Nature, 2024, book section 7, pp. 145–197. https://doi.org/10.1007/978-3-031-50081-7_7.
- [65] Markus Sommerfeld, J. D. S. C. C., Martin Dörenkämper, “Impact of wind profiles on ground-generation airborne wind energy system performance,” 2023. <https://doi.org/10.5194/wes-8-1153-2023>.
- [66] Tan, J., “Improving the Techno-Economic Performance of Wave Energy Converters,” Ph.D. thesis, TU Delft, 2022. <https://doi.org/10.4233/uuid:de50235b-1d2a-43f3-bcfa-1dd5f570ab5a>.
- [67] Falnes, J., “Ocean waves and Oscillating systems,” *Ocean Engineering*, Vol. 30, No. 7, 2003, p. 953. [https://doi.org/10.1016/S0029-8018\(02\)00070-7](https://doi.org/10.1016/S0029-8018(02)00070-7).
- [68] Riyanto, R., and Rahmawati, S., “Hydrostatic Stiffness as Displacement Boundary Condition of Floating Cylindrical Structural Analysis in Waves,” , 2019. <https://doi.org/10.5220/0010058501310137>.
- [69] Babarit, A., Delhommeau, G., Kurnia, R., Singh, G., Daubisse, J., and Guével, P., “NEMOH,” , 2022. <https://lheea.ec-nantes.fr/valorisation/logiciels-et-brevets/nemoh-presentation>.
- [70] Ruehl, K., Michelén Ströfer, C., Kanner, S., Lawson, M., and Yu, Y.-H., *Preliminary Verification and Validation of WEC-Sim, an Open-Source Wave Energy Converter Design Tool*, Vol. 9, 2014. <https://doi.org/10.1115/OMAE2014-24312>.
- [71] Wilson, P. A., *Basic Naval Architecture*, Springer International Publishing, Cham, 2018. https://doi.org/10.1007/978-3-319-72805-6_3.
- [72] Jonas W. Ringsberg, X. L. E. J., Shun-Han Yang, and Kamf, J., “Mooring forces in a floating point-absorbing WEC system – a comparison between full-scale measurements and numerical simulations,” *Ships and Offshore Structures*, Vol. 15, 2020, pp. 70–81. <https://doi.org/10.1080/17445302.2020.1746122>.

- [73] Moses F. Oduori, T. O. M., Enoch K. Musyoka, “Material Selection for a Manual Winch Rope Drum,” *International Journal of Materials and Metallurgical Engineering*, Vol. 10, 2016.
- [74] DNV, “Lifting Appliances,” , 2013. <https://files.engineering.com/download.aspx?folder=b6a75e18-2d9e-4d25-8ed7-90344e376b73&file=standard2-22.pdf>.
- [75] S. Gupta, e. a., “Experiment on Hydraulic Power Take-Off Unit (PTO) for Point Absorber Wave Energy Converter (PA-WEC),” , 2024. https://link.springer.com/chapter/10.1007/978-981-99-7827-4_61.
- [76] R. Joshi, e. a., “Techno-economic analysis of power smoothing solutions for pumping airborne wind energy systems,” 2022. <https://iopscience.iop.org/article/10.1088/1742-6596/2265/4/042069/meta>.
- [77] Hagen, L. v., Petrick, K., Wilhelm, S., and Schmehl, R., “Life-Cycle Assessment of a Multi-Megawatt Airborne Wind Energy System,” *Energies*, 2023.
- [78] Hagen, L. v., “Life Cycle Assessment of Multi-Megawatt Airborne Wind Energy,” Ph.D. thesis, 2021.
- [79] Schaeffer-Oil, “512 ECOSHIELD™ BIODEGRADABLE HYDRAULIC FLUID ISO 32, 46 68,” , 2023. <https://www.schaefferoil.com/documents/213-512-td.pdf>.
- [80] Diinef, “Ground stations for Airborne Wind Energy,” , 2024. <https://www.diinef.com/kopi-av-airborne-wind>.
- [81] K.T. Waskito, e. a., “Design of hydraulic power take-off systems unit parameters for multi-point absorbers wave energy converter,” 2024. <https://www.sciencedirect.com/science/article/pii/S2352484723015676>.
- [82] L. Gao, e. a., “Modeling and Discretization of Hydraulic Actuated Telescopic Boom System in Port-Hamiltonian Formulation,” 2019. https://www.researchgate.net/publication/335162050_Modeling_and_Discretization_of_Hydraulic_Actuated_Telescopic_Boom_System_in_Port-Hamiltonian_Formulation.
- [83] Dickson, S. P., Vanegas-Cantarero, M. M., Bloise-Thomaz, T., Jeffrey, H., and J., M., “Life cycle assessment of a point-absorber wave energy array,” *Renewable Energy*, Vol. 190, 2022, pp. 1078–1088. <https://doi.org/10.1016/j.renene.2022.04.010>, <https://www.sciencedirect.com/science/article/pii/S0960148122004712>.
- [84] Gavazzo, N., “Life cycle assessment and productivity analysis of a point absorber wave energy converter,” *Politecnico di Torino*, 2022, p. 72. <http://webthesis.biblio.polito.it/id/ep rint/24951>.
- [85] “Review of mooring design for floating wave energy converters,” *Renewable and Sustainable Energy Reviews*, Vol. 111, 2019, pp. 595–621. <https://doi.org/10.1016/j.rser.2019.05.027>.
- [86] “Preventing Exposures to Lead in Telecommunications: What Every Member Should Know,” , 2023.
- [87] Jones, C., “Why offshore wind plans must include communication networks,” , 2022. <https://www.renewableenergyworld.com/wind-power/why-offshore-wind-plans-must-include-communication-networks/>.
- [88] “World’s largest offshore wind farm gets full mobile connectivity,” , 2021. <https://www.boldyn.com/news/worlds-largest-offshore-wind-farm-gets-full-mobile-connectivity>.

- [89] Vermillion, C., Cobb, M., Fagiano, L., Leuthold, R., Diehl, M., Smith, R. S., Wood, T. A., Rapp, S., Schmehl, R., Olinger, D., and Demetriou, M., “Electricity in the air: Insights from two decades of advanced control research and experimental flight testing of airborne wind energy systems,” *Annual Reviews in Control*, Vol. 52, 2021, pp. 330–357. <https://doi.org/10.1016/j.arcontrol.2021.03.002>.
- [90] Ringwood, J. V., Zhan, S., and Faedo, N., “Empowering wave energy with control technology: Possibilities and pitfalls,” *Annual Reviews in Control*, Vol. 55, 2023, pp. 18–44. <https://doi.org/10.1016/j.arcontrol.2023.04.004>.
- [91] Ringwood, J. V., Bacelli, G., and Fusco, F., “Energy-Maximizing Control of Wave-Energy Converters The Development of Control System Technology to Optimize Their Operation,” *Ieee Control Systems Magazine*, Vol. 34, No. 5, 2014, pp. 30–55. <https://doi.org/10.1109/Mcs.2014.2333253>.
- [92] Thematica, “The under the surface technology that’s connecting the power sector to a cleaner energy future,” , 2023. <https://www.thematica.com/the-under-the-surface-technology-thats-connecting-the-power-sector-to-a-cleaner-energy-future/>.
- [93] Cables, E., “IEC Cable,” , 2024. <https://www.elandcables.com/electrical-cable-and-accessories/cables-by-standard/iec-cable>.
- [94] Schachner, J., “Power Connections for Offshore Wind Farms,” Ph.D. thesis, 2004.
- [95] Salari, M. E., Coleman, J., and Toal, D., “Analysis of direct interconnection technique for offshore airborne wind energy systems under normal and fault conditions,” *Renewable Energy*, Vol. 131, 2019, pp. 284–296.
- [96] Nieradzinska, K., MacIver, C., and Gill, S., “Optioneering analysis for connecting Dogger Bank offshore wind farms to the GB electricity network,” *Renewable Energy*, Vol. 91, 2016, pp. 120–129.
- [97] Joshi, R., and Trevisi, F., “Reference economic model for airborne wind energy systems,” , 2023. <https://doi.org/10.5281/zenodo.8114627>.
- [98] Giglio, E., Petracca, E., Paduano, B., Moscoloni, C., Giorgi, G., and Sirigu, S. A., “Estimating the Cost of Wave Energy Converters at an Early Design Stage: A Bottom-Up Approach,” *Sustainability*, Vol. 15, No. 8, 2023. <https://doi.org/10.3390/su15086756>.
- [99] NOAA, “Global Self-consistent, Hierarchical, High-resolution, Geography Database (GSHHG),” , 2024. <https://www.ngdc.noaa.gov/mgg/shorelines/>.
- [100] Salma, V., Friedl, F., and Schmehl, R., “Improving reliability and safety of airborne wind energy systems,” *Wind Energy*, Vol. 23, No. 2, 2019, pp. 340–356. <https://doi.org/10.1002/we.2433>.
- [101] Ambühl, S., “Reliability of Wave Energy Converters,” Ph.D. thesis, Aalborg University, Aalborg, Denmark, 2015. <https://doi.org/10.13052/rp-9788793379053>.
- [102] Okoro, U. G., Kolios, A., Lopez, P. E., Cui, L., and Sheng, Q., “Wave Energy Converter System Safety Analysis,” , 2015. <http://repository.futminna.edu.ng:8080/jspui/handle/123456789/2791>.
- [103] Coe, R. G., Yu, Y.-H., and Rij, J. V., “A Survey of WEC Reliability, Survival and Design Practices,” *Wave Energy Potential, Behavior and Extraction*, 2017. <https://doi.org/10.3390/en11010004>.
- [104] TPM, E., and –, I. G., “Supply chains, energy chain analysis, and life cycle assessment,” , 2023. <https://brightspace.tudelft.nl/d21/1e/content/597774/viewContent/3535353/View>.

- [105] Coutinho, K., “Life cycle assessment of a soft-wing airborne wind energy system and its application within a hybrid power plant configurations,” , 2024.
- [106] Reddy, A. M., Das, S. K., and R., K., “Life cycle assessment of processing alternate sands for sustainable construction: Coal mine overburden sand versus manufactured sand,” *Journal of Building Engineering*, Vol. 75, 2023, p. 107042. <https://doi.org/10.1016/j.jobe.2023.107042>.
- [107] Garcia-Teruel, A., “Life cycle assessment of floating offshore wind farms: An evaluation of operation and maintenance,” 2022. <https://www.sciencedirect.com/science/article/pii/S0306261921013520>.
- [108] Energies, P., “Electricity Generation and CO₂ Emissions,” , 2016. <https://www.planete-energies.com/en/media/article/electricity-generation-and-related-co2-emissions>.
- [109] McNeill, Schratzberger, M., Thompson, M. S., Couce, E., Szostek, C. L., Baxter, H., Nicola J. Beaumont, S. C. W., Somerfield, P. J., Lemasson, A. J., Knights, A. M., Edwards-Jones, A., Nunes, J., Pascoe, C., and Louise, C., “The global impact of offshore wind farms on ecosystem services,” *Ocean Coastal Management*, Vol. 249, 2024, p. 107023. <https://doi.org/10.1016/j.ocecoaman.2024.107023>, <https://www.sciencedirect.com/science/article/pii/S0964569124000085>.
- [110] Dinh, V. N., and Mckeogh, E., “Offshore Wind Energy: Technology Opportunities and Challenges: Energy and Geotechnics,” 2019.
- [111] “Construction of an offshore wind plant: Everything you’d like to know about offshore wind farm construction,” , 2023.
- [112] Spyroudi, A., “End-of-life planning in offshore wind,” *Catapult Offshore Renewable Energy*, 2021.
- [113] “OCEAN ENERGY: Development Evaluation Protocol.” *Hydraulics Maritime Research Centre (HMRC)*, 2003.
- [114] “RAMS Engineering,” , 2023. <https://www.byhon.it/rams-engineering/>.
- [115] Li Shen, e. a., Liping Sun, “Reliability Assessment of Point-Absorber Wave Energy Converters Based on FMEA,” *12th International Conference on Quality, Reliability, Risk, Maintenance, and Safety Engineering*, IET Conference Proceedings, 2022, pp. 829–834. <https://doi.org/10.1049/icp.2022.2970>.
- [116] “Dutch Offshore Wind Innovation Guide,” Report, Wind and Water Works, 2024.
- [117] Towner-Roethe, H., “Hornsea Project Four: Outline Offshore Operations and Maintenance Plan (tracked),” Report, 2022.
- [118] Zhang, Y., “Wind turbine blade damage detection using aerodynamic noise,” 2024. <https://doi.org/10.4233/uuid:a45acef5-5ef9-4797-be5e-08498566ec8a>.
- [119] Polycase, “IP68 Enclosures,” , 2024. <https://www.polycase.com/ip68-enclosures>.
- [120] “Subsea Cables: Maintenance/Repair Operations,” , 2023.
- [121] “Hydraulic Services,” , 2024. <https://www.dphydraulics.ie/services>.
- [122] “Floating wind anchors and moorings: suction pile anchors,” , 2024. <https://www.sptoffshore.com/floating-wind-anchors-and-moorings/>.
- [123] “Innovative in-line mooring buoyancy solution for floating offshore wind,” , 2023. <https://www.balmoraloffshore.com/information/press/274-in-line-mooring-buoyancy-developed-for-floating-wind-and-surf-sectors>.

- [124] "Gentle Driving of Piles," , 2024. <https://www.vibrotwist.com/home>.
- [125] A. Tsetas, S. S. G., E. Kementzetidis, "Gentle Driving of Piles: Field Observations, Quantitative Analysis and Further Development," *Offshore Technology Conference*, 2024. <https://doi.org/10.4043/35156-MS>.